THE ANALYSIS OF TOPPLING FAILURE USING MODELS AND NUMERICAL METHODS

by

Abdurrahim Özgenoğlu B.Sc., M.Sc.

A thesis submitted to the University of London (Imperial College of Science and Technology) for the Degree of Master of Philosophy in the Faculty of Engineering

February 1978

ABSTRACT

This thesis describes research into toppling failure of rock slopes, carried out using both physical and numerical methods of investigation. Chapter 1 introduces the subject and reviews previous work in this area. Chapter 2 reports investigations into the mode of failure of a real slope using base friction models. Chapters 3, 4 and 5 are devoted to toppling analysis by means of simple physical models (base friction and tilting frame), limiting equilibrium, and numerical modelling (dynamic relaxation) respectively. A summary of the conclusions is given in Chapter 6.

ACKNOWLEDGEMENTS

The author wishes to express his gratitude to Dr. J.W. Bray for his supervision and to Dr. G. Hocking for his help and advice on computer work.

Thanks are also due to Mr. J.P. Jenkins who corrected the English, and Miss M.T.M. Chock who typed the thesis.

CONTENTS

LIST OF FIGURES

LIST OF FIGURES (continued)

LIST OF FIGURES (continued)

LIST OF FIGURES (continued)

LIST OF PLATES

LIST OF PLATES (continued)

LIST OF TABLES

CHAPTER ONE

INTRODUCTION

1.1 General

Now, it is a fact well known by everybody concerned with rock engineering that the stability of slopes in rock is controlled primarily by the planes of weakness or structural discontinuities - namely joints, faults, bedding planes etc. - within it. This is a natural outcome of the fact that the strength of the discontinuities is much less than that of the intact rock. Apart from the orientation, inclination, frequency, continuity and surface characteristics of these features, presence of groundwater pressure influences the behaviour of the slope as a major factor. Seismic acceleration forces due to blasting, rock mass strength, slope geometry, stresses and deformations in the slope, climatic conditions and time could be cited as the other points that should be taken into consideration when a detailed analysis is to be done[1].

In order to avoid loss of life, money and time a rational design of slopes is essential with a balance between economics on one side and safety on the other. However this is not an easy task because of the complex and variable nature of the rock; so, every effort should be made with the available tools at hand. In this context, the close collaboration between geologist and engineer must be emphasized. Many people on various occasions put stress to the utmost need and

importance of the geologist's contribution for a sound and healthy understanding of the media[2,3].

1.2 Methods of Slope Stability Analysis

Slopes in rock can be analysed with three different techniques[4]. These are:

a. Empirical and observational approach

b. Limit equilibrium approach

c. Stress analysis approach

The empirical method makes use of previous experience together with the study of models and the performance of the prototype itself. The limit equilibrium method is based on the strength characteristics of the rock mass, specifically those of the discontinuities, and normally utilizes the Coulomb-Navier failure criterion. The third method, i.e. the stress analysis approach, involves the study of the deformation and strength characteristics of the rock mass.

a. Physical models may yield important information regarding the behaviour of a prototype provided simulitude laws are observed, but this is very difficult to achieve because it is seldom possible to vary each of the parameters independently. Despite its limitations physical models have been used extensively by investigators. Barton's[5] sophisticated two-dimensional model where the strength and behaviour of rough joints were reproduced, and Heuze' and Goodman's[6] interesting three-dimensional model where water was introduced to promote

motion of blocks are examples of gravity loaded models. To investigate the behaviour of rock slopes in sedimentary rock structure Stacey[1] built up both two and three dimensional models which were loaded in a centrifuge. Although it is difficult to produce reliable quantitative results, physical models remain very valuable for the conduct of kinematic studies. In this context the base friction technique has been used extensively by various researchers[7,8,9,10] despite its qualitative nature. This method is discussed in Chapter Two in detail and the tests conducted are reported in Chapters Two and Three. Obviously it is preferable to replace the physical models with numerical solutions which fulfill the same purpose but are not subject to some of the limitations inherent in the former. In such an attempt St. John[11] tried to simulate the Barton's[5] two-dimensional slope model by using the finite element technique but could not get satisfactory results for various reasons.

b. The limit equilibrium method of analysis simply works out the balance of disturbing and resisting forces against sliding on a pre-defined surface. Since the method produces a definite answer in the form of factor of safety it has found an extensive use in rock mechanics, having been used for many years to evaluate the stability of soil slopes. For ease of operation and speed of application calculations have been reduced to a graphical or tabular presentation. In this connection attention is drawn to a set of slope charts for circular and plane failures designed by Hoek & Bray[12]. Although this technique is very efficient in estimating the stability of

excavated slopes it requires the failure mode to be known or to be guessed with reasonable certainty in order to define a slip surface upon which the limiting conditions will be examined. Jennings[13] considered the case of a plane failure on a stepped surface taking into account the continuity of joints and thus tried to obtain a better representation of the behaviour of the rock mass in nature. But the assumption that rock behaves in a rigid-perfectly plastic manner (non-deformable block) is the shortcoming of this method because the progressive nature of failure which is a complex phenomenon is not taken into account. For analysis of three-dimensional cases Londe and his co-workers[14,15], and John[16] have used the stereographic projection as a powerful tool in such a way that the frictional and cohesive strength of the discontinuities and all forces including water pressure could be taken into account. As an alternative to graphical techniques, the analytical models (vectors) as discussed by Wittke[17] and Goodman & Taylor[18] appeared to be advantageous in their ability to handle the rotational and toppling modes of block failures in addition to sliding modes. As a final remark about this method of analysis one should bear in mind that the reliability of the technique depends on how reliable and representative the input data are and the assumptions made.

c. Design methods based on <u>stress analysis</u> have been advancing rapidly recently with the newly developing numerical techniques and increasing computer capacities. The necessity for an exceptionally high level of experimental skill and the amount of time required to carry out a complete analysis made

the photoelastic method of stress analysis[19,20] unattractive, especially with the emergence of powerful Finite Element[21] and Finite Difference[22] techniques as alternatives. The only advantage of the photoelastic technique was its applicability to three-dimensional problems, and this has been diminishing because of extension of the capability of numerical techniques from two to three dimensional cases[1,11,23]. The attempts made by Mahtab & Goodman[23], St. John[24], and Stacey[1] in using the Finite Element method to analyse three-dimensional jointed rock slopes although not fully satisfactory have shown the versatility of numerical techniques. A relatively new method of stress analysis, namely the Boundary Integral Equation method, has been receiving an increasing amount of attention recently for analysing the stress distribution around underground excavations[25,26]. This technique offers certain definite advantages such as considerable reductions in computer storage and time, and data preparation when compared with the finite element method. To the author's knowledge, the method has not been adopted yet for slope stability analysis. While Goodman and Taylor[18] have noted the difficulties in the finite difference method in matching the boundaries and treating the variation in material properties, Cundall[27] has demonstrated the versatility of the technique when large scale movements in blocky rock systems are to be modelled: such movements cannot be analysed by the finite element method. On the other hand, St. John[11] supports the finite element method saying "..... any material behaviour may be simulated providing it can be adequately defined".

In this respect he points out that the method is capable of treating arbitrary boundary conditions, any initial stress conditions, inhomogeneity, and also inelastic and non-linear behaviour.

Some of the methods available for the analysis of jointed rock masses and their capabilities and limitations have been summarised by Stacey[1] in the form of a table which is reproduced as Table 1.1 here.

1.3 Slope Failure Mechanisms

An understanding of the way in which rock masses move in slopes is of considerable importance in slope design, and is a necessary prerequisite for carrying out a proper limiting equilibrium analysis, and also for deciding the precautionary steps which should be taken to avoid instability. Knill[36], Hutchinson[37], and Coates[38], to name only a few, have classified the slope failures according to the mechanics of failure. Hutchinson[37] made the most comprehensive classification under the title of "Geomorphological Classification of Mass Movements on Slopes". He considered three main groups of behaviour: Creep, Frozen Ground Phenomena and Landslides, and subdivided them further as seen in Table 1.2. Knill's[36] classification follows more or less the same path with three main categories: a) Rock Falls b) Rock Slides c) Creep. He described the rock falls as the sliding or rolling down of loose rocks developed on the slope, weathering being the primary cause of loosening. Toppling failures were included in this category. Rock slides have been further sub-classified

Table 1.1- Summary of numerical methods of analysis for jointed rock masses (After Stacey[1]).

Reference	Brief description of method	Capabilities				Remarks
		Non-homogeneous material	Arbitrary boundary shapes	Discontinuities	Large deformations	
Tarasova[28]	Elastic method in which equivalent elastic moduli for the rock mass are calculated	No	No	Yes	No	Deals with alternating hard and soft layers i.e. anisotropic system
Pinto[29]	As above, but equivalent moduli are calculated in 3 dimensions	No	No	Yes	No	As above, but deals with orthotropic material as well
Zienkiewicz, Cheung and Stagg[30]	Finite element approach, incorporating anisotropic properties	Yes	Yes	Yes	No	For analysis of stratified material
Duncan and Goodman[31]	As above, but incorporating equivalent orthotropic properties	Yes	Yes	Yes	No	For analysis of block jointed material with or without softer materials on joints
Zienkiewicz, Valliappan & King[32]	Iterative finite element approach	Yes	Yes	No	No	"No-tension" iterative approach redistributes any tensile stresses which are calculated assuming linearly elastic properties. Suitable for extensively fractured rock but does not actually handle discontinuities as separate entities
Zienkiewicz, Best, Dullage and Stagg[33]	Iterative finite element approach to handle one or two sets of discontinuities	Yes	Yes	Yes	No	Iterative "no-tension" approach redistributes stresses, for application to the cases of single or double laminarity. An alternative approach to double laminarity is to assign single laminarity different orientation to alternating elements
Malina[34]	Iterative finite element approach to handle one or more sets of discontinuities	Yes	Yes	Yes	No	Handles pre-existing discontinuities as well as the formation of new fractures. Intact material and discontinuity strengths are represented by Mohr envelopes.
Goodman, Taylor and Brekke[35]	Iterative finite element approach incorporating special "joint" elements	Yes	Yes	Yes	Yes	Discontinuities are modelled individually by elements with specified force-displacement relationships, allowing large deformations. Zienkiewicz et al (33) describe similar elements based on stress-strain relationships
Cundall[27]	Iterative approach based on force-displacement relationships	No	Yes	Yes	Yes	Collapse of structures modelled with ease. Intact rock is assumed to be rigid, and "rock blocks" are modelled individually
Stacey[1]	Iterative finite element approach to handle one or more sets of discontinuities	Yes	Yes	Yes	No	Handles pre-existing discontinuities, allowing tension across joints in some cases, and corrects for tensile opening of one joint set associated with shear failure on another set

Table 1.2- Geomorphological classification of mass movements on slopes (After Hutchinson[37]).

CREEP

1. Shallow, predominantly seasonal creep; Mantle creep
   - (a) Soil creep
   - (b) Talus creep
2. Deep-seated continuous creep; Mass creep
3. Progressive creep

FROZEN GROUND PHENOMENA

4. Freeze-thaw movements
   - (a) Cambering and valley bulging
   - (b) Solifluction sheets & lobes
   - (c) Stone streams
   - (d) Rock glaciers

LANDSLIDES

5. Translational slides
   - (a) Rock slides; block glides
   - (b) Slab, or flake slides
   - (c) Detritus, or debris slides
   - (d) Mudflows
     - (i) Climatic mudflows
     - (ii) Volcanic mudflows, or lahars
   - (e) Bog flows; bog bursts
   - (f) Flow failures
     - (i) Loess flows
     - (ii) Flow slides
6. Rotational slips
   - (a) Single rotational slips
   - (b) Multiple rotational slips
     - (i) In stiff, fissured clays
     - (ii) In soft, extra-sensitive clays; clay flows
   - (c) Successive, or stepped rotational slips
7. Falls
   - (a) Stone and boulder falls
   - (b) Rock and soil falls
8. Sub-aqueous slides
   - (a) Flow slides
   - (b) Under-consolidated clay slides

into uniplanar or multiplanar translational slides, rotational slides or a combination of both translational and rotational slides. Translational slides are said to occur along geological planes of weakness such as bedding planes, joints, faults, etc. when the shear resistance along the plane(s) is exceeded. Slopes cut in intensely and randomly jointed hard rock may fail by rotation of mass on a more or less circular arc which is typical of soil slopes. Creep is the time-dependent deformation that most rock types exhibit. Coates[38], apart from rock fall, rotational and plane shears, introduces "block flow" replacing creep (see Fig. 1.1). He visualises this method of failure as being a general break-down of the rock mass as a consequence of crushing at the points of highest stress in the brittle rock blocks comprising the mass. Piteau[39] considers creep as a form of block flow failure. Richards[40] recognises six basic types of slope

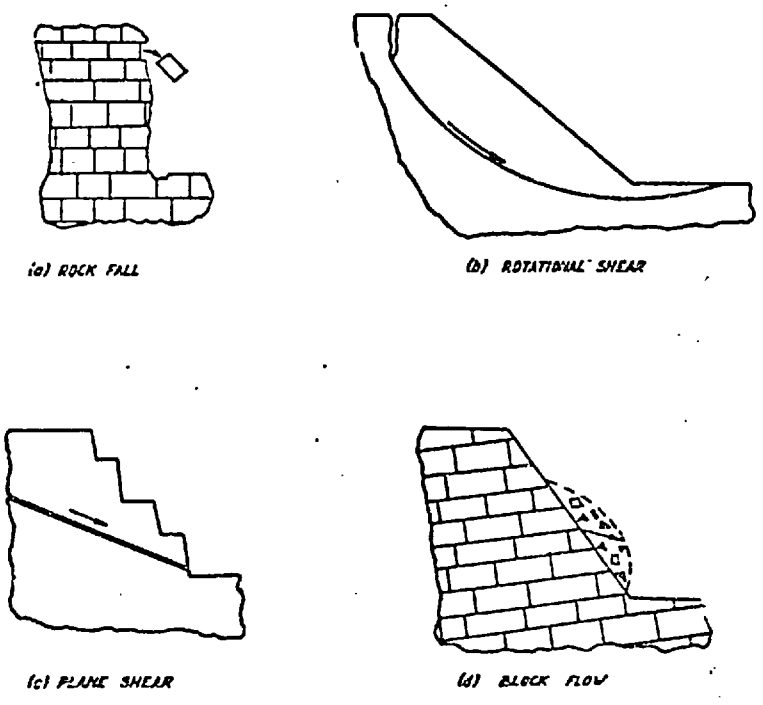

Figure 1.1- Classification of types of slope failure(After Coates[38]).

failure in rock masses which are shown diagrammatically in Fig. 1.2. Toppling is taken into account as a separate mode of failure in this classification. Ravelling failure of Richards should correspond to block flow failure of Coates.

Jennings[13], Piteau[39], and Goodman & Bray[41] have gone further splitting the specific modes of failure into sub-classes. Jennings proposed four separate modes of failure involving planes or combinations of planes and put forward mathematical theories for each case for the stability analysis. They are:

a. Plane failure mode.
b. The conjugate joint zone failure mode involving failure on three mean planes.
c. The conjugate joint block failure mode.
d. Three dimensional wedge failure.

Piteau[39], considering the significant failure types postulated by Jennings[13], grouped the modes of failure on preferred planes of weakness as follows:

a. Line failure modes (Fig. 1.3).
   (i) Plane failure mode.
   (ii) Stepped joint failure mode.
b. Conjugate planes - failure modes (Fig. 1.4).
   (i) Conjugate planes - zone failure mode.
   (ii) Conjugate planes - block failure mode.
c. Wedge failure mode.

In a recent paper, Goodman & Bray[41] gave several kinds of

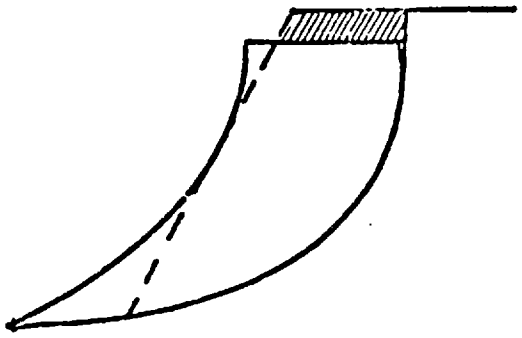

1). Circular failure

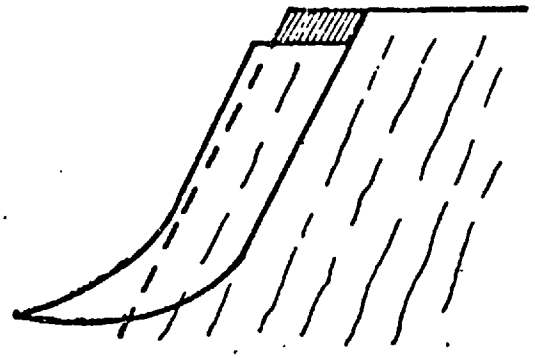

2). Non-circular failure

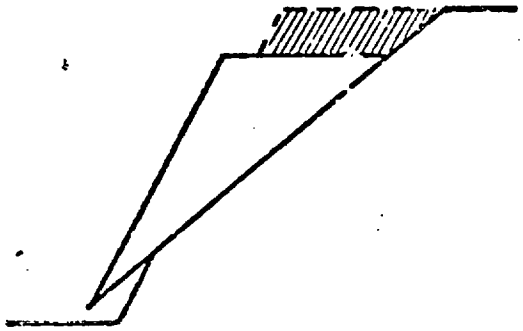

3). Plane failure

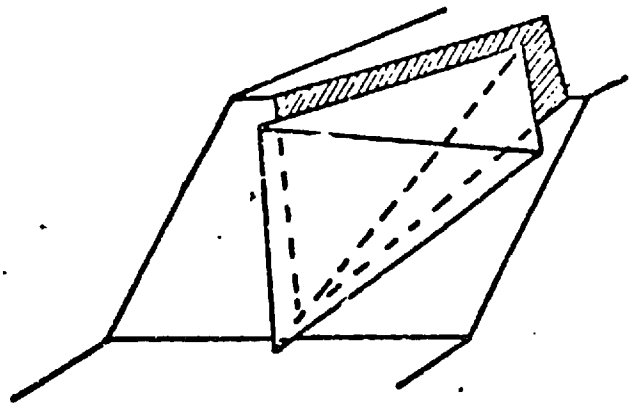

4). Wedge failure

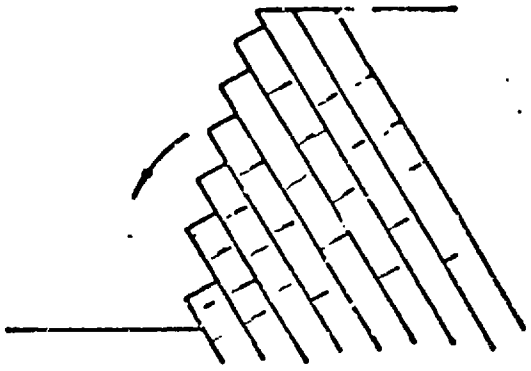

5). Toppling failure

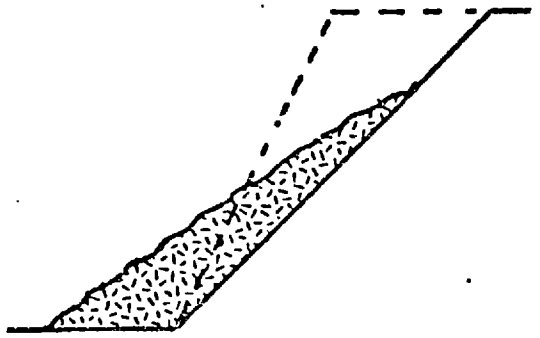

6). Ravelling failure

Figure 1.2- Mechanisms of slope failure (After Richards[40]).

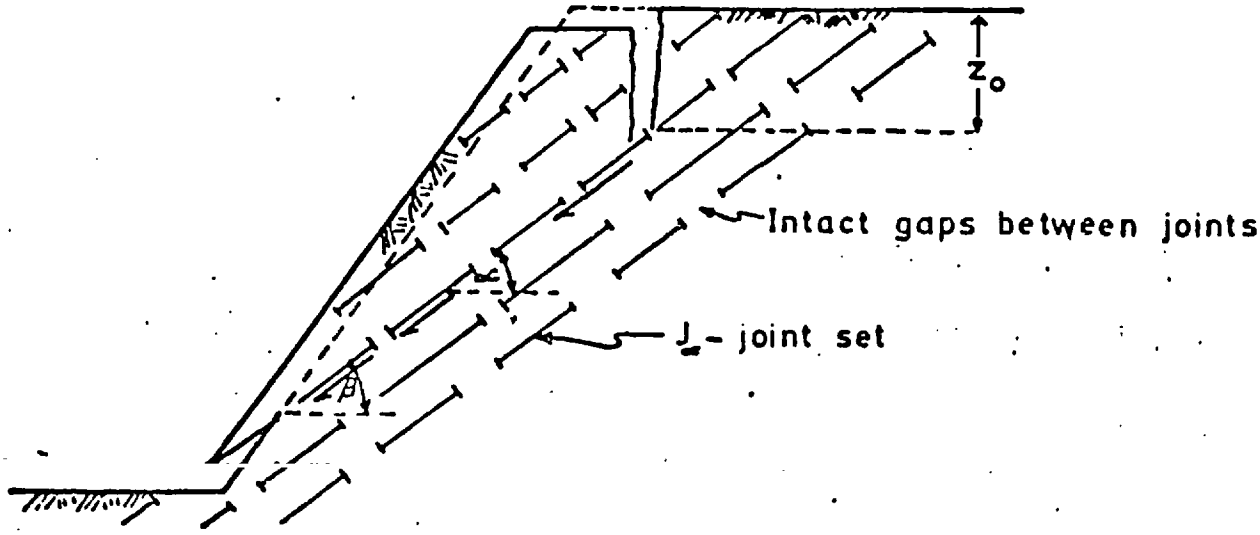

i) plane failure mode

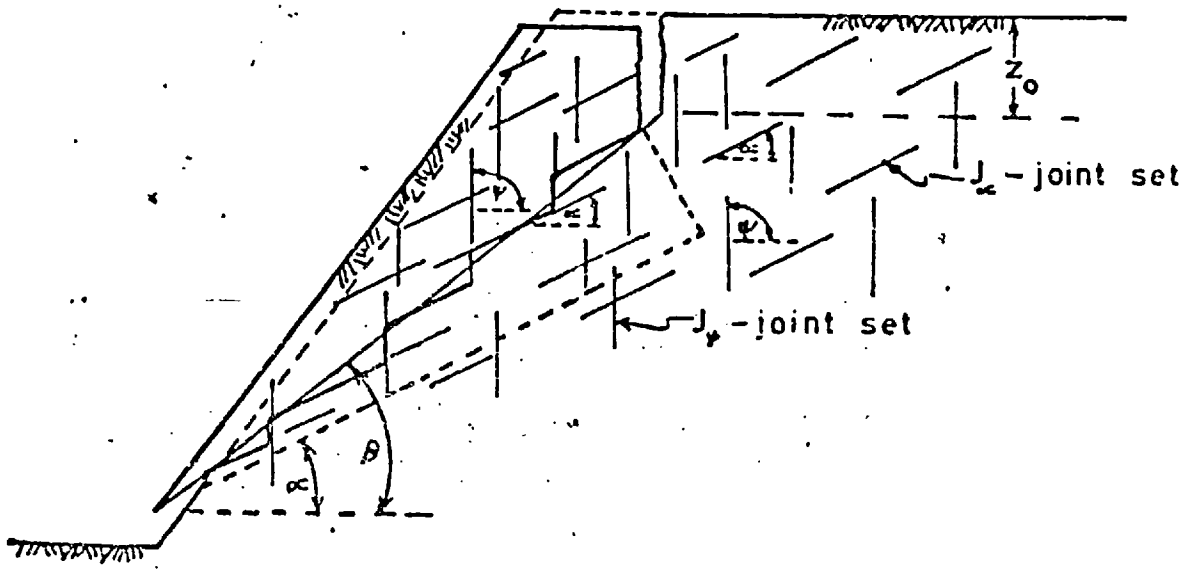

ii) stepped joint failure mode

Figure 1.3- Line failure modes (After Piteau[39]).

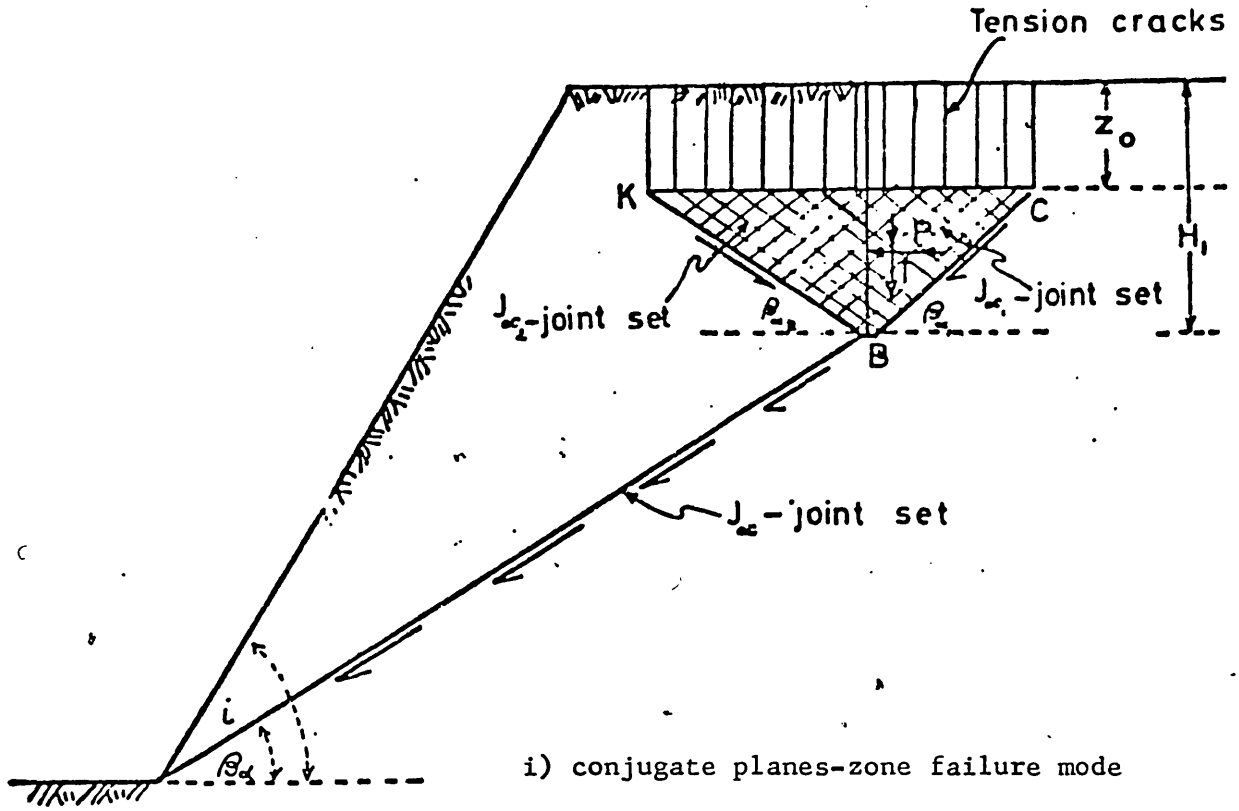

i) conjugate planes-zone failure mode

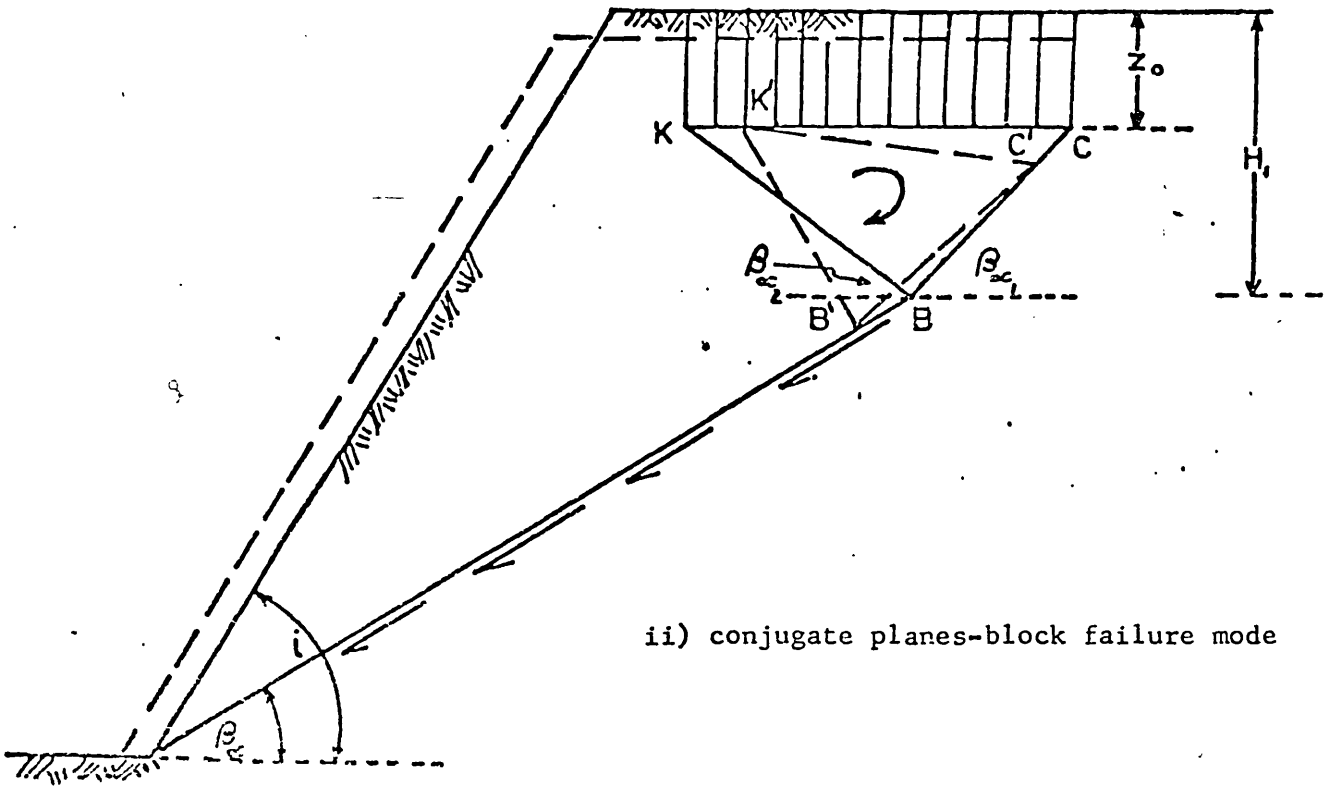

ii) conjugate planes-block failure mode

Figure 1.4- Conjugate planes-failure modes (After Piteau[39]).

failure mechanisms involving overturning of columns. They classified them as:

a. Flexural toppling

B. Block toppling

c. Block-flexure toppling

which are shown in Figure 1.5. They also indicated the possibility of induced toppling and named it as "secondary toppling". Figure 1.6 shows several examples of such secondary toppling modes.

Consequently, it can be said that practically all the modes of failure in rock slopes are structurally controlled unless the rock is intensely and irregularly jointed whence it behaves like an isotropic soil. Failure through intact rock material alone is hardly possible as pointed out by Terzaghi[42].

1.4 Previous Work on Toppling

Although toppling has long been observed in the field as a deformational mechanism, surprisingly it is only recently considered to be a fundamental mode of failure in jointed rock slopes. The idea first originated from Bray[43] in 1969, and has been flourishing around himself since. However John[44] reports that the overturning failure of rock slopes was first analysed by himself in 1964 for a highway project, it cannot be considered as a major effort but an isolated work. Bray's theoretical findings soon have been backed by physical and numerical model studies of Barton[5], Ashby[45], Müller & Hofmann[46],

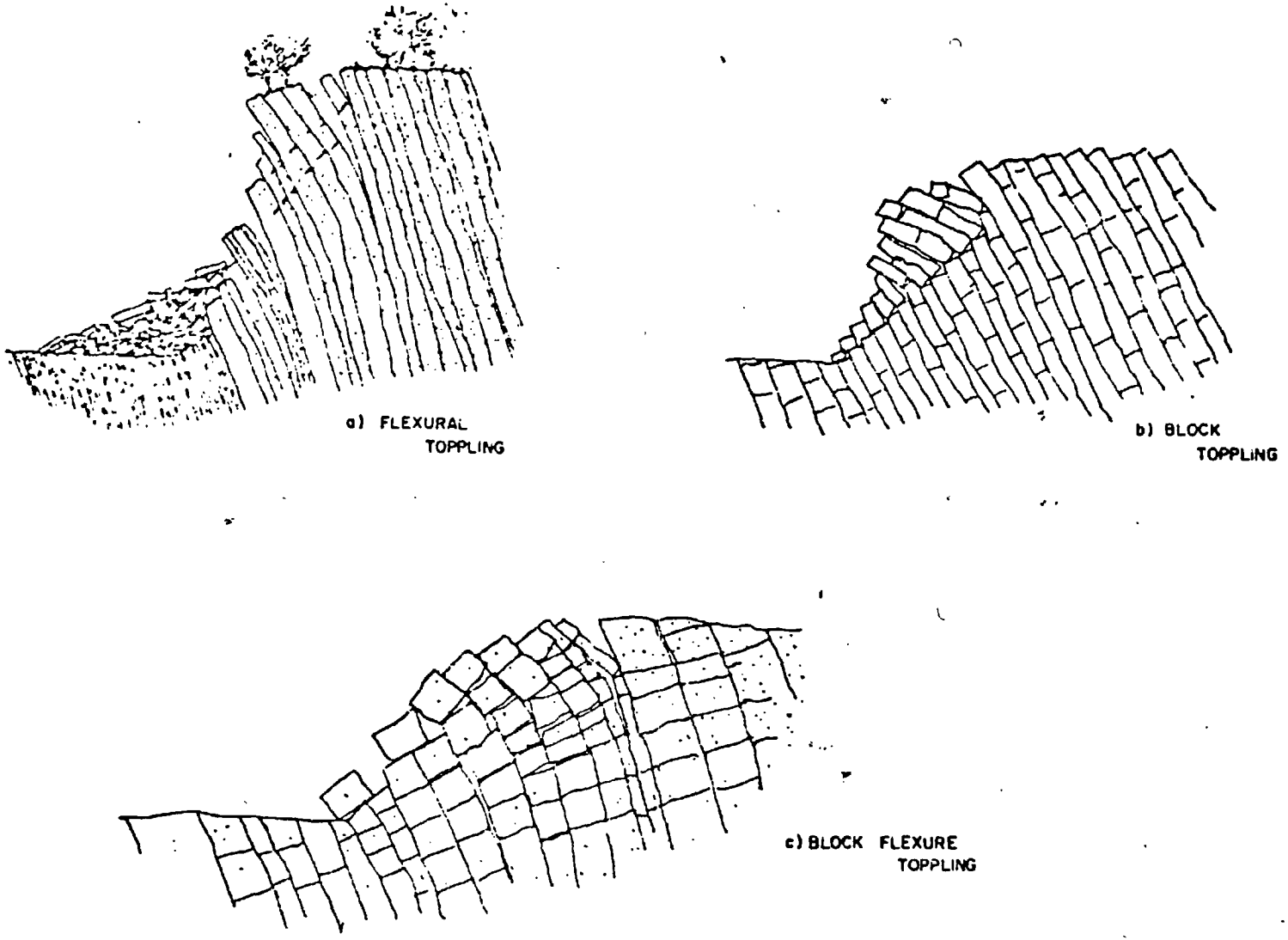

Figure 1.5- Common classes of topples: a)flexural toppling, b)block toppling, c)block flexure toppling (After Goodman and Bray[41]).

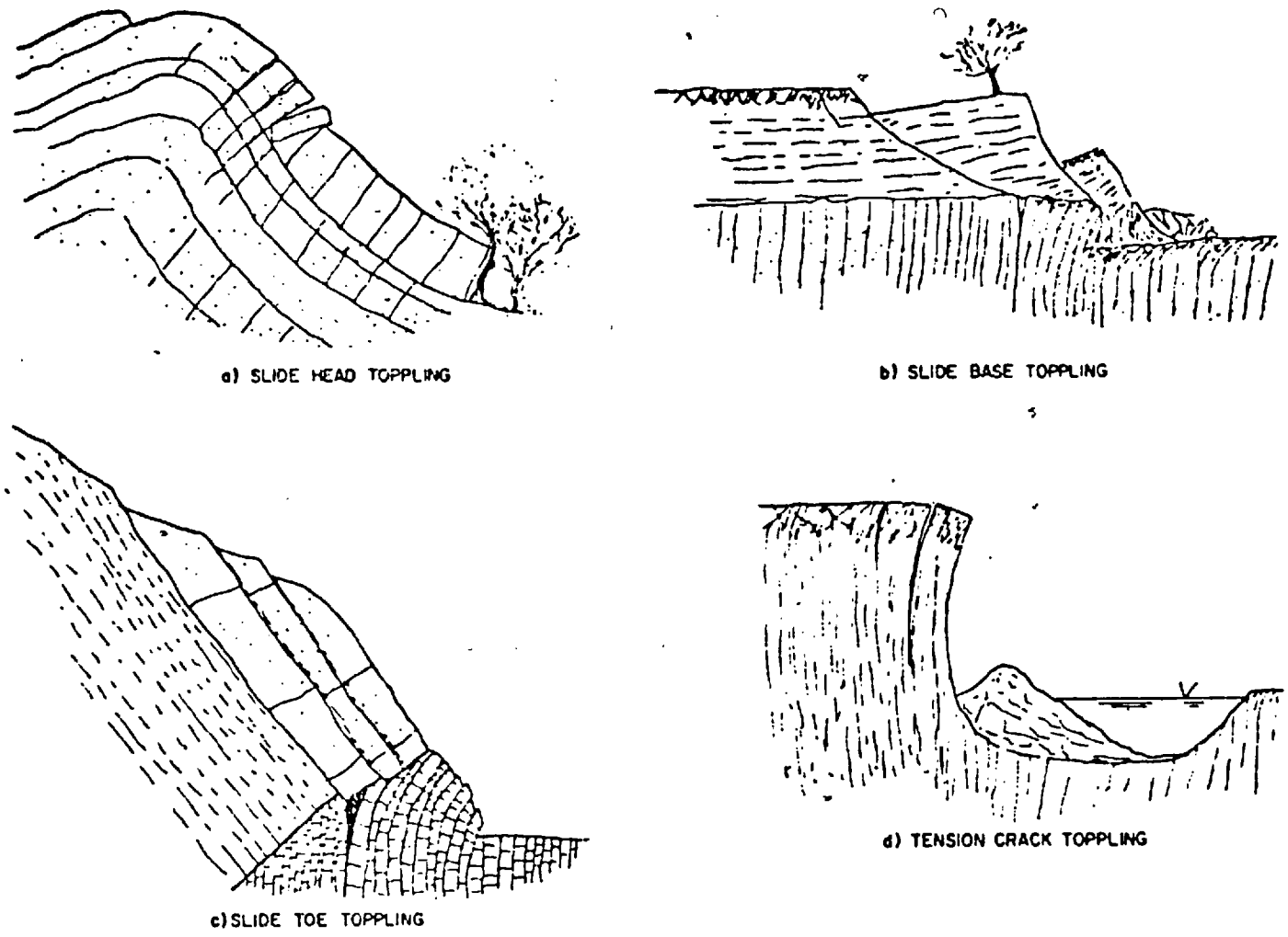

Figure 1.6- Secondary toppling modes: a) slide head toppling; b) slide base toppling; c) slide toe toppling; d) tension crack toppling (After Goodman & Bray[41]).

and Cundall[22] respectively. Ashby's remarkable work, in this context, laid down the foundation for further analyses. Soon after the model test confirmation of toppling as a failure mechanism field examples of toppling failures were reported by de Freitas & Watters[47], indicating its existence in nature as well. The following is the list of authors with their contributions in evaluation of toppling in chronological order. They are going to be referred throughout the thesis when necessary.

BRAY[43] (1969): Put forward the concept of toppling as a behavioural mode for jointed rock slopes with a theoretical basis.

JOHN[44] (1970): Stressed the need of a check for overturning failure, particularly in steep slopes, apart from the primary shear failures. Noted the joint spacing as a governing factor in this mechanism. Introduced an arbitrary criterion for the stability limit against overturning of individual rock elements defining an overturning wedge at the base of the element and assumed that stable conditions exist as long as the resultant (weight or weight and hydrostatic thrust) is within this wedge. With a simple graph showed the effect of the slope angle and hydrostatic thrust for plane conditions, based on the criterion put forward. Made an attempt to analyse the overturning failure in three dimensions using refe-rence hemisphere.

MÜLLER & HOFMANN[48] (1970): Reported "overturning of the top of the slope with subsequent rock falls" as the first of three

main successive stages of deformation and failure during the excavation of regularly jointed rock slope models built to investigate the complicated kinematics and varying failure behaviour of rock masses. Noted the significance of regular jointing with high continuity in determining this mode of behaviour. Also, emphasized the necessity to understand the possible kinematics of the various zones and their combined action in endangering the rock mass of the slope in addition to investigating the system of joints in the critical zone.

BARTON[5] (Jan. 1971): Conducted a series of two-dimensional jointed slope model tests on a tilting frame reproducing the strength and behaviour of rough joints by the creation of sets of tensile fractures in a weak brittle material. Observed several toppling failures beside translational shear and translational shear with tensile opening. Noted the importance of the relative orientation of the primary and secondary joints with respect to the gravity field in implementing the mode of failure. Reported that for toppling shear failure to occur either a higher frictional resistance on the joint set dipping into the slope (sliding set) than on the near vertical (overhanging) set potentially involved in toppling shear or an angle of dip for the sliding set low enough to preclude shear failure on this set has to exist. Pointed out the role played by the frictional resistance in controlling the post-vertical angle required for relative shear to initiate. Described toppling a totally self inhibiting mechanism for dilatant joints considering the

necessity of relative shear across the sub-vertical joint set for its initiation and therefore ruled out the possibility of deep seated loosening of the jointed rock mass to yield a toppling failure in conventional open pit slopes of 30^{o} to 60^{o}, and consequently restricted this type of failures to steep benches where blast damage could render suitable joint configurations prone to toppling failure.

CUNDALL[22] (Feb. 1971): Produced computer drawn diagrams of the spectacular progressive toppling mechanism in idealized block models using a finite difference approach where realistic friction laws have been incorporated allowing unlimited block movement. In support of Barton's[5] findings, demonstrated that the mechanism of toppling was governed by relative shear along sub-vertical joints which in turn was controlled by the friction coefficient of shearing surfaces.

HOEK & BOYD[48] (July 1971): Discussed the basic mechanisms of sliding and toppling of a discrete block. Using the base friction modelling technique demonstrated the importance of toppling as a mode of failure and showed that the final configuration could easily be confused with one of the more familiar sliding modes.

ASHBY[45] (1971): Undertook an extensive modelling work (mainly tilting frame tests) in an attempt to understand and define the toppling phenomenon manipulating the frictional characteristics of columns and the thru-going discontinuity, and the number of columns essentially. Remarked the following points from his observations:

a. Toppling must be considered in conjunction with sliding displacement at the toe.

b. The stability (of the model) is controlled dominantly by the frictional characteristics of the throughgoing discontinuity at the toe, the geometrical relationship of the columnar joints, and only to a slight extent by the frictional characteristics of the column surfaces.

c. Reduction in factor of safety of a predicted sliding could be as much as 70% due to toppling.

d. The least stable high angle joint (toppling set) orientation is 65^{o}.

e. Tension crack displacement at the crest occurs prior to toe displacement.

f. While base friction models (plaster blocks) give less stable configurations, numerical models (Cundall's Dynamic Relaxation) yield slightly more stable configurations as compared to tilting frame tests. Also, delineated three zones of behaviour from his experiments, such as:

   i. a region of sliding - generally restricted to the toe block along the incline

   ii. a region of toppling columns and blocks with step failure by sliding when the dip of low angle discontinuities exceeds the friction angle of blocks

   iii. an approximately triangular slab region in which no movement occurs.

ST. JOHN[11] (Jan. 1972): Made an attempt to simulate Ashby's toppling block model with a simple finite element idealization. However obtained the typical block rotation that occurs, failed to get toppling induced partings between blocks because of the inherent limitation (of infinitesimal strain) of the finite element technique.

WATTERS[49] (1972): While investigating the stability of slopes in Scottish Highlands confirmed the existence of toppling in nature too. Discussed the approaches to isolate toppling and toppling/sliding modes of failure from those of translational shear from field observations. Concluded that slopes designed to satisfy a translational shear mechanism, and judged as "safe" may well fail if a toppling or toppling/sliding mechanism can develop.

DE FREITAS & WATTERS[47] (1973): Described three field examples of toppling which came from contrasting structural settings, each involving a different scale of mass movement; so, indicated that this mode of failure requires neither unusual geological conditions, nor unusual geological materials in order to develop, but the reverse seems to be true. Pointed out that toppling failures could develop in a variety of rock types such as sandstones, shales, granulites, and schists. Noted, also, the sensitivity of toppling failure to the lateral restraints provided by the margins of the moving mass.

STACEY[1] (1973): Observed toppling, although not deep seated, in his two dimensional small scale models which were subjected

to large centrifugal accelerations in a centrifuge to simulate gravitational loading, even though the bedding planes forming the continuous columns were dipping into the slope with an inclination of only 33^{o} to the horizontal. Reported the occurrence of toppling exclusively for the ratio of joint spacing to bedding plane spacing of 1 but not of 1.87, 2.76 and 3.74 cases underlining the effect of block geometry upon the mode of failure.

GOODMAN[8] (1973): Noted the following points after a simple two-dimensional kinematic model study in an attempt to demonstrate the importance of detailed geological observations on the modes of behaviour (under varying initial stress conditions):

a. The toe region has great importance in a rock slope with a potentially toppling joint set. Toe flexure takes place when horizontal stresses are significant.
b. An analysis of toppling must take into account the overturning moment on individual columns, the resistance through overturning of the toe portion of the slope, and the flexural strength of the overturning material.
c. Toppling of vertical columns does not compromise the overall stability of a steep rock slope; it is a local failure condition restricted to the vicinity of the slope itself.

HOEK & BRAY[12] (1974): Though briefly, touched on toppling as a mode of failure beside failure by sliding and warned

the design engineers against its increasing danger with steepening discontinuity angle and slope angle. Also, recommended reinforcement by rockbolts or cables tying tall slender rock columns together to form wider blocks to prevent toppling. The importance of identification and anchorage of the "keystone" which prevents the front face of the slope from moving was emphasized too.

GEOROGIANNOPOULOS[50] (Sept. 1974): Tried to find a way to judge about toppling mode of failure relying entirely on models (tilt frame and base friction). Come up with the conclusion that the outward rotation of the slope upper surface (exactly opposite to that of circular failure) seems to be the best judgement about the toppling mode of failure. Proposed a crude rule, as well, to judge about the depth of disturbance.

BAYNES[51] (June 1975): Compared the theoretical model postulated (by himself) using the previously published model studies with the detailed field evidence. Indicated that the field evidence tends to support the various hypothesis proposed. On the basis of this field evidence, however limited, formulated some very crude design guidelines for toppling failures.

GOODMAN & BRAY[41] (1976): Discussed toppling in its wide spectrum indicating that it may occur in slopes cut quite a variety of rocks, under various circumstances, and in different ways with very serious consequences if overlooked. Examined a limit equilibrium analysis for the special case of block

toppling on a stepped base producing the required support force at the toe of the slope to achieve a specified factor of safety.

1.5 Scope of the Thesis

When this study was undertaken, very little was known about toppling failure in the form of quantitative analysis. Therefore it was proposed to develop a design criterion so that the practising engineer would be provided with simple design charts or graphs to solve his problem safely and easily. For this purpose the author has chosen to examine situations of steadily increasing complexity in an effort to understand this mode of behaviour in depth. Also, the tools used to explore toppling were from simple to complex in nature, starting with base friction models and ending with dynamic relaxation computer simulation respectively. But everything has not gone as planned and the aim of the research could not be reached. The author was unfortunate enough firstly, having been restricted in time and secondly, receiving no encouragement in tackling such a vast and complex topic which deserves more time and much more effort. However, the author has undoubtedly made some useful contributions to the subject such as testing and modifying a Dynamic Relaxation Block Program to handle differently shaped blocks, limit equilibrium analysis of multiple block systems, testing and evaluation of base friction model tests in appreciation of toppling problems and finally enlightening of the mode of a real slope failure from the field

using base friction technique.

1.6 Conclusions

While designing slopes in rock toppling should be given important consideration beside conventional sliding, especially when columnar or layered structures are in question because, now, it is a world-wide known fact that it (toppling) can involve large volumes of rock mass with serious deformations far distant from the slope face. However, although a great deal of research has been going on for some time receiving an increasing attention every day, the present level of knowledge offers very little to the practising slope engineer in the way of quantifiable parameters on which to base a slope design when faced with the problem of toppling. Quoting from Goodman & Bray[41]: "Suffice it to say that our understanding and appreciation of this behavioural mode is but in its infancy".

REFERENCES

1. STACEY, T.R. Stability of rock slopes in mining and civil engineering situations. Dr.Sc. Thesis, University of Pretoria, 1973.
2. HOEK, E. Rock Engineering. Inaugural lecture, Imperial College of Science and Technology, London, 1971.
3. PITEAU, D.R. Geological factors significant to the stability of slopes cut in rock. Proc. Symp. on Open Pit Mine Planning, Johannesburg, Sept. 1970.
4. GOODMAN, R.E. and DUNCAN, J.M. The role of structure and solid mechanics in the design of surface and underground excavations in rock. Structure, Solid Mechanics and Engineering Design, (Proc. Civil Eng. Materials Conf., Southampton, 1969), Part 2, 1971.
5. BARTON, N.R. A model study of the behaviour of steep excavated slopes. Ph.D. Thesis, Univ. of London (Imperial College), 1971.
6. HEUZE', F.E. and GOODMAN, R.E. A design procedure for high cuts in jointed hard rock - Three dimensional solutions. Report to the U.S. Bureau of Reclamation, Denver, Colo., Contract 14-06-D-6990 by Geotechnical Engineering, Univ. of California, Berkeley.
7. WHYTE, R.J. A study of progressive hangingwall caving of Chambishi Coppermine in Zambia using the base friction model concept. M.Sc. Thesis, Univ. of London (Imperial College), 1973, 86p.

8. GOODMAN, R.E. Geological investigations to evaluate stability. Proc. 2nd Symp. of Stability for Open Pit Mining, Vancouver, Nov. 1971, Publishers AIME, New York.

9. SOTO, C.A. A comparative study of slope modelling techniques for fractured ground. M.Sc. Thesis, Univ. of London (Imperial College), 1974.

10. HAMMETT, R.D. A study of the behaviour of discontinuous rock masses. Ph.D. Thesis, James Cook Univ. of N. Queensland, Australia, 1975.

11. ST. JOHN, C.M. Numerical and observational methods of determining the behaviour of rock slopes in open cast mines, Ph.D. Thesis, Univ. of London (Imperial College), 1972.

12. HOEK, E. and BRAY, J.W. Rock Slope Engineering. The Inst. of Mining & Metall. (Publishers) London, 1974, 309p.

13. JENNINGS, J.E. A mathematical theory for the calculation of the stability of slopes in open cast mines. Proc. Symp. on Open Pit Mine Planning, Johannesburg, 1970.

14. LONDE, P., VIGIER, G., and VORMERINGER, R. Stability of rock slopes - A three dimensional study. J. Soil Mech. & Found. Div. ASCE Vol. 95, No. SM1, 1969.

15. LONDE, P., VIGIER, G., and VORMERINGER, R. Stability of rock slopes - Graphical methods. J. Soil Mech. & Found. Div. ASCE Vol. 96, No. SM4, 1970.

16. JOHN, K.W. Graphical stability analysis of slopes in jointed rock. J. Soil Mech. & Found. Div., ASCE, Vol. 34, No. SM2, 1968.

17. WITTKE, W.W. Methods to analyse the stability of rock slopes, with and without additional loading (in German),

Felsmechanik und Ingenieurgeologie, Vol. 30. Suppl. II 1965 (English translation from Rock Mechanics Information Service, Imperial College, London).

18. GOODMAN, R.E. and TAYLOR, R.L. Methods of analysis for rock slopes and abutments: A review of recent developments. Proc. 8th Symp. Rock Mech.: Failure and Breakage of Rock, Fairhurst Ed. AIME, pp.303-320.

19. LA ROCHELLE, P. The short term stability of slopes in London clay. Ph.D. Thesis, Univ. of London (Imperial College), 1960.

20. LONG, A.E. Problems in designing stable open-pit mine slopes. Canad. Min. & Met. Bull. 1964, Vol. 57, pp.741-746.

21. ZIENKIEWICZ, O.C. The Finite Element Method in Engineering Science, McGraw-Hill Publ. Comp., London, 1971.

22. CUNDALL, P.A. The measurement and analysis of accelerations in rock slopes. Ph.D. Thesis, Univ. of London (Imperial College), 1971.

23. MAHTAB, M.A. and GOODMAN, R.E. Three-dimensional finite element analysis of jointed rock slopes. Proc. 2nd Cong. I.S.R.M., Belgrade, 1970, Paper 7-12.

24. ST. JOHN, C.M. Three dimensional analysis of jointed rock slopes. Symp. on Rock Fracture I.S.R.M. Nancy, 1971.

25. HOCKING, G., BROWN, E.T. and WATSON, J.O. Three dimensional elastic stress analysis of underground openings by the boundary integral equation method. Progress Report No. 16, Rock Mechanics Project, Imperial College, London, April 1976.

26. BRAY, J.W. A program for two-dimensional stress analysis using the boundary element method. Progress Report No. 16, Rock Mechanics Project, Imperial College, London, April 1976.

27. CUNDALL, P.A. A computer model for simulating progressive, large-scale movements in blocky rock systems. Symp. on Rock Fracture, I.S.R.M. Nancy, 1971.

28. TARASOVA, I.V. Influence of fissures on the deformability of rock foundations. Soil Mech. & Found. Eng. (translated from Russian), No. 2, 1968, pp.110-113.

29. PINTO, J.L. Stresses and strains in an anisotropic-orthotropic body. Proc. 1st Congress of the International Society for Rock Mechanics, Lisbon, 1966, V.1, pp.625-635.

30. ZIENKIEWICZ, O.C., CHEUNG, Y.K. and STAGG, K.G. Stresses in anisotropic media with particular reference to problems in rock mechanics. Journal of Strain Analysis, Vol. 1, No. 2, 1966, pp.172-182.

31. DUNCAN, J.M. and GOODMAN, R.E. Finite element analysis of slopes in jointed rock. Contract Report, U.S. Army Engineer Waterways Experiment Station, Corps of Engineers, No. S-68-3, Feb. 1968, 247p.

32. ZIENKIEWICZ, O.C., VALLIAPPAN, S. and KING, I.P. Stress analysis of rock as a "no-tension" material. Geotechnique, Vol. 18, 1968, pp.56-66.

33. ZIENKIEWICZ, O.C., BEST, B., DULLAGE, C. and STAGG, K.G. Analysis of non-linear problems in rock mechanics with particular reference to jointed rock systems. Proc. 2nd Congress of the I.S.R.M., Belgrade, 1970, Vol. 3, No. 8-14.

34. MALINA, H. The numerical determination of stresses and deformations in rock taking into account discontinuities. Rock Mechanics, Vol. 2, 1970, pp.1-16.

35. GOODMAN, R.E., TAYLOR, R.L. and BREKKE, T.L. A model for the mechanics of jointed rock. J. Soil Mech. & Found. Div. ASCE, Vol. 94, No. SM3, 1968, pp.637-659.

36. KNILL, J.L. Types of slope failures in rock. Geological Society of London, Engineering Group, Symposium on Rock Slopes, Imperial College, London, Jan. 1967.

37. HUTCHINSON, J.N. Mass movement. Encyclopedia of Geomorphology (Ed. R.E. Fairbridge), Reinhold, 1968, pp.688-695.

38. COATES, D.F. Rock Mechanics Principles. Department of Energy, Mines and Resources, Mines Branch Monograph 874, 1970.

39. PITEAU, D.R. Engineering geology contribution to the study of stability of slopes in rock with particular reference to De Beers Mine. Ph.D. Thesis, Univ. of the Witwatersrand, Johannesburg, 1970.

40. RICHARDS, L.R. The shear strength of joints in weathered rock. Ph.D. Thesis, Univ. of London (Imperial College), April, 1975.

41. GOODMAN, R.E. and BRAY, J.W. Toppling of rock slopes. Proc. Conf. on Rock Engineering for Foundations & Slopes, ASCE, Boulder, Colo., Vol. 2, 1976.

42. TERZAGHI, K. Stability of steep slopes in hard unweathered rock. Geotechnique, Vol. 12, 1962, pp.251-270.

43. BRAY, J. Seminar on toppling failure. Rock Mech. Dept. Imperial College, London, 1969.

44. JOHN, K.W. Three-dimensional stability analyses of slopes in jointed rock. Proc. Symp. on Open Pit Mine Planning, Johannesburg, 1970.

45. ASHBY, J. Sliding and toppling modes of ailure in models and jointed rock slopes. M.Sc. Thesis, Univ. of London (Imperial College), 1971, 40p.

46. MÜLLER, L. and HOFMANN, H. Selection, compilation and assessment of geological data for the slope problem. Proc. Symp. on Open Pit Mine Planning, Johannesburg, 1970.

47. DE FREITAS, M.H. and WATTERS, R.J. Some field examples of toppling failure. Geotechnique, Vol. 23, No. 4, 1973.

48. HOEK, E. and BOYD, J.M. Stability of slopes in jointed rock. Rock Mechanics Progress Report No. 6, Imperial College, London, July 1971.

49. WATTERS, R.J. Slope stability in the metamorphic rocks of the Scottish Highlands. Ph.D. Thesis, Univ. of London (Imperial College), 1972.

50. GEROGIANNOPOULOS, N. The use of surface displacement monitoring in slopes to predict failure mode and location of failure surface. M.Sc. Thesis, Univ. of London (Imperial College), 1974, 37p.

51. BAYNES, F.J. A study of the toppling failure mode with special reference to field examples from North Devon. M.Sc. Thesis, Univ. of London (Imperial College), June 1975.

CHAPTER TWO

BACK ANALYSIS OF A FAILURE TO FIND OUT THE FAILURE MECHANISM

2.1 Introduction

This chapter summarises the work done to explain the 1967 failure of the Old Delabole Slate Quarry. Most of the information and data needed for this investigation has been collected from the Field Reports of groups of Rock Mechanics M.Sc. students (Imperial College). Though none of these groups has directly been involved in the 1967 failure, many of them made back analysis of it to get some strength parameters to assess the stability of their own region neighbouring the failure area. Postulations put forward regarding the mode of failure remain unproven so far. As an attempt, the author has thought the base friction technique to be helpful in identifying the real mechanism.

2.2 Old Delabole Slate Quarry

2.2.1 - Introduction -

The Old Delabole Slate Quarry is situated 2 miles south of Tintagel, Cornwall, as an elliptical excavation 500 feet deep. "All the rock in the Quarry is highly metamorphosed, good cleavage characterising the whole"[1]. Mainly two types of slate occur, differing slightly on a lithological basis. They are of Upper Devonian age and named as blue-grey and green-grey slates. In the western face of the Quarry a third

type, "Silver grey Woolgarden", is observed as this part of the Quarry was down thrown by a major fault.

Cleavage is a well defined feature throughout the Quarry with a dip of 20° - 30°, and a dip direction of 245° - 260°. Spacing is in millimetric scale. Cleavage surfaces are fairly smooth and closed generally. Bedding planes possess the same dip angle as cleavage, therefore they are obscured almost completely. The rock does not split along bedding, so this feature can be regarded as insignificant.

The measurements taken all around the pit reveal that serval joint sets exist throughout the Quarry, most of them being steeper than 70°, in particular on the western side. There is a considerable scatter in their orientations as shown in Figure 2.1. Wedge joints (wrinkles) and the joints forming the bench faces (shorters) are the characteristic features on the east and west side of the Quarry respectively. Roughness and undulations along the strike of joint surfaces exist in general, "Especially those at right angles to the cleavage planes exhibit very wavy surfaces on all scales"[1]. There has not been a systematic and detailed investigation of the continuity and frequency of joint sets, but it is considered that most of them may be accepted as continuous planes as related to the slope height.

The area is traversed by families of parallel faults mostly and random faults occasionally. In general, they are steep and some are associated with joint sets. Richards[2] mentions about the low angle faults as having anisotropic characteristics ranging from 2° to 40°, depending on the

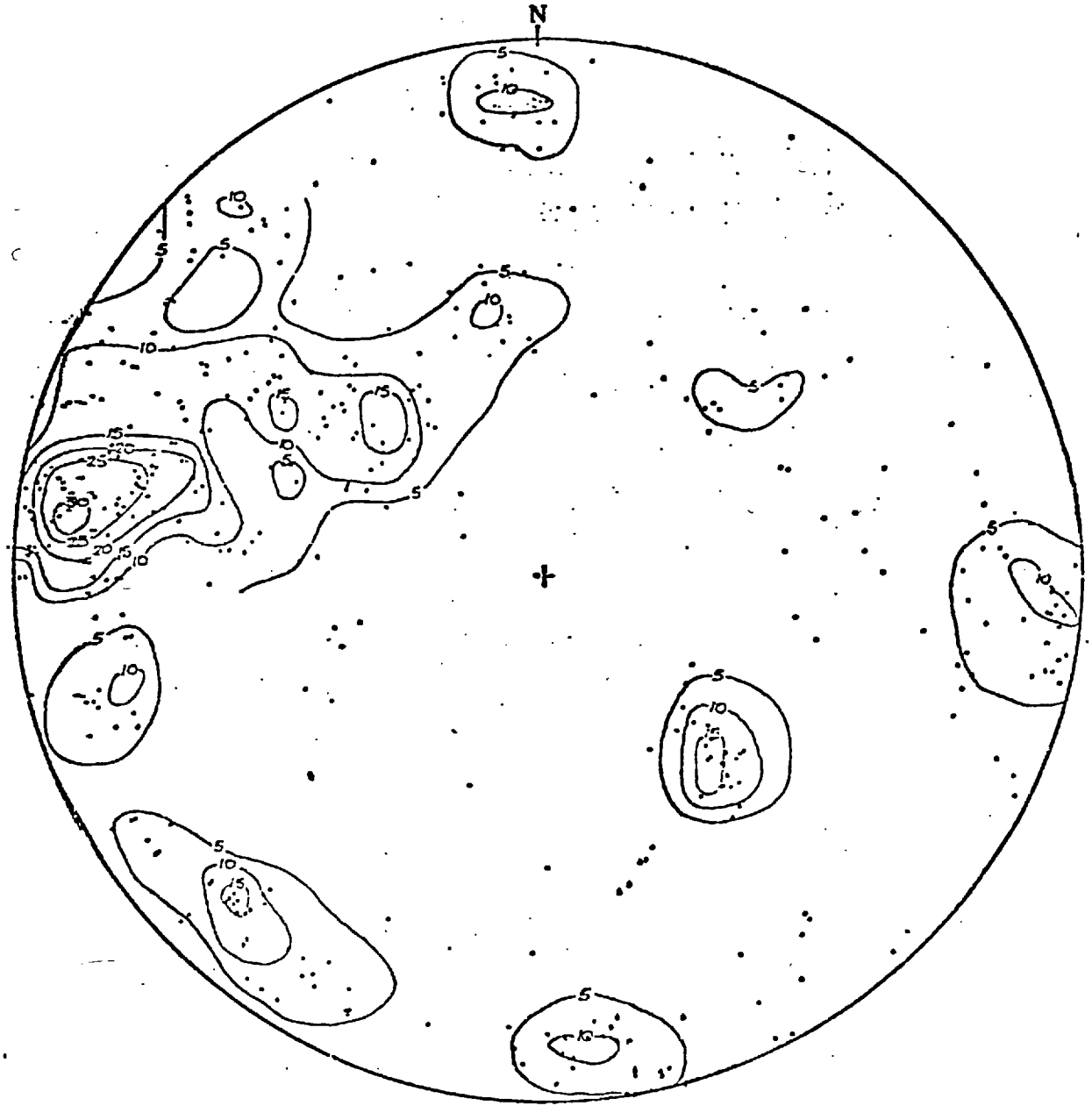

Figure 2.1- Polar stereonet of joints with pole-count contours

(Compiled by G.Hocking)

direction. Since these faults carry gouge and have thicknesses up to 1 meter, they may become critical from the stability point of view.

Though groundwater is one of the most important factors influencing the stability of rock slopes; it is the least known in Delabole Quarry. Estimation of the present phreatic surface from the face seepages is difficult because their levels vary considerably over a short horizontal distance, and there is not sufficient borehole information. Slate is defined as the most impermeable intact rock[3], so it is evident that the flow patterns are dependent on discontinuities acting as channels for water flow. This fact should be the explanation for differential face seepage. Nevertheless, an average groundwater level at elevation of about 425 feet, supported by the observations on east and west side of the pit, will not be too wrong. Daily rainfall records dating back some 50 years reveal that the total annual amount varies between 35 inches and 55 inches (Figure 2.2). It is understood that one or two days per annum are likely to receive up to 1.75 inches.

2.2.2 -Strength Properties-

The strength characteristics of Delabole Slate has been studied extensively by Richards[2]. A brief summary is given below.

A. Intact Material

(i) Available failure theories do not describe the anisotropic behaviour of this slate accurately. Therefore,

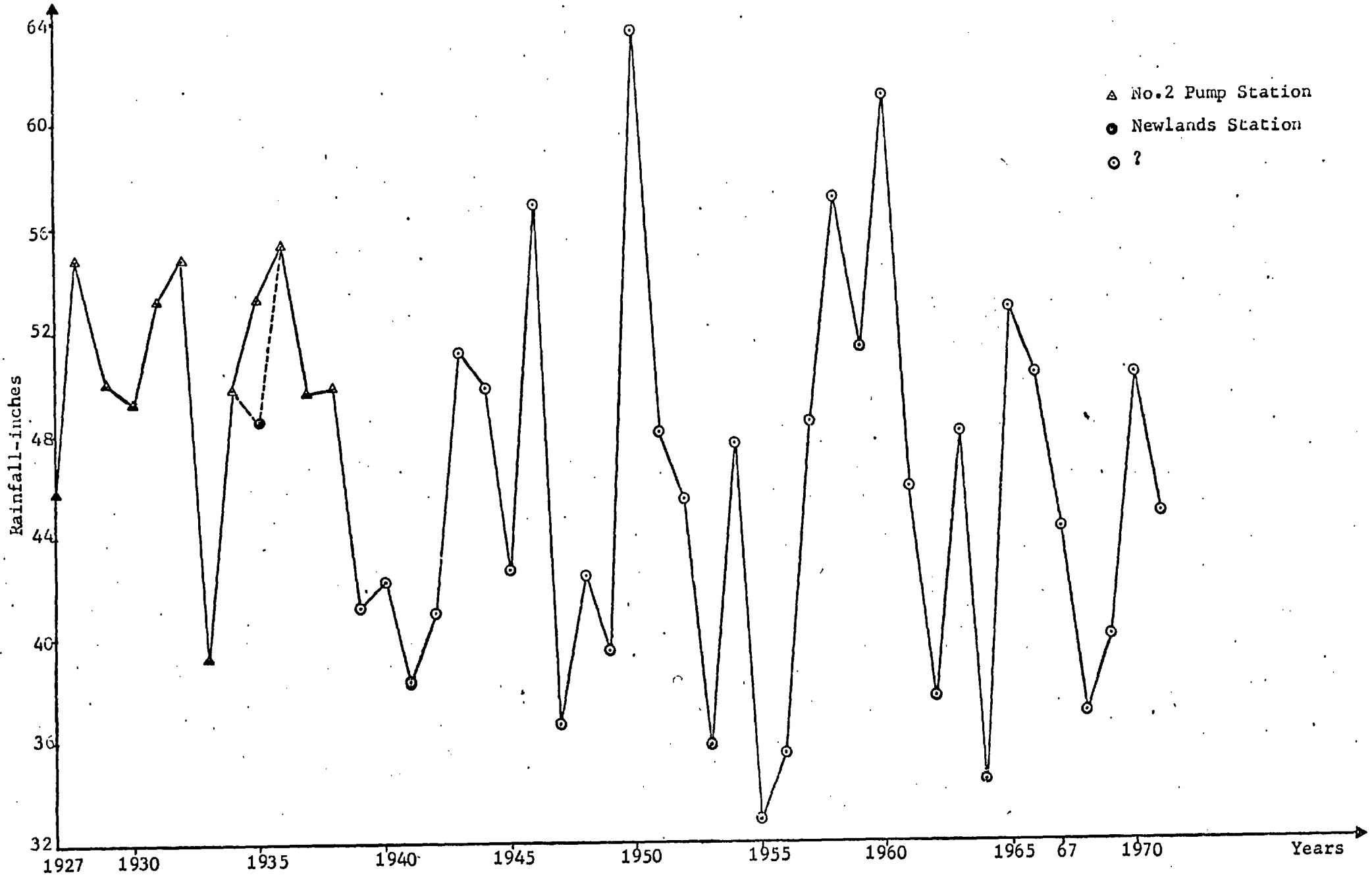

Figure 2.2- Rainfall records at Delabole Quarry.

empirical curves are fitted.

(ii) Minimum strength is observed when the angle between the maximum principal stress and the normal to the plane of anisotropy (i.e. the cleavage planes) is 45^{o}, is contrary to Jaeger's "Single Plane of Weakness Theory", which predicts this angle to be 60^{o}.

(iii) Uniaxial compressive strength ranges from 22 to 185 MN/m^2.

(iv) Shear strength parameters vary considerably for different sample orientations and for different methods of analysis.

B. Discontinuities

Direct shear tests on either polished or parted cleavage surfaces gave the following results:

(i) The average peak value of dry friction angle is about 30^{o}. Contrary to general observations, the residual friction angle is greater with a value of 33^{o}.

(ii) Water acts as a lubricant and reduces the friction angle down to 20^{o}.

(iii) Apparent cohesion intercept of 0.20 MN/m^2 is obtained when extrapolation is done.

(iv) The effect of the sliding direction relative to cleavage planes is insignificant.

(v) The effect of the sliding direction relative to surface roughness features is found to be very important. For example, an increase of 45^{o} in friction angle has been observed when the shearing direction was normal to the surface ridges of a joint (for low normal loads).

(vi) Effect of lithology is very little.

(vii) Surface staining, due to weathering, increases the friction angle irrespective of its degree.

C. Fault Gouge

(i) Dry fault gouge can have a friction angle as high as 32° indicating no deleterrous weathering effects on the material. However, another sample gives a friction angle of 17°.

(ii) Natural gouge material is relatively insensitive to water with a drop of 6.5° in friction angle when tested wet.

2.2.3 -1967 Failure-

On March 4th, 1967, a large scale fall occurred on the western wall of the Quarry. It involved a large volume of material which covered the main haulage road to the pit bottom (see Figure 2.3). The failure zone extends from the third bench at the top (level 575 ft.) down to the 350 ft. level. It seemed to be a plane failure consisting of two slide surfaces. The upper one is steeper and dips with an angle of approximately 70° - 75° down to the level 425 ft. The lower surface has an inclination of about 40° - 45° as determined with rough survey techniques. Figures 2.4 and 2.5 show the slope profiles drawn using the field measurements and the aerial photography topographic map respectively.

The following observations are of interest to note:

1. Slope crest constitutes a moving zone with large and small (open) tension cracks. The large tension crack lies at the top along Bench 1 (617.3') with two smaller ones

Figure 2.3- Photograph of 1967 failure.

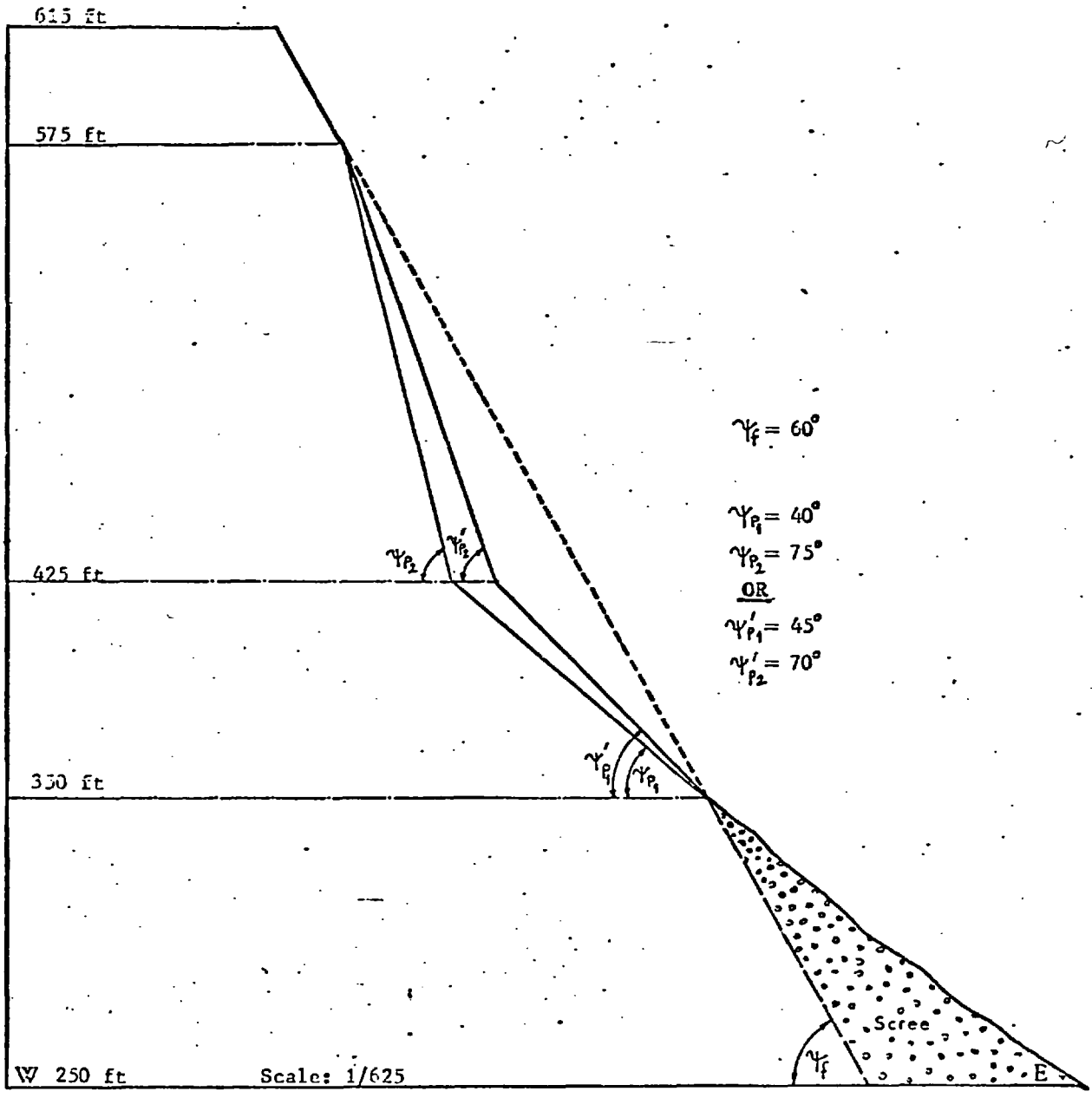

Figure 2.4- Approximate slope profiles..

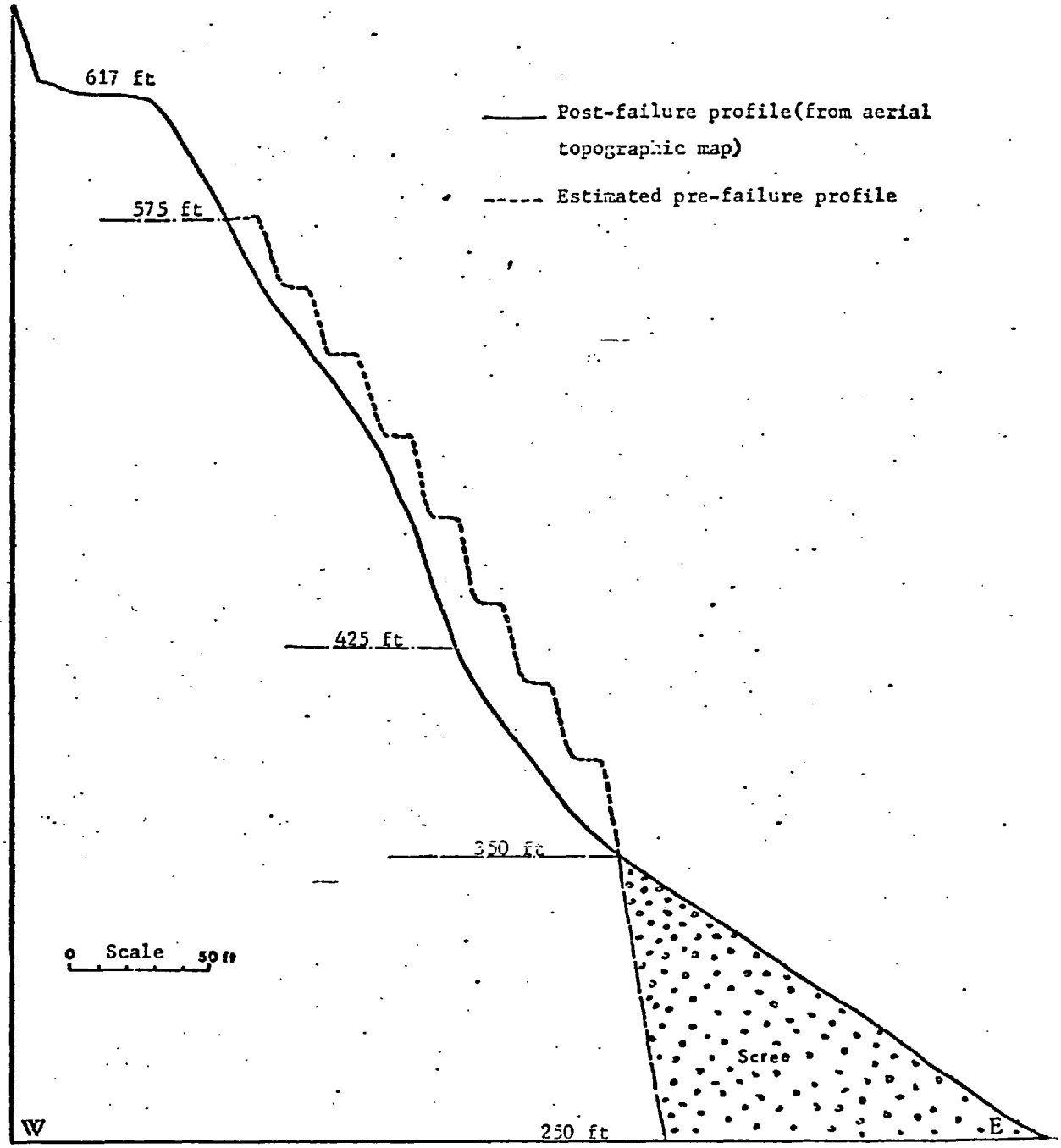

Figure 2.5- Section through 1967 Failure zone.

close to the rear wall. Bench 2, at a lower position, also accommodates a small tension crack as shown in Figure 2.6.

2. Upper failure surface is planar and well-defined. It can be considered as an inclined tension crack. There is speculation about this surface to be a fault plane.

3. Intersection between upper and lower surfaces is not well-defined. Indications are such that a fault passes along this intersection but its orientation is not known exactly. Further considerations will be given to this point later on.

4. The lower surface is pretty rough and irregular as compared to the upper one. It has a stepped appearance. Though the weathering and the seepage should have changed its original character since 1967, it is not very difficult to appreciate the difference between these two surfaces.

5. Scree of the failed material lies at the bottom of the pit. It is interesting to note that the rock is highly disintegrated. A boulder, for example, can hardly be seen. Again weathering should have played a role in this matter, but this is not supposed to be the whole answer.

2.2.3.1 - Structural geology -

Restricted access to the area limited the information needed to evaluate the structural geology and the stability. However, the investigations made at the adjoining parts of the fall revealed that the features in the Quarry west face generally fell into well defined sets, which either followed the cleavage or dipped nearly vertically. The following are of importance:

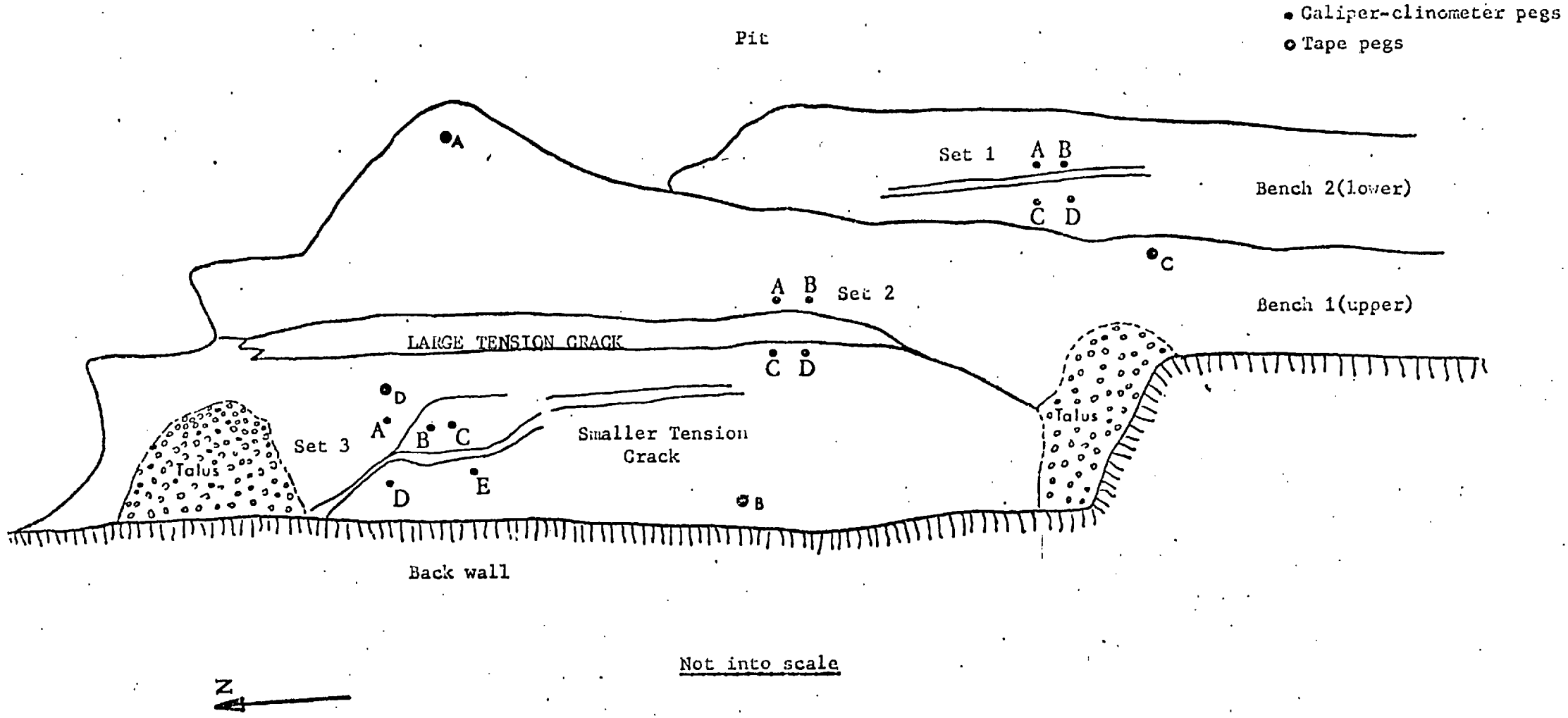

Figure 2.6- Rough plan of the slope crest('67 Failure zone) with peg locations.

1. Joints: Almost all of the joints appeared to be dipping at angles greater than 70°. The most important joint set striking nearly parallel to the slope face (i.e. dip direction of 100° - 105°) has an inclination of 70° to 90°. It has been observed that this set is highly persistent in extent and is associated with a series of parallel faults. Indeed, this is the set mentioned as "shorters" previously, and will be called "Joint Set A" from now on. The second steep joint set, in a sense, is a mirror image of the first one dipping into the slope with an angle of 85°. This set is also found to be associated with another set of faults, and will be called "Joint Set B". The third joint set of interest lies flat showing quite a variation both in inclination and orientation (30° - 65° and 90° - 130° being the dip and dip direction respectively). It is observed that this third set "Joint Set C", is scarce, isolated and not continuous.

2. Cleavage: Cleavage maintains its general trend, but a reduction in the dip angle has been observed. Towards the upper part of the north of the fall 10° of inclination was measured. This anomaly can be explained with the occurrence of Woolgarden rock which has been described as having an unreliable cleavage by Leese and Setchell[1].

3. Faults: Two groups of faults are identified - thrust faults on cleavage, or transgressing it at a low angle, and a more obvious group at right angles to these at dips from 90° to 70°, dip direction 90° to 120°. The latter is associated with shorters and has a frequency of about 6 meters at the failure area. The traces of this group can be followed at

the south wall of the pit. All the faults carry gouge material.

2.2.3.2 - Lithology -

A lithological boundary between grey slates found at the bottom of the pit and green slates at pit rim level has been traced in the area to the north of the fall at approximately 420 feet elevation dipping at an angle of approximately 45^{o} to the east and has probably been produced by faulting. A distinct difference in rock mass behaviour was observed between these two rock types although Richards[2] found slight variation on shear strength for different lithology. In the upper part of the slopes of the western wall, the green slates graduating to Woolgarden beds appear to be much looser, blocks are separated very frequently by open joints and along the cleavage. At the bottom of the slope the grey slates graduate to black phyllites which are obviously more massive. They have closed or tight joints in the main and are much more competent.

2.2.3.3 - Groundwater conditions -

Seepage mostly occurs at elevation 425 feet, but some water also issues at 475 feet. Though no correlation exists with the neighbouring faces, east side of the pit conforms to 425 feet elevation yielding a lower bound of water table (well water level records exist at the Quarry but are too far distant from the site to warrant extrapolation of data).

Reference to rainfall records show that there was no marked or unusual rainfall during January or February, the months preceding the failure, but it should be kept in mind

that the fall took place at the end of the rainy period.

2.2.3.4 - Tension crack monitoring and previous failures -

Existence of the tension cracks at the crest is reported to be 1943 predated[4] and the records show that they have been monitored since 1948. This indicates that the area is unstable over a considerable period of time and a progressive failure is underway. Measurements currently being carried out imply that a complex failure mechanism with block rotations is occurring. Analysis of relative moments suggest that the rock mass near the slope face is moving towards the pit and the wedge of rock between the tension cracks is tilting in the opposite direction with some subsidence (peg movements of set 2 of Bench 1 in Figure 2.6).

Reference to photographs in the Quarry Museum show that failures have been occurring along the western wall at least since 1890. It is understood that failures similar to 1967 fall have occurred three times indicating they were controlled to an important extent by the structure of the area. The failure mechanisms that might be involved will be dealt with in detail in the next part.

2.3 Analysis

2.3.1 - Introduction -

Failed slopes are a very valuable source of information to assess the stability of critical ones. Strength parameters, cohesion (c) and friction angle (ϕ), can easily be obtained through a process of back analysis. However,

for these parameters to be of any practical value the real failure mechanism must be defined. Since there is not strong evidence in the 1967 fall in favour of one or another failure mechanism, all the possibilities will be considered, and checked either analytically or experimentally, or in both ways against the field observations, disregarding the improbable ones. In dealing with many uncertainties related to discontinuities the Base Friction technique is thought to be helpful.

2.3.2 - Modes of Failure -

In postulating a mechanism, post-failure geometry should be accounted for. There was no doubt about the upper face. It was either a "shorter" or a fault behaving as an inclined tension crack. On the other hand, the lower face appeared to be extremely difficult to interpret. In the light of the site investigation carried out, the following failure mechanisms were considered:

(a) Shear failure through intact material.
(b) Undercutting due to weathering.
(c) Sliding in one way or another.
(d) Toppling.

(a) When the stresses in the rock mass due to its own weight were compared with the strength of the rock it was realised that any major shearing through intact material was strictly impossible. Even the lowest strength recorded by Richards[2] (20 MN/m^2) is several times the stresses computed (2 MN/m^2).

(b) It was proposed[4] that an undefined fault (may be the probable so-called "Lithology fault" mentioned earlier)

could create an environment for undercutting through weathering of the gouge. Thus, the wedge formed at the top would push the lower portion outwards and the shear strength along a sort of composite surface of shorters and cleavages would be mobilized as shown in Figure 2.7 below:

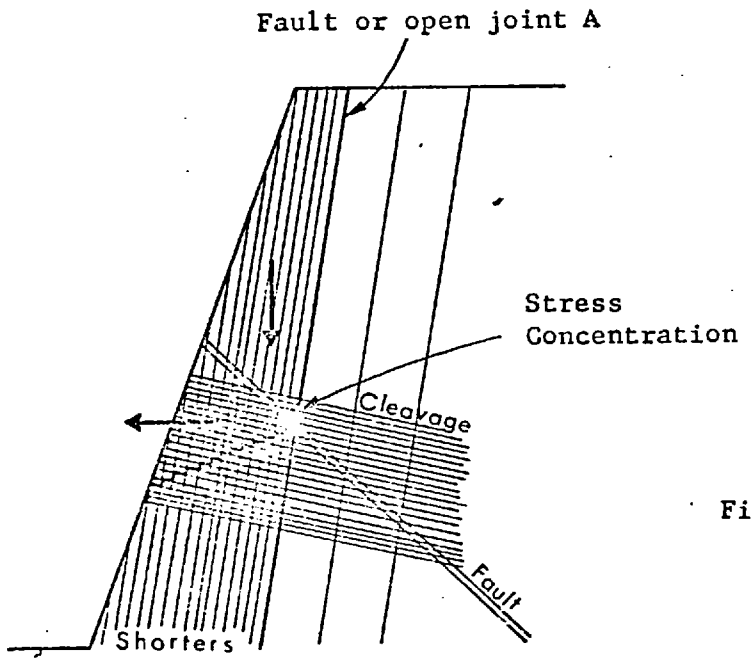

Figure 2.7- Undercutting failure mechanism.

The base friction technique has been employed to check the validity of this postulate. Tests with different fault orientations did not appear to be reproducing the real mechanism as will be discussed later on.

(c) Lack of any major throughgoing discontinuity comparable with the lower slide surface and its stepped character led the analysis to the same assumption again - formation of a composite failure surface. In fact such a stepped surface was observed at a location along the western wall in a smaller scale reinforcing the assumption. Thus, the analytical approach illustrated in Figure 2.8(a) has been attempted. The following assumptions were made:

- vertical tension crack appearing on the slope face with $c = 0$ $\phi = 0^{\circ}$
- 40° of angle stepped lower surface formed by cleavage planes, inclined into the slope with an apparent dip angle of 6° ($i = 40+6 = 46^{\circ}$) and joints (shorters) dipping towards the pit an angle of 80°
- friction angle of 20° (due to water lubrication) and apparent cohesion of 30 lbf/in^2 along lower surface; so, effective angle of friction, ϕ_e, of 66° ($\phi_e = \phi + i = 20 + 46 = 66^{\circ}$)
- slope angle of 70°

The following equations given by Hoek and Bray[3] for plane failure yielded Figure 2.8(b): Factor of safety versus depth of water in tension crack for zero and 30 lbf/in^2 cohesion values.

$$F = \frac{cA + (W.\mathrm{Cos}\psi_p - U - V.\mathrm{Sin}\psi_p)\mathrm{Tan}\phi}{W.\mathrm{Sin}\psi_p + V.\mathrm{Cos}\psi_p}$$

where,

$$A = (H-Z).\mathrm{Cosec}\psi_p$$

$$U = \tfrac{1}{2}\,\gamma_w.Z_w(H-Z).\mathrm{Cosec}\psi_p$$

$$V = \tfrac{1}{2}\,\gamma_w.Z_w^2$$

$$W = \tfrac{1}{2}\,\gamma H^2\left[(1-Z/H)^2\mathrm{Cot}\psi_p(\mathrm{Cot}\psi_p.\mathrm{Tan}\psi_f-1)\right]$$

As shown in Figure 2.8(b) the slope is stable for a half filled tension crack even for $c = 0$, and obviously stability increases with cohesion, that is, for the slope to be unstable two thirds

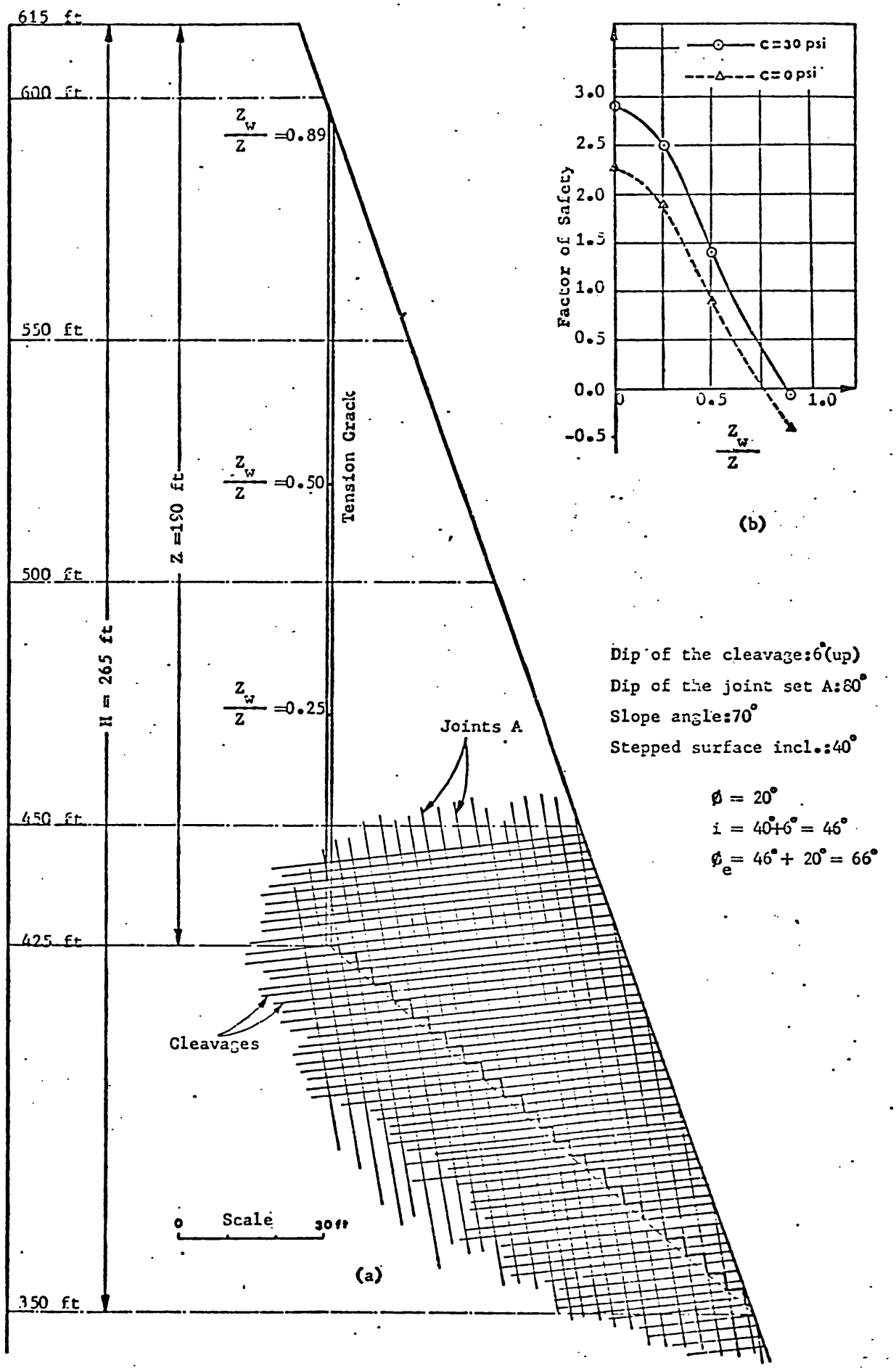

Figure 2.8- Analytical approach.

of the tension crack must be full of water when c = 30 $\ell bf/in^2$. Although, as previously mentioned, there was no record of unusual rainfall before the fall, the possibility of high water level cannot be disregarded completely because the blockage of drainage channels with impermeable materials can produce effective heads above water table.

(d) Being a steep slope in vertically jointed rock, consideration was given to a toppling mode of failure. The following evidence was found supporting the involvement of such a mechanism.

(i) The existence of a toppling joint set (associated with a series of faults as mentioned earlier), though not as frequent and consistent as shorters, well enough to produce toppling.

(ii) The stepped failure surface which is a characteristic feature of toppling[5,6,7,8].

(iii) The analysis of the measurements currently being carried out on tension cracks indicates that a complex mode of block movements is progressively underway which is most likely produced by toppling -wedging interaction as simply illustrated in Figure 2.9.

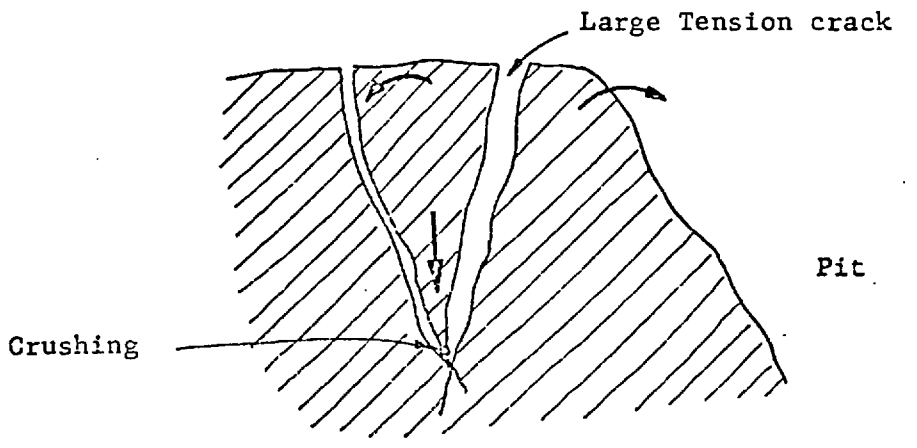

Figure 2.9- Monitored slope crest movements.

2.3.3 - Laboratory Work -

In order to verify the possible failure mechanisms put forward in Section 2.3.2 and hence to discover the real slope behaviour, a series of tests have been performed on base friction frame. While doing this, the effect of geometrical variations of parameters on rock mass behaviour has also been investigated. At the end, an attempt was made to simulate the groundwater conditions on a rather simple model.

The features and their geometrical characteristics are listed below. The features are also illustrated in Figure 2.10. Undefined parameters such as Joint A spacing or slope angle, and small scale parameters like cleavage spacing were varied to examine their effect upon the slope behaviour.

Feature	Dip Angle	Spacing (mm)
Joint A	70^{o}	10, 25, 33, 40, 50, 66
Joint B	$\overline{85}^{o}$*	20, 25, 50
Joint C	50^{o}	40
Cleavage (apparent)	$\overline{5}^{o}$, $\overline{10}^{o}$, $\overline{15}^{o}$	10, 20, 40
Fault	0^{o}, $\overline{30}^{o}$, $\overline{45}^{o}$, $\overline{60}^{o}$, 90^{o}, 45^{o}, 70^{o}	5, 10 (thickness)

Slope Angle: 50^{o}, 60^{o}, 65^{o}, 70^{o}, 75^{o}

Scale: 1/200

*The bar (-) indicates the feature dipping into the slope.

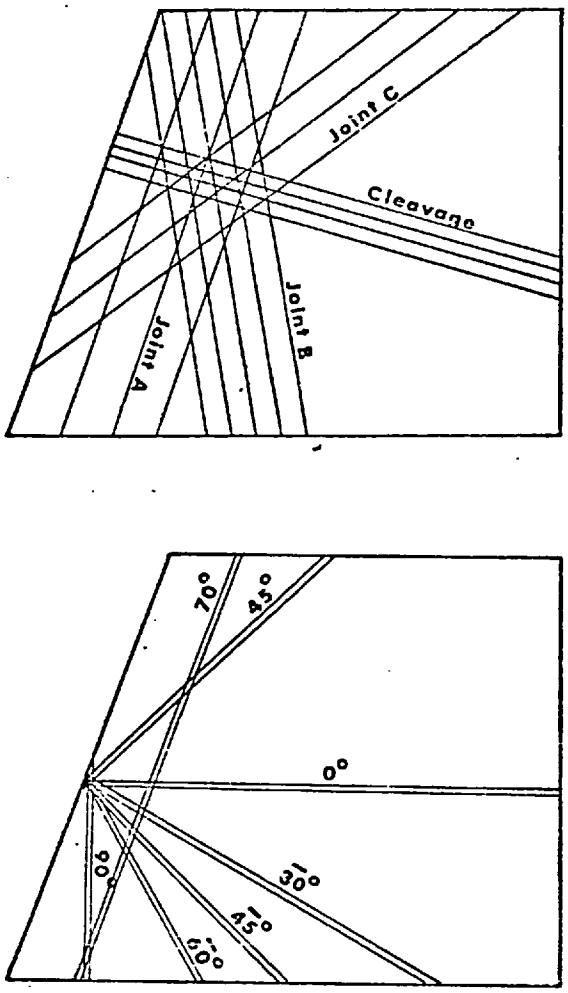

Figure 2.10- Features modelled:(a)joints and cleavage,(b)faults.

2.3.3.1 - Base friction technique (Theory, Apparatus, Material)

The base friction technique has been described elsewhere[9,10] and has been used by many investigators[10,11,12]. It simply works on the principle of simulation of gravitational loading by frictional forces. Being a two dimensional and horizontally constructed modelling technique it is very easy, quick and economic to operate, and a variety of model materials from deformable mixture to rigid blocks to simulate different behaviours can be used. On the other hand, its qualitative

nature coming from the difficulty of fulfilling the laws of similitude limits its exploitation. However, as a step towards its quantitative usage, in a recent work Bray[13] has analytically demonstrated that in general, velocities in the base friction model correspond to acceleration in the real situation. A suggestion from the same author seems very promising. He recommends developing a computer program to simulate the base friction technique, so that one can vary any parameter including joint characteristics.

Tests have been conducted on the large frame designed by Whyte[10]. An attempt has been made to produce a low friction angle material, at least as low as 30^{o} to be equivalent to the dry friction angle of slate. In this respect mica and ballotini were tried, but satisfactory results could not be obtained. Mica flakes laid down and decreased the friction between the material and sandpaper rather than the cut joints. Ballotini helped to bring down the friction angle to 37^{o} when used in large proportions (36 - 37% by weight), but in this case the material became very brittle. Eventually the following mixture was found to be optimum;

Material	% by Weight
Flour	51
Sand	12
Vegetable Oil	13
Ballotini	24

This mixture gave a friction angle of $\phi = 40 - 41^{o}$, and compacted density of 1.33 gr/cm^{3}.

2.3.3.2 - Method adopted -

After compaction and consolidation of the slab, the following sequential procedure was adopted to lessen the likelihood of "healing" the discontinuities.

(i) The slope geometry and the discontinuities are marked to scale faintly.

(ii) The slope geometry is cut.

(iii) Each set of discontinuities is cut in sequence, either starting from top or from bottom. Continuous sets are to be cut before cross joints, if any.

(iv) The excess material around the slope boundary removed.

Note: To simulate the field conditions a bit better significance may be given to the order of cutting the joints, that is, the tight discontinuity set should be cut first and the rather open set last.

Photographs were taken to keep a record of movements and a timing procedure was implemented when the behaviour of two slopes was to be compared closely. When a model turned out to be stable, the configuration of the slope was changed by sharpening the slope angle and/or inserting an additional discontinuity set to make full use of the model.

The validity of the failure mechanisms postulated in Section 2.3.2 is checked against the post-failure slope geometry and behaviour in the field, namely:

(i) Post-failure slope profile.

(ii) Formation of tension cracks at the crest.

(iii) Block movements at the top corresponding to tension

crack monitoring information.

A. Simple Sliding as the Mode of Failure (Plate 2.I)

The following assumptions are made:

(i) Slope is dry.

(ii) There exists three continuous discontinuities:

Joint A: dips into the pit with an angle of 70° to match the upper failure face

Joint C: dips into the pit with an angle of 40° to match the lower surface

Cleavage: dips into the slope with an apparent angle of 15°

(iii) $\phi = 30^{\circ}$, $c = 0$ for both joint sets.

(iv) Slope angle is 60°.

To overcome the limitation imposed by the model material having a friction angle of approximately 40°, reference was made to the Factor of Safety equation for plane failure, dry slope case given by Hoek and Bray[3] (page 141).

where

$F = \cot\psi_p . \tan\phi$ $(c = 0)$

ψ_p = dip of the failure plane

ϕ = angle of friction on failure plane

For an increase of 10° in friction angle when accompanied by the same amount of increase in the dip of the failure plane, the Factor of Safety did not change considerably. Therefore, joint set C is modelled having a 50° dip angle.

A fairly simple sliding took place along joint C as shown in photograph (b), but contrary to the general tendency, it occurred along an undaylighted discontinuity passing close to the toe. Crushing of the sharp-pointed tip of the large wedge produced by the slope face and joints A and C occurred and being very near to slope face facilitated this movement. Thus, quite a large volume of rock mass was involved in the slide. Joints A at the top acted as inclined tension cracks at the beginning of the slide. Since the joint sets intersected at an acute angle, jacking of columns and blocks by the driving of wedges was observed throughout the test, along the main sliding surface in particular (photograph b). Columns at the top parted along cleavages while passing the intersection point (shown by arrow) as shown in photographs c and d. Removal of the failed material produced sliding of the remaining triangular body at the top and the joint C along which the slide took place became the new slope face (photographs e and f).

It is obvious that none of the field post-failure observations have been reproduced. Even the slope profile could not be attained. Nevertheless, in another test with continuity arrangements, the post-failure profile was obtained but nothing more than this. Another model lacking the cleavage planes failed in a similar manner to the one pictured in Plate I, indicating that the cleavage is not an active agent in the mechanism, its function being limited to producing smaller blocks.

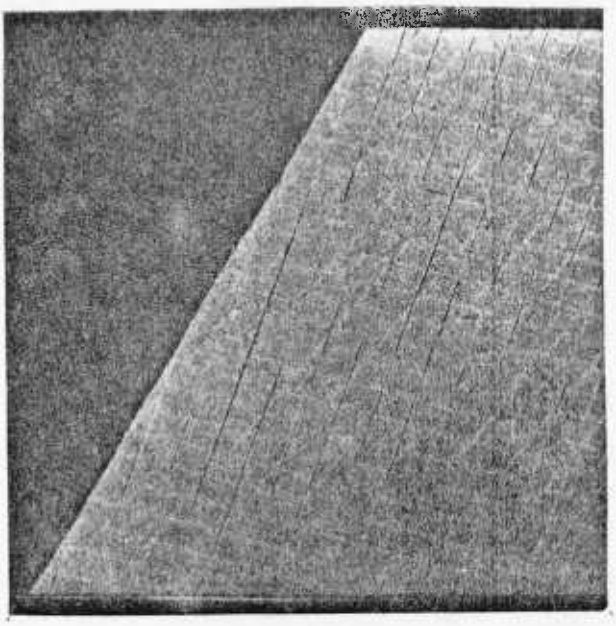

a

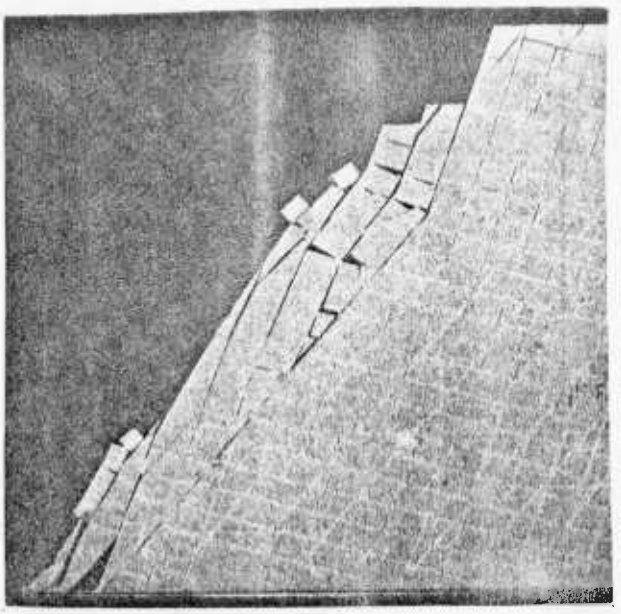

d

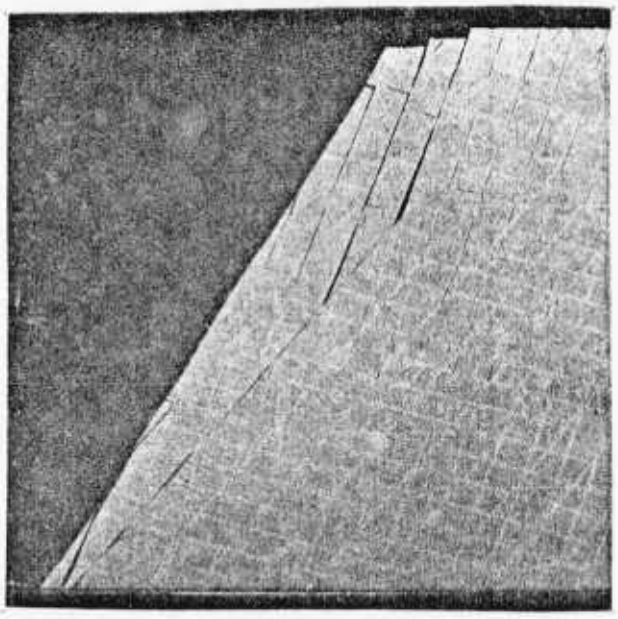

b

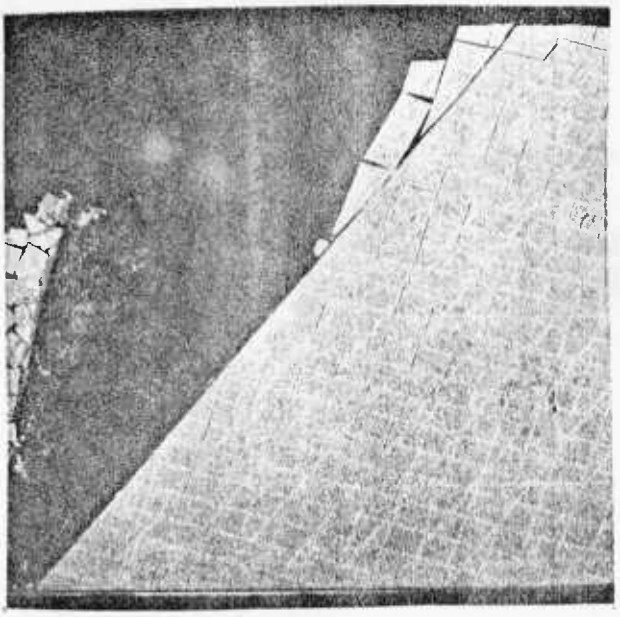

e

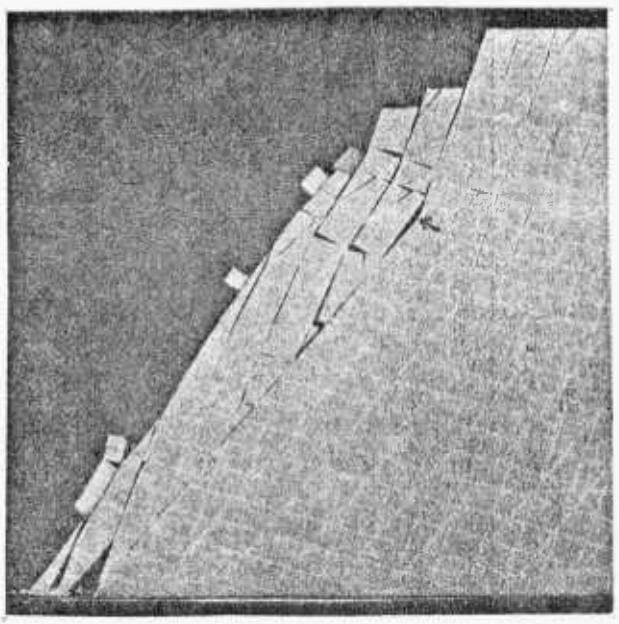

c

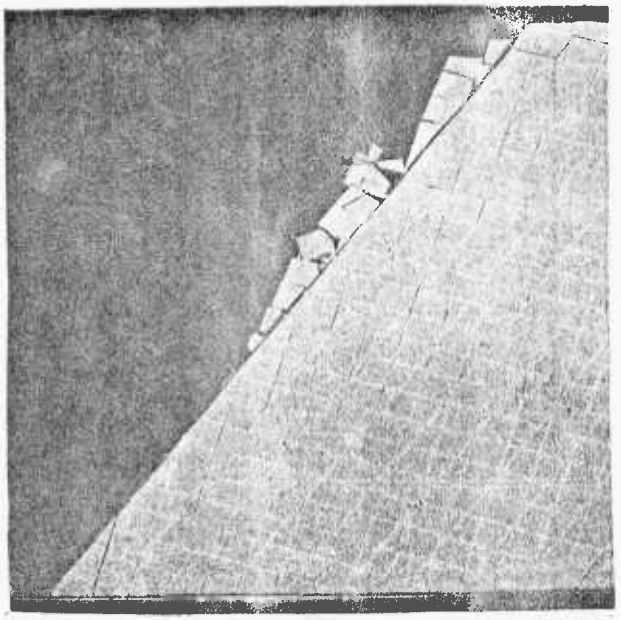

f

PLATE 2.I- Simple sliding as the mode of failure.

B. Undercutting, Through the Weathering of Fault Gouge, As the Mode of Failure (Plate 2.II)

In this test, joint set C is removed from the system while a fault is introduced. The fault is inclined at 45° to the horizontal dipping into the slope and is represented by two parallel cuts being 10 mm apart throughout the rock mass. To represent the fault gouge the compacted strip of material between the cuts is replaced with a loose one. Neither joint set A nor cleavage planes, having dip angles of 70° and $\bar{5}^{o}$ respectively, cut across the fault but are continuous on both sides. Above the fault, joint set A (or another fault set) has a spacing of 5 cm, cleavage has 2 cm. Below the fault both features are 1 cm apart spaced to facilitate the formation of a composite failure surface. The slope angle is 70° (photograph a).

Fault gouge was excavated in stages. No movement was observed when a distance equivalent to the above fault spacing of joint A was removed (photograph b). Then, full spacing was excavated (photograph c) which ended up with sliding of a full column of joint A to fill the gap. Pressure exerted by this column was not high enough to produce a "pop-out" underneath, combining closely spaced joint and cleavage planes (photograph d). Even the joints C placed an echelon along a 40° plane (photograph e) did not help very much because all of the rock bridges could not be fractured to mobilise sliding, but separation along joint A took place as a result of compression (photograph f). No better picture has been obtained for the case where two joint A columns were undermined.

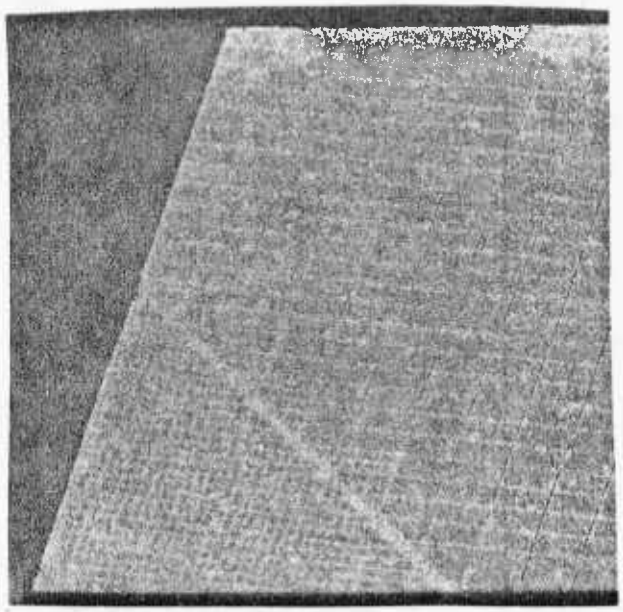

a

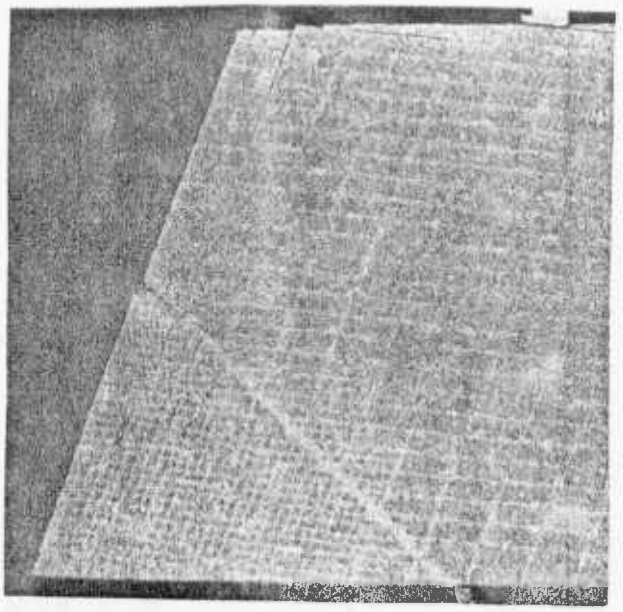

d

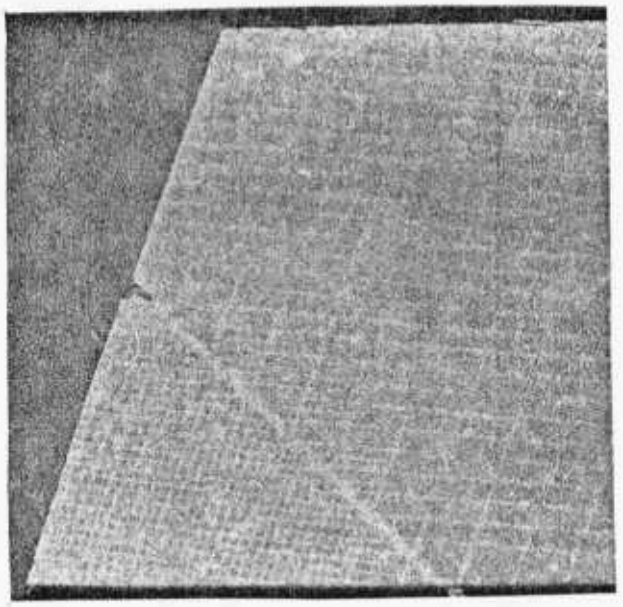

b

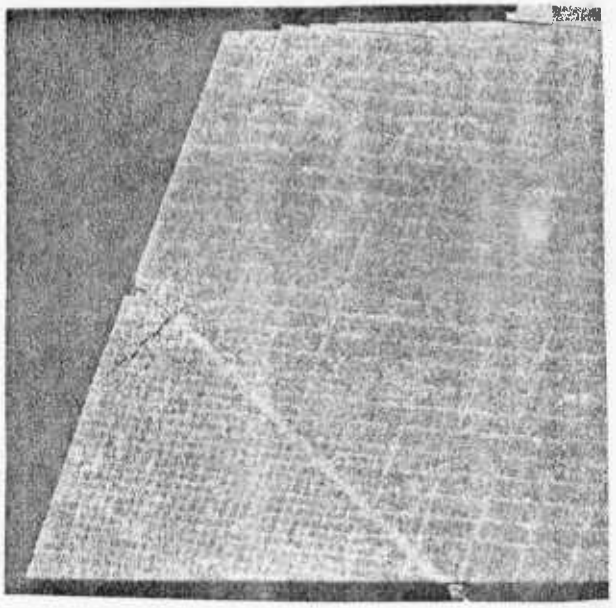

e

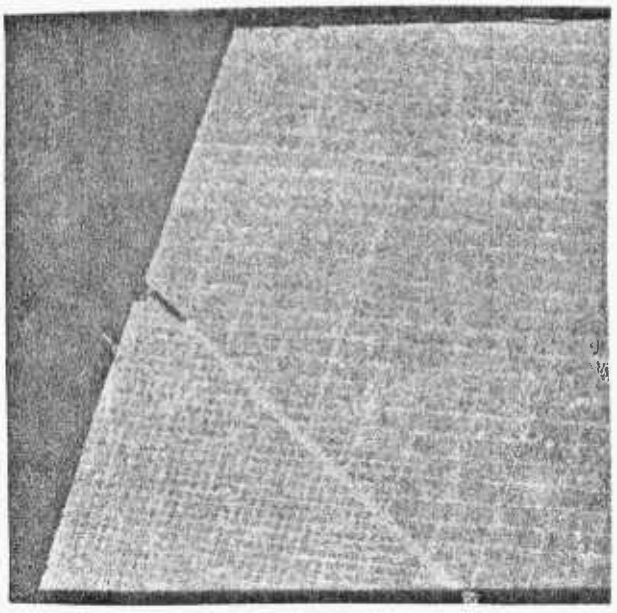

c

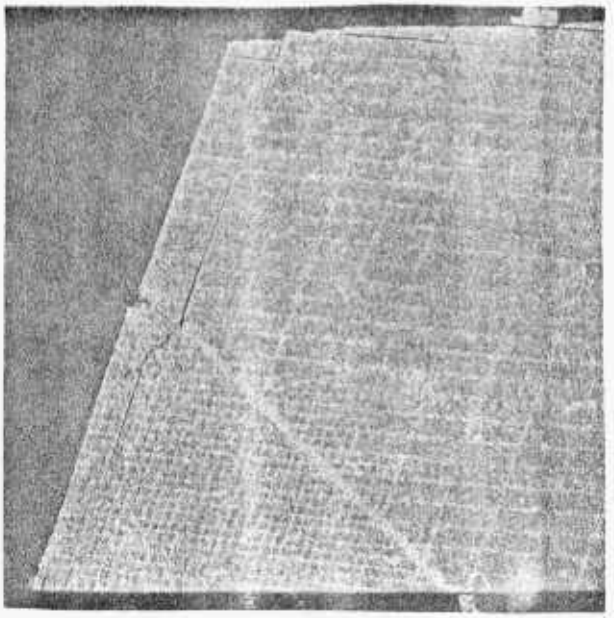

f

PLATE 2.II- Undercutting(through the weathering of fault gouge) as the mode of failure.

As a result it became clear that none of the post-failure conditions, even the slope profile, was obtainable with this failure mechanism.

C. Toppling as the Mode of Failure (Plate 2.III)

Again a dry slope is considered. Joint set C is not present in the system while set B is included with an inclination of 85° dipping into the slope. Joint A and cleavage are still predominant features having 70° and $\bar{5}^{\circ}$ dip angles respectively. Slope angle is 60° (see photograph a).

Plate 2.III shows a typical model of the several similar ones where toppling occurred, together with sliding. A close examination of the upper half of the slope (photograph b) indicates that both rotation and sliding of joint B columns are taking place. Sliding dominates mainly at the top through wedging of diamond shaped blocks, especially along the joint A, shown by an arrow which becomes the boundary of disturbance. On the other hand, toppling is predominant in the lower part and the rock mass starts to dilate here. As a result of these movements two tension cracks are produced at the crest along joints B. An important feature to be noted is that the wedging of the sliding block at the top marked "X" coincides with the tension crack monitoring data from the field and the assumptions made earlier. Dilation of the rock mass associated with toppling of joint B columns continues, but, due to the overturning resistance of the toe of the slope, it is very slow (photograph c). To facilitate further rotation, cleavage

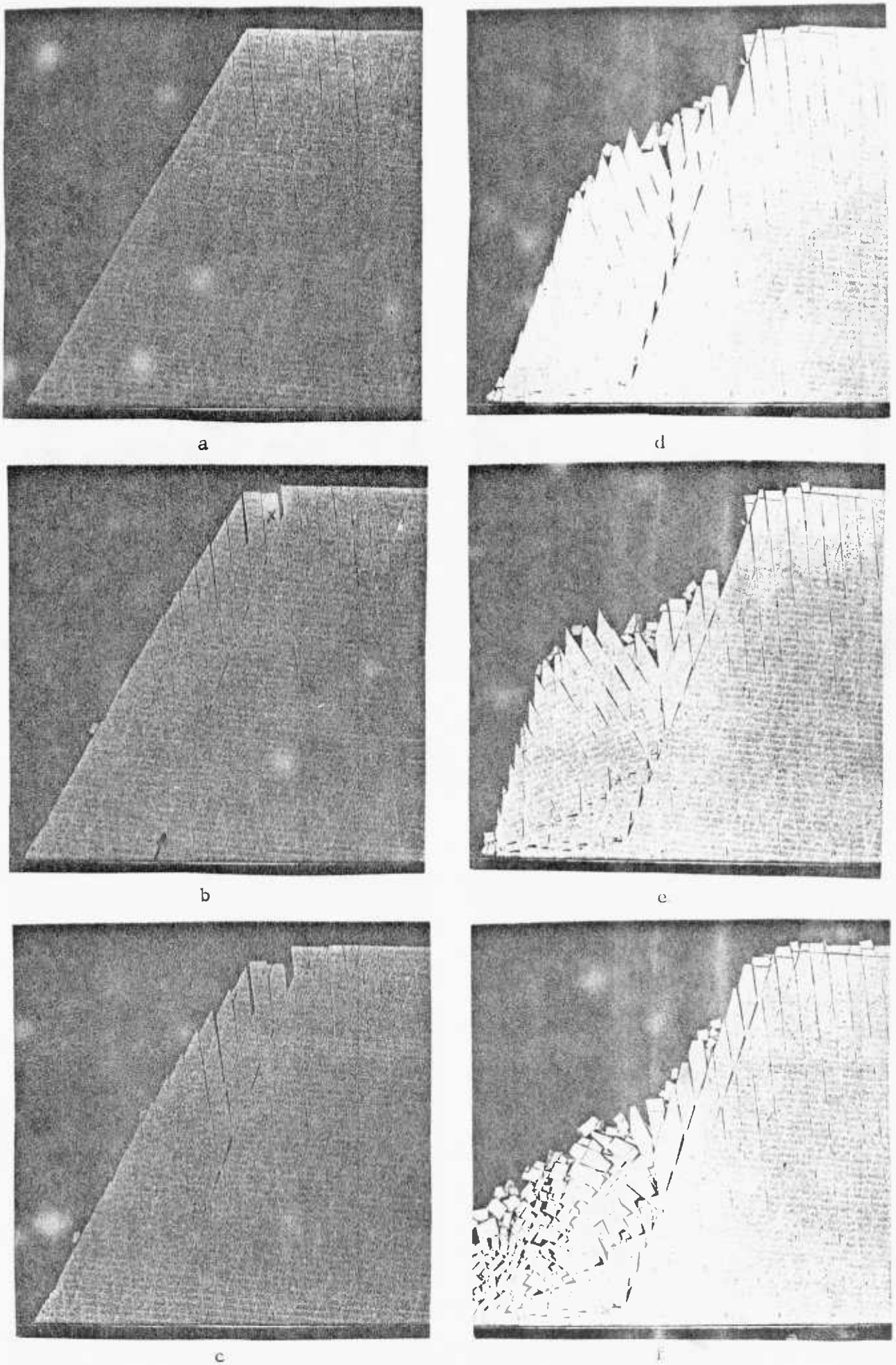

PLATE 2.III- Toppling as the mode of failure.

planes at the toe open up first (photograph d), then a stepped pattern involving cleavages and joints B develops (photograph e). From now on the toppling accelerates and ends up with complete collapse of the slope face (photograph f). The repeating nature of the mechanism can be seen in photographs d, e and f where the movements (rotation and sliding) at the top of the next column (of joint A) are readily observable.

As a result of this test it became clear that almost all the post-failure conditions were reproduceable with a toppling mechanism. Tension cracks, and block movements at the crest were produced. The slope profile with a stepped lower surface was also produced. But the volume of rock mass involved in the failure was larger and the toppling extended down to the toe giving rise to a longer stepped surface. This discrepancy might be attributed to the imposition of the steel frame at the bottom as a discontinuity. However the test conducted removing this effect revealed that the steel frame had no influence at all and the stepped pattern started nearly from the toe again as shown in Plate 2.IV. Even the further division of 5 cm thick joint A columns into 1 cm ones to facilitate the formation of a stepped surface in an upper position did not help because of wedge action. On the other hand, the stepped surface was formed in proper position in the following cases:

a. Repetition of failure after the first one (Plate 2.V)

The broken material from the first column failure provided lateral support preventing the toppling mechanism from extending to the toe of the second column. Actually,

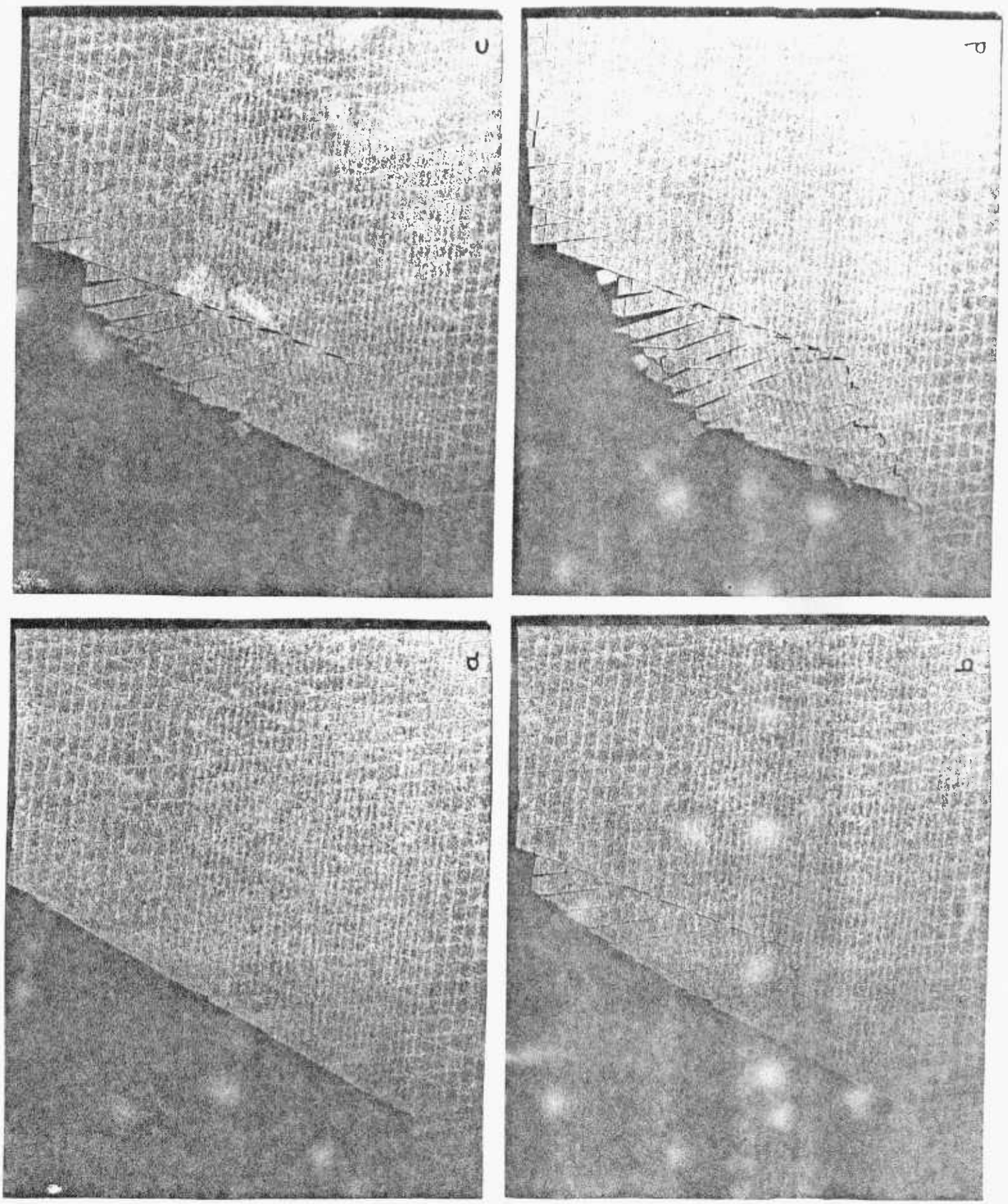

PLATE 2.IV- Toppling model without the influence of steel frame at the bottom of the slope.

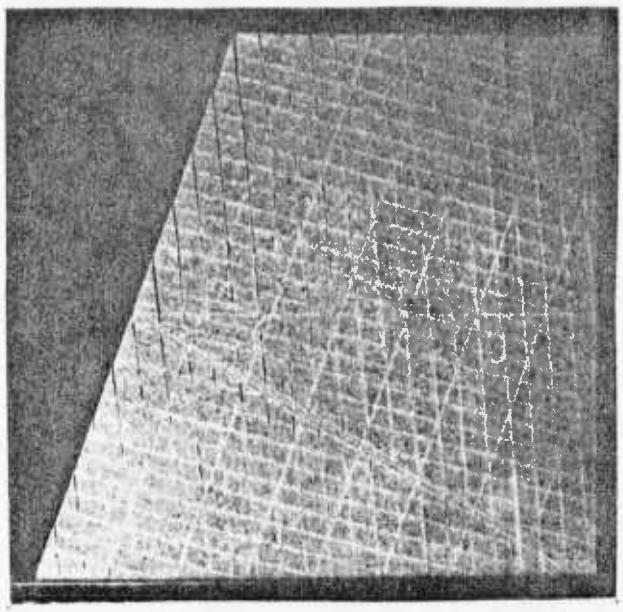

a

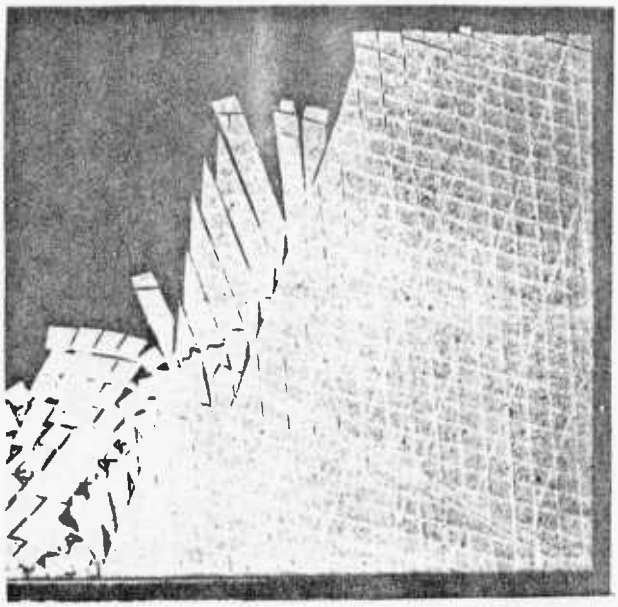

d

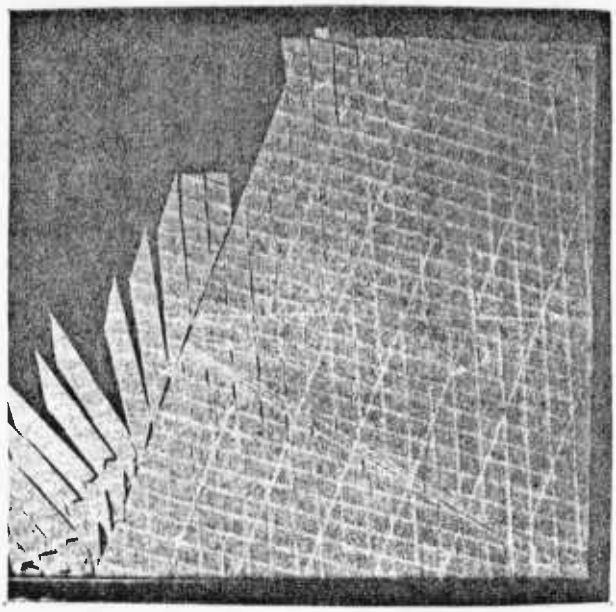

b

e

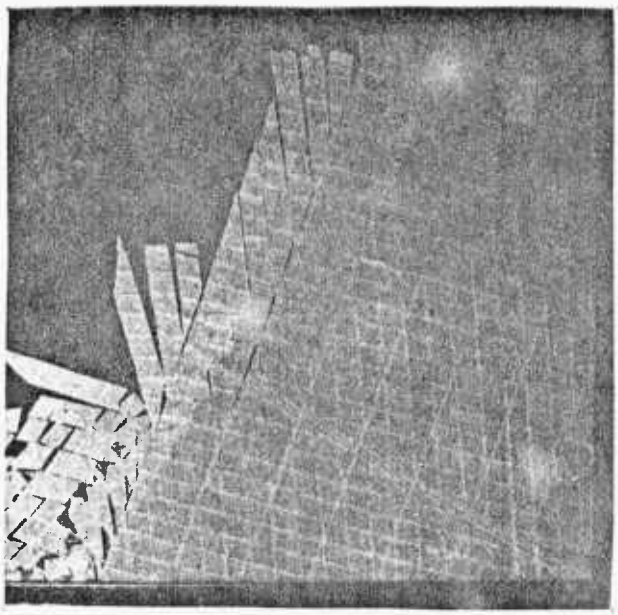

c

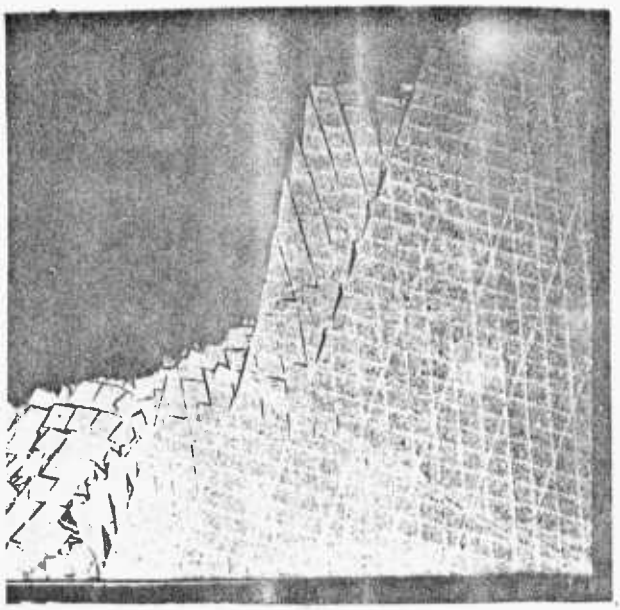

f

PLATE 2.V- Formation of the stepped failure surface in the proper position due to repetition of failure.

the slope geometry altered and the top of the failed material acted as a new pit bottom. In this respect it is true to say that stepped pattern again started from the toe. Nevertheless it became clear that there had been a resistance to further extension of toppling in the field. The source of this resistance should be the more competent and sound nature of the grey slates forming the lower part of the pit.

b. Termination of toppling set joint B at the middle of the slope due to presence of a discontinuity (Plate 2.VI)

The earlier mentioned probable, so called, "Lithology" fault could be a boundary for joint B set and might stop the failure spreading to the bottom. The test shown in Plate 2.VI has confirmed this idea. A stepped surface formed well above the toe involving closely spaced cleavage planes and shorters (joint A) as shown by an arrow in photograph d.

2.3.4 - Influence of Certain Geometrical Parameters on the Stability of the Slope -

Several tests have been conducted to investigate the influence of the following parameters on the behaviour of the slope.

(i) Cleavage spacing
(ii) Cleavage inclination
(iii) Joint set A spacing
(iv) Joint set B spacing
(v) Fault inclination
(vi) Slope angle

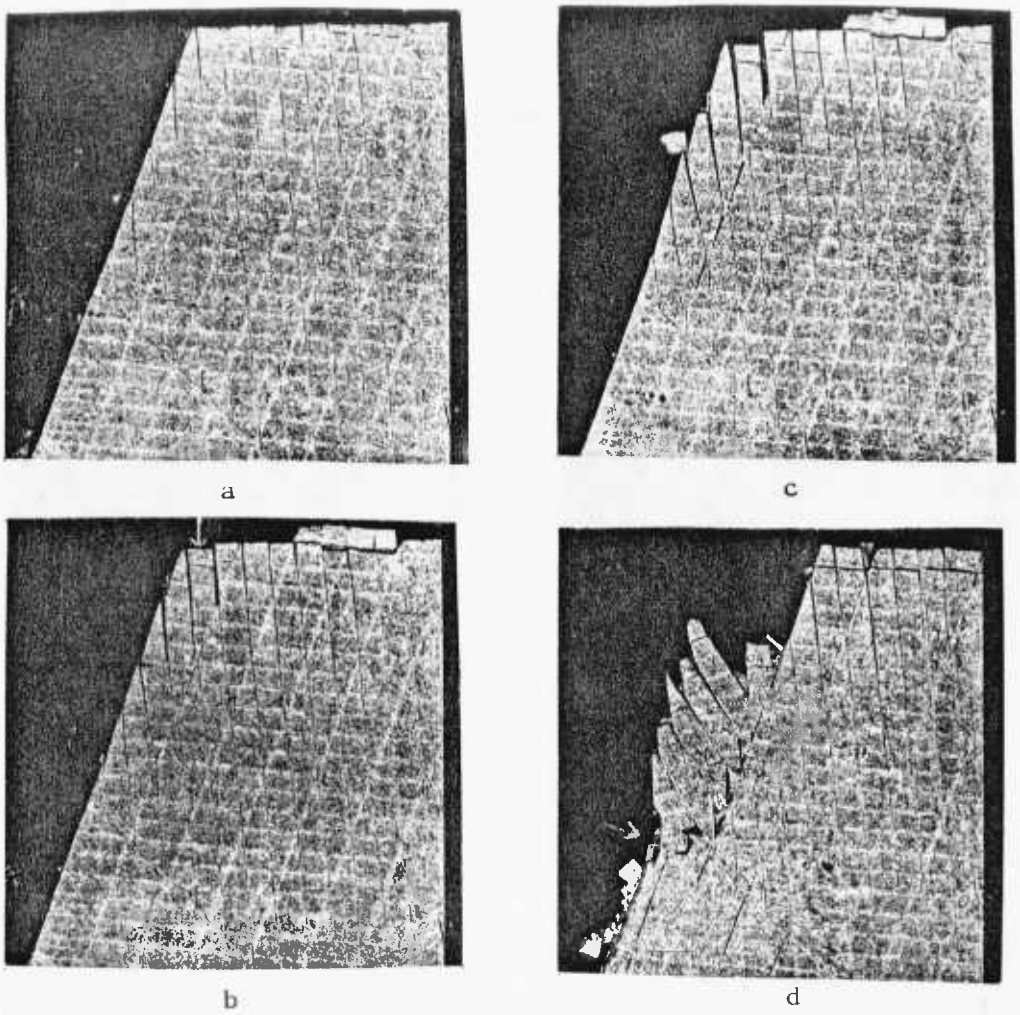

Plate 2.VI- Formation of the stepped failure surface in the proper position due to termination of toppling set in the middle of the slope.

The number of joint A columns failed at the slope surface is taken as the criterion of comparison for most of the cases. Two sets of analysis has been made:

(a) Single variations: only one parameter changed each time.

(b) Double variations: two parameters change at a time but one of them has been proven to be uninfluential from the "single variation" analysis. So, the number of variables is reduced to one practically.

Owing to limited time, each parameter was varied two times usually for a set of constants. However, the same parameter is checked within the same test and also for another

set of constants.

The necessary information is given adjacent to the graphs which are self-explanatory. Nevertheless in summary the results are: (Figures 2.11, 2.12, 2.13, and 2.14).

(i) Cleavage spacing and inclination do not affect the volume of rock involved in the failure.

(ii) As the slope angle or fault inclination increases, so does the number of failing joint A columns.

(iii) An increase in joint A spacing or in joint B spacing decreases the number of failing joint A columns, the latter only slightly.

(iv) Stepped surface angle increases with increasing cleavage inclination and/or slope angle.

2.3.5 - Groundwater Simulation -

An attempt has been made to simulate the groundwater conditions, on a single column model for simplicity. Artificial cork was employed to manipulate the friction angle, ϕ, and assess the effect of material density, if any. The cork was in the form of a $\frac{1}{2}$ inch thick sheet having a density of 0.3 gr/cm^3 less than the quarter of that of the deformable mixture (1.33 gr/cm^3). The friction angle between cut surfaces was found to be 42° - 44°, nearly the same as for the deformable material. Dry lubricant P.T.F.E. brought down the ϕ to 29° - 30°, equal to the dry friction angle of slate when sprayed on one of the contact surfaces only, and to 18° - 20° equal to the wet friction angle of slate, when sprayed on both of the contact surfaces.

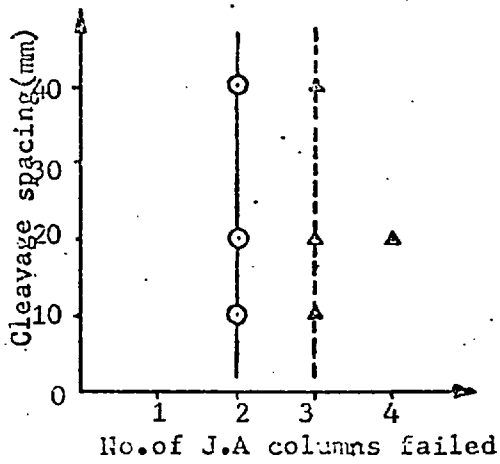

J.A: 70°(40mm)
J.B: 85°(25mm)
Clea.10°(40mm)
(20mm)
(10mm)

$\psi_f = 65°$

J.A: 70°(33mm)
J.B: 85°(25mm)
Clea. 5°(40mm)
(20mm)
(10mm)

$\psi_f = 70°$

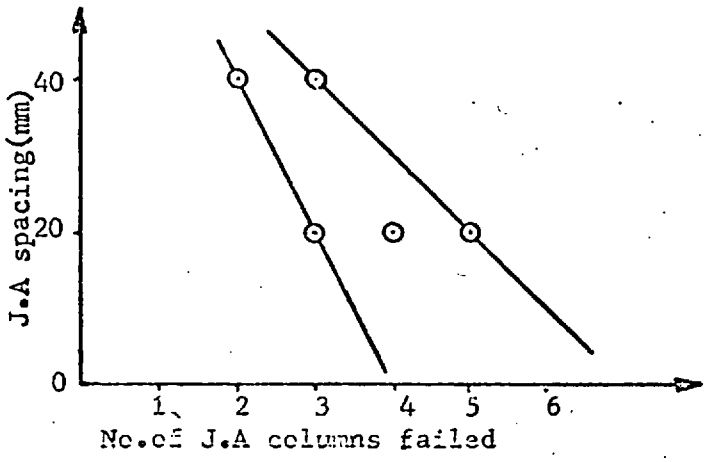

J.A: 70°(40mm)
(20mm)
J.B: 85°(25mm)
Clea.10°(40mm)

$\psi_f = 70°$

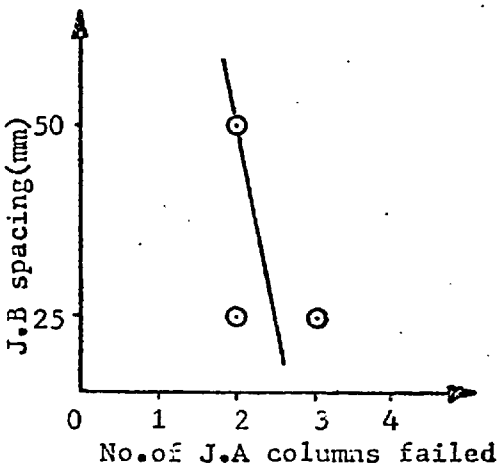

J.A: 70°(40mm)
J.B: 85°(50mm)
(25mm)
Clea.10°(10mm)

$\psi_f = 70°$

KEY TO THE ABBREVIATIONS

J.A ——→ Joint set A
J.B ——→ Joint set B
Clea.——→ Cleavage
ψ_f ——→ Slope angle

Note: The angle following the feature is the dip angle of it. The figure in paranthesis indicates the spacing(in the model).

Figure 2.11- Single Variation of Parameters.

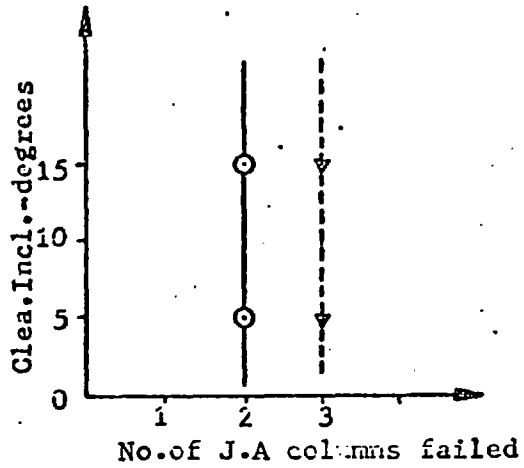

J.A: 70°(33mm)
J.B: 85°(25mm)
Clea.15°(10mm)
5°(10mm)
ψ_f =60°

J.A: 70°(33mm)
J.B: 85°(25mm)
Clea.15°(10mm)
5°(10mm)
ψ_f =70°

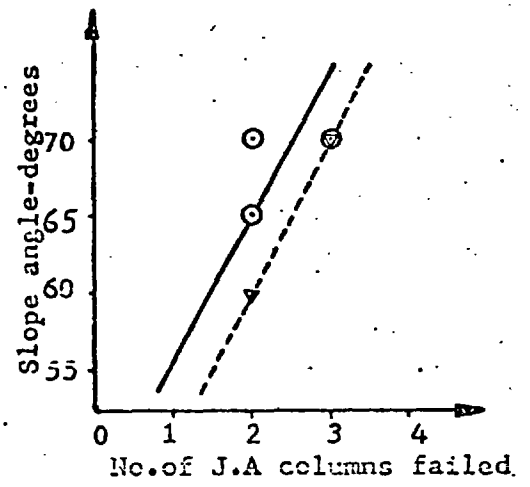

J.A: 70°(40mm)
J.B: 85°(25mm)
Clea.10°(10mm)
ψ_f =65°
70°

J.A: 70°(33mm)
J.B: 85°(25mm)
Clea. 5°(10mm)
ψ_f=60°
70°

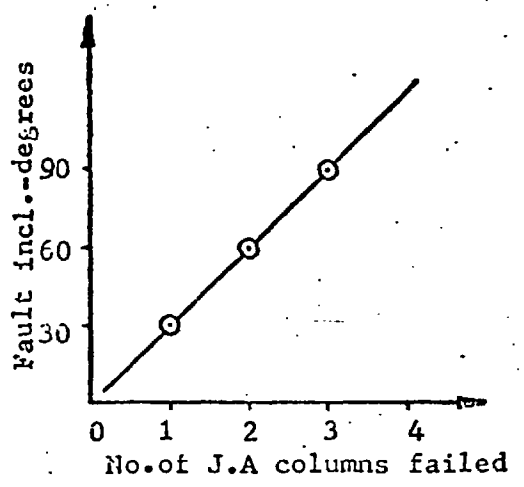

J.A: 70°(66mm)
J.B: 85°(25mm)
Clea.15°(20mm)
Fault: 30°(10mm thick)
60°(10mm thick)
90°(5mm thick)
ψ_f=70°

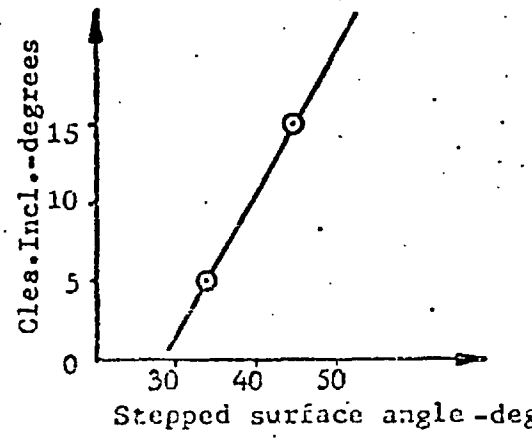

J.A: 70°(33mm)
J.B: 85°(25mm)
Clea.15°(10mm)
5°(10mm)
ψ_f=60°

Note: No.of J.A columns failed is same for both cases and is equal to 2.

Figure 2.12- Other single variations.

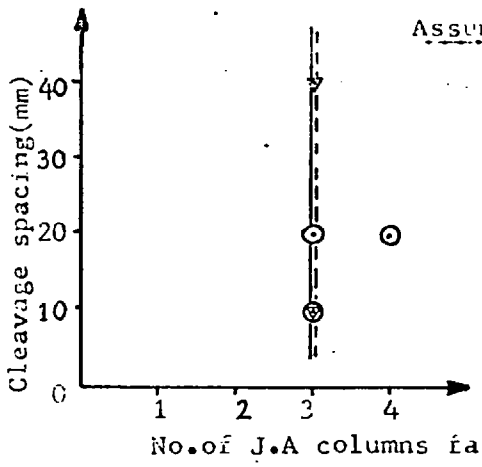

Assumption: Cleavage inclination is constant

J.A: 70° (33mm)	J.A: 70° (33mm)
J.B: 85° (25mm)	J.B: 85° (25mm)
Clea. 5° (20mm) 15° (10mm)	Clea. 15° (10mm) 5° (40mm)
ψ_f=70°	ψ_f=70°

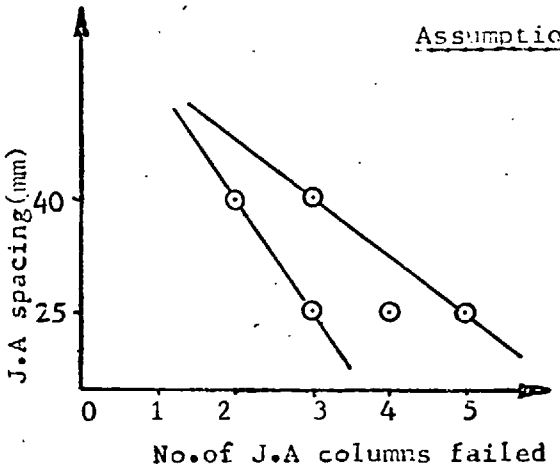

Assumption: Cleavage spacing is constant.

J.A: 70° (40mm) (25mm)
J.B: 85° (25mm)
Clea. 10° (20mm) (10mm)
ψ_f=70°

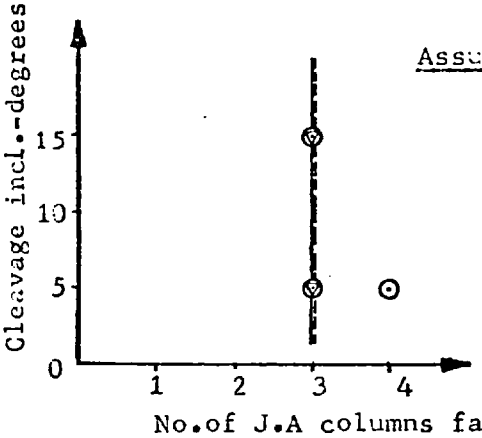

Assumption::Cleavage spacing is constant.

J.A: 70°(33mm)	J.A: 70°(33mm)
J.B: 85°(25mm)	J.B: 85°(25mm)
Clea. 15°(10mm) 5°(20mm)	Clea. 15°(10mm) 5°(40mm)
ψ_f=70°	ψ_f=70°

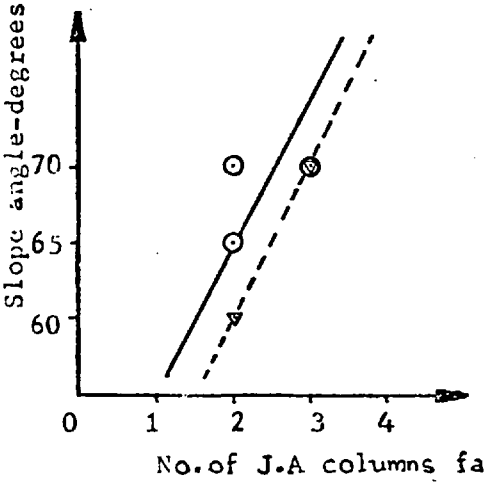

Assumptions:

Clea. spac. const.	Clea. incl. const.
J.A: 70°(40mm)	J.A: 70°(33mm)
J.B: 85°(25mm)	J.B: 85°(25mm)
Clea. 10°(10mm) (20mm)	Clea. 5°(10mm) 15°(10mm)
ψ_f=70° 65°	ψ_f=70° 60°

Figure 2.13- Double variation of parameters.

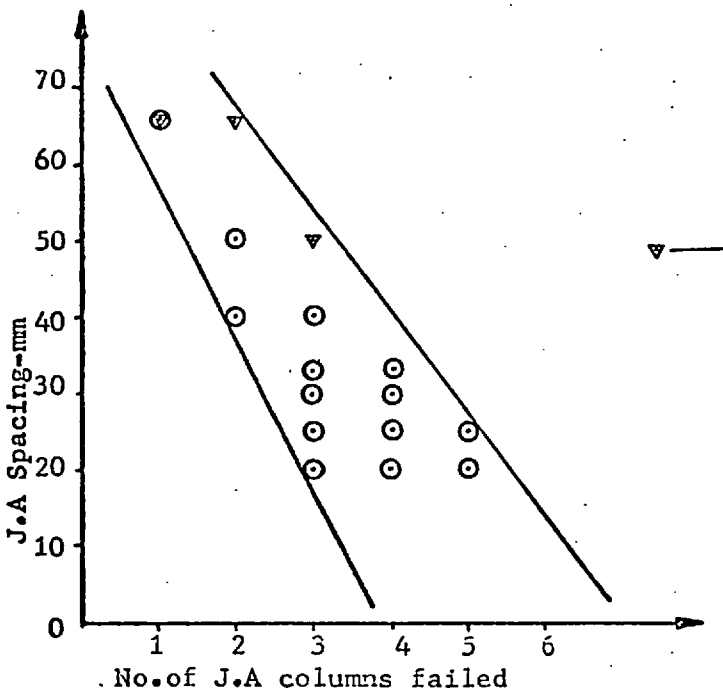

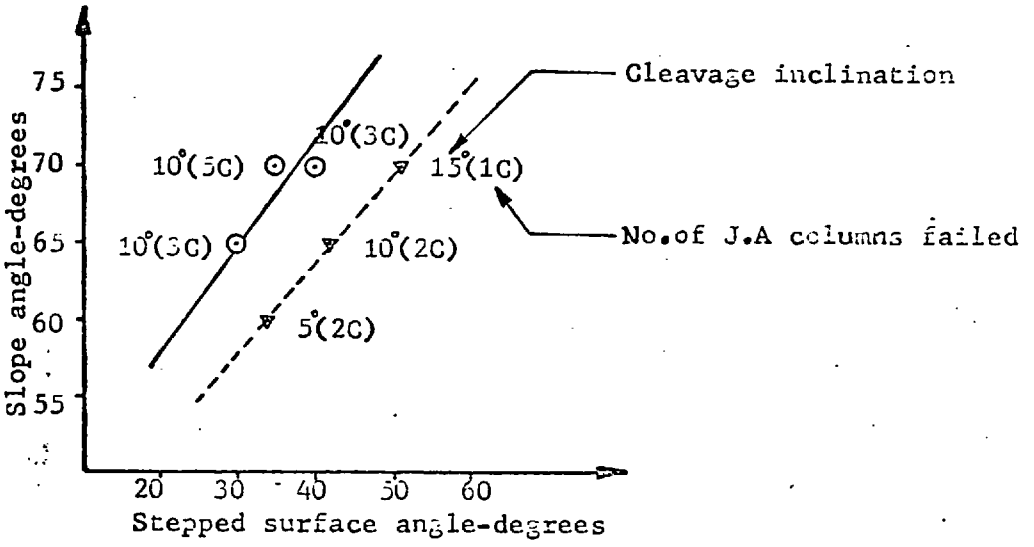

Constant cleavage inclination. The total distance of failed J.A columns at the slope crest is 12-15cm(in the model).

Increasing cleavage inclination. The total distance of failed J.A columns at the slope crest is 6.5-8cm(in the model).

Figure 2.14- Multiple Variation of Parameters.

As important as the lubrication effect, water has an uplift effect in the slope reducing the factor of safety. An attempt was made to simulate this effect by rotating the model (within its horizontal plane) by an appropriate angle to the direction of the moving belt, in such a way that the resultant of the weight and water (force) vectors coincides with the direction of belt movement.

The model which produced single column failures was chosen for this analysis and only this single column (e.g. joint A) was considered throughout the tests. It was assumed that water pressure acts along joint A alone with a water pressure distribution as shown in Figure 2.15. Half and fully saturated slopes were examined by rotating the model 12^{o} and 47.5^{o} respectively. The effect of uplift force was studied on both models constructed from the deformable mixture and cork, whereas the effect of water lubrication was investigated with cork model only. To be able to compare the models more precisely, timing was adopted and photographs were taken at regular time intervals.

The following is a summary of the observations made:

1. Failure occurs more quickly in the mixture model while the cork model is more liable to toppling (plate 2.VII).
2. The introduction of water uplift forces, in the case of half saturated slope, speeded up the failure for both types of model materials, and increased the amount of toppling for cork at the same time. Even a completely different picture was obtained for the fully saturated slope case where the "hangover" of column occurred

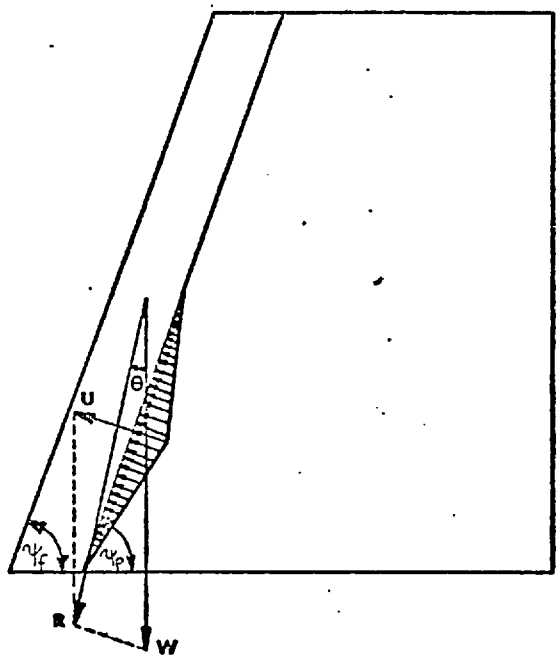

(a)

$W = 2.704 \times 10^6$ lb.
$U = 0.56 \times 10^6$ lb.
$\theta = 12°$
$\psi_f = 70°$
$\psi_p = 70°$

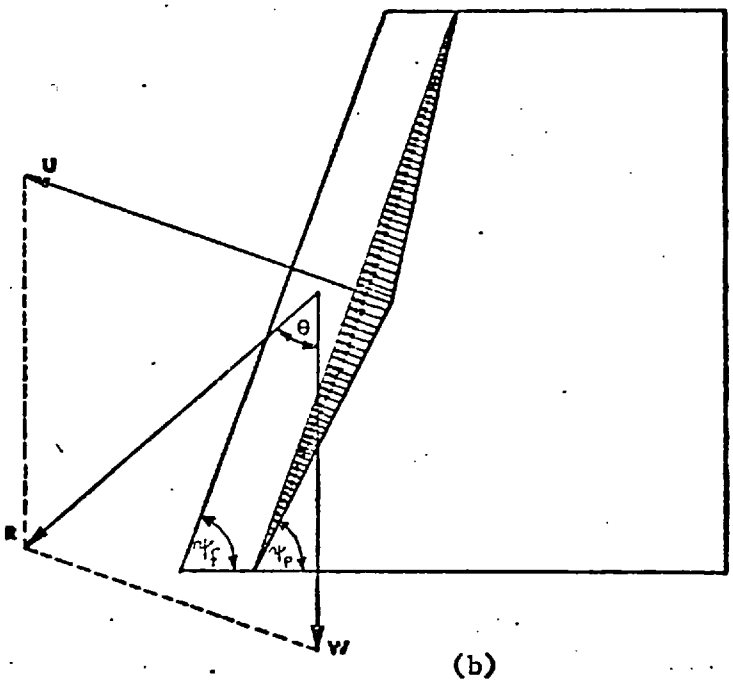

(b)

$W = 2.704 \times 10^6$ lb.
$U = 2.23 \times 10^6$ lb.
$\theta = 47.5°$
$\psi_f = 70°$
$\psi_p = 70°$

Figure 2.15- Groundwater simulation for single column: (a) Half saturated slope, (b) Fully saturated slope.

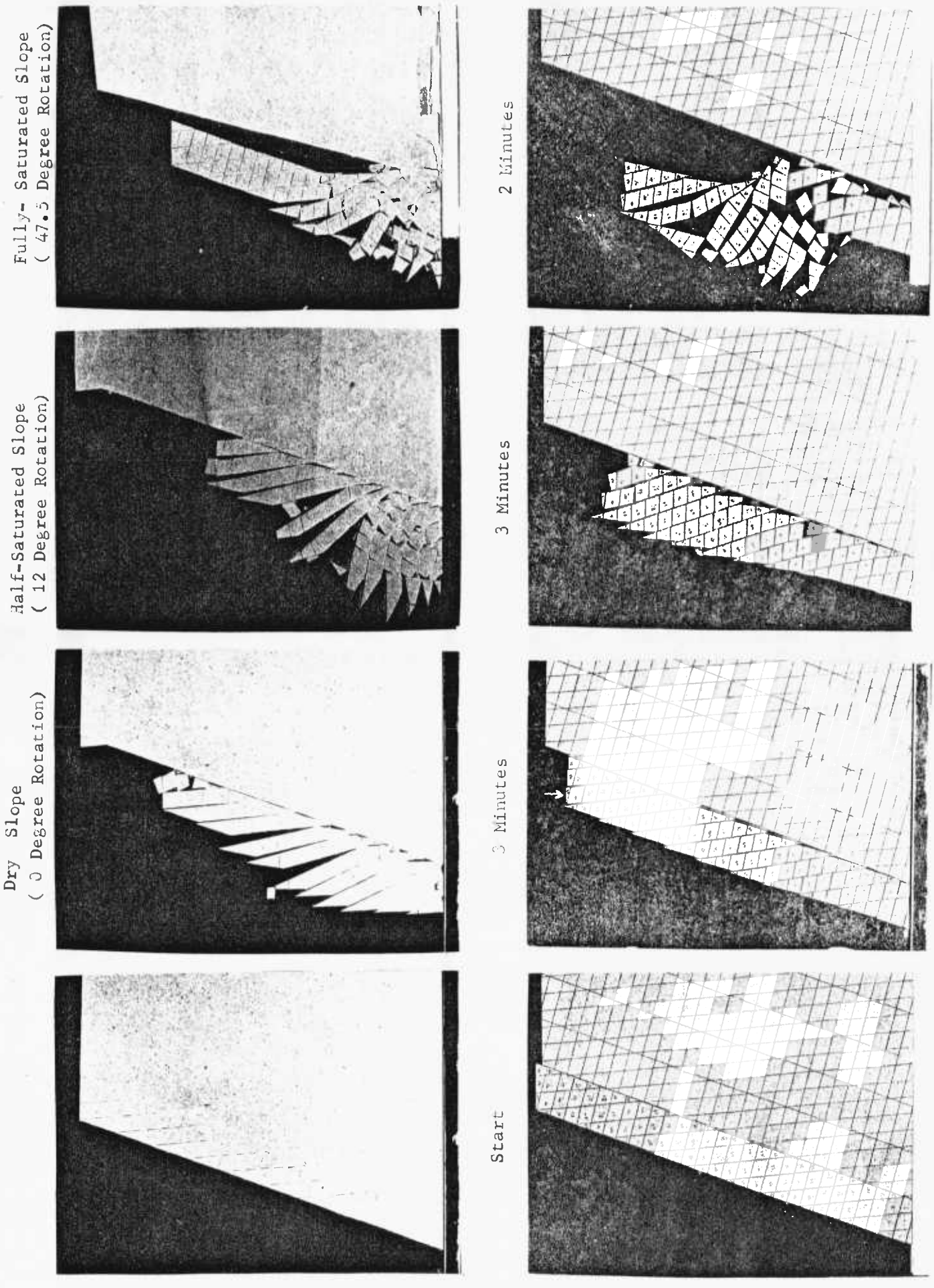

PLATE 2.VII- Comparison of deformable mixture and cork sheet models.

(plate 2.VII).

3. Reduction in friction angle ϕ due to water lubrication increased the speed of movements (plates 2.VIII and 2.IX).
4. The greater ϕ, the more predominant the toppling (plates 2.VIII and 2.IX).

Cork has some advantages and disadvantages as compared to the deformable mixture.

Advantages are:

1. Friction angle can be controlled throughout the model and lower values can be attained.
2. No healing and sticking of the joints which might give misleading observations.
3. It does not erode. This is a good point, especially at the top of the slope. Since there is no distortion of the material, the movements (subsidence e.g.) can be followed realistically.
4. Repetition of any test is easy and unchangeable (consistent) once the model is cut.
5. Ground water conditions
   a. reduction in ϕ
   b. uplift force

   can be simulated easily and practically.
6. Any configuration can be prepared easily.
7. Blocks can be numbered and traced during the test.
8. Material properties and composition do not change test to test.

Disadvantages are:

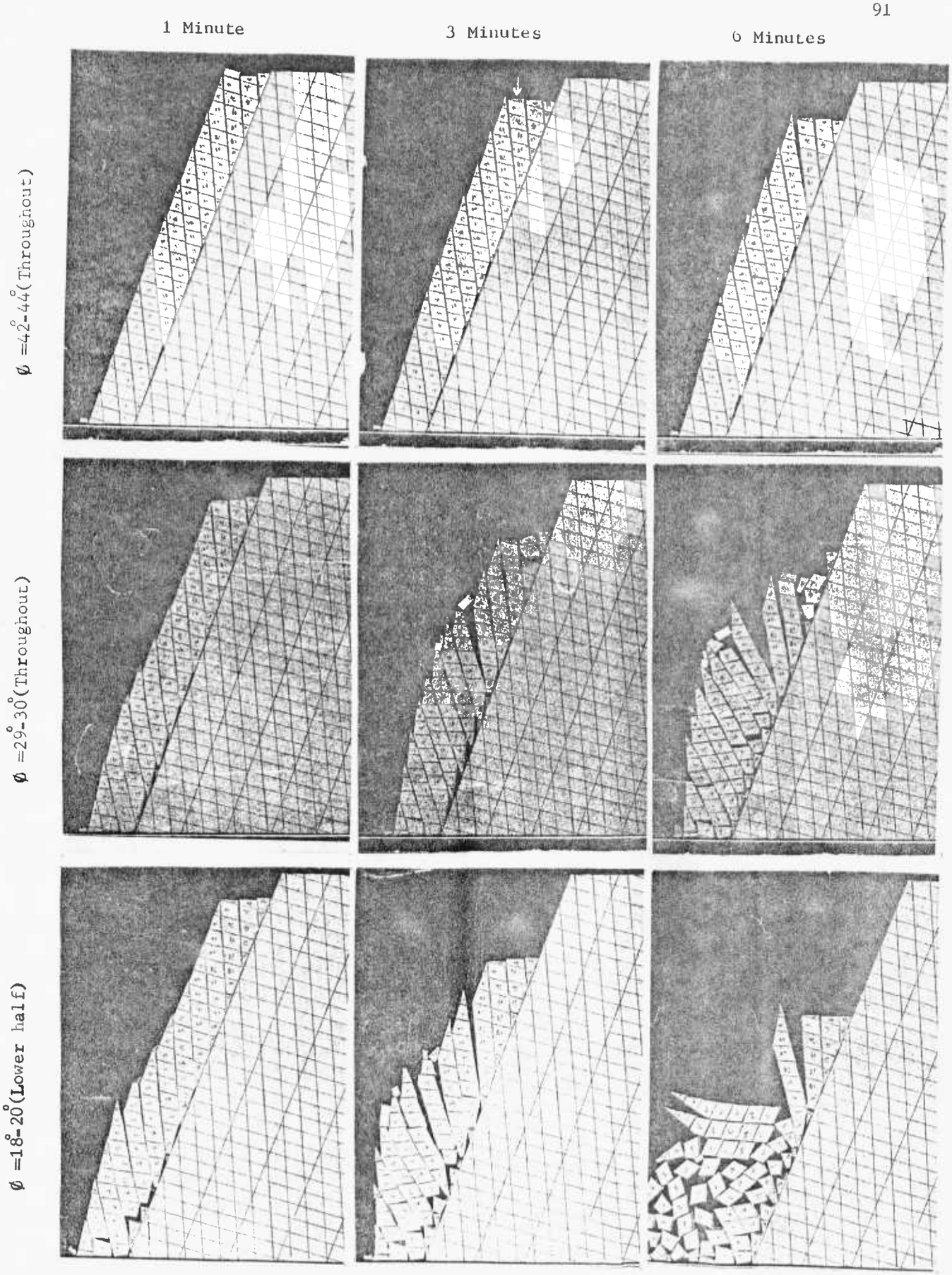

Note: All are dry slopes(no rotation)

PLATE 2.VIII- Cork sheet models with different friction angles.

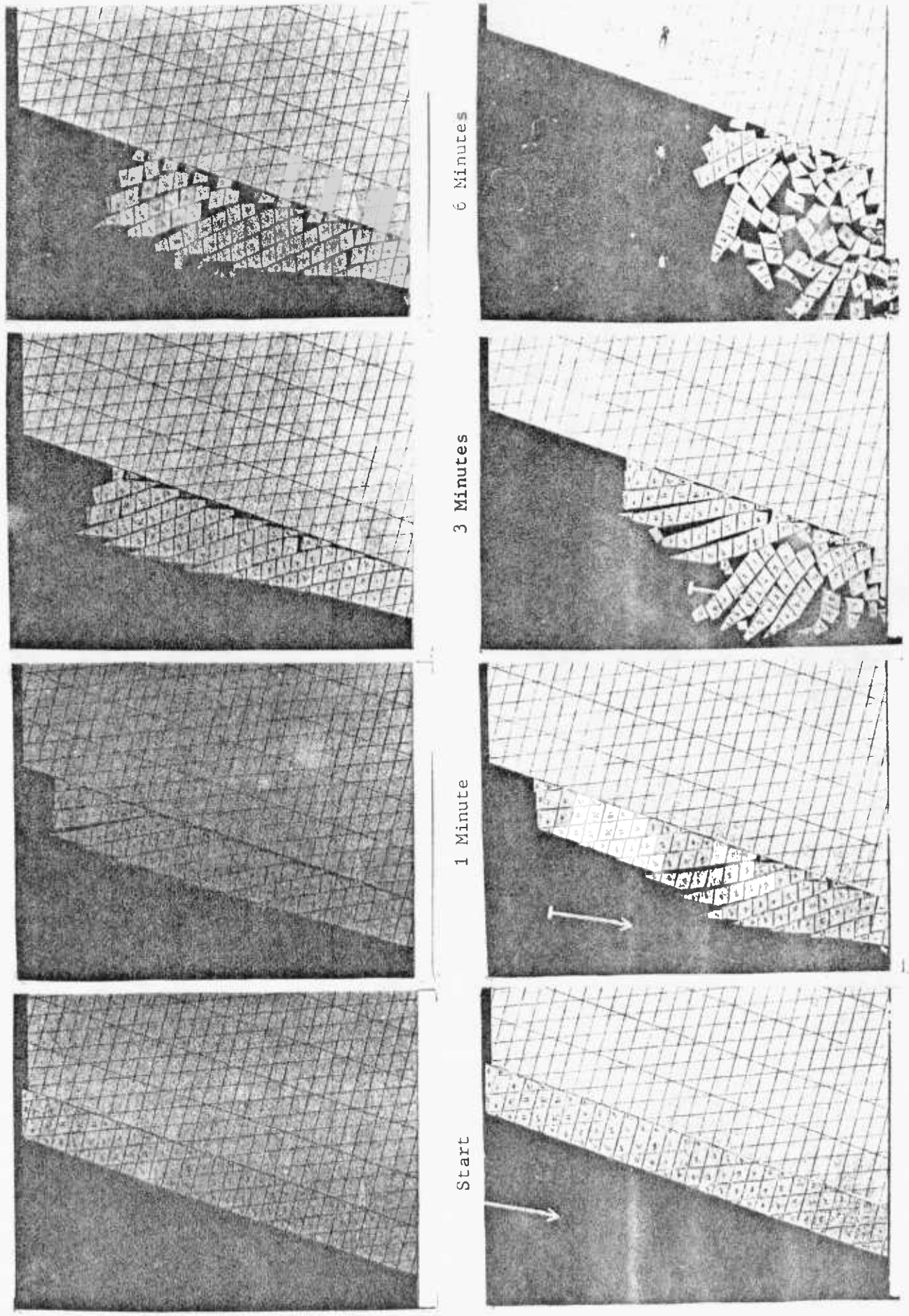

Notes: 1) Both are half saturated slopes(12° rotation). 2)Arrow in the lower pictures indicates the belt flow.

PLATE 2.IX- Simulation of water pressure and water lubrication with cork sheet models.

1. No failure through intact material can be exercised. This is the main disadvantage because this type of failure should be under consideration every time.
2. It is not dense, therefore difficulties arise during the experiment. Namely, blocks or columns do spring like movements from time to time. That is to say, consistent and steady movements are difficult to get because of the nature of the material itself (cork) and the sandpaper. Sudden motions, jerks could well change the pattern of displacements.
3. It is difficult to cut it. Smooth surfaces are not easy to obtain.

2.4 Discussion of Results and Conclusions

2.4.1 - Discussion of Results -

As a whole, the Old Delabole Slate Quarry presents rather a complex structure with several joint sets, various faults and a ubiquitous feature of cleavage. The Western wall of the pit exhibits an even more complicated structure with changing rock mass properties associated with lithological variations. When this complexity is added to the inadequacy of field information, regarding the continuity, frequency and strength characteristics of discontinuities, groundwater flow pattern, the dimensions of the problem grow due to numerous assumptions that can be made. On the other hand, restricted time, and limitations imposed by the base friction technique prevented some aspects of the problem being investigated in depth and judgement had to be made in such cases. For example,

if the strength and deformational properties of intact rock were correctly scaled, undercutting might have produced a failure similar to the real one, or, if it were possible to simulate the groundwater effects realistically in the sliding mode of failure, tension cracks would most probably open up at the crest. But, the author doubts the monitored block movements at the crest would occur which is supposed to be a phenomenon unique to toppling and sliding joint sets existing together. If the simulation of momentum were exact, the failed material would be more disintegrated, especially in toppling failure, because of falling columns. It is the author's opinion that the scree in the field is well broken, mainly due to occurrence of soft and loose Woolgarden rock, but the toppling mechanism should contribute to disintegration.

Analytical sliding analysis revealed that the failure in this mode was only possible with high water levels in tension crack which cannot be ruled out completely in spite of the average rainfall recorded during the months preceding the failure, because the occurrence of impermeable barriers to water flow increasing the effective head is a likelihood. However, even the sufficient water pressure was attained, as pointed out earlier, it is hardly expected of this mechanism to produce block rotation at the crest.

Contrary to other mechanisms, the toppling mode of failure was found to be independent of water pressure to take place. Actually, it was not a pure toppling but a combination of toppling and sliding helping each other. This mechanism appeared to be reproducing the field conditions with its

progressive and repeating character and more important than these with its post-failure geometry. In the light of the results of the site investigation, the essential feature for this type of failure to occur was determined to be the "toppling set", whether it is the joint set B or a group of faults associated with it. The "sliding set", whether being the joint set A or the associated faults, affected toppling in three ways: first, by producing very active wedges forcing the joint B columns to topple, second, by confining the extension of toppling (through accommodation of wedge slidings along), and thirdly, by taking part in the formation of the stress release path (stepped surface) which was an important phenomenon in the mechanism because the overturning resistance of the toe has been relieved. The preliminary function of the cleavage was bound to be taking part in the formation of stepped surface together with joint set A. (Contribution of isolated joints C could also be expected).

Finally, the author wants to make a comment on his observations which is rather open to argument in many ways. In several tests, particularly in multiple column failure models, it has been observed that a series of parallel tension cracks formed (along joints B - toppling set) at the slope crest before the collapse (see plate 2.III photograph b, and plate 2.V photographs c and e). It was thought that this could be connected with the toppling failure. Therefore, it is deduced that the occurrence of a series of parallel tension cracks at a slope crest in the field can be taken as an indication of a toppling mechanism. Actually, this is the case

in the 1967 failure area where a couple of parallel cracks do occur at the slope crest, as shown in Figure 2.6.

2.4.2 - Conclusions -

From the investigation made the following conclusions can be drawn:

(i) It is most likely that the 1967 failure was produced by a complex mechanism of toppling and sliding interaction, the toppling being the dominant behaviour. Sliding was in the form of driving wedges and was confined to the upper part of the slope mostly.

(ii) This mechanism appeared to have a progressive and repeating character.

(iii) The features and their roles in the failure process are, in the order of importance, as follows:

- Toppling set: Joint set B (or associated faults): produced the potential toppling columns.
- Sliding set: Joint set A(or associated faults): helped toppling in many ways, as discussed in the previous section.
- Cleavage: took part in the formation of the lower failure surface with joint set A.
- (Lithology) fault (if any): stopped toppling to extend down to the toe.
- Joint C's (isolated): helped the development of the lower failure surface.

(iv) Presence of water which acted as a lubricant as well as uplift agent, speeded up the failure.

(v) The extent and frequency of joint set B and the frequency of joint set A have influenced the size of the failure, while the cleavage frequency was neutral.

(vi) Occurrence of parallel tension cracks at the slope crest could be related to involvement of the toppling mechanism.

REFERENCES

1. LEESE,C.E. and SETCHELL, J. Notes on Delabole Slate Quarry. Trans. of the Royal Geological Soc. of Cornwall, Vol. XVII, Part 1, 1937.
2. RICHARDS, L.R. Strength properties of Delabole slates. Imperial College Rock Mechanics Research Report No. 22, May 1973, 27p.
3. HOEK, E. and BRAY, J.W. Rock Slope Engineering. The Inst. of Mining & Metall. (Publishers), London 1974, 309p.
4. BOYD, J.W. Personal Communication, Imperial College, 1974.
5. CUNDALL, P.A. The measurement and analysis of accelerations in rock slopes. Ph.D. Thesis, Univ. of London (Imperial College), 1971.
6. ASHBY, J.P. Sliding and toppling modes of failure in models and jointed rock slopes. M.Sc. Thesis, Univ. of London (Imperial College), 1971, 40p.
7. SOTO, C.A. A comparative study of slope modelling techniques for fractured ground. M.Sc. Thesis, Univ. of London (Imperial College), 1974.
8. GEROGIANNOPOULOS, N. The use of surface displacement monitoring in slopes to predict failure mode and location of failure surface. M.Sc. Thesis, Univ. of London (Imperial College), 1974, 37p.
9. ERGUVANLI, K.A. and GOODMAN, R.E. Applications of models to engineering geology for rock excavations. Bull. of the Assoc. of Eng. Geologist, Vol. IX, No. 2, 1972.

10. WHYTE, R.J. A study of progressive hangingwall caving at Chambishi Coppermine in Zambia using the base friction model concept. M.Sc. Thesis, Univ. of London (Imperial College), 1973, 86p.

11. GOODMAN, R.E. Geological investigations to evaluate stability. Proc. 2nd Symp. of Stability for Open Pit Mining, Vancouver, Nov. 1971, Publishers AIME, New York.

12. HAMMETT, R.D. A study of the behaviour of discontinuous rock masses. Ph.D. Thesis, James Cook Univ. of N. Queensland, Australia 1975.

13. BRAY, J.W. Methods of analysing discontinua in situations where slip and separation may produce significant displacements. Imperial College Rock Mechanics Technical Report No. 1, July 1975, 5p.

CHAPTER THREE

PHYSICAL MODEL TESTS

3.1 General

Simple physical modelling techniques, namely base friction and tilting frame, have been chosen to start with in understanding the basic mechanics of toppling failure. Base friction models, in particular, were thought to be very useful to study the kinematics of the rock mass forming the slope. The response of the models to varying parameters would be noted both qualitatively and quantitatively (whenever possible) to establish some empirical design criteria. For this purpose over 50 base friction tests were run. Tilting frame tests were not as extensive as originally planned because of inconsistent frictional characteristics of the block surfaces. Therefore, only very basic tests were conducted for comparison purposes.

3.2 Base Friction Models

This technique has been explained in Chapter Two (Section 2.3.3), together with the theory, the apparatus and material used, and the method adopted. Since nothing has been altered they will not be repeated here with the exception of the friction angle of the model material (loose mixture of flour, fine sand, vegetable oil and ballotini) which is 40 - 41 degrees. Timing was done for comparison purposes, and pictures were taken regularly for documentation and comparison.

Every effort was made to be precise in preparation and execution of the tests. Much attention was focussed on gathering information that would lead to a quantitative assessment of toppling failure. For this reason some of the tests were repeated two or even three times. As the behaviour of the slopes was not predictable, a detailed test programme was not made beforehand, but the "plan as you test" method was adopted instead.

3.2.1 - Description of Test Parameters -

The following parameters were varied independently to examine their influence on the mode of behaviour:

- Slope angle (60^{o}, 65^{o}, 70^{o}, 80^{o})
- Slope height (12", 15", 18", 21", 24")
- Joint dip (70^{o}, 80^{o})
- Number of columns (various)

Figure 3.1 illustrates the parameters together with the other terms that have been used throughout this chapter.

Slopes containing only one joint set, which dips into the slope to promote toppling, were constructed to begin with, and for the sake of simplicity the joint spacing of one inch was kept constant for all models unless the effective slope height was to be increased; then the slab was cut into 0.75" or 0.5" thick columns. A second joint set crossing the main one perpendicularly in a staggered manner to form blocks of 1" x 2" was included in the models at a later stage. The consistency and repeatability characteristics of the base friction technique have been under heavy investigation for most of the tests to see to what extent the test yields re-

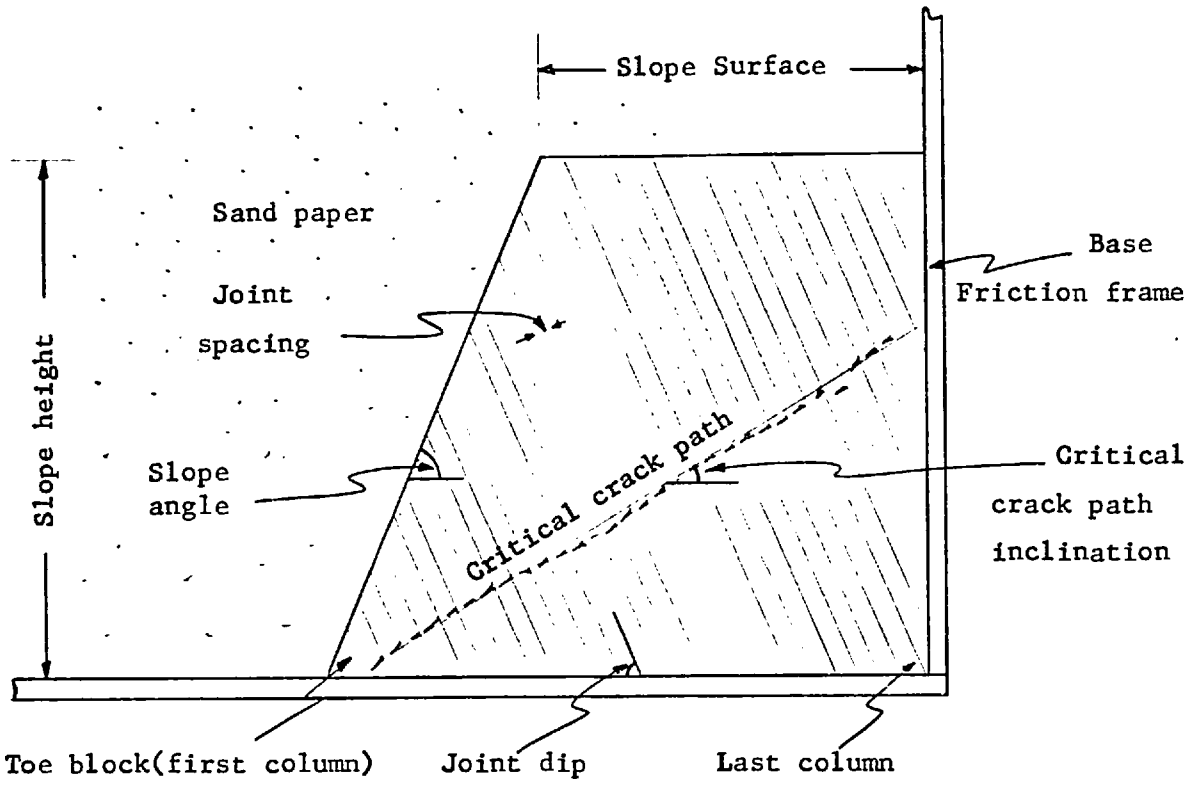

Figure 3.1- Test parameters

liable information. Therefore, two identical models were constructed symmetrically on each side of the base friction table and tested simultaneously as long as both models could be accommodated. The effect of boundaries are important in any physical modelling technique, and this was given much consideration as will be seen in the following pages.

To be able to evaluate and compare the test results the "critical crack path" with its developing time and inclination was closely monitored. The critical crack path can be defined as the irregular line(s) of fractures forming in the middle of the slope and extending mostly from the toe to the bottom of a tension crack. The position of tension cracks were also noted whenever possible.

3.2.2 - Tests Performed -

Because of limited space some of the tests will not be illustrated here, but they are all summarised in Tables 3.1 and 3.2. Table 3.1 lists the experiments in the order in which they were conducted, and Table 3.2 presents them in a form arranged to indicate the ultimate slope behaviour. Since the photographs are self-explanatory, detailed explanations will be avoided, but some comments will be made in the following descriptions.

MODEL 1 (R & L) - See Plate 3-I

The two slopes, one on the left (LS) and the other on the right (RS), were made with a 60^{o} slope angle, 12 in. slope height, and a joint set with a spacing of 1 in. and a dip of 80^{o}. As after 3 minutes of running time there was no sign of any instability, a vertical cut was made at the toe of the right slope right down to the steel frame, as in Plate 3-I(b). This operation altered the slope geometry in favour of instability, and the rotation of columns produced a toppling failure. The toe cut affected the slope behaviour because,

a. slope height was increased by 25%,

b. slope angle was increased, becoming 30^{o}

at the critical toe region, thus giving rise to the formation of long, slender blocks which were liable to topple easily.

c. Restraint at the toe was released.

The first critical crack path with an inclination of 32.5^{o} was followed by others as the columns bent forward, all merging at the toe.

Table 3.1 Base Friction Tests.

MODEL NO.	SLOPE ANGLE	SLOPE HEIGHT	JOINT DIP	CR.C. PATH DEV. T.	CR.C. PATH INCL.	REMARKS
1(R)	60°	12"	80°	10 m.	32.5°	First stable. Toe cut vertically → S. Height became 15". Then failed.
1(L)	60°	12"	80°	11 m.	30°	Quicker because of fresh sand paper. Restraint removed by cutting toe vertically.
2(R)	80°	15"	80°	2 m.	21.5°	No restraint at the beginning. Failure path is curved.
2(L)	80°	12"	80°	2 m.	28°	Restraint at the beginning. Quick failure as compared to 1(L).
3(R)	60°	12"	80°	-	-	Slope stands on the model material. Toe block removed. Still stable.
3(L)	60°	12"	80°	6 m.	28° - 29°	Slope stands on steel frame. Backward rotation at the upper part of slope face.
4(R)	60°	12"	80°	-	-	Similar to 3(L). No instability.
4(L)	60°	12"	80°	10 m.	25.5°	Similar to 3(R). First stable. Strip of tin placed horizontally → failure.
5(R)	60°	15"	80°	13 m.	21°	Restraint at the beginning → stable. Toe cut vertically → unstable.

Table 3.1 (continued)

MODEL NO.	SLOPE ANGLE	SLOPE HEIGHT	JOINT DIP	CR. C. PATH DEV. T.	CR. C. PATH INCL.	REMARKS
5(L)	60°	15"	80°	15 m.	32° - 34°	Restraint at start → stable. Hor. discontinuity cut at bottom → failure.
6(R)	60°	12"	70°	30.5 m.	31.5°	Slab unconsolidated. Toe blocks removed to initiate failure.
6(L)	60°	12"	70°	34.5 m.	40°	Consolidation forgotten. Failure initiated after toe blocks removed.
7(R)	60°	15"	70°	11.5 m.	31°	Triangular toe block removed.
7(L)	60°	15"	70°	12.5 m.	34.5°	Triangular toe block removed. Dilation of rock mass and backward rotation.
8(R)	60°	18"	70°	17 m.	36°	Backward rotation. Very similar to 8(L).
8(L)	60°	18"	70°	18.5 m.	37.5°	Backward rotation. Very similar to 8(R).
9(R)	60°	21"	70°	21 m.	33.5°	
9(L)	60°	21"	70°	25 m.	37.5°	
10(R)	60°	24"	70°	42 m.	41°	Buckling of columns into "S" shape. Three types of intact failure observed.
11(R)	70°	24"	70°	1 m.	34.5°	

Table 3.1 (continued)

MODEL NO.	SLOPE ANGLE	SLOPE HEIGHT	JOINT DIP	JOINT SPAC.	CR. C. PATH DEV. T.	CR. C. PATH INCL.	REMARKS
12(R)	70°	24"	70°	1"	1 m.	33.5°	Backward rotation due to toe support. "S" configuration.
13(R)	60°	24"	70°	1"	2 m.	33.5°	
14(L)	70°	12"	80°	1"	2 m.	25°	Irregular crack pattern.
15(L)	80°	12"	80°	1"	3-4 m.	38°	
2'(L)	80°	12"	80°	1"	2 m.	22°	Critical path passed above toe on contrary to 2(L).
$2'_1$(L)	80°	15"	80°	1"	2 m.	27°	Toe block fails by tensile bending. Fold structure developed.
4'(L)	60°	12"	80°	1"	40 m.	27.5°	Limit equilibrium case?
$2'_R$(L)	80°	12"	80°	1"	2 m.	30°	Stepped crack pattern.
5'(L)	60°	11¼"	80°	¾"	22 m.	23° (27.5°-34.5°)	Stable .'. Horizontal cut made at bottom.
$14'_1$(L)	70°	11¼"	80°	¾"	2 m.	28.5°(U) 21.5°(L)	Upper path control toppling.

Table 3.1 (continued)

MODEL NO.	SLOPE ANGLE	SLOPE HEIGHT	JOINT DIP	JOINT SPAC.	CR. C. PATH DEV. T.	CR. C. PATH INCL.	REMARKS
11'(L) or 12'(L)	70°	12"	70°	½"	¾ m.	33°	Critical path didn't pass through toe. Fracturing at slope face.
10'(L)	60°	12"	70°	½"	-	-	Stable slope. Continued from previous test → joints not recut.
$10'_1$(L)	65°	12"	70°	½"	-	-	Stable slope. Limiting equilibrium. Joints recut.
$11'_R$(L) or $12'_R$(L)	70°	12"	70°	½"	<1 m.	33.5°	Critical path passed through toe. Backward rotation.
11_R(L) or 12_R(L)	70°	12"	70°	½"	¾ m.	38°	Critical path passed below toe. Curved slope profile at the end.
4"(L)	60°	12"	80°	1"x2"	-	-	Stable slope.
$4''_1$(L)	65°	12"	80°	1"x2"	-	-	Local displacement at crest. Limiting equilibrium?
$4''_2$(L)	70°	12"	80°	1"x2"	14 m	-	Instability confined to slope face and crest.

Table 3.1 (continued)

MODEL NO.	SLOPE ANGLE	SLOPE HEIGHT	JOINT DIP	JOINT SPAC.	CR. C. PATH DEV. T.	CR. C. PATH INCL.	REMARKS
14"(L)	70°	12"	80°	1"x2"	-	-	Block columns formed.
11"(L) or 12"(L)	70°	18"	70°	$\frac{3}{4}$"x$\frac{3}{2}$"	2.5 m.	-	Cross joints opened up in a stepped manner. Toe region stable.
$11'_1$(L) or $12'_1$(L)	65°	18"	70°	$\frac{3}{4}$"x$\frac{3}{2}$"	-	-	No signs of instability.
$11'_S$(L) or $12'_S$(L)	70°	18"	70°	$\frac{3}{4}$"x$\frac{3}{2}$"	$\frac{1}{2}$ m.	-	A quick failure. Instability extends to toe. Model on steel frame.
$11''_{S1}$(L) or $12''_{S1}$(L)	70°	11$\frac{1}{4}$"	70°	$\frac{3}{4}$"x$\frac{3}{2}$"	1.5 m.	-	Opening up and closing down of joints continuously.
$11''_{S2}$(L) or $12''_{S2}$(L)	70°	9"	70°	$\frac{3}{4}$"x$\frac{3}{2}$"	4 m.	-	
14D (L)	70°	12"	80°	1"	5 m.	26°	Sawtooth pattern joint delayed rotation.

Note: (R) Stands for the model constructed on the right hand side of the Base Friction Table.
(L) Stands for the model on the left.

Subscript R indicates repetition.
Single prime (') indicates boundary-effect-free model.
Double prime (") indicates cross jointed model.

Table 3.2 Base Friction Test Results.

MODEL NO.	SLOPE ANGLE	HEIGHT/ J. SPACING	JOINT DIP	CR.C. PATH DEV. T.	CR.C. PATH INCL.	REMARKS	SLOPE BEHAVIOUR
1(R)	60°	12	80°	-	-	Restraint at the toe	S
1(L)	"	"	"	-	-	Restraint at the toe	S
3(R)	"	"	"	-	-	Slope on model material	S
3(L)	"	"	"	6 m.	28°-29°	Slope on steel frame	U
4(R)	"	"	"	-	-	Slope on steel frame	S
4(L)	"	"	"	-	-	Slope on model material	S
4(L)	"	"	"	10 m.	25.5°	Strip of tin at slope bottom	U
4'(L)	"	"	"	40 m.	27.5°	Very long run	L.E.
4"(L)	"	"	"	-	-	1" x 2" blocks, staggered	S
6(R)	"	"	70°	30.5 m.	31.5°	Unconsolidated slab, on steel frame	L.E.
6(L)	"	"	"	34.5 m.	40°	Toe blocks removed, long run	L.E.
1 (R)	"	15	80°	7 m.	32.5°	A vertical cut of 3" at toe	U
1 (L)	"	"	"	1 m.	30°	A vertical cut of 3" at toe	U
5(R)	"	"	"	-	-	Restraint at the toe	S
5(R)	"	"	"	-	-	Horizontal cut at the bottom	S
5(L)	"	"	"	-	-	Restraint at the bottom	S
5(L)	"	"	"	9 m.	32°-34°	Horizontal cut to release restraint	U
5'(L)	"	"	"	-	-	Joint spacing = ¾"	S
5'(L)	"	"	"	16 m.	23°	Horizontal cut at the bottom	U
7(R)	"	"	70°	11.5 m.	31°	Triangular toe block removed	U

Table 3.2 (continued)

MODEL NO.	SLOPE ANGLE	HEIGHT/ J. SPACING	JOINT DIP	CR.C. PATH DEV. T.	CR.C. PATH INCL.	REMARKS	SLOPE BEHAVIOUR
7(L)	60°	15	70°	12.5 m.	34.5°	Triangular toe block removed	U
5(R)	"	18	80°	4 m.	21°	A vertical cut of 3" at toe	U
8(R)	"	"	70°	17 m.	36°	Slope on steel frame	U
8(L)	"	"	"	18.5 m.	37.5°	Slope on steel frame	U
9(R)	"	21	70°	21 m.	33.5°	Slope on steel frame	U
9(L)	"	"	"	25 m.	37.5°	Slope on steel frame	U
10(R)	"	24	"	42 m.	41°	Slope surface = 10" → 22 columns	L.E.
10'(L)	"	"	"	-	-	Joints not re-cut, short run (5 m)	S
13(R)	"	"	"	2 m.	33.5°	Slope on steel frame. Slope surf. = 8" → 20 columns	U
$4''_1$(L)	65°	12	80°	-	-	Local displacements at crest, 18 m run	L.E.
$10'_1$(L)	"	24	70°	-	-	20 minutes of run	S
$11''_1$(L)	"	"	"	—	—	10 minutes of run	S
$4''_2$(L)	70°	12	80°	14 m.	-	Slope on model material	U
14(L)	"	"	"	2 m.	25°	Slope on steel frame	U
14"(L)	"	"	"	1-2 m.	-	Slope on steel frame	U
14D(L)	"	"	"	5 m.	26°	Sawtooth pattern joint	U
$11''_{S2}$(L)	"	"	70°	4 m.	-	Slope on steel frame	U
$14'_1$(L)	"	15	80°	2 m.	28.5° 21.5°	Slope on model material	U
$11''_{S1}$(L)	"	"	70°	1.5 m.	-	Slope on steel frame	U

Table 3.2 (continued)

MODEL NO.	SLOPE ANGLE	HEIGHT/ J. SPACING	JOINT DIP	CR.G. PATH DEV. T.	CR.G. PATH INCL.	REMARKS	SLOPE BEHAVIOUR
11(R)	70^{o}	24	70^{o}	1 m.	34.5^{o}	Slope surface = 10" → 17 columns	U
12(R)	"	"	"	1 m.	33.5^{o}	Slope on steel frame, 22 columns	U
11'(L)	"	"	"	¾ m.	33^{o}	B.E.F.M., Critical path didn't pass through toe	U
$11'_{R}$(L)	"	"	"	< 1 m.	33.5^{o}	B.E.F.M., Critical path passed through toe	U
11_{R}(L)	"	"	"	¾ m.	38^{o}	Critical path passed through toe (slope on St. Frame)	U
11"(L)	"	"	"	2.5 m.	-	B.E.F.M. Toe region stays intact	U
$11''_{S}$(L)	"	"	"	½ m.	-	Slope on steel frame, toe unstable	U
2(L)	80^{o}	12	80^{o}	2 m.	28^{o}	Slope on model material → restraint at toe	U
15(L)	"	"	"	2-3 m.	38^{o}	Slope on steel frame	U
2'(L)	"	"	"	3 m.	22^{o}	B.E.F.M., Critical path didn't pass through toe	U
$2'_{R}$(L)	"	"	"	2 m.	30^{o}	B.E.F.M., Critical path passed through toe	U
2(R)	"	15	"	2 m.	21.5^{o}	Slope on steel frame; Vertical cut of 3" at toe	U
$2'_{1}$(L)	"	"	"	2 m.	27^{o}	B.E.F.M.	U

Abbreviations:

S = Stable slope
U = Unstable slope
L.E. = Slope in Limit Equilibrium
B.E.F.M. = Boundary Effect Free Model

PLATE 3.I- Base Friction Model No.1.

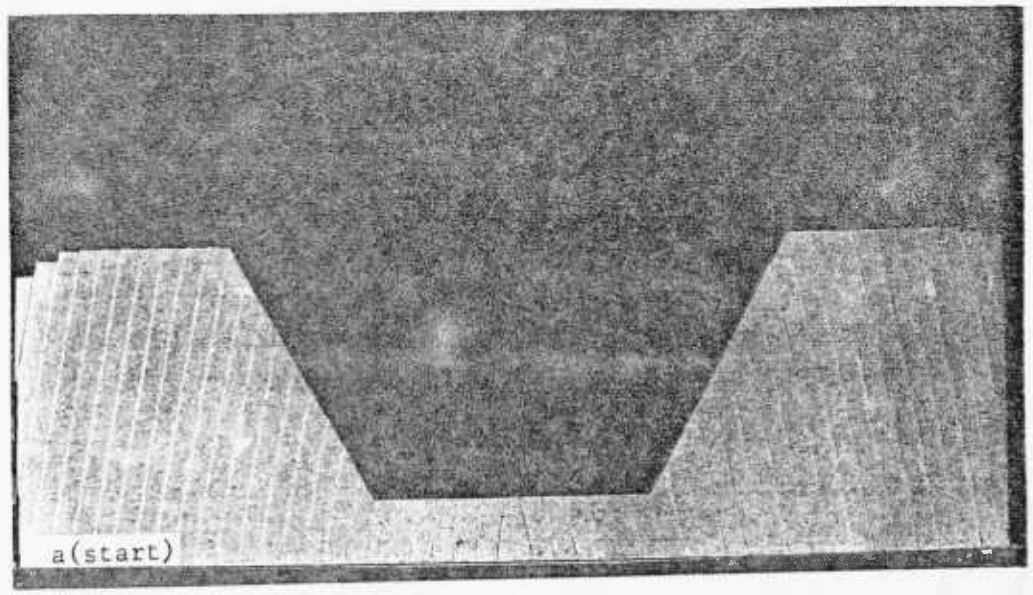
a(start)

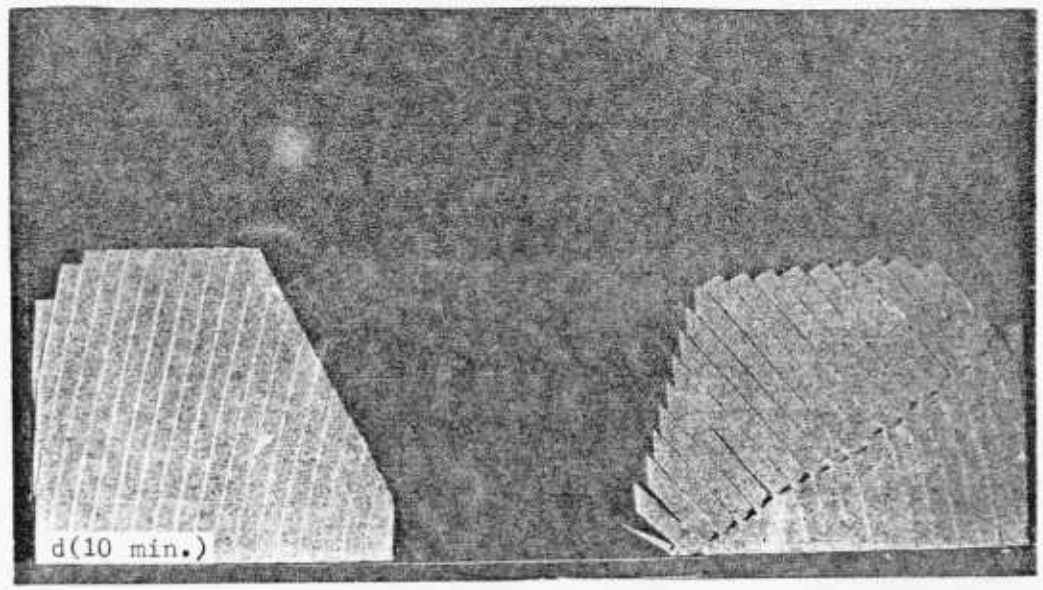
d(10 min.)

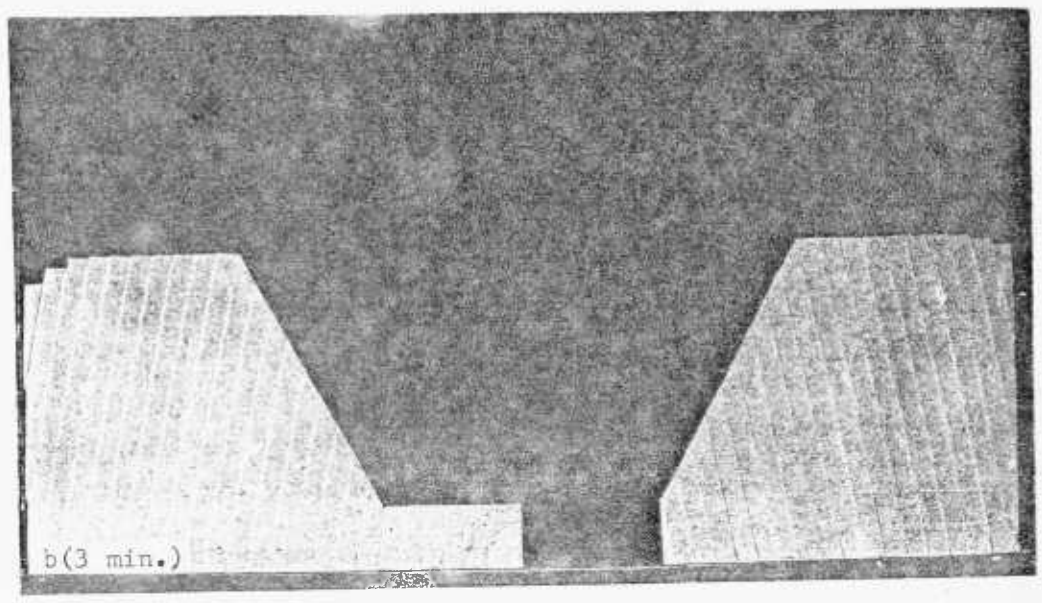
b(3 min.)

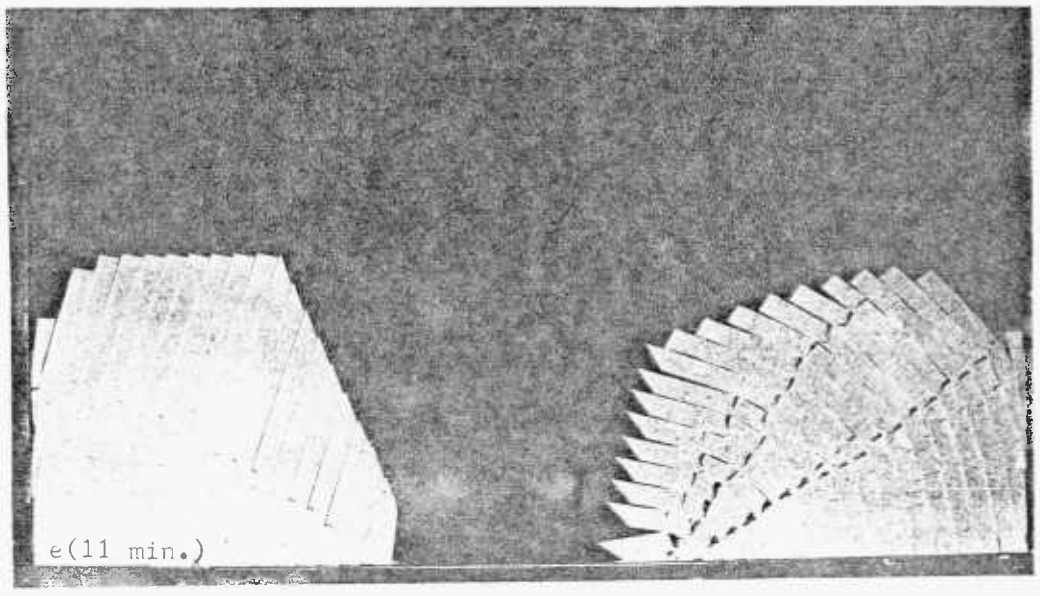
e(11 min.)

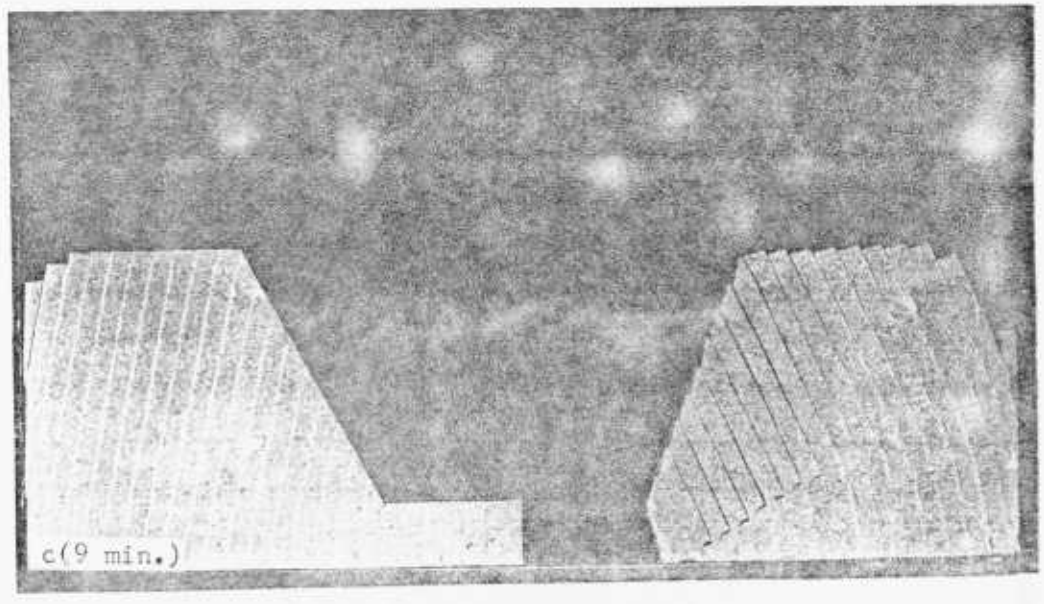
c(9 min.)

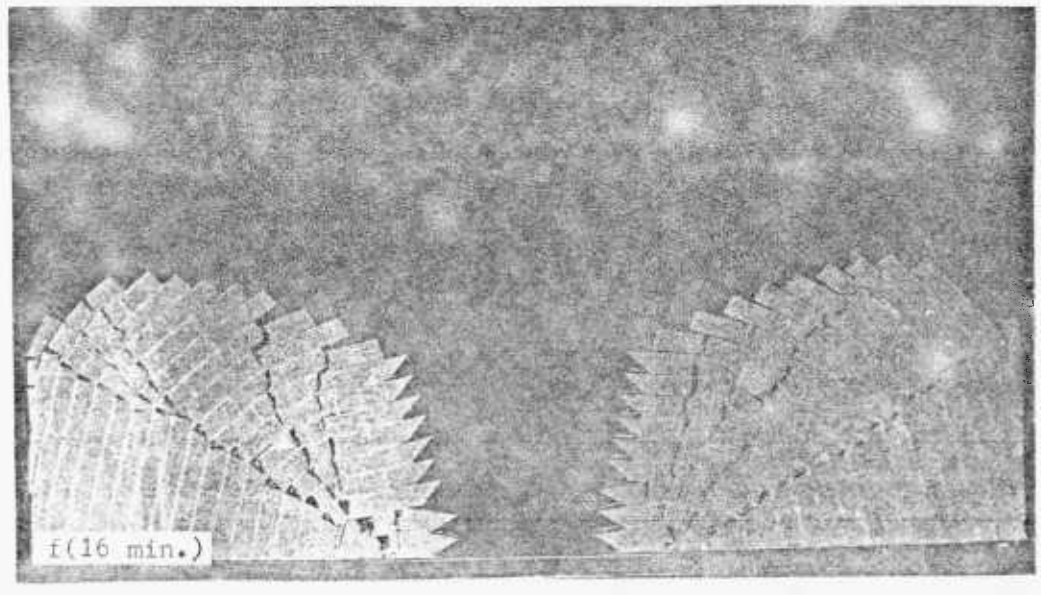
f(16 min.)

The left slope (LS) also remained stable until a vertical toe cut was made. Eventually it failed like the RS with a critical crack path inclination of 30°. The quicker path development in this slope could be attributed to the fresh sandpaper on this side of the belt. Nevertheless, photograph (f) demonstrates the consistency of the tests conducted on either side of the base friction table.

MODEL 2 (R & L) - See Plate 3-II

Same as model No. 1, except for the slope angle which was 80°. At the start, the right slope had a vertical toe cut while the restraint at the toe of the left slope was still present in order to make the test similar to the second stage of model 1 (photograph (b)). Both slopes failed quickly. The presence of restraint could not save the left slope from failure in this case due to the steep slope angle. The right slope failed with a critical crack path angle (c.c.p.a.) of 21.5° as compared to 28° for the left slope, the former being more disturbed as a consequence of the toe cut.

MODELS 3 and 4 (R & L) - See Plate 3-III

Slopes, one resting on the steel frame and the other resting on the model material, were constructed to see the influence of base material in terms of its frictional characteristics and stiffness properties. To be able to compare with Model 1, as far as the toe restraint and the general slope behaviour are concerned, the same slope geometry (slope height = 12", slope angle = 60°, joint dip = 80°) was cut.

PLATE 3.II- Base Friction Model No.2.

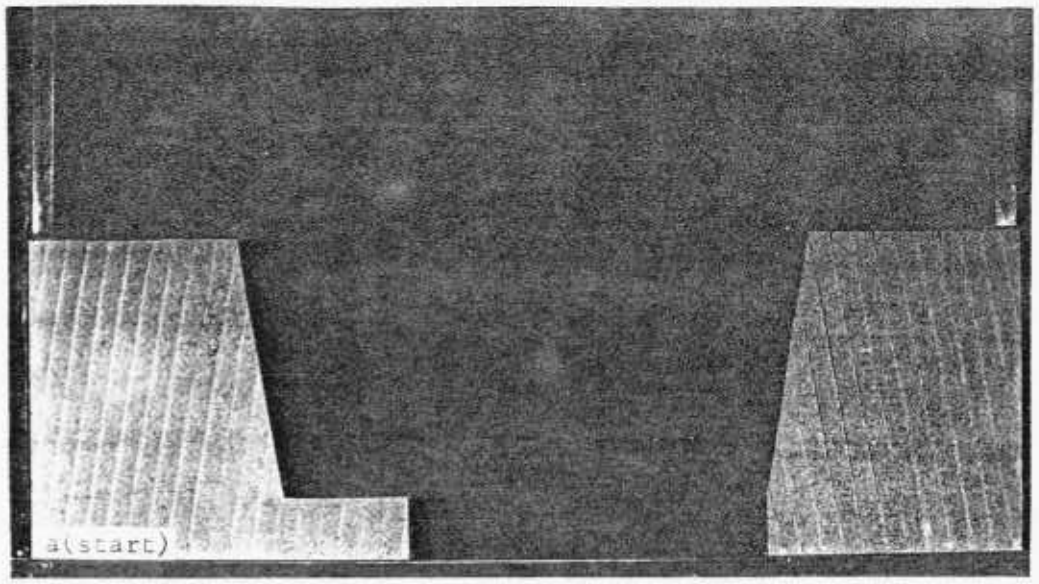
a(start)

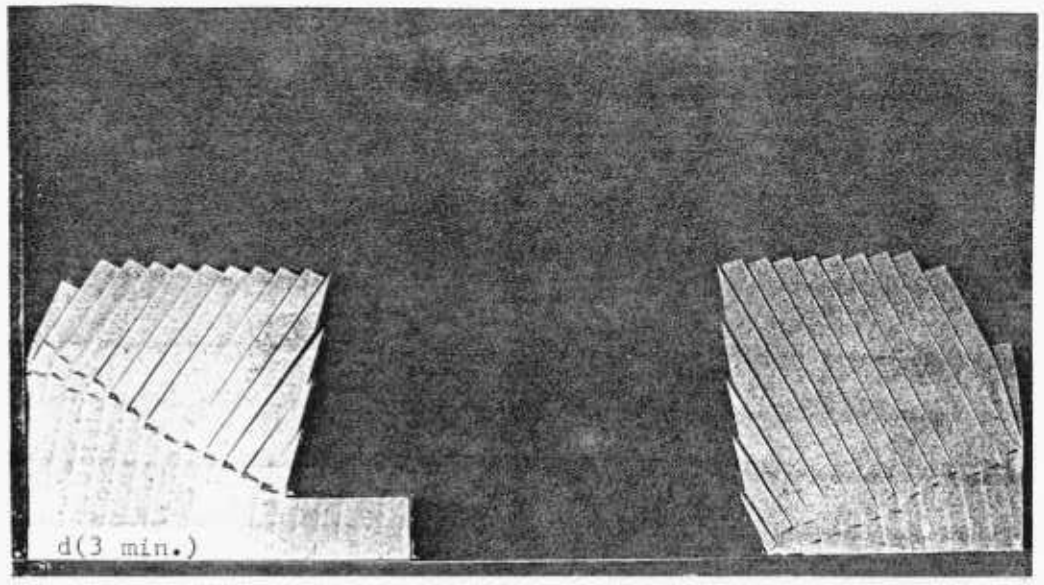
d(3 min.)

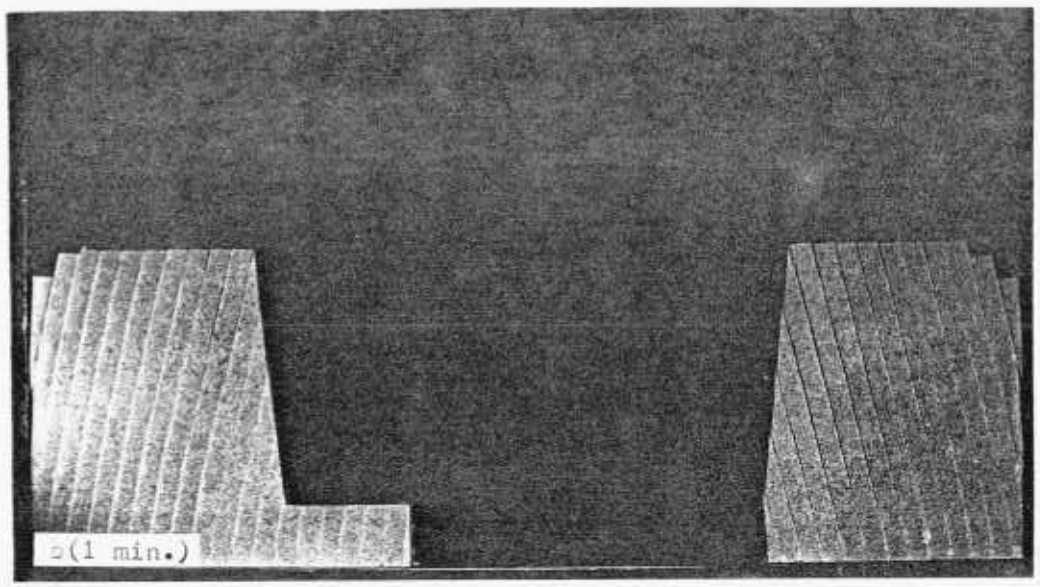
b(1 min.)

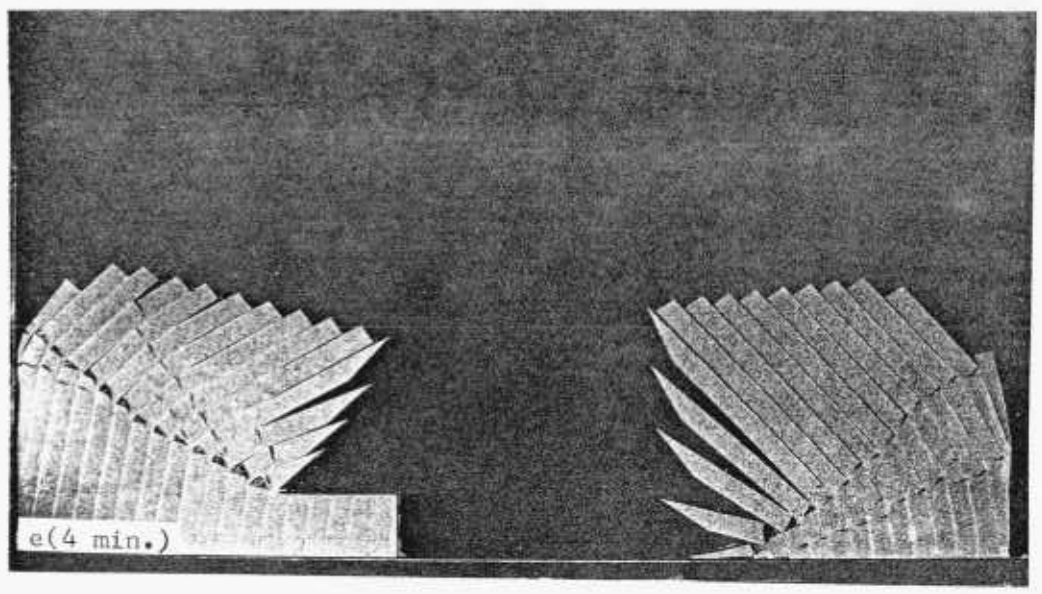
e(4 min.)

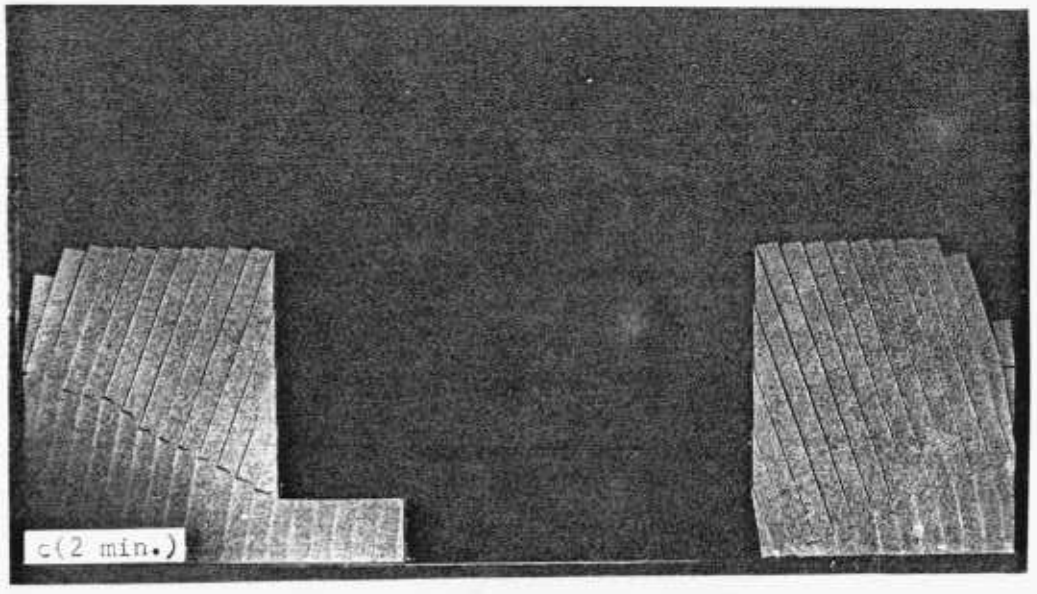
c(2 min.)

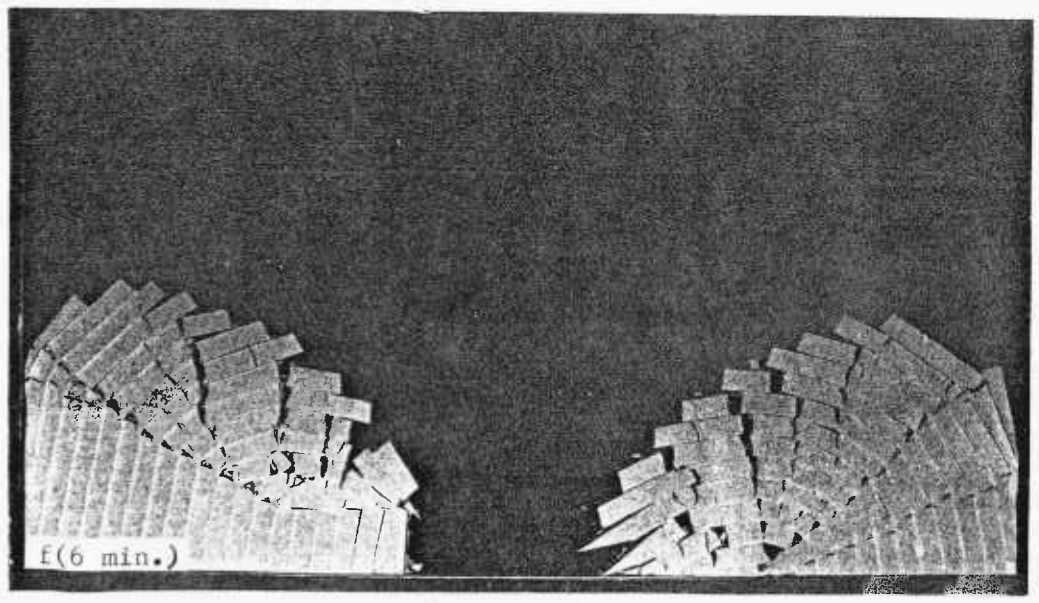
f(6 min.)

Model 3 was repeated as Model 4, changing the position of the slopes. Slopes resting on the model material, i.e. 3(R) and 4(L), remained stable agreeing with each other, and also indicating the stability of the 60° slope whether toe restraint is present or not, when compared to Model 1. On the other hand, slopes resting on the steel frame did not agree with each other; while 3(L) was developing a critical cr. path in 6 minutes. 4(R) remained stable although the triangular toe block was displaced and the columns shown by arrows were slightly rotated. This discrepancy might come from the quality of sandpaper again, in other words, fresh sandpaper could have caused a higher simulated gravitational loading for the slopes constructed on the left hand side of the frame.

As slope 3(R) did not respond to the removal of the toe block it was cut through at an inclination of 28°, which happened to be the c.c.p.a. for 3(L), to initiate failure. Slope 4(L), although slowly, also failed after the horizontal cut at the bottom of the slope was replaced with a strip of tin, most likely due to the reduction in friction angle along the horizontal discontinuity. But, slope 4(R) was not quite responsive to the artifical critical crack path cut similar to the one formed in slope 4(L).

MODEL 5 (R & L) - See Plate 3-IV

This test demonstrates how the toe blocks control the mechanical behaviour of a toppling slope. As the 60° slopes (15" high) showed no sign of instability a horizontal

PLATE 3.III- Base Friction Models No.3 and 4.

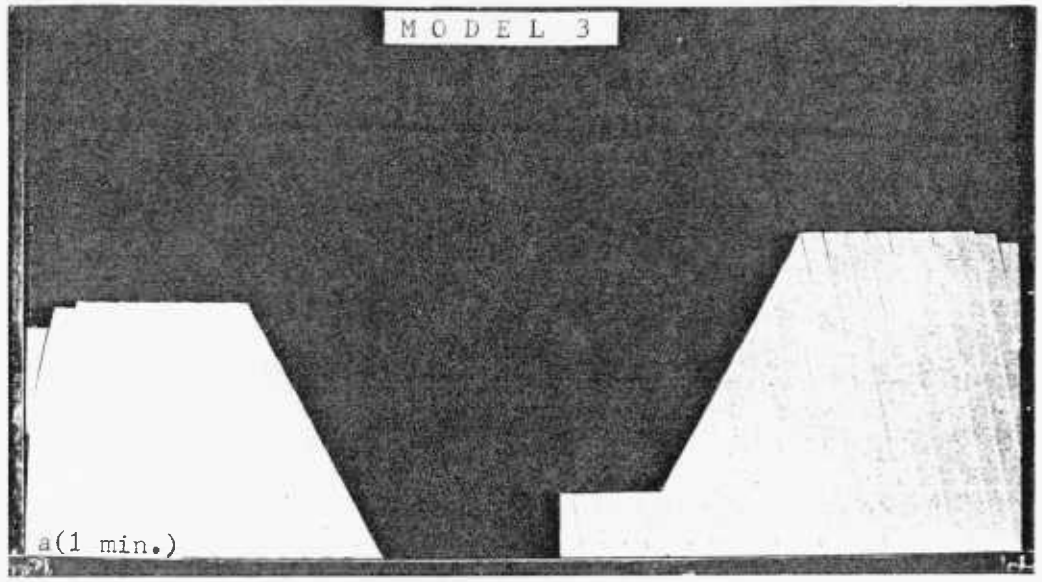
MODEL 3
a(1 min.)

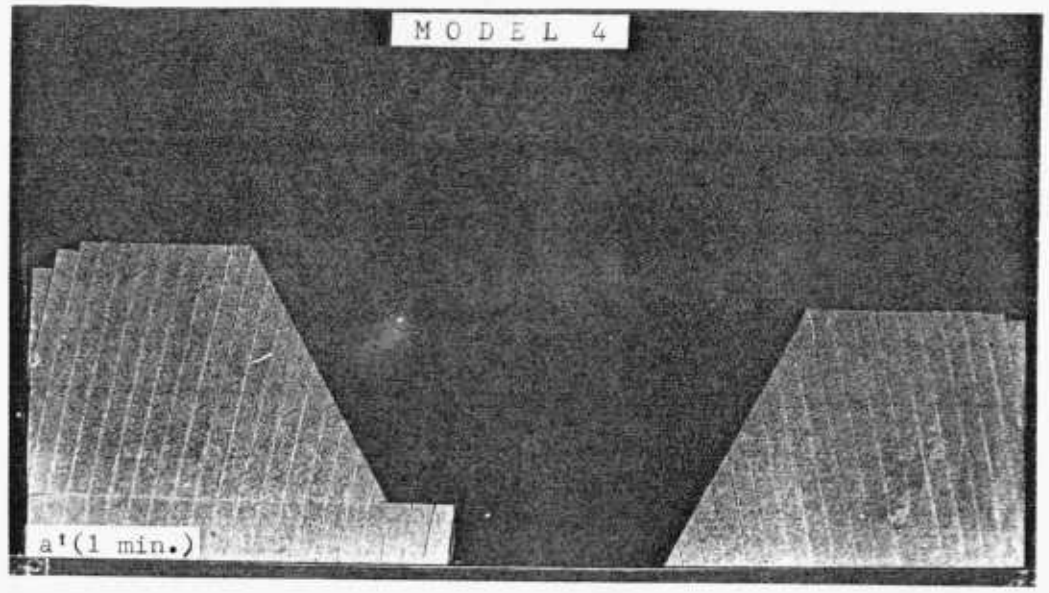
MODEL 4
a'(1 min.)

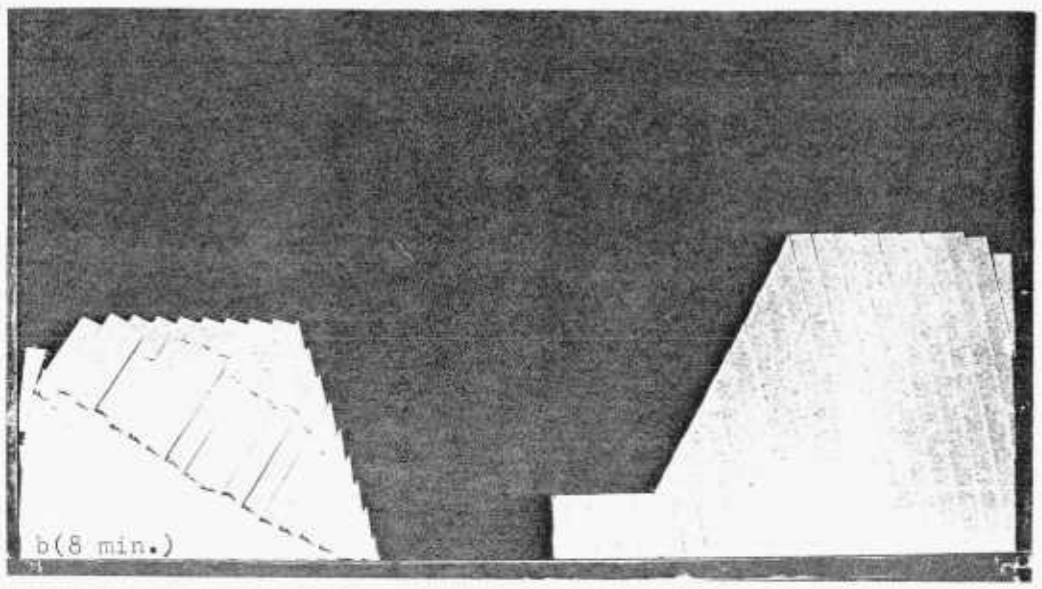
b(8 min.)

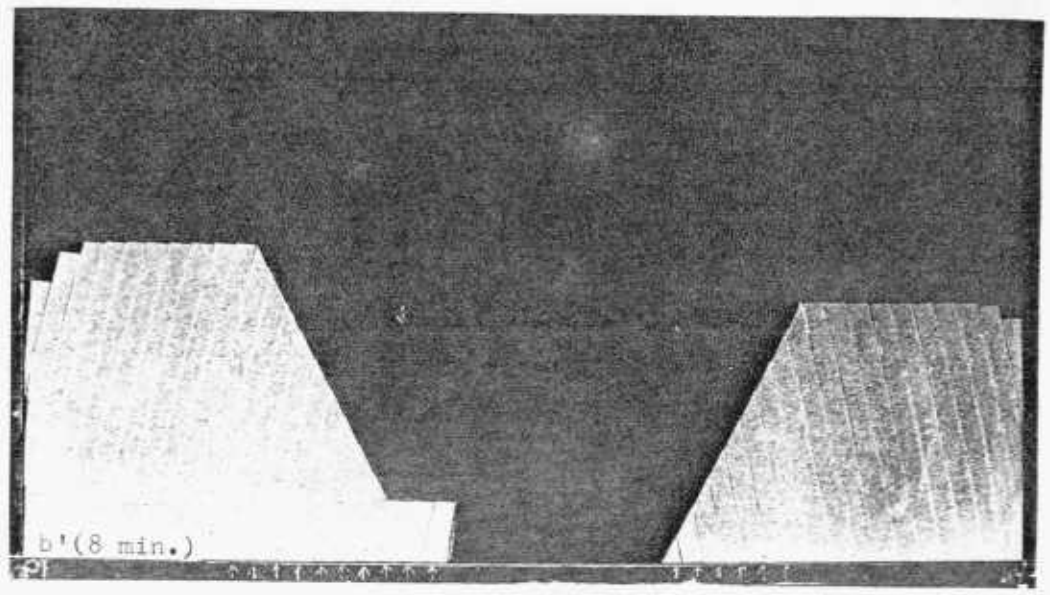
b'(8 min.)

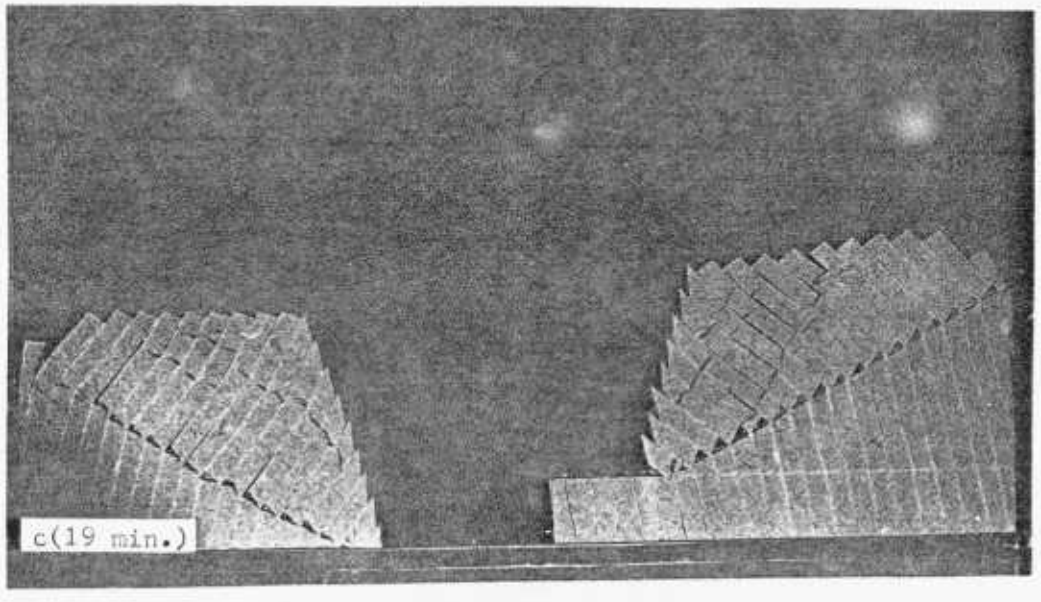
c(19 min.)

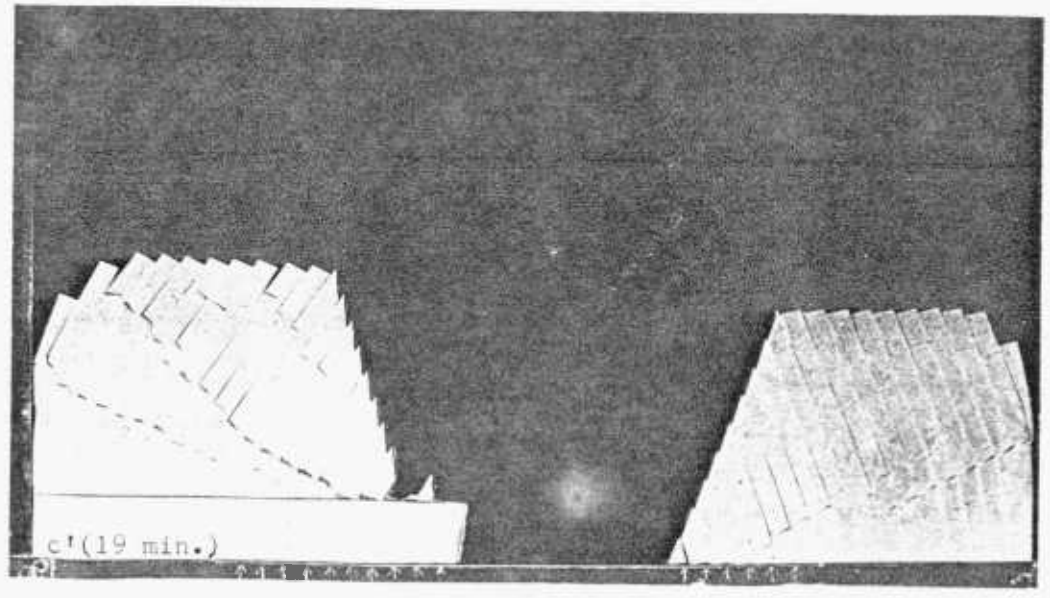
c'(19 min.)

cut was made at the bottom of both slopes to remove the restraint, and thus promote toppling. After a while the right slope was cut vertically at the toe because it was felt that the stability would be maintained in spite of the horizontal cut. The left slope was left untouched. First, the right slope failed, and, soon after, the left one followed it. Although both slopes were unstable at the end they failed differently forming completely different fracture patterns. As illustrated by photograph (f) the fracture pattern in the right slope was a radiating type, all paths joining at the toe (thus heavily crushing this zone), the last one being parallel to the slope face. The fractures in the left slope developed parallel to the first critical crack path, the last one crossing the slope face. The simple reason for the different fracture patterns was the different restraints shown by the toe blocks, depending on their geomtry. The vertical cut in the right slope produced long and slender toe block(s) which failed easily through tensile bending offering little resistance to rotation. So, a fold structure developed. On the other hand, the toe block(s) of the left slope opposed toppling action considerably, and because of their geometry preferred sliding and slow rotation rather than flexural yielding. From the comparison of critical crack path angles (21^{o} for RS against 32^{o} - 34^{o} of left) one might deduce that the degree of resistance shown by the toe block(s) also determined the extent of the disturbance in the rock mass.

MODEL 6 (R & L) - See Plate 3-V

Unfortunately, this model was not properly consoli-

PLATE 3.IV- Base Friction Model No.5.

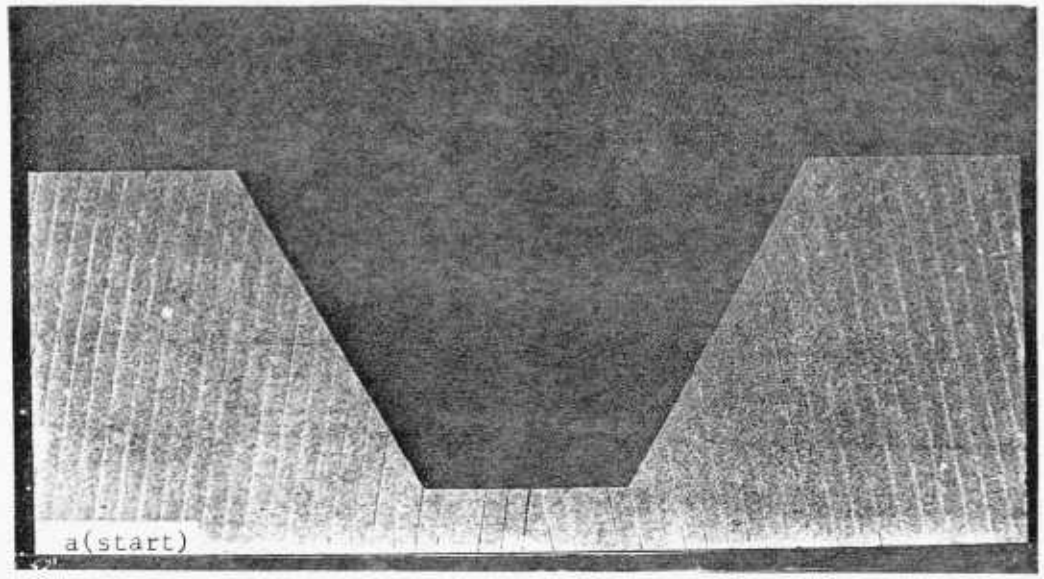
a(start)

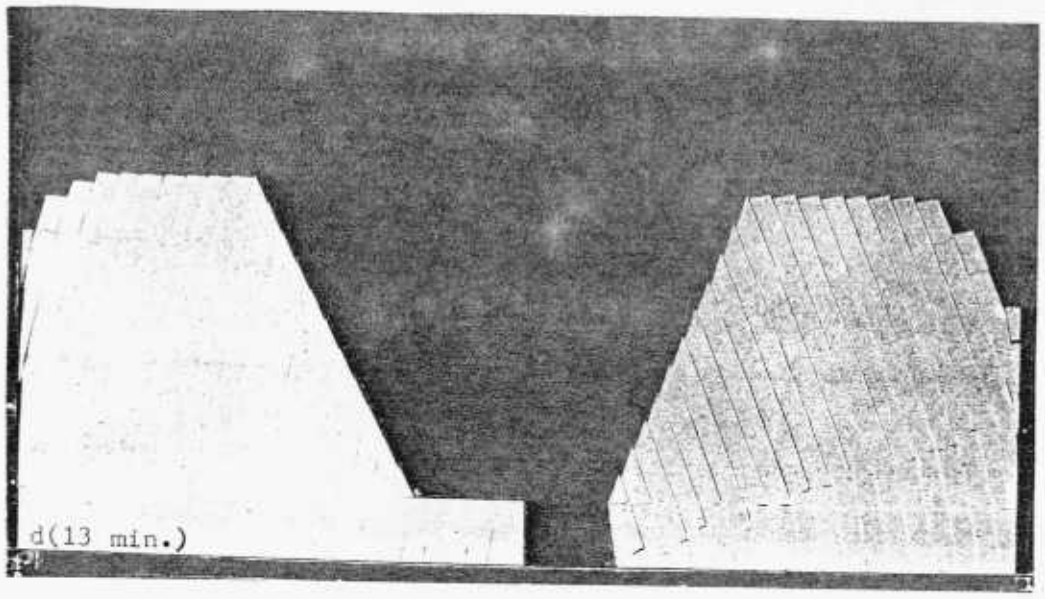
d(13 min.)

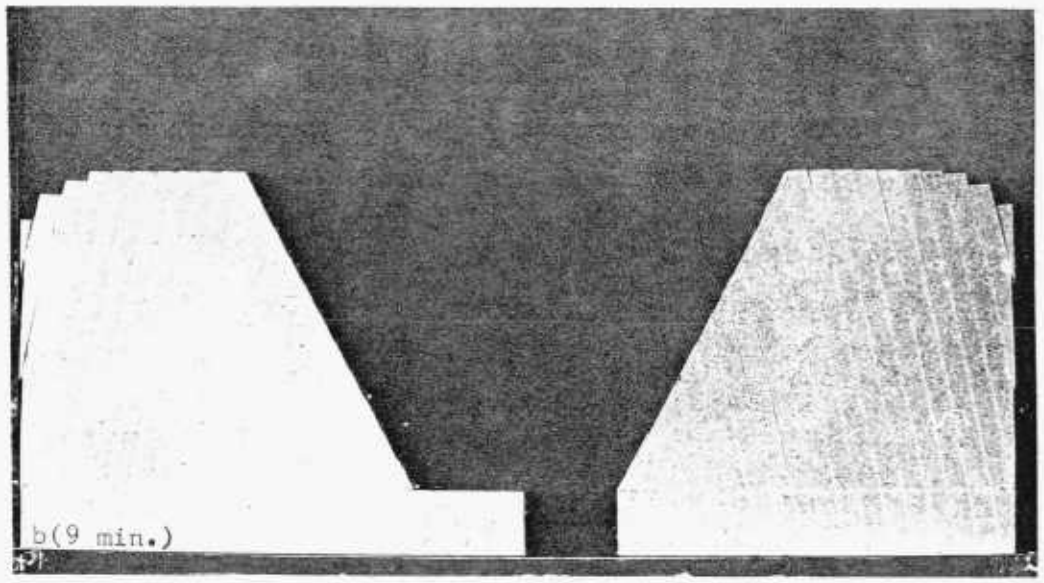
b(9 min.)

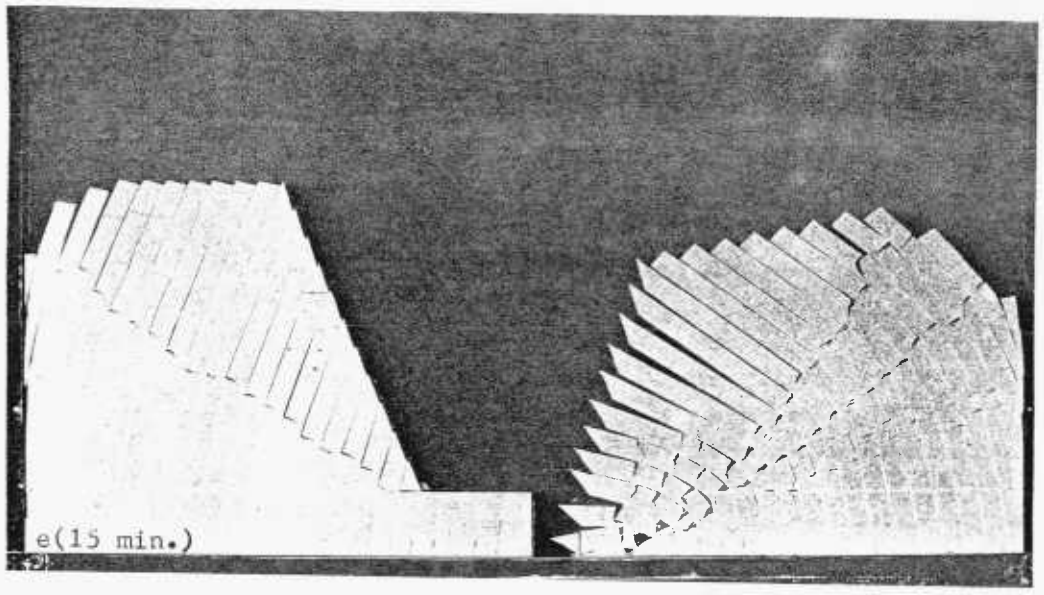
e(15 min.)

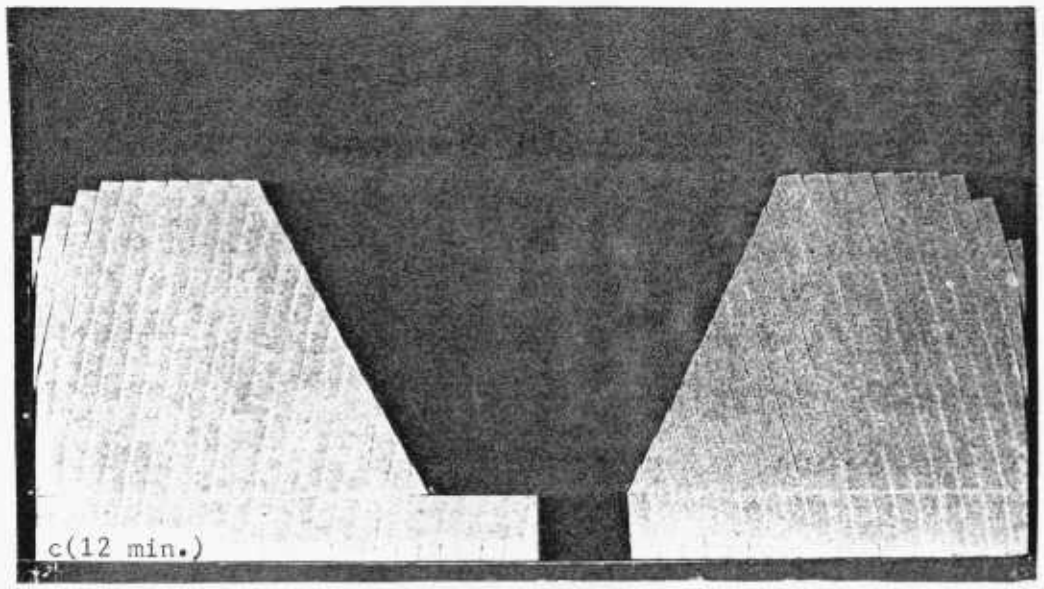
c(12 min.)

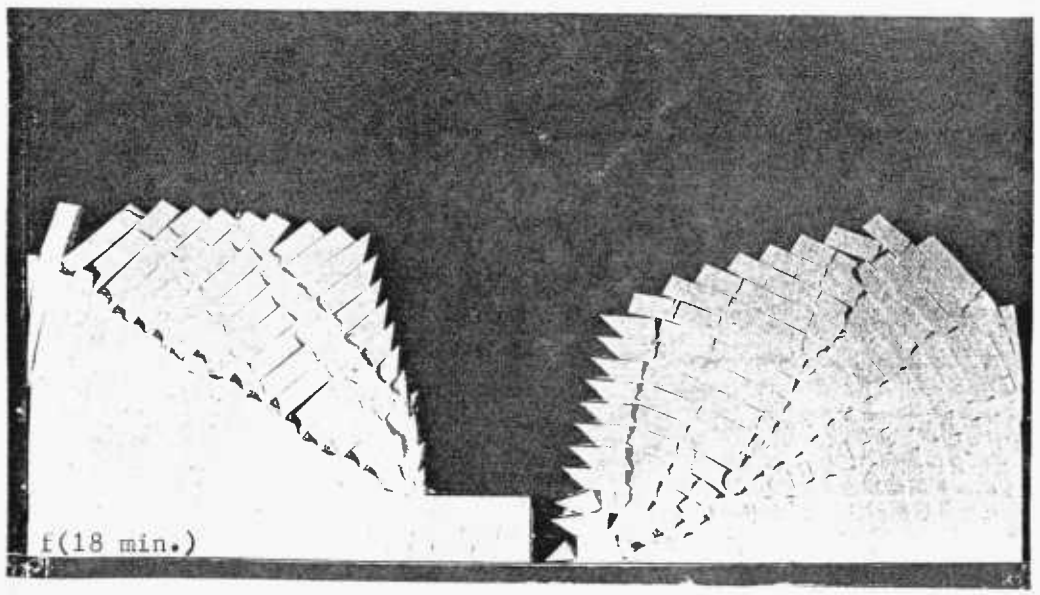
f(18 min.)

dated; however, it was an interesting test to demonstrate the support provided by the toe block(s) against rotation. Both slopes, resting on the steel frame, were a copy of 3(L) or 4(R) with the exception of joint dip which was 70° in this test. A run of 30 minutes did not make any considerable change in slope configurations, but the mobilisation of shear strength along the joints was recognizable from the displacements along the slope face. Even the lying down of the little triangular block at the toe did not suffice to bring about failure, but the block next to it seemed to be the key one, and as this block was taken away toppling was initiated with the formation of a critical crack path within a minute in the right slope, and within a couple of minutes in the left slope.

MODELS 8 and 9 (R & L) - See Plate 3-VI

To investigate the influence of slope height on the behaviour of a rock slope traversed by a toppling joint set, Models 8 and 9 were built having slope heights of 18" and 21" respectively. The other dimensions were identical: slope angle = 60°, joint dip = 70°, joint spacing = 1". Contrary to expectations it took longer for the higher slope to fail. To find out whether this outcome was coincidental Test No. 10 which will not be described here, was carried out with a slope height of 24". Surprisingly enough it needed even more time (42 minutes) to develop a critical crack path as the sign of instability, thus confirming the reliability of Models 8 and 9. The reason for this behaviour was sought, and eventually it

PLATE 3.V- Base Friction Model No.6.

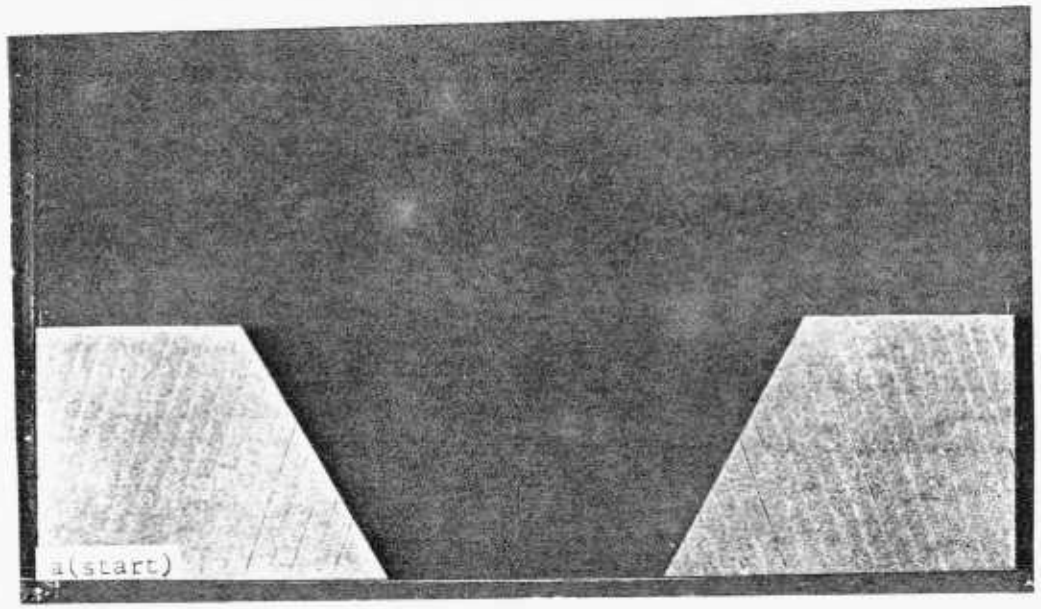
a(start)

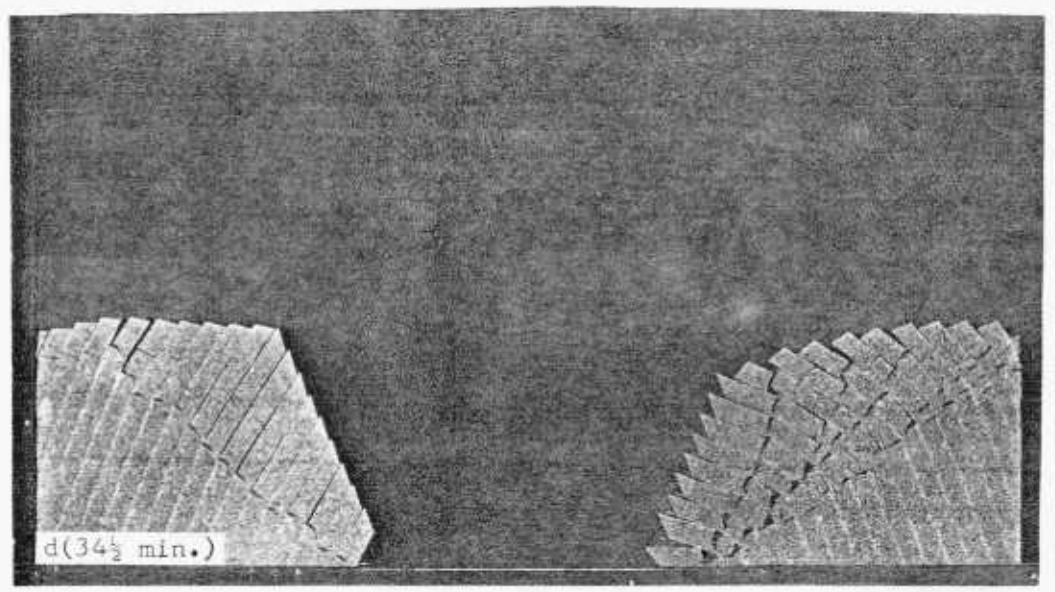
d(34½ min.)

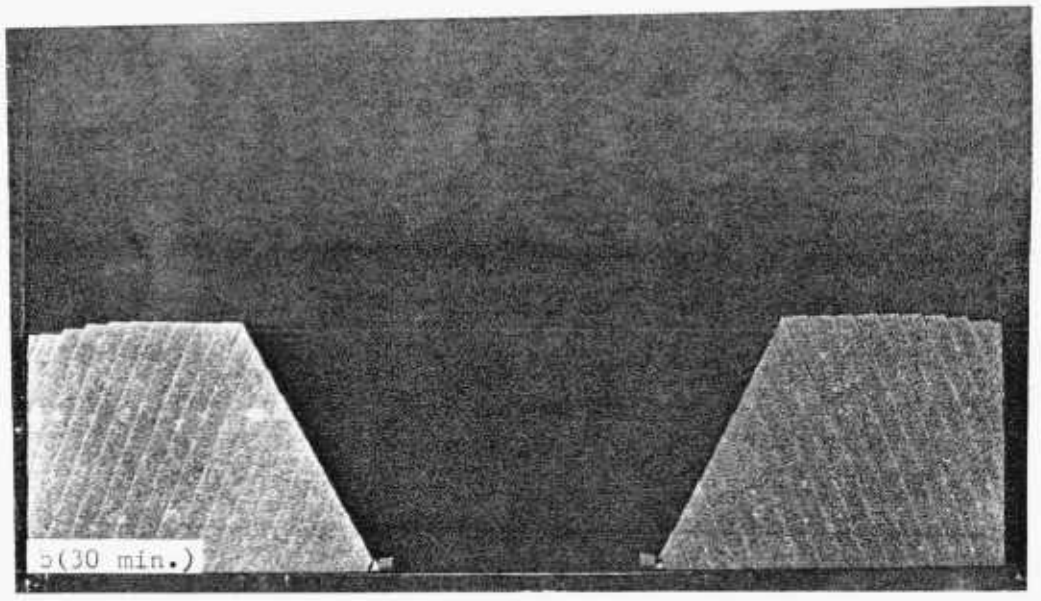
b(30 min.)

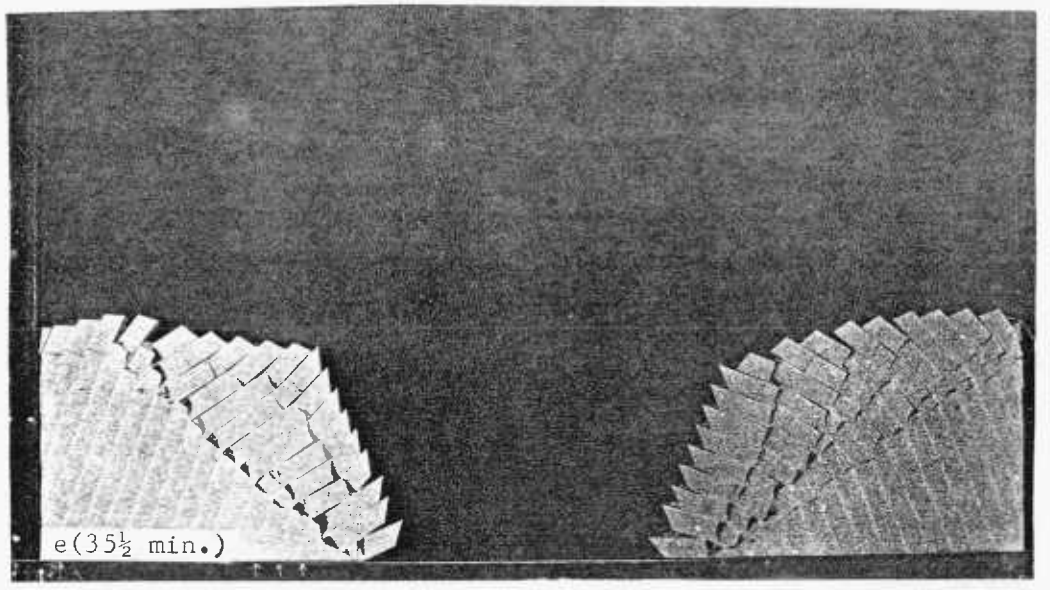
e(35½ min.)

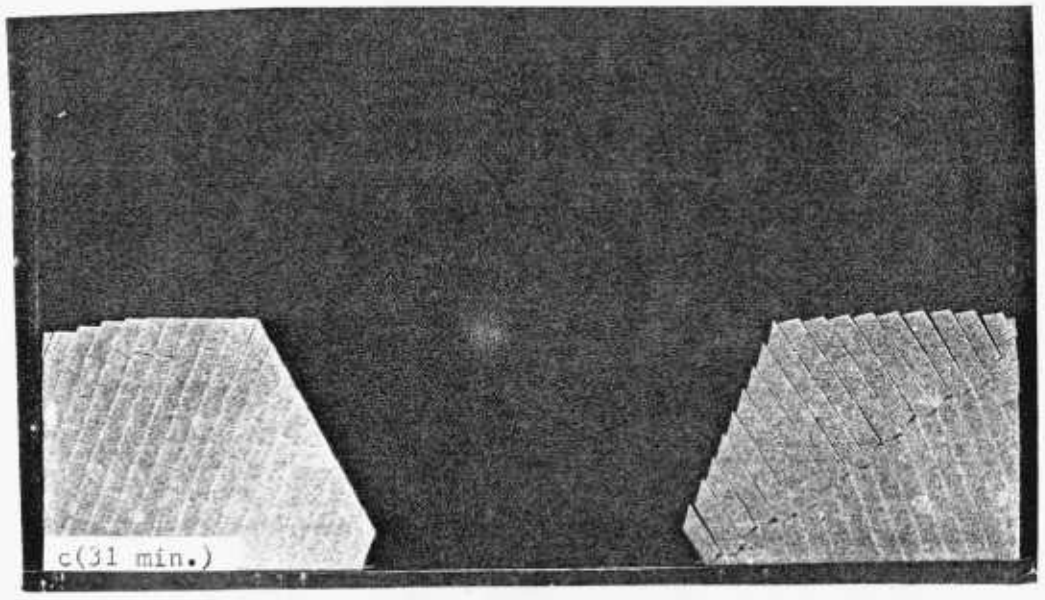
c(31 min.)

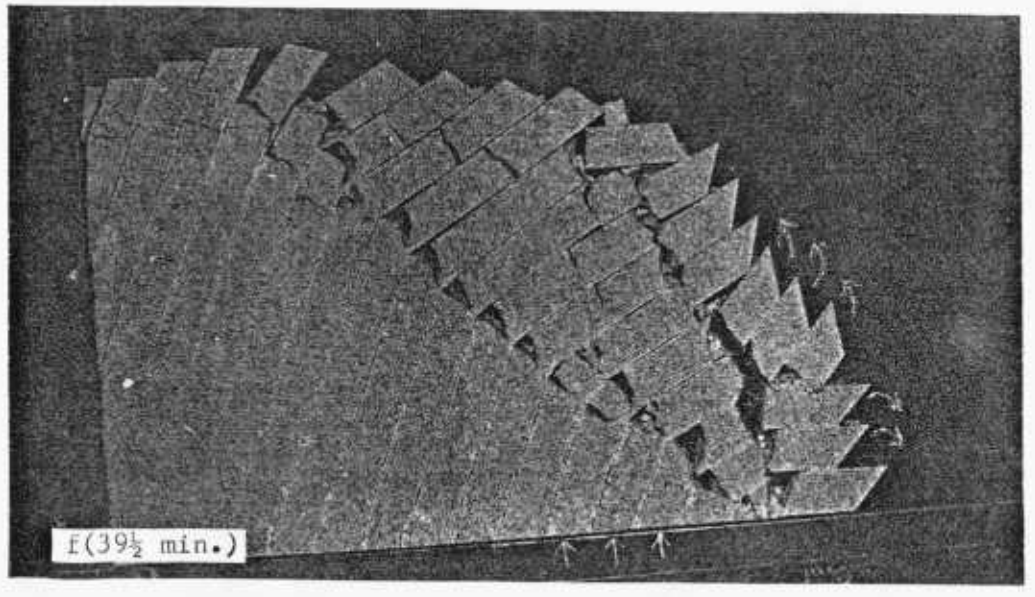
f(39½ min.)

was found that the number of columns comprising the slope bottom was increasing with height because the slope surface was being kept constant (10") for all models. Consequently, it was thought that with the increasing number of columns at the lower part of the slope, the overall flexural strength of the columns was also increasing, thus producing a greater resistance to rotation. This phenomenon was further investigated with model 13 where the number of columns at the bottom was brought down to 20 from 22 (of Model 10), and the failure started to take place in 2 minutes incredibly. On the other hand, comparison of Models 9(R) and 13 supports the general trend that as the slopes get higher, the more unstable they become. Increasing the slope height from 21" to 24" dropped the failure initiation time from 21 minutes to 2 minutes (slope angle = 60^{o}, joint dip = 70^{o} for both models). Although there seems to be a contradiction between this and previous findings regarding the slope height versus stability, there is not, in fact, because this time the numbers of columns constituting the bottom of the slopes were equal (20 columns).

The test results covering Models 6, 7, 8, 9 and 10 are presented graphically in Figure 3.2. Table 3.3 also summarizes the results of the tests carried out to examine the slope height variation. From these, together with the test photographs one can draw the following conclusions:

a. Tests were conformable with each other, but right slopes of every model failed earlier, while the critical crack path angles for left slopes were greater.

b. Quite a resemblance was found between right and left slope

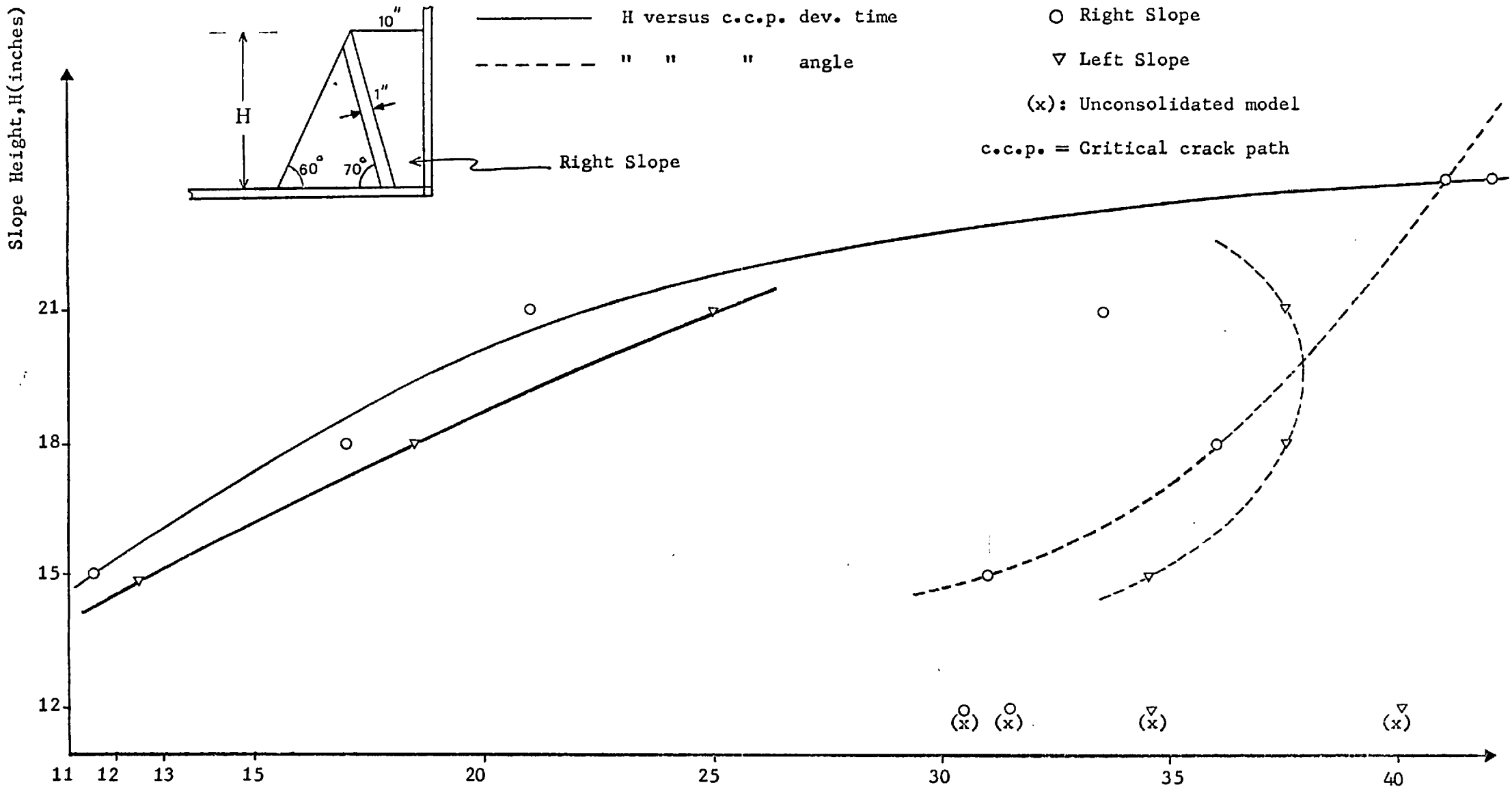

Figure 3.2- Effect of slope height on critical crack path parameters.

MODEL NO.	SLOPE ANGLE	JOINT DIP	SLOPE HEIGHT	CR. CRACK PATH DEV. TIME (min)		CR. CRACK PATH INC.		REMARKS
				R. SLOPE	L. SLOPE	R. SLOPE	L. SLOPE	
6	60°	70°	12"	30	34	31.5°	40°	Consolidation of model forgotten. Triangular adjacent toe blocks removed.
7	60°	70°	15"	11.5	13	31°	34.5°	Triangular toe blocks removed.
8	60°	70°	18"	17	18.5	36°	37.5°	
9	60°	70°	21"	22	25	33.5°	38.5°	
10	60°	70°	24"	40	-	41°	-	Only right slope built.

Table 3.3 Slope Height Variations.

PLATE 3.VI- Base Friction Models No.8 and 9.

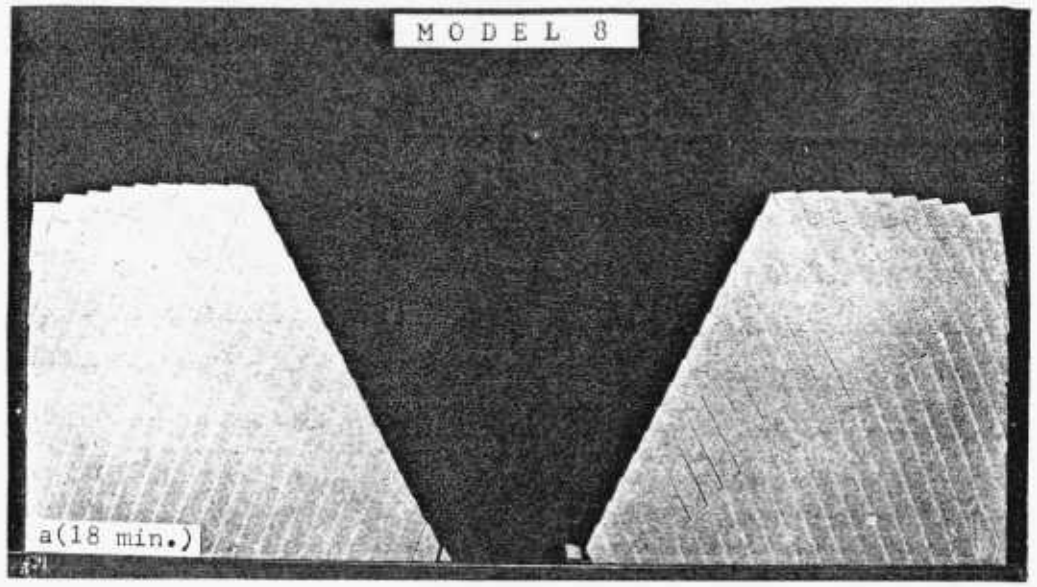
MODEL 8
a(18 min.)

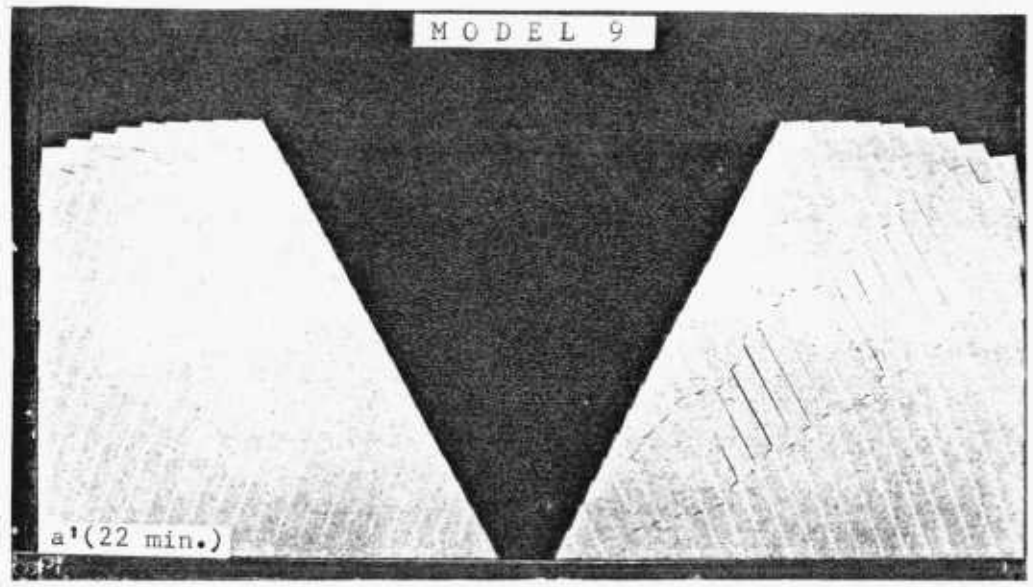
MODEL 9
a'(22 min.)

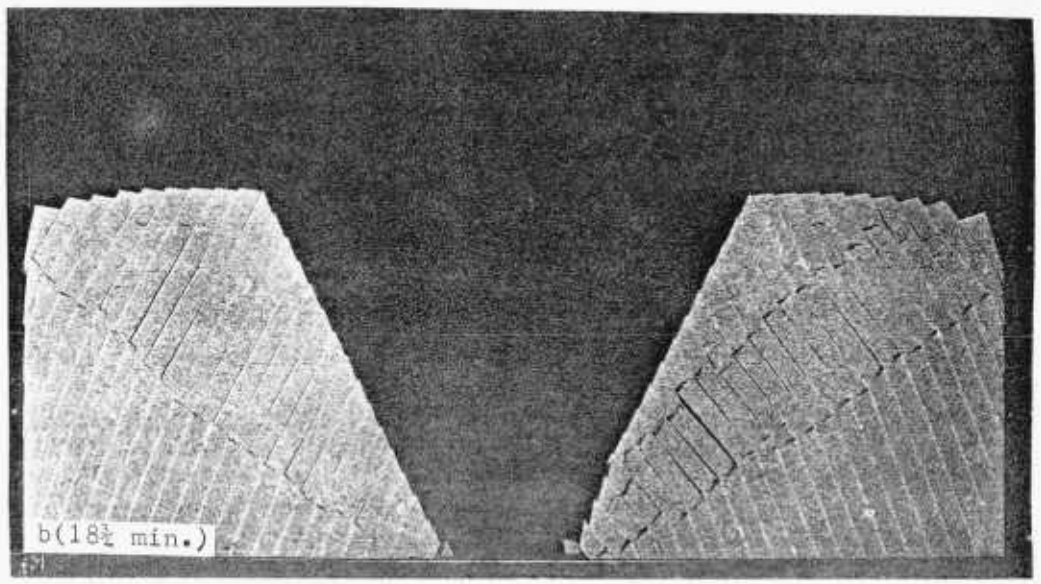
b(18½ min.)

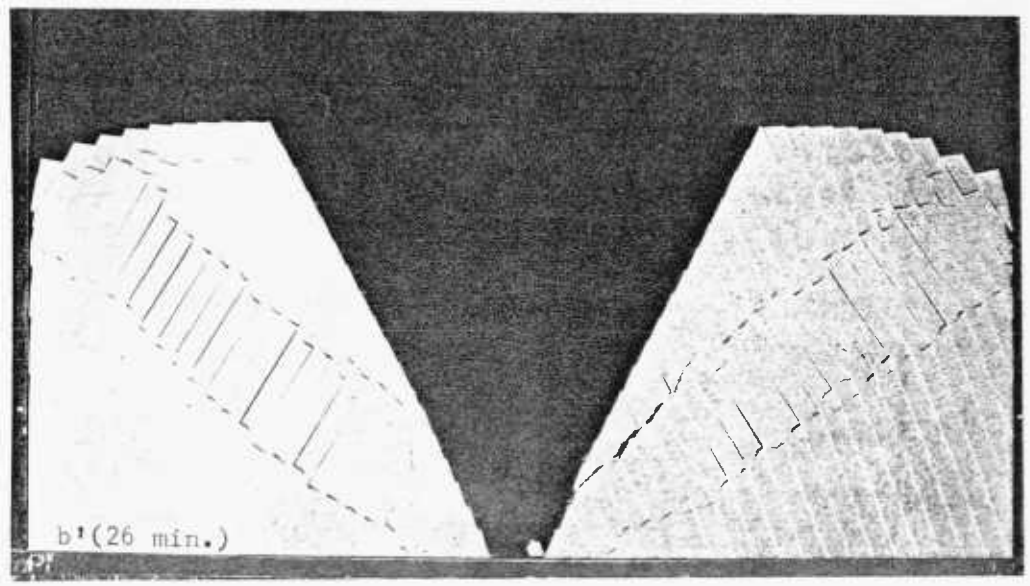
b'(26 min.)

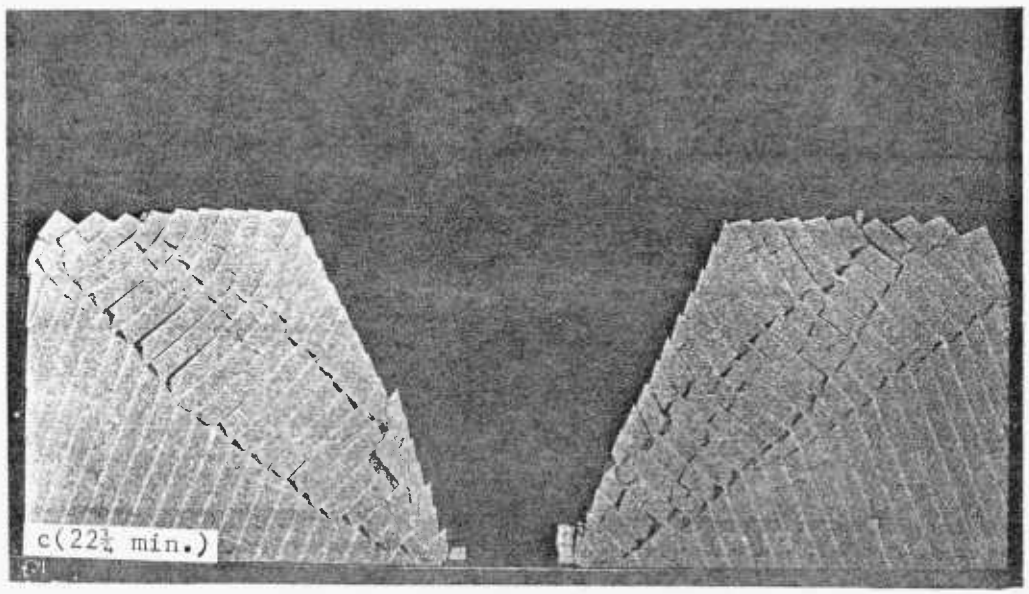
c(22½ min.)

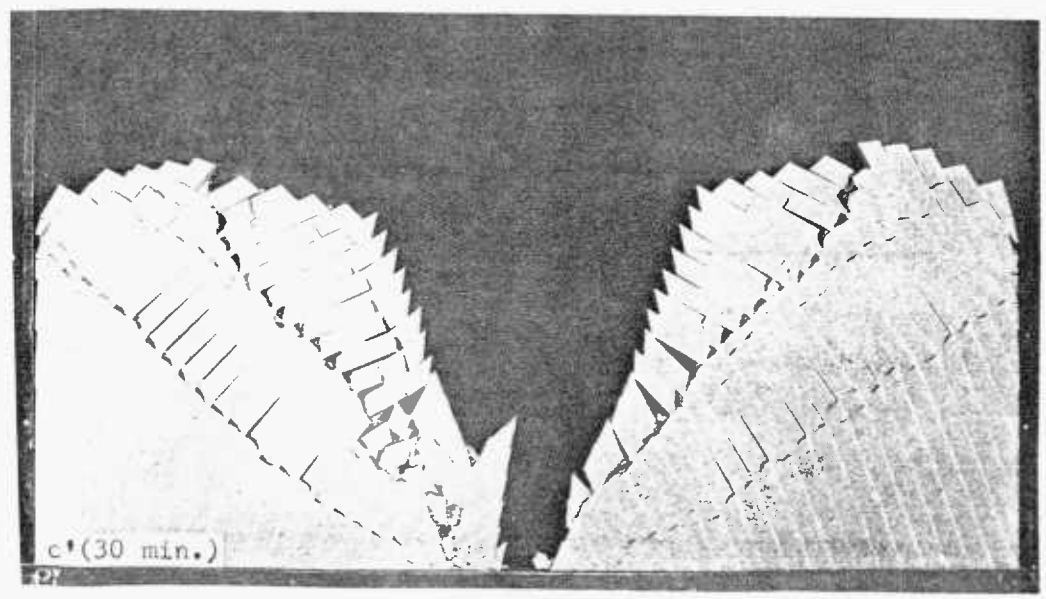
c'(30 min.)

behaviour. Almost the same sort of critical crack path developed in both slopes. A depression formed in both slope surfaces. The slope face rotated upward in both of them.

Another interesting failure, which was observed in Models 8 and 9 especially, was the formation of "kink bands" described by Hammett[1] as the zone of rotating block columns. Although he related this phenomenon specifically to underground openings, this seems to be unjustified for the simple reason that each whole column may not always rotate in one piece especially when the slope is made up of long, slender and/or low flexural strength columns, but instead they break into pieces forming isolated zones of columns which rotate almost independently instead.

MODELS 11 and 12 (R) - See Plate 3-VII

Models 11 and 12 were designed to study the variation of slope angle and the number of columns forming the base of the slope. Both models had a slope angle of 70^{o}, a joint dip of 70^{o} and a height of 24", the only difference being the number of columns at the base which was 17 for Model 11 and 22 for Model 12. Both slopes cracked after a minute to form the critical crack paths at about the same inclination. Similar movements took place in both slopes, such as the formation of a wedge in the middle and consequent crushing of the toe region, dilation of the mass and bulging of the slope face, and a seemingly backward rotation of columns at the slope face due to toe support.

MODEL 11

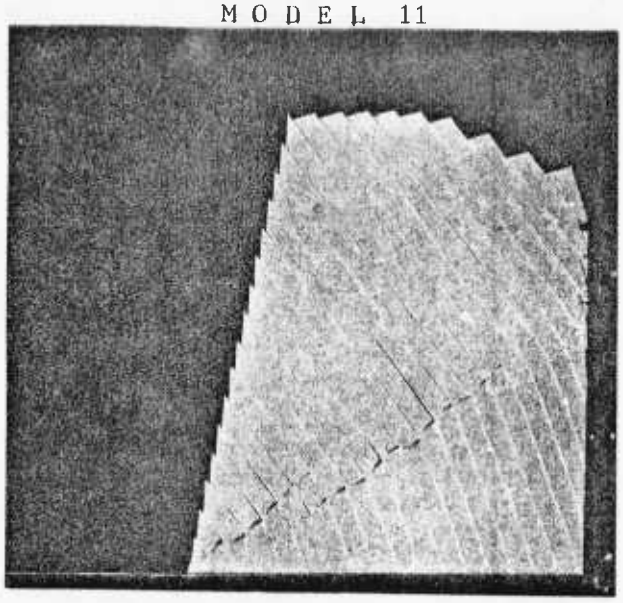

a(2 min.)

MODEL 12

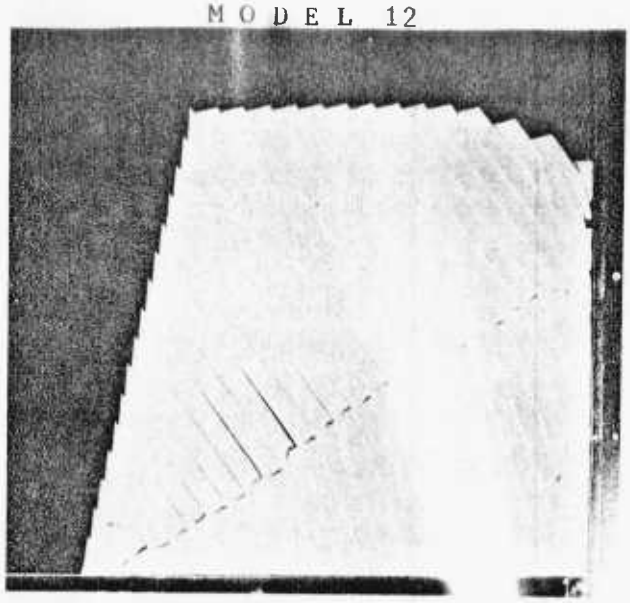

a'(2 min.)

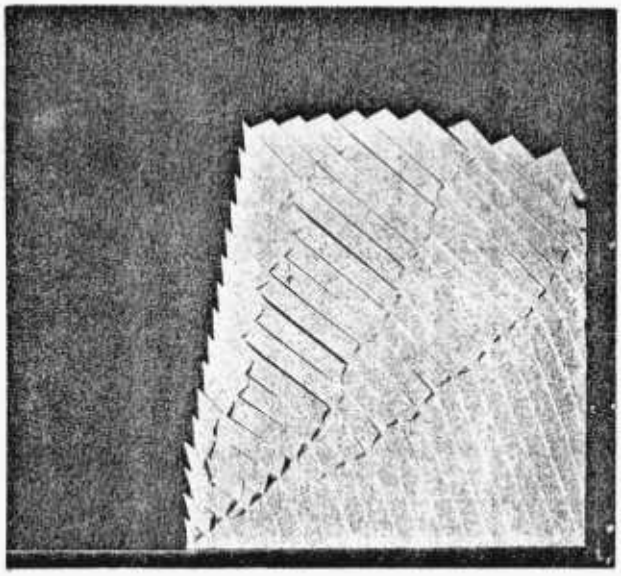

b(3 min.)

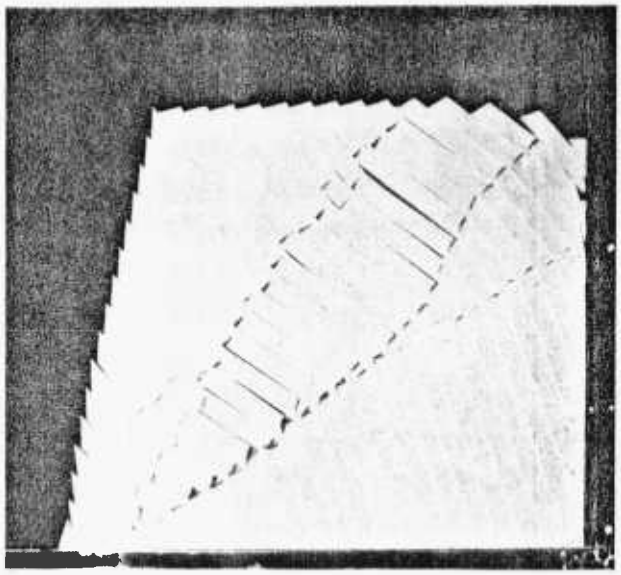

b'(3 min.)

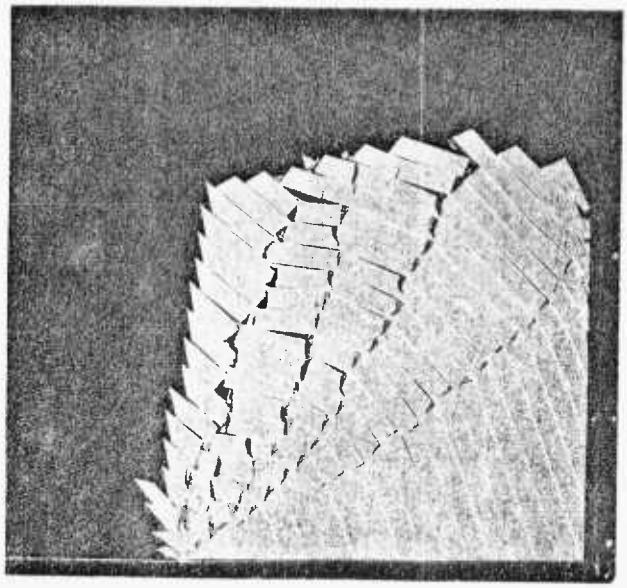

c(4 min.)

PLATE 3.VII- Base Friction Models No. 11 and 12.

Contrary to earlier observations, the number of columns appeared to have no effect in these tests. This could be explained with the increasing slope angle. It may be assumed that when a slope is steeper than a critical inclination (60^{o} seems to be quite a probable value) the other parameters, such as number of columns for instance, count for little. As a matter of fact, comparison of Models 12 and 10, both having the same number of columns (22), reveals the significance of slope angle variation: An increment of 10^{o} (from 60^{o} to 70^{o}) in slope angle reduced the critical crack path development time drastically from 42 minutes to 1 minute only.

MODEL 2'(L) - See Plate 3-VIII

To investigate the influence of boundaries some of the previous slopes were reconstructed so as to lessen the boundary effects. Model 2'(L) was built as a boundary-effect-free counterpart of Model 2(L). The distance from the pit bottom to the steel frame boundary was equal to the slope height, while the slope surface was extended to three times the slope height. In this test too, it took 2 minutes for the first line of cracks to appear within the slope, but it was a little flatter. As far as the kinematics of the rock mass was concerned, both slopes appeared to be quite in agreement as seen in the photographs, the only exception being the location of the critical crack path which passed above the toe in Model 2'(L).

PLATE 3.VIII- Base Friction Model No.2'.

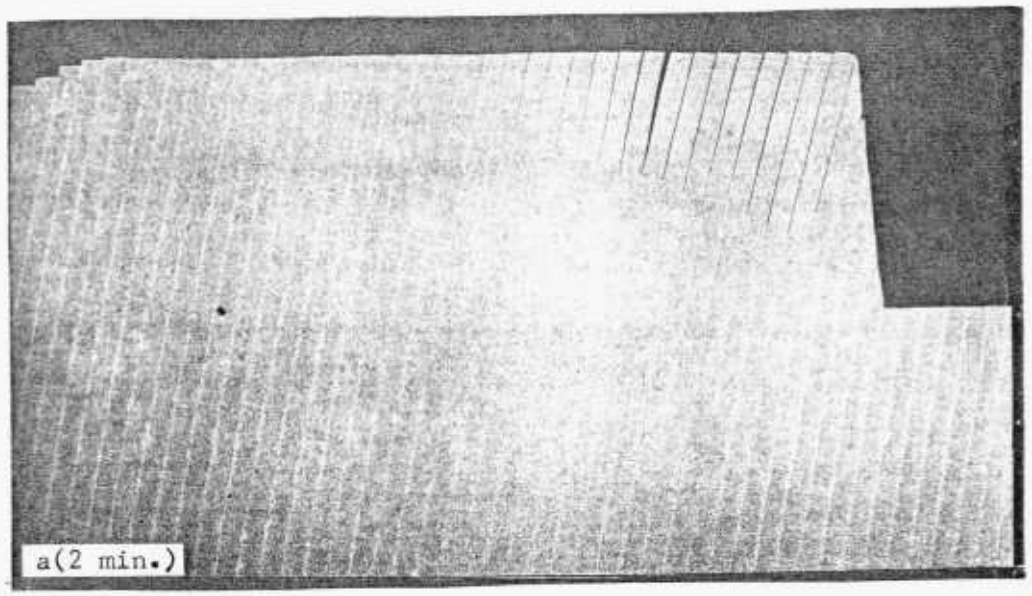

a(2 min.)

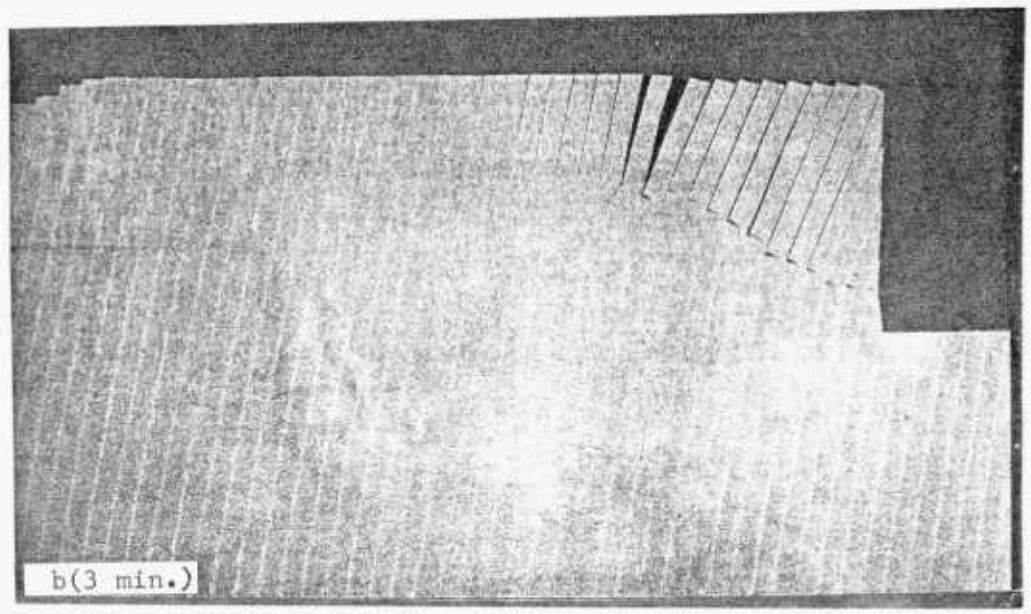

b(3 min.)

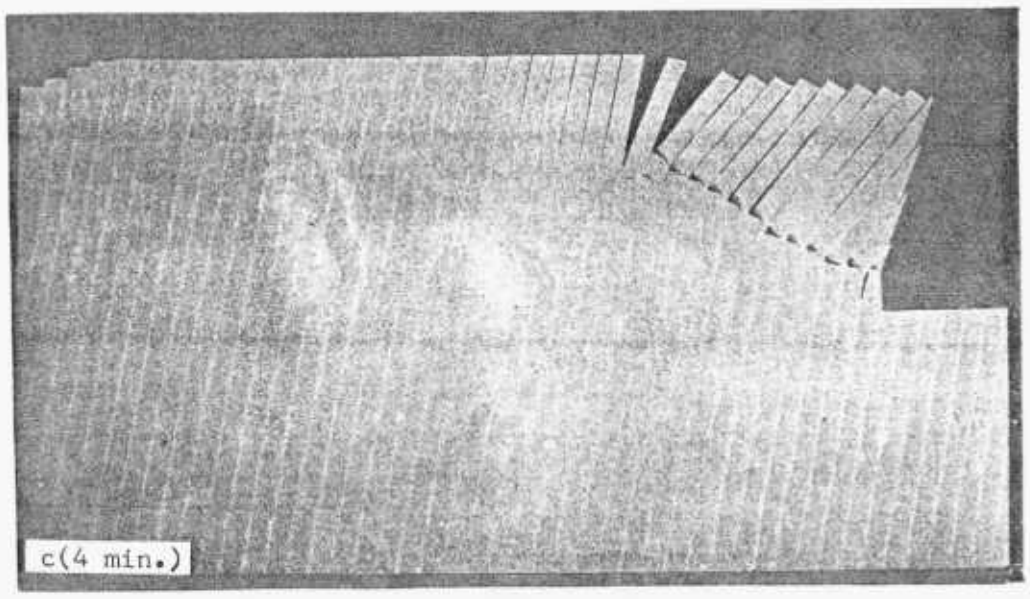

c(4 min.)

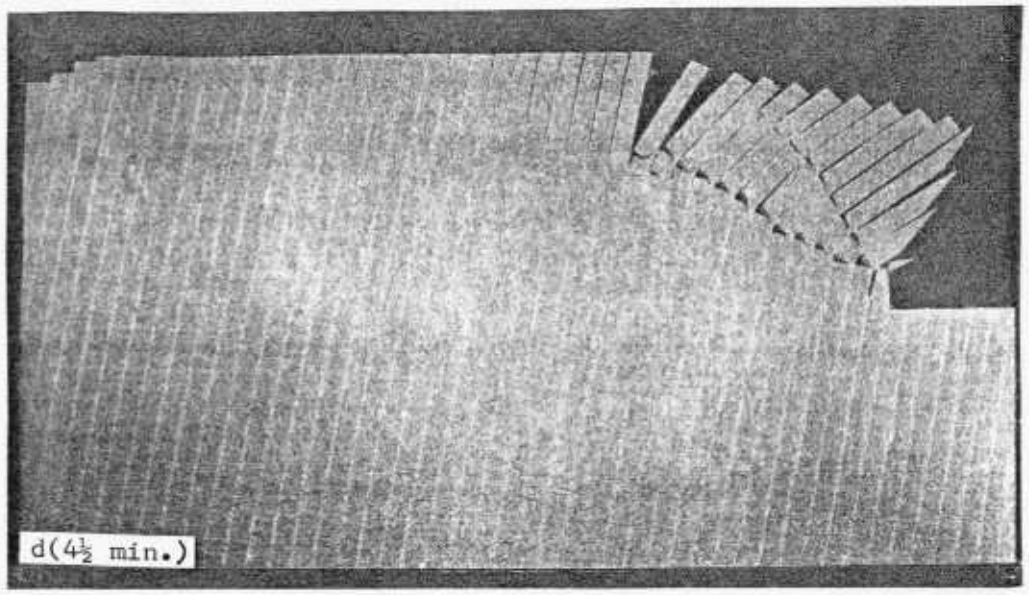

d(4½ min.)

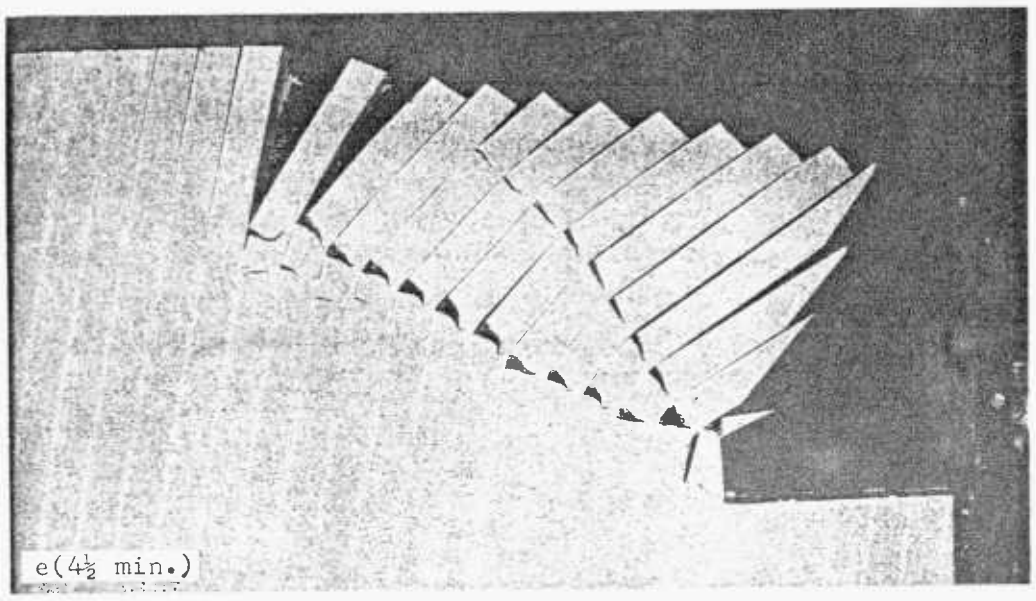

e(4½ min.)

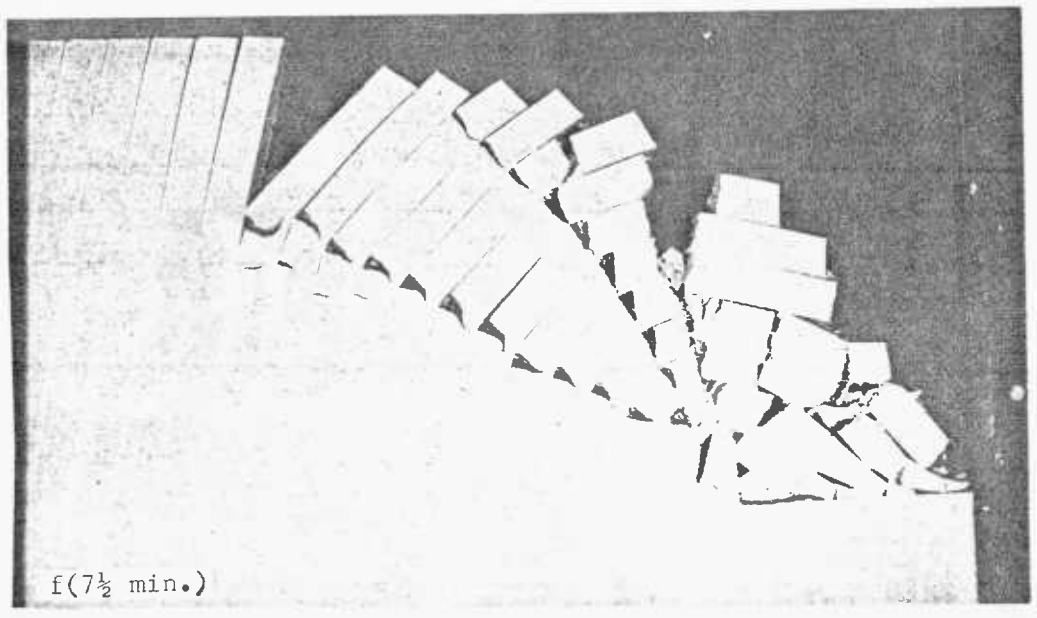

f(7½ min.)

MODEL $2'_1$(L) - See Plate 3-IX

This model exhibits the adverse effects of deepening a slope. Increasing the slope height from 12" (Model 2'(L)) to 15" (this model) increased the extent of disturbance behind the crest drastically. As one may gather from the photographs the disturbance in this model extended more than twice the height of the slope, whereas in the previous model it was equal to the slope height. However, in another test repeating the Model 2'(L) the critical crack path passed through the toe and the disturbance at the top was equal to twice the slope height. Fresh sandpaper might also be considered as the cause of the discrepancy.

The following aspects of the model behaviour should also be noted:

a. -the easy and quick yielding of the toe block(s), first by tensile fracturing at the bottom, then by rotation owing to its columnar character produced by steep slope inclination,

b. -formation of a series of tension cracks at the top, starting from the back and proceeding towards the crest.

MODELS 11 and 11' - See Plate 3-X

To study the boundary effects further Test 11' was run duplicating Model 11. To be able to accommodate the model on the table as boundary-effect-free the slope height and the joint spacing were halved. Thus, the ratio of slope height to joint spacing remained constant. Normally, one would have thought that the reduction in scale should have

PLATE 3.IX- Base Friction Model No.$2'_1$.

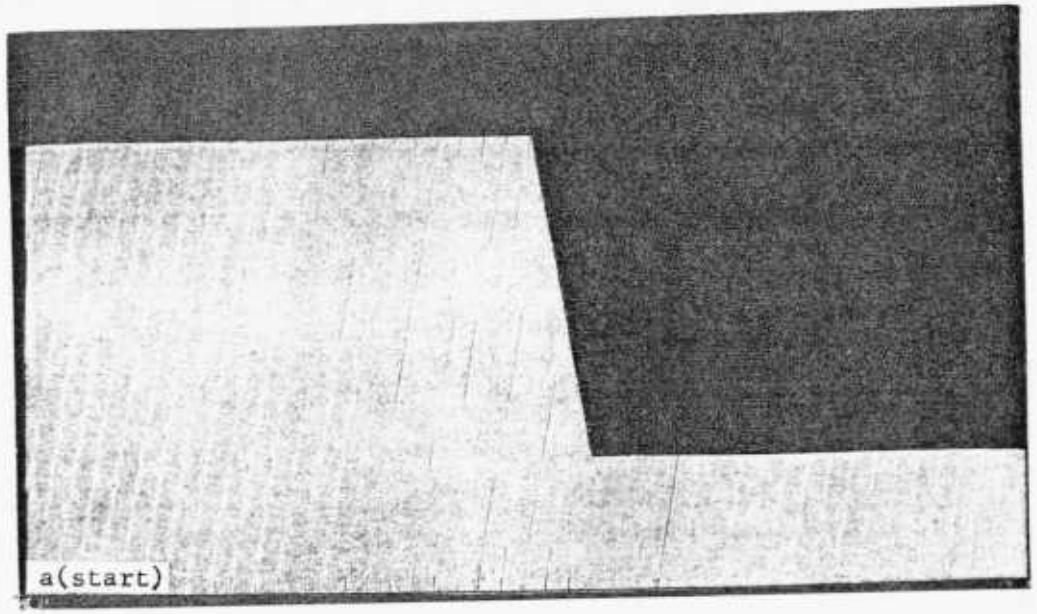
a(start)

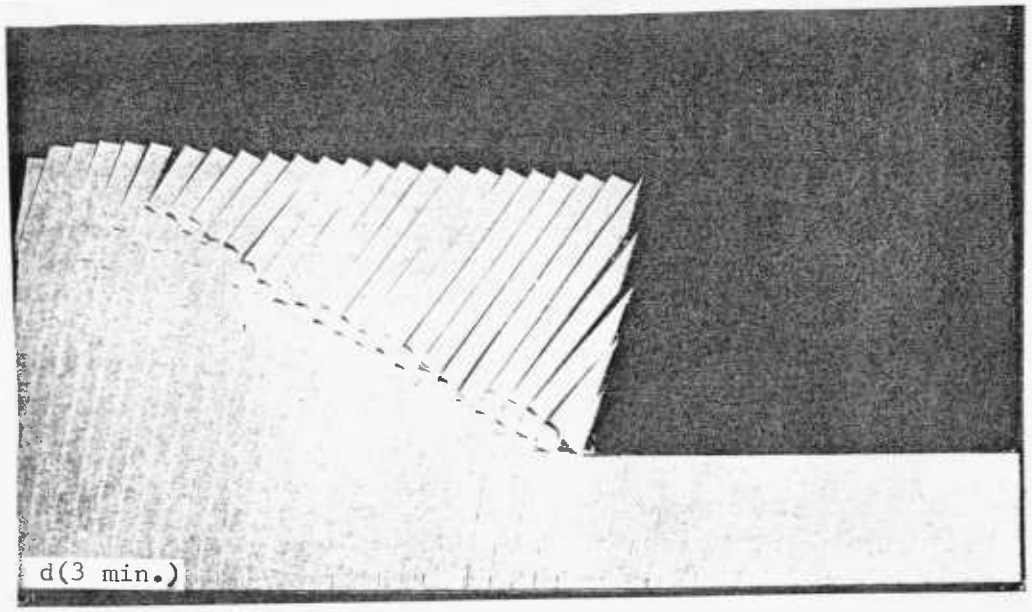
d(3 min.)

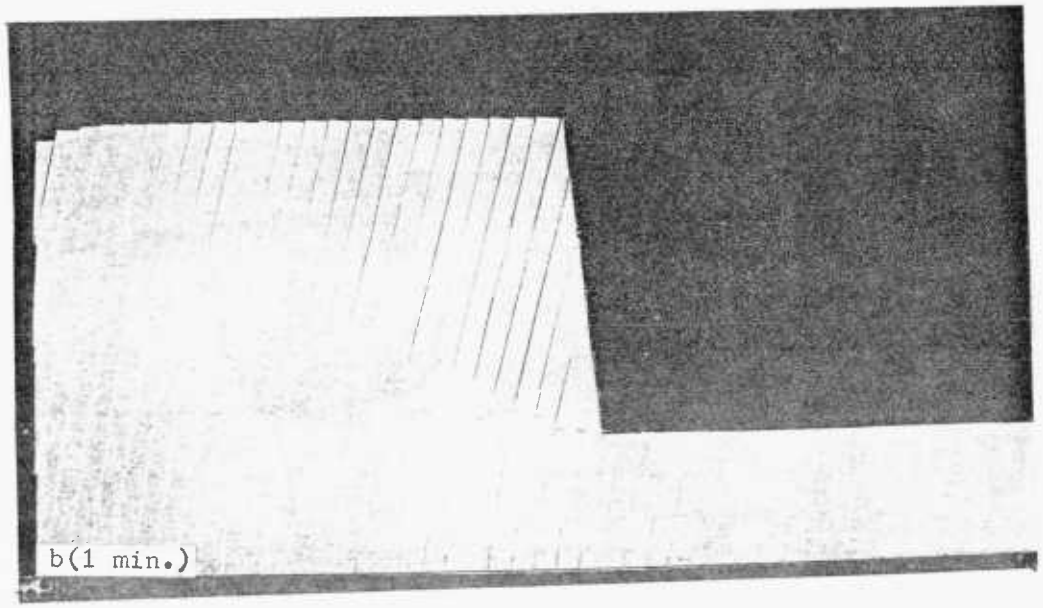
b(1 min.)

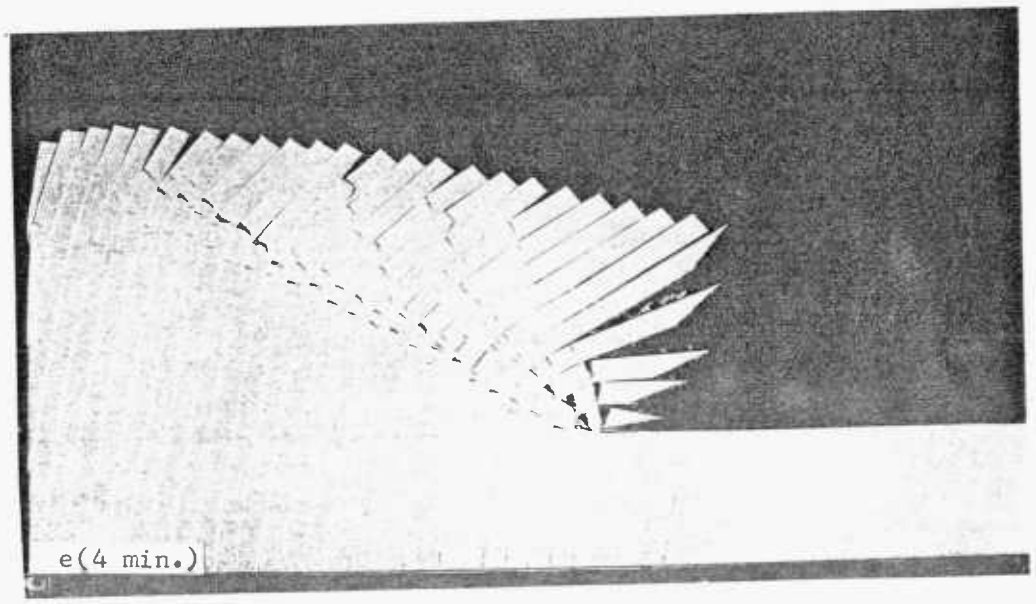
e(4 min.)

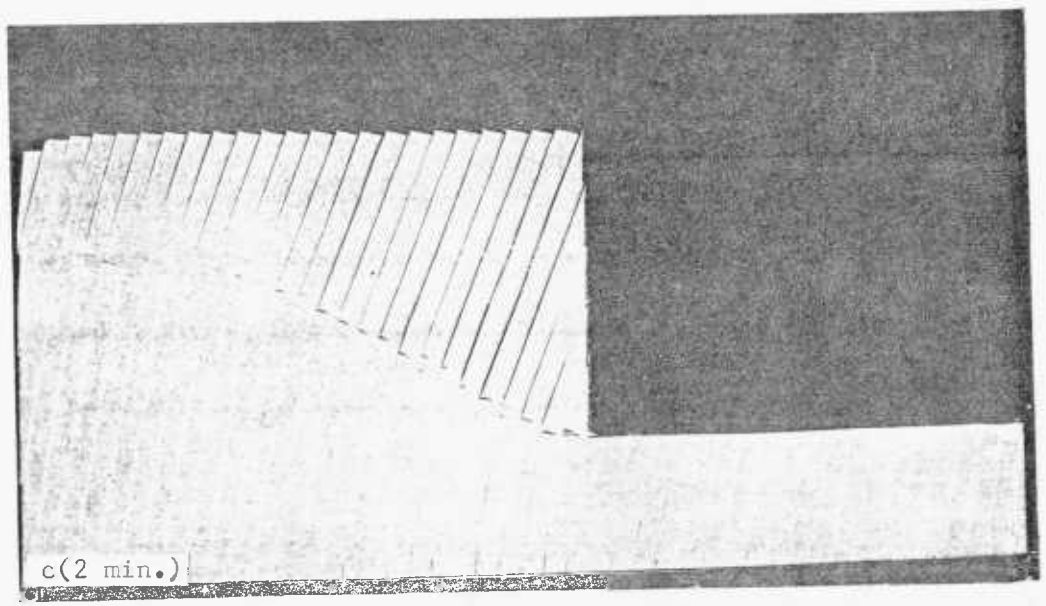
c(2 min.)

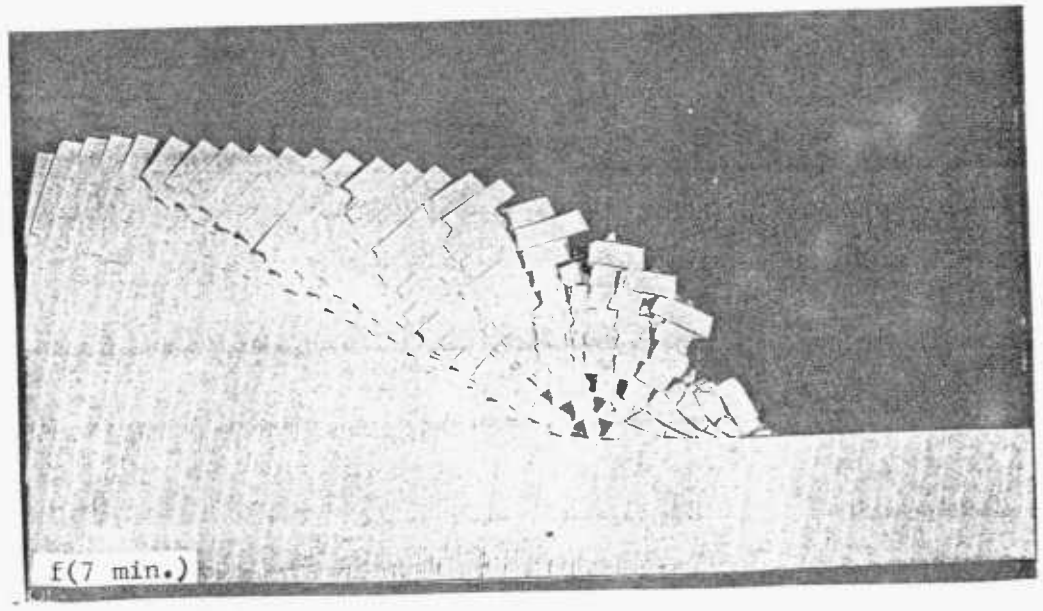
f(7 min.)

involved the third dimension, namely the thickness of the slab, for a better adjustment of column flexural strength. But this was not practicable in this instance.

As can be seen in the photographs both slopes failed within a minute forming the critical crack paths of almost equal inclination. The general trend of movements was identical, Model 11' being a bit quicker probably because of the less used sandpaper on left hand side again. Obviously, the important disagreement between these two tests was the striking of the critical crack path above the toe point in Model 11'. The occurrence of the same thing in Model 2'(L), if not a coincidence, leads one to the conclusion that the boundary-effect-free slopes, which are presumably more representative of real ones, yield not at the toe but above it. This is probably because of the support provided by the material surrounding the toe to make this zone firmer and stronger in boundary-effect-free models.

MODEL $11'_R$ - See Plate 3-XI

As the reproduction of Model 11' this test displays a very good example of repeatability as far as the base friction modelling technique is concerned. The critical crack path formation time and inclination, mass behaviour, and even the location of tension cracks were reproduced in this test. The only discrepancy was the route of the critical crack path in the toe region. As happened in Model $2'_R$(L) when conducted as the duplicate of 2'(L), this duplication too let the critical crack path pass through the toe point, dis-

PLATE 3.X- Base Friction Models No. 11 and 11'.

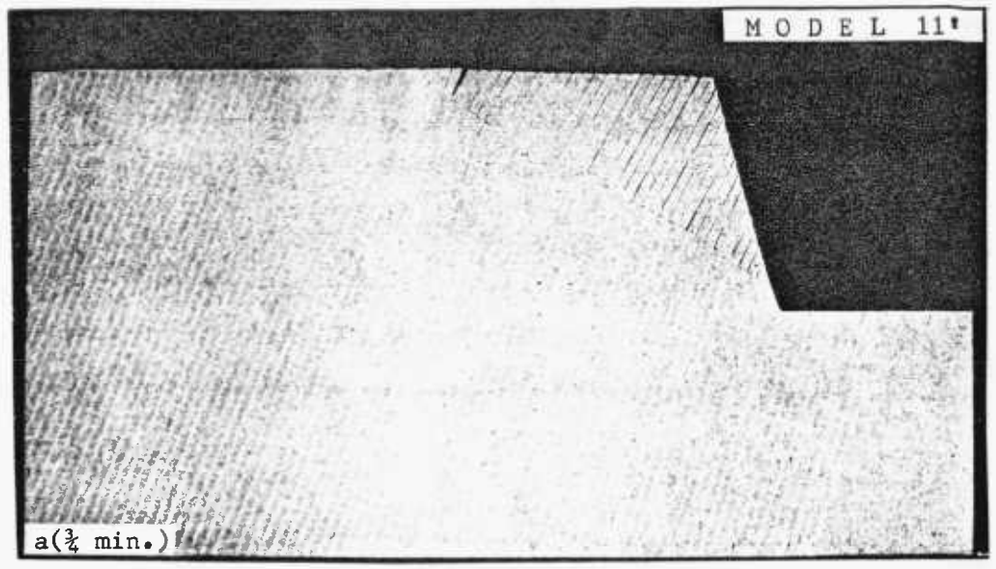
MODEL 11'
a(¾ min.)

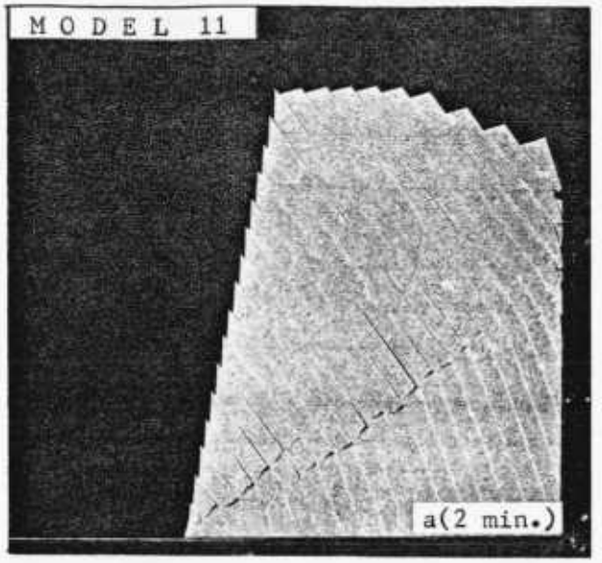
MODEL 11
a(2 min.)

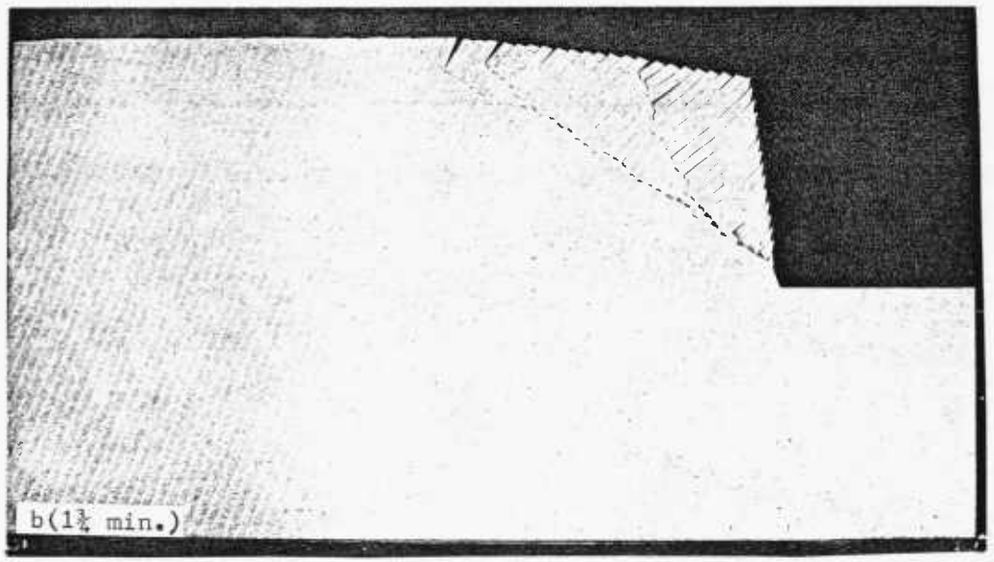
b(1¾ min.)

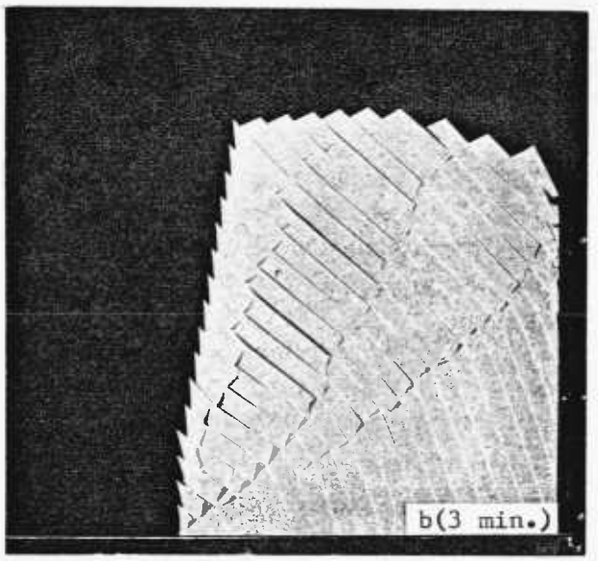
b(3 min.)

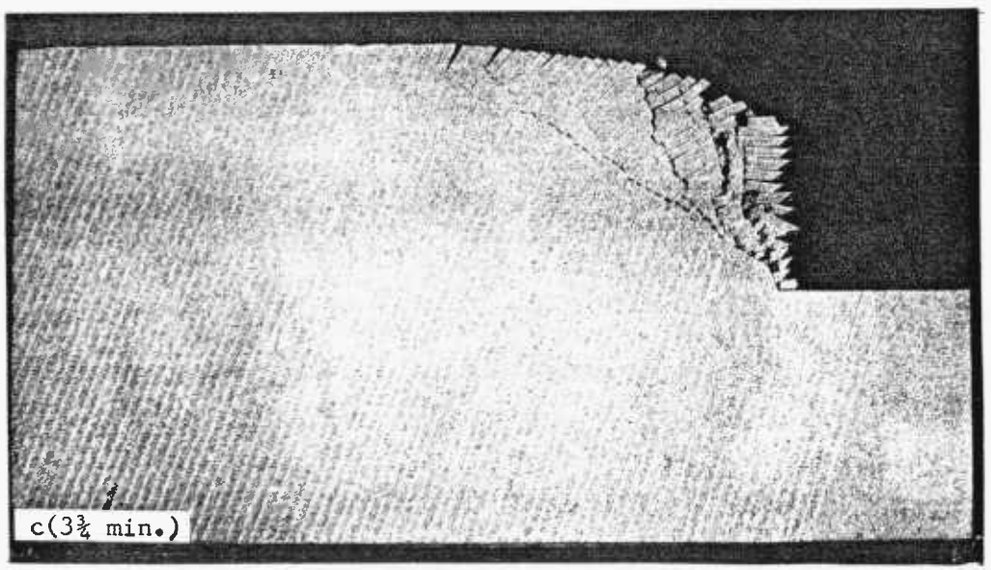
c(3¾ min.)

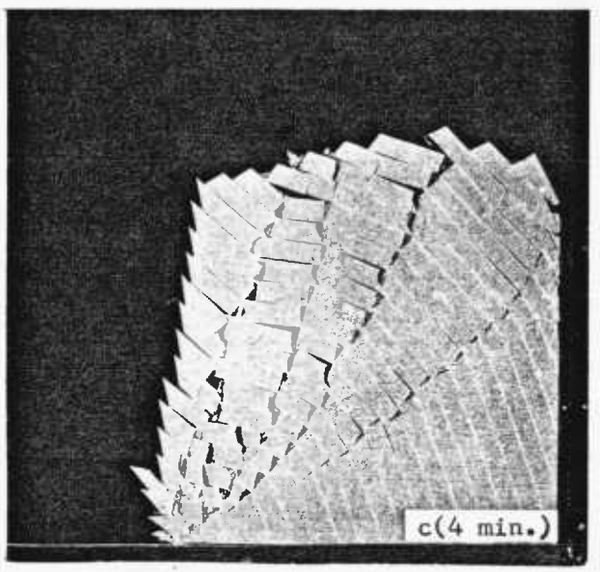
c(4 min.)

PLATE 3.XI- Base Friction Model No.$11'_R$.

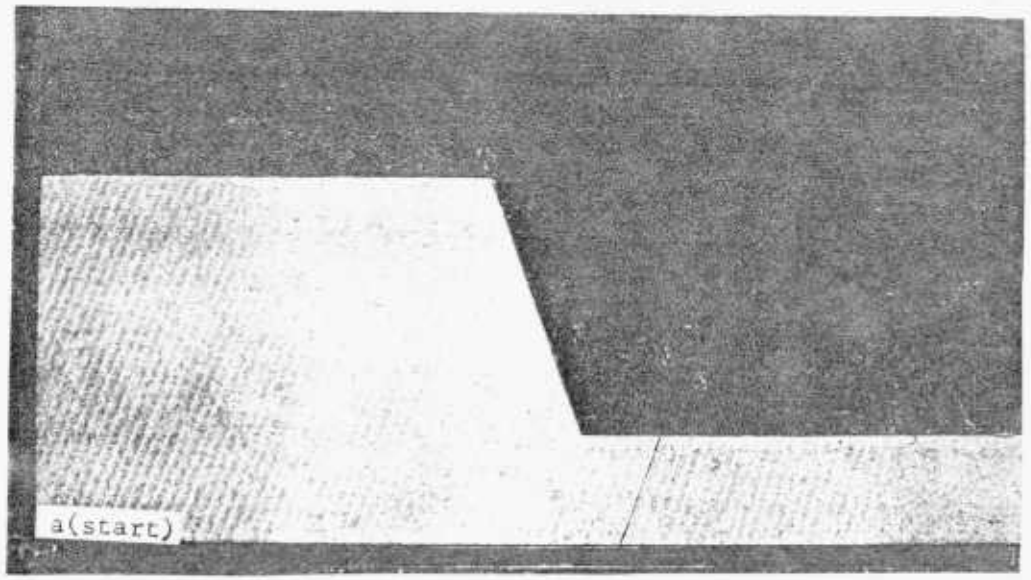
a(start)

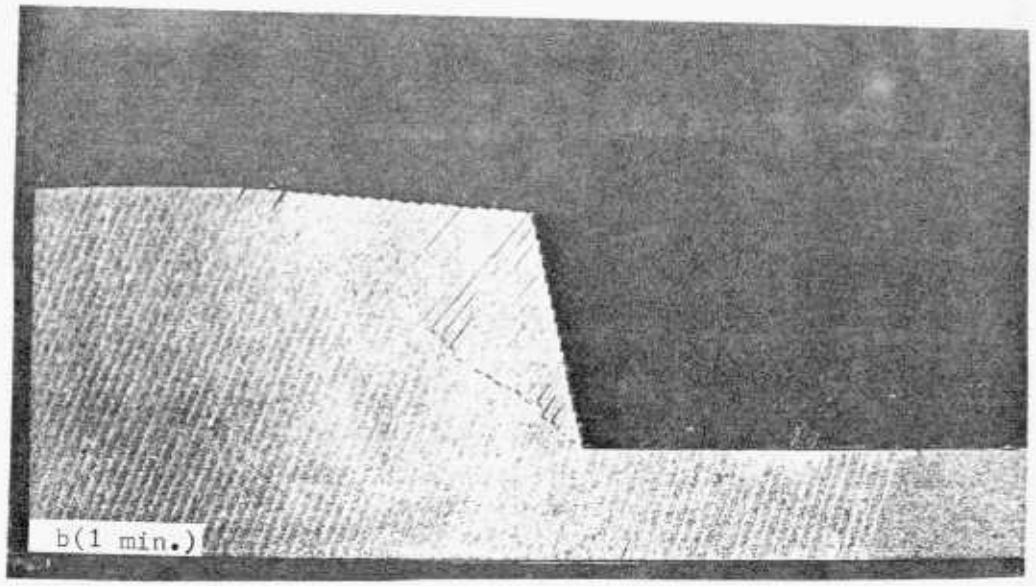
b(1 min.)

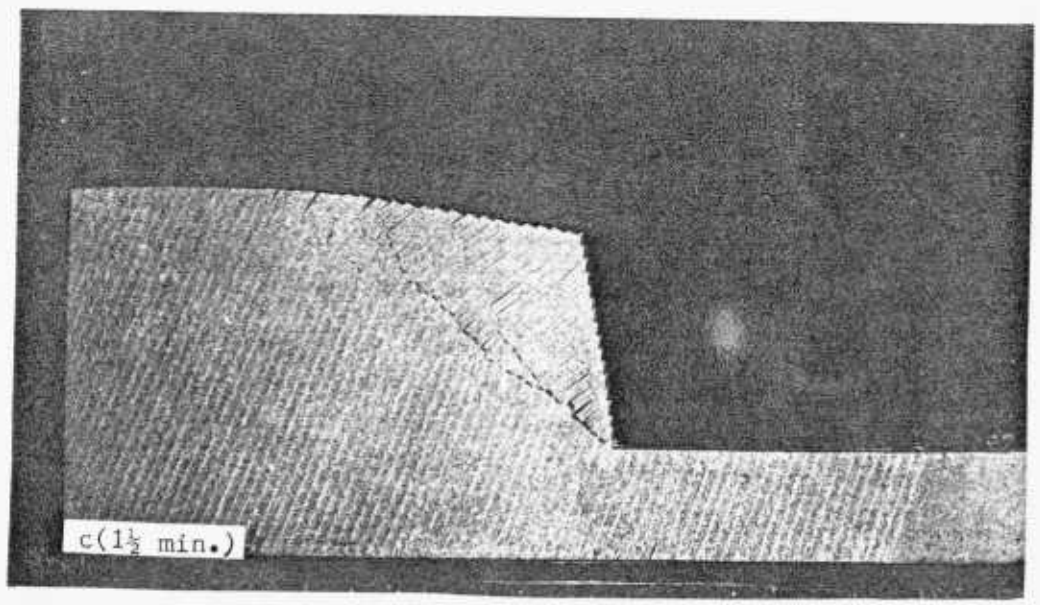
c(1½ min.)

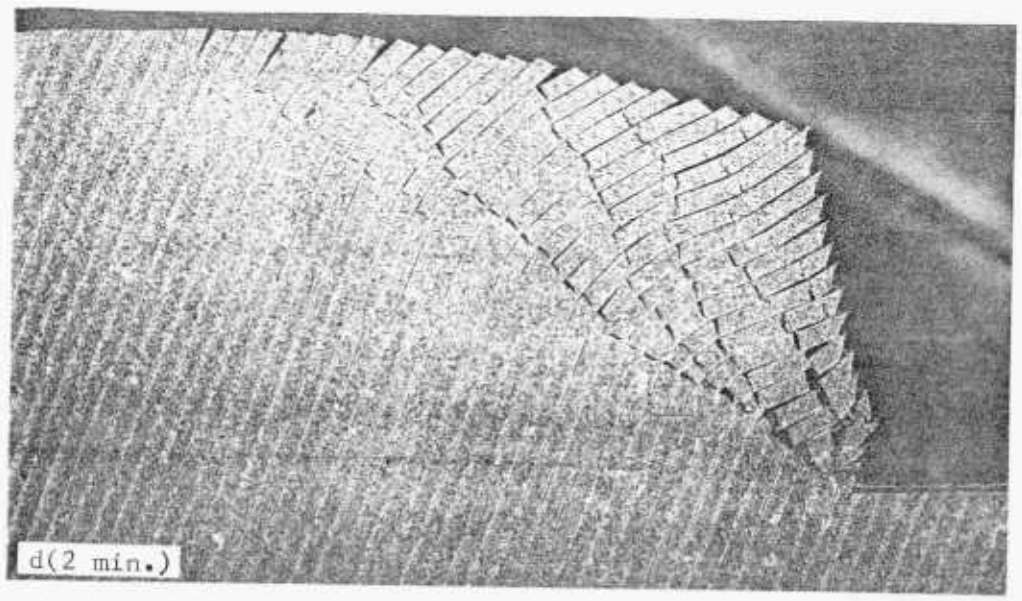
d(2 min.)

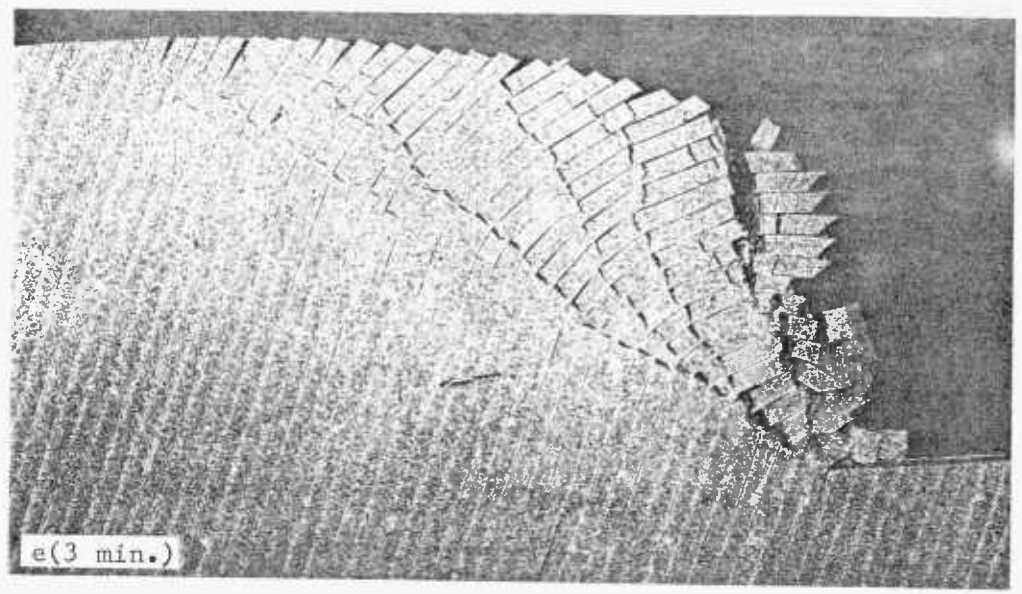
e(3 min.)

agreeing with the original model. The peculiarity common to both duplicate models was the depth below the pit bottom which was halved as compared to the originals. One wonders whether this difference in model geometry could lead to such a seemingly consistent anomaly.

MODELS 11" and $11''_S$ - See Plate 3-XII

To investigate the role played by cross joints on the mode of behaviour, tests 11" and $11''_S$ were run, the former being boundary-effect-free to be able to compare with Model 11' or $11'_R$; the latter was to be compared with Model 11. Staggered cross joints were implemented at regular intervals of 2" to form a brick pattern. So, the slopes were made up of 2" x 1" blocks.

Failure was initiated in these models with the opening up of cross joints in a stepped manner. As the rotation of blocks in a columnar fashion continued, edge contacts turned to point contacts producing corner crushing and tensile fractures. Staggering disappeared with rotation and continuous surfaces, though very rough, were formed to accommodate sliding. In the beginning the toe region remained intact, but instability spread down progressively. However, the newly formed columns of blocks having a greater thickness stabilized the slope extensively unless they were undermined at the toe.

As far as the boundary-effect-free models were concerned, failure initiation took longer in the cross-jointed slope. But, Model $11''_S$, in this respect, was in agreement

PLATE 3.XIII- Base Friction Models No.$11''$ and $11''_S$.

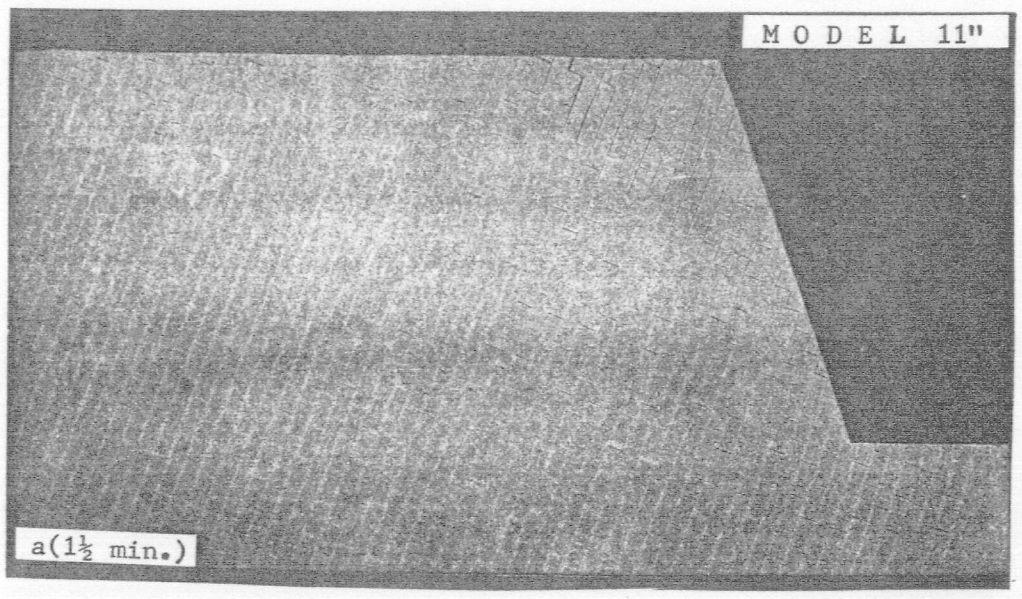
MODEL 11"
a(1½ min.)

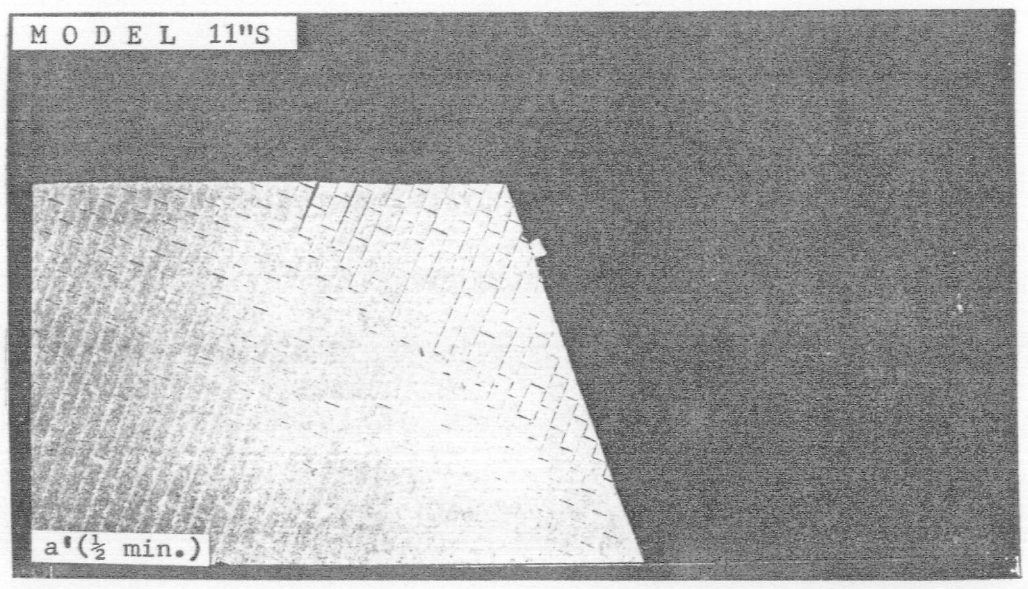
MODEL 11"S
a'(½ min.)

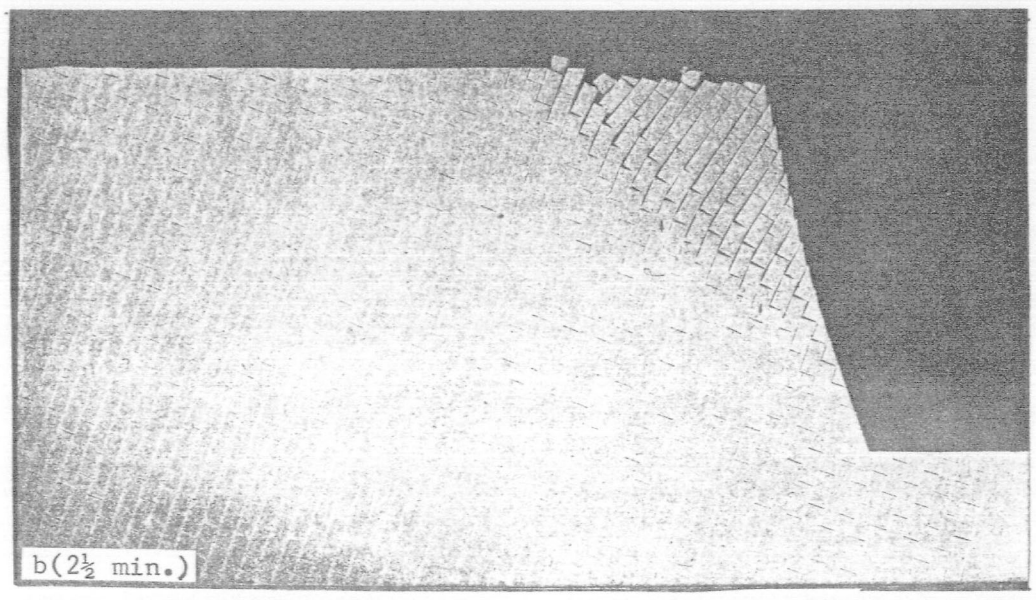
b(2½ min.)

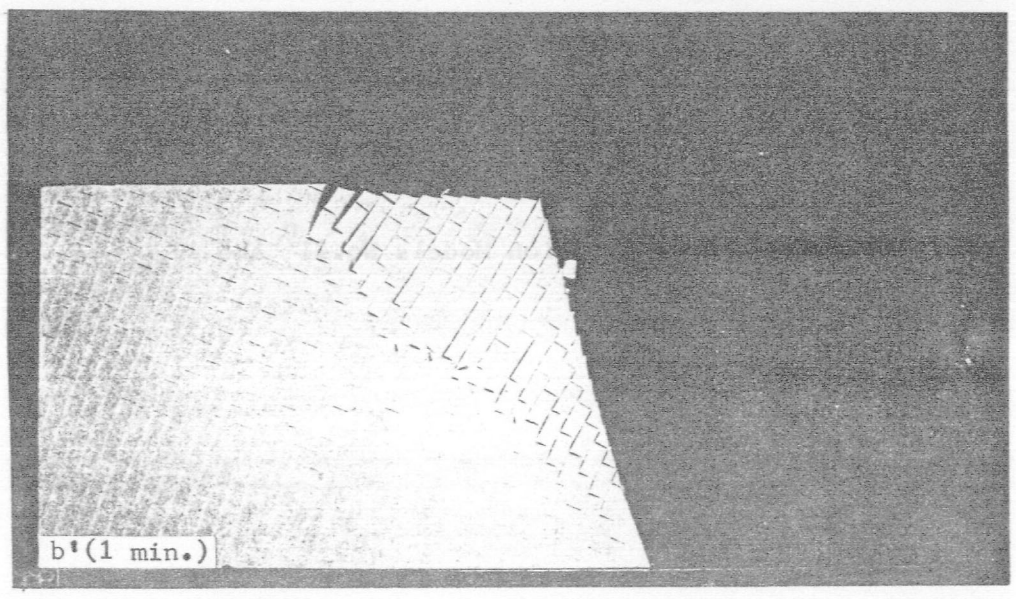
b'(1 min.)

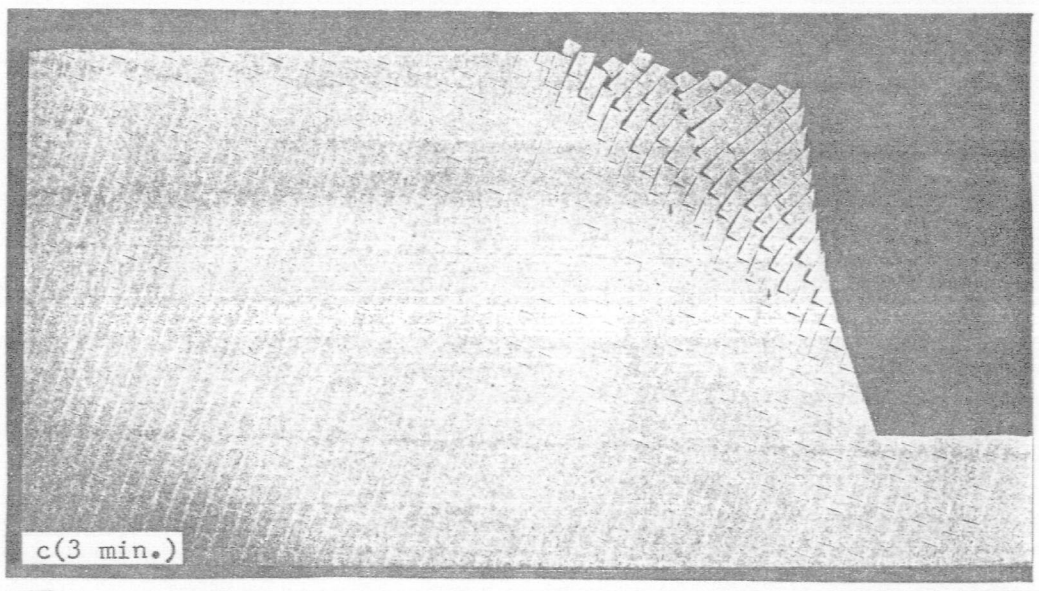
c(3 min.)

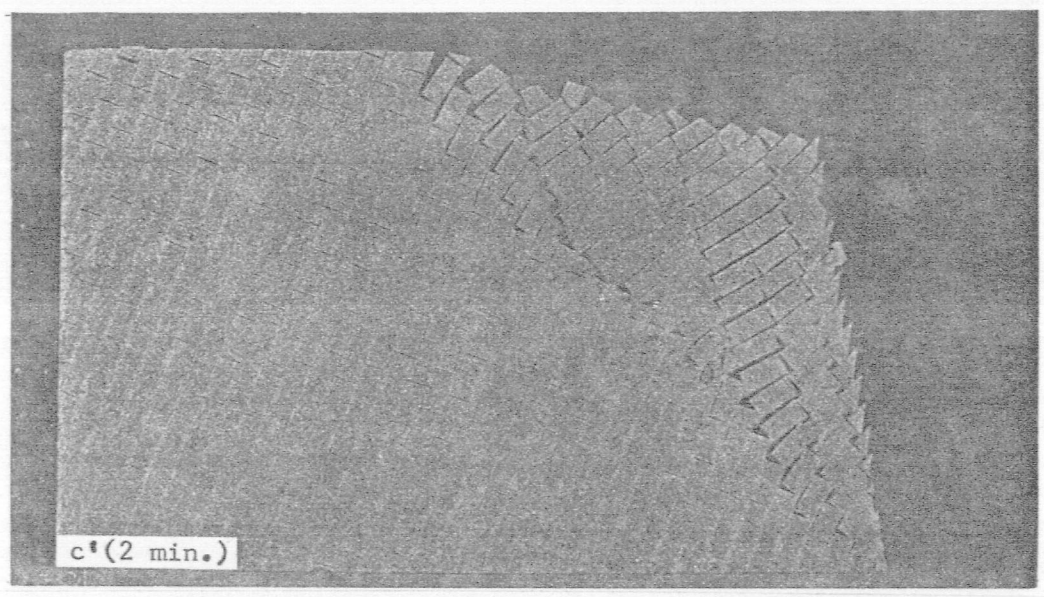
c'(2 min.)

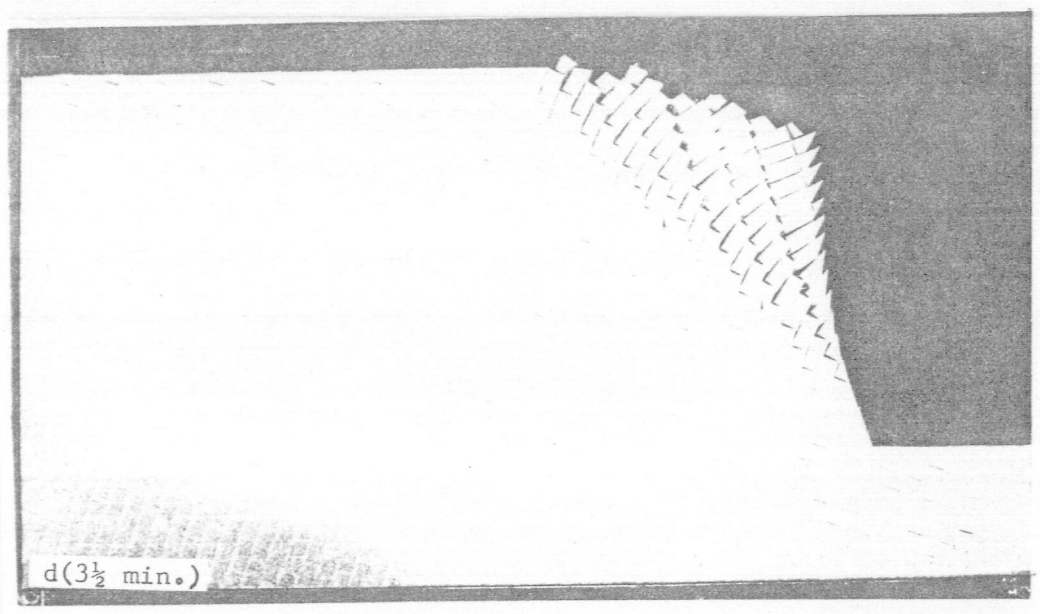
d(3½ min.)

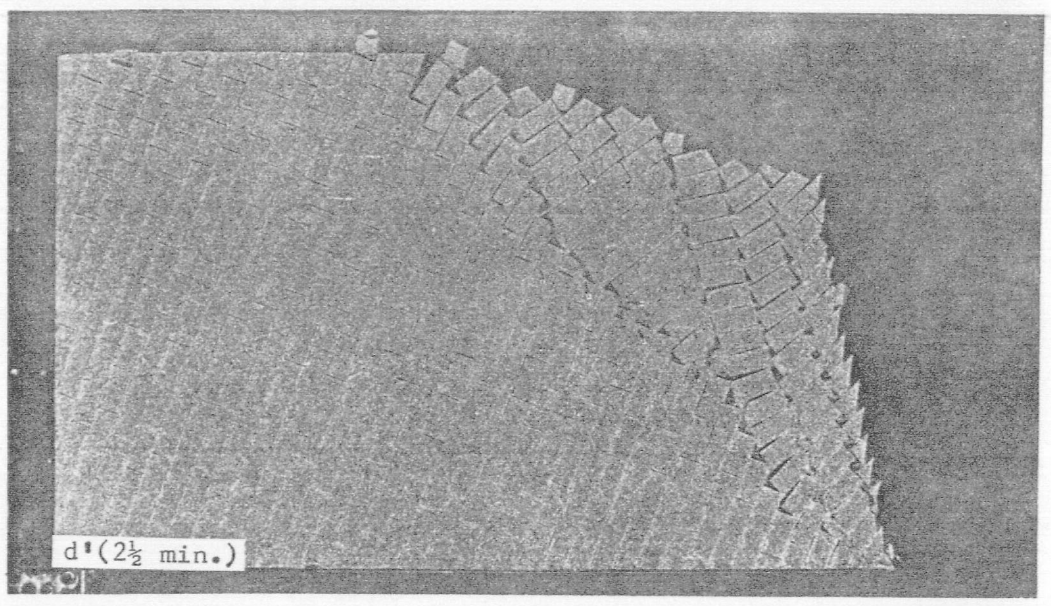
d'(2½ min.)

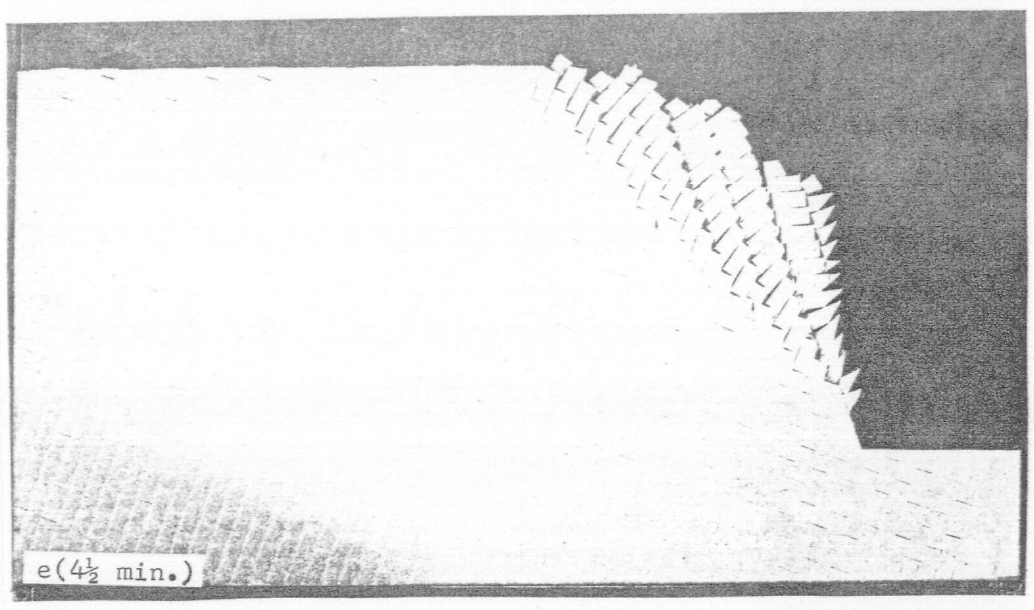
e(4½ min.)

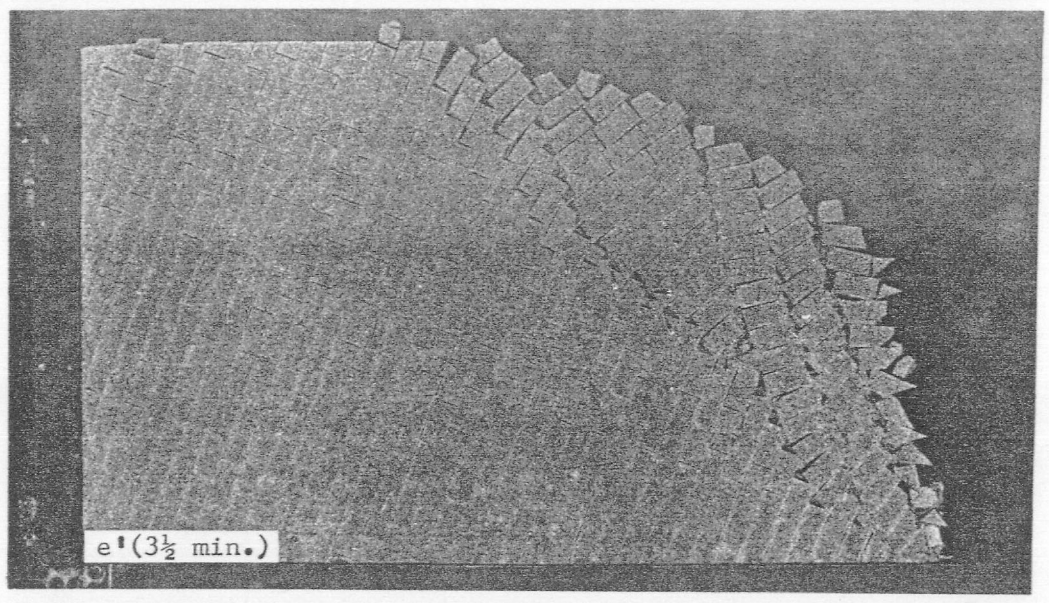
e'(3½ min.)

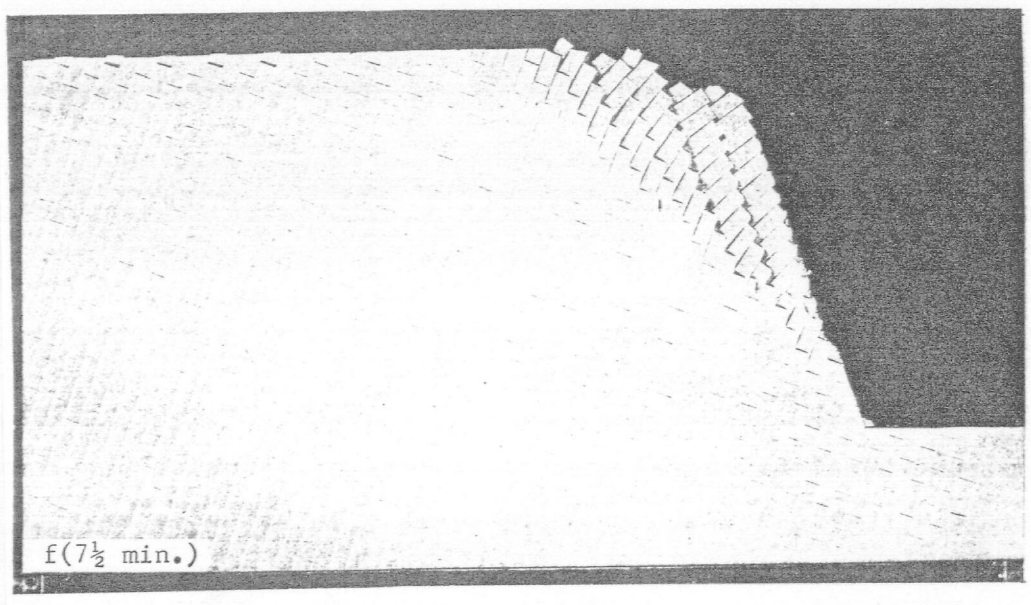
f(7½ min.)

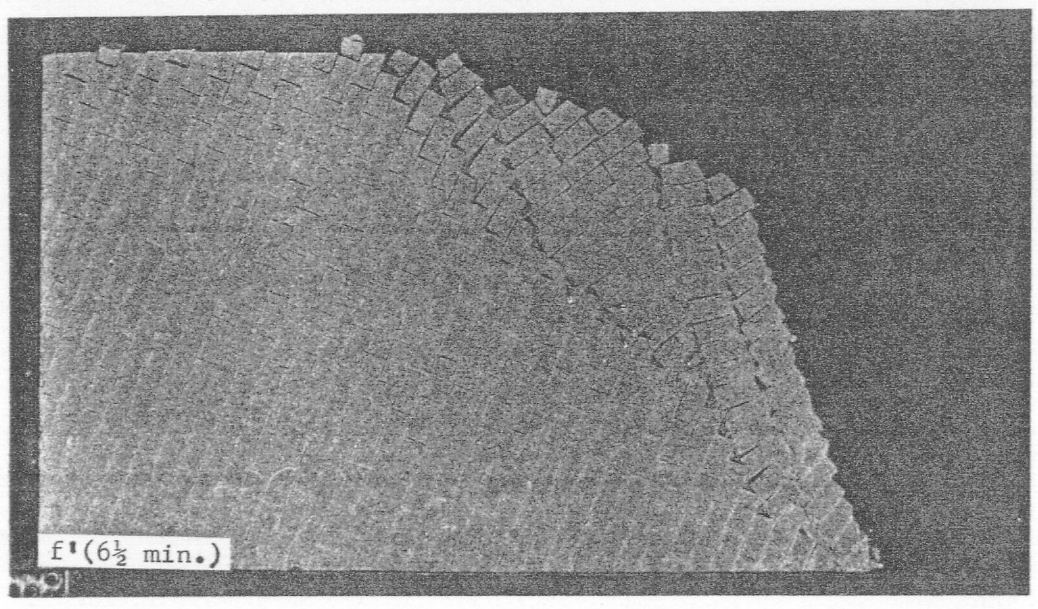
f'(6½ min.)

with its continuous column counterpart (Model 11 or 12) displaying the signs of instability soon after the start. This observation pronounces the significance of boundary effects for cross-jointed models as opposed to the continuous column ones. A feature common to both cross-jointed slopes was that a considerably lower volume of the rock mass was involved and disturbed in the failure. The prevention of stress concentrations due to the presence of cross joints which ease the rotation might be the reason why instability is confined to a region which does not extend far behind the crest.

Model $11''_S$ together with $11''_{S1}$ and $11''_{S2}$ indicated that the reduction in slope height was followed by an increase in failure initiation time thus giving rise to a more stable slope as opposed to the continuous column slopes discussed earlier.

MODELS 14 and 14D - See Plate 3-XIII

To understand to what extent and in what way the joint roughness could affect the toppling mechanism Model 14D was built having a saw-tooth pattern joint which passed through the crest. Although the inter-columnar shear was inhibited along this particular joint, failure took place in a manner very similar to Model 14. Even the critical crack path inclination was nearly the same. The main influence exerted by the joint roughness was the retarding of failure because the teeth could not be sheared and the columns on both sides of the saw-tooth joint acted as a single one thus altering

PLATE 3.XIII- Base Friction Models No.14 and 14D.

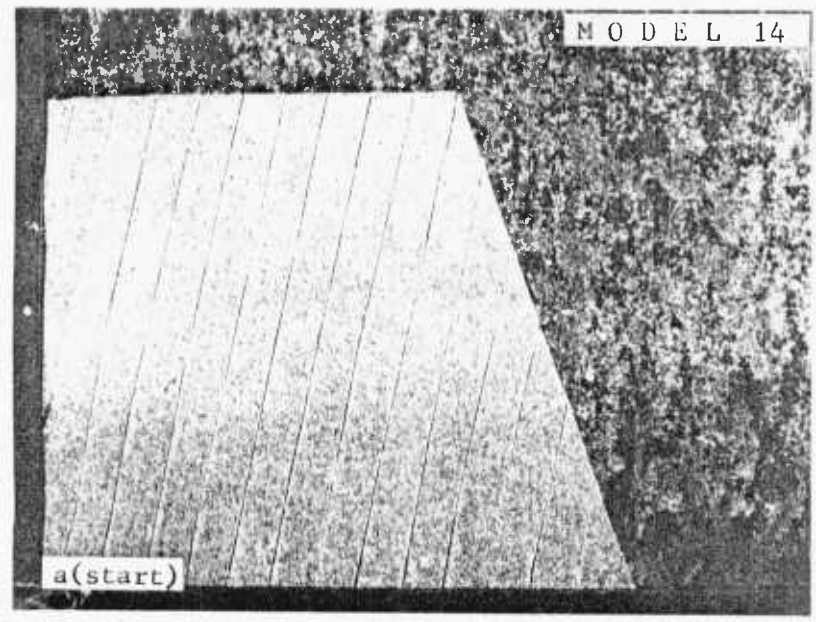
MODEL 14
a(start)

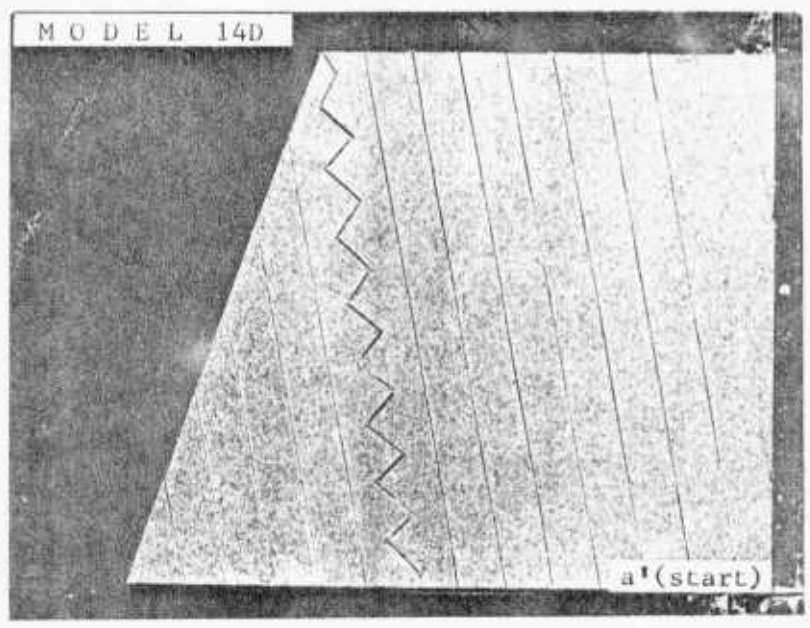
MODEL 14D
a'(start)

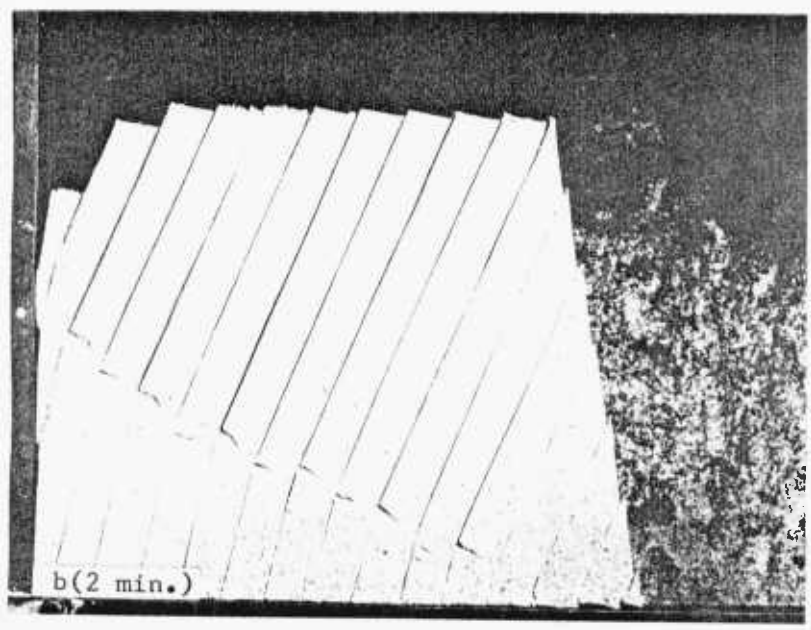
b(2 min.)

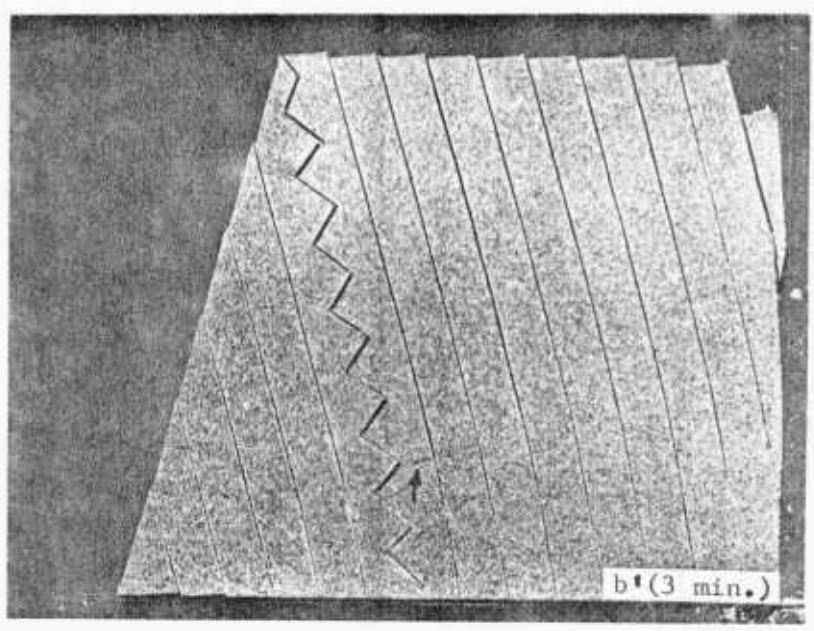
b'(3 min.)

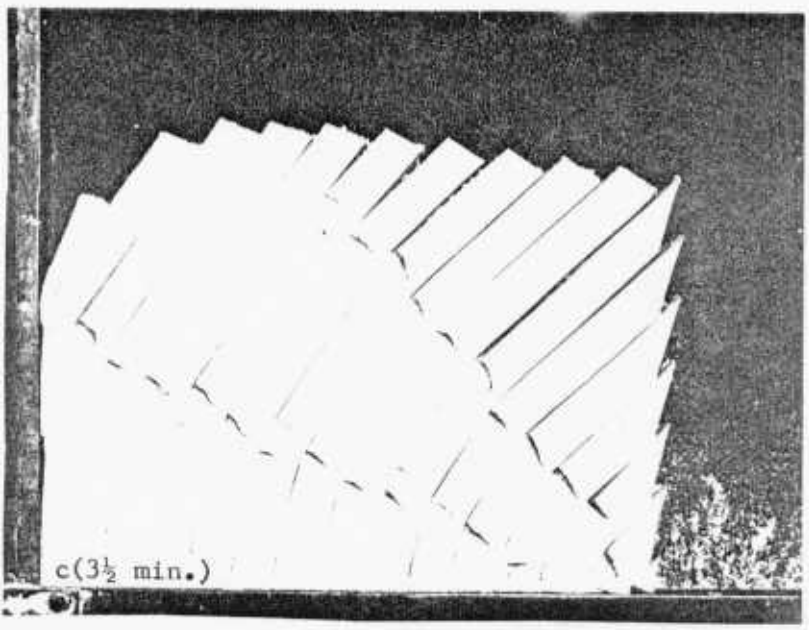
c(3½ min.)

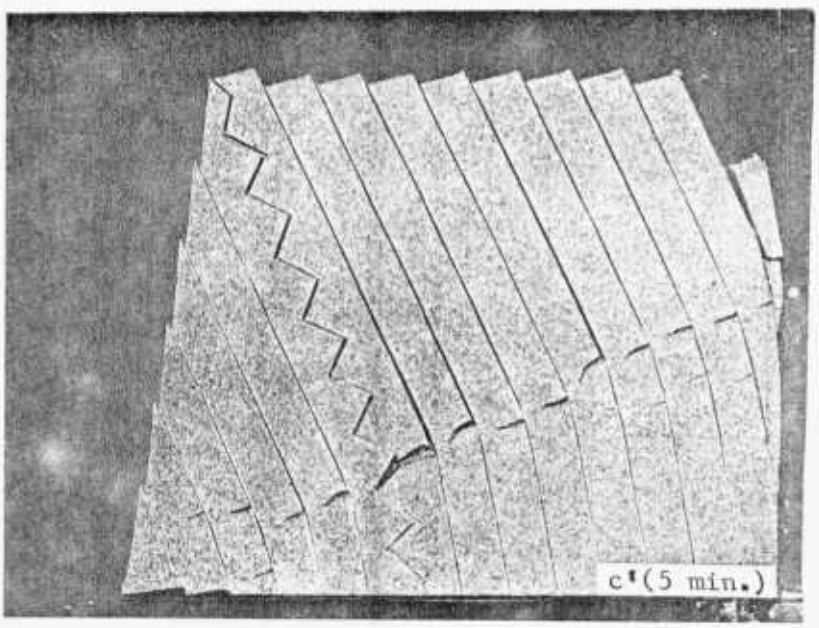
c'(5 min.)

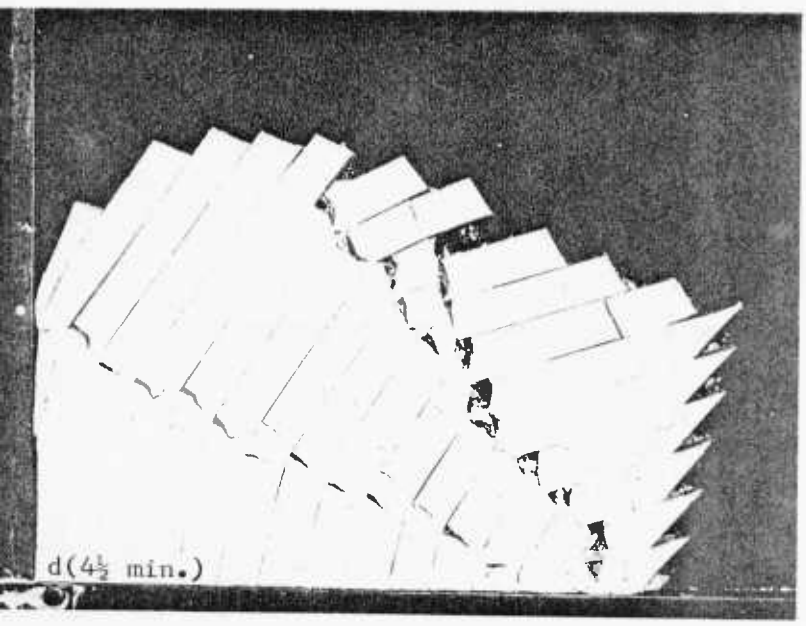
d(4½ min.)

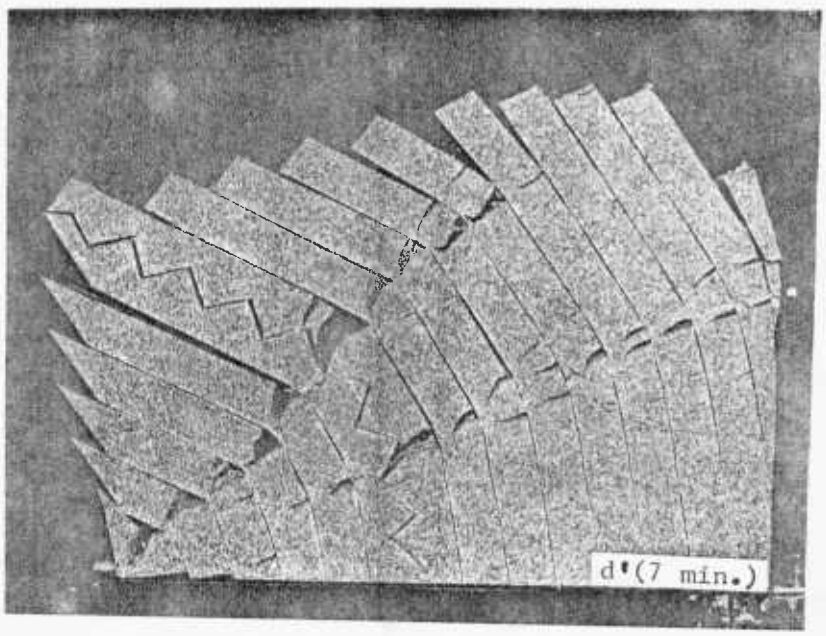
d'(7 min.)

the geometry (width doubled) in favour of stability. On the other hand, the flexural strengths of these two particular columns were weakened at peak points where the effective joint spacing contracts. As a matter of fact the first crack appeared in such a critical location as shown by an arrow in photograph (b') of Plate 3-XIII. Naturally enough the path followed a course offering the least resistance to rotation and in this respect it involved a part of the saw-tooth joint.

3.3 Tilting Frame Tests

Tilting frame is a simple two-dimensional modelling technique designed and used first by Barton[2]. Then Ashby[3] made extensive use of it in exploring the toppling mode of failure. Gerogiannopoulos[4] and Soto[5] also found this technique helpful in dealing with jointed rock slopes. Soto, in particular, studied the technique itself while comparing it with the base friction method, and pinpointed its shortcomings with some recommendations as to how to overcome them.

To describe it briefly, the tilting frame is made up of a pivoted incline driven by a motor to rotate in a vertical plane up to 40^{o} to the horizontal. The motor is reversible and provided with a microswitch stop to ensure that the frame returns to the horizontal before the test starts. The incline rotates with a speed of approximately 8.33^{o}/min. To complete the frame a perspex back is attached to the incline to support the model which is composed of discrete blocks usually cast from plaster.

In the beginning, bearing in mind the successful

work done by Ashby[3], it was planned to undertake a very detailed study with the tilting frame. It would cover Ashby's and Soto's suggestions as well as the new ideas such as adapting the deformable mixture of base friction to the tilting frame. Therefore, cubic (one inch) and rhombohedral blocks (45^{o}, 60^{o}, 75^{o}) were cast from plaster besides the continuous columns. As the preliminary tests revealed that intolerably inconsistent friction coefficients existed between the different surfaces of the blocks, the plans to carry out further investigation were abandoned. No attempts were made to improve the conditions because of limited time. Figure 3.3 shows the distribution of the friction angle (ϕ) of a single plaster block (1 inch cube) tested on the plaster incline by simple sliding. As illustrated, tests made at different locations on the same face, and different faces (of the same block) on the same location gave by no means tolerable results. Even the repetition (same location, same face) yielded different ϕ values. Inconsistent values were further obtained regarding the presence of contact with the perspex back. The main source of the discrepancy should come from the wearing down of small scale asperities as the test goes on. Figure 3.3(b) confirms this clearly. All of the five faces yielded decreasing friction angles with changing locations to A, B, and C consecutively for the case of contact with the perspex back. Surprisingly enough, the value of 36^{o} given by Ashby[3] was only attained once, although the plaster/water ratio (60/40) of the blocks was the same.

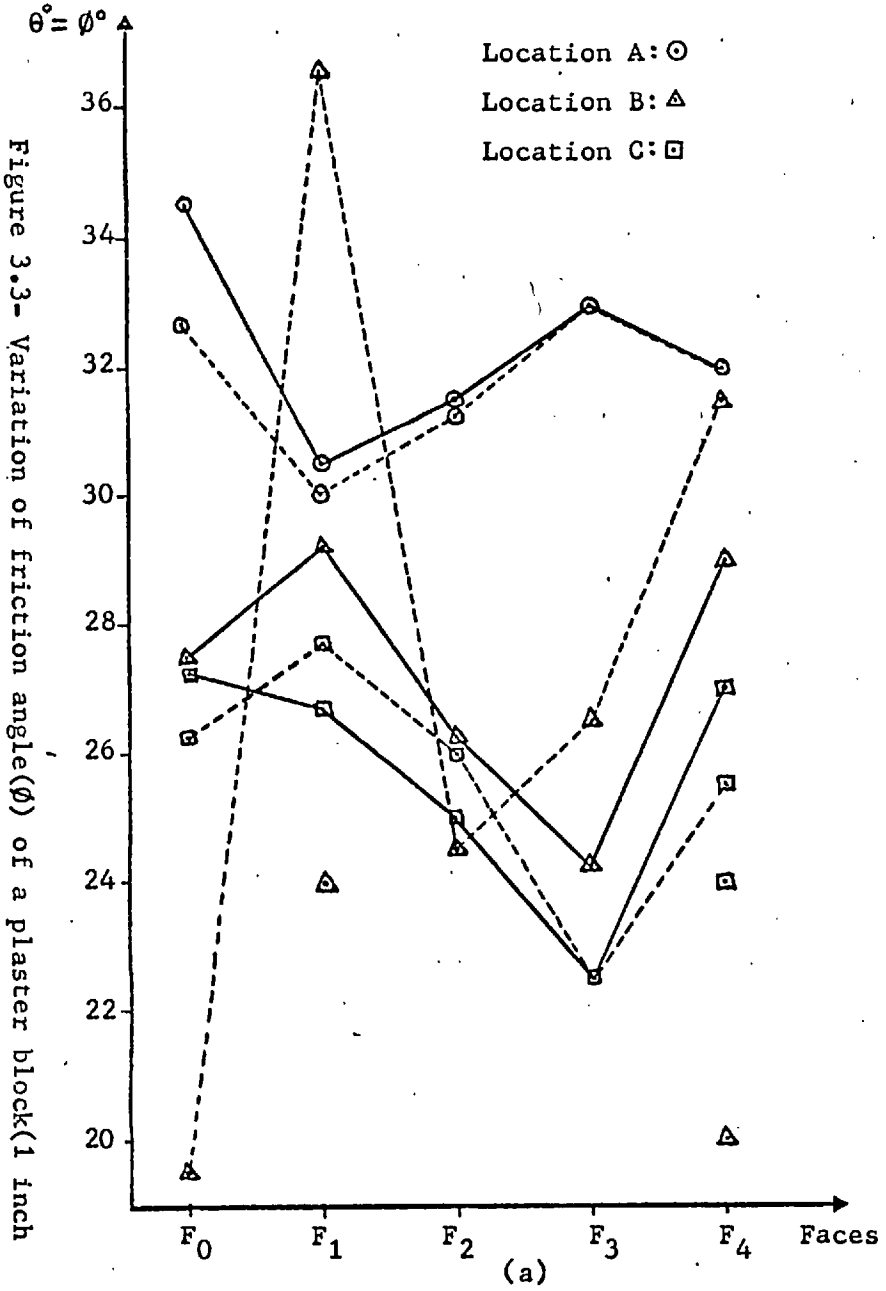

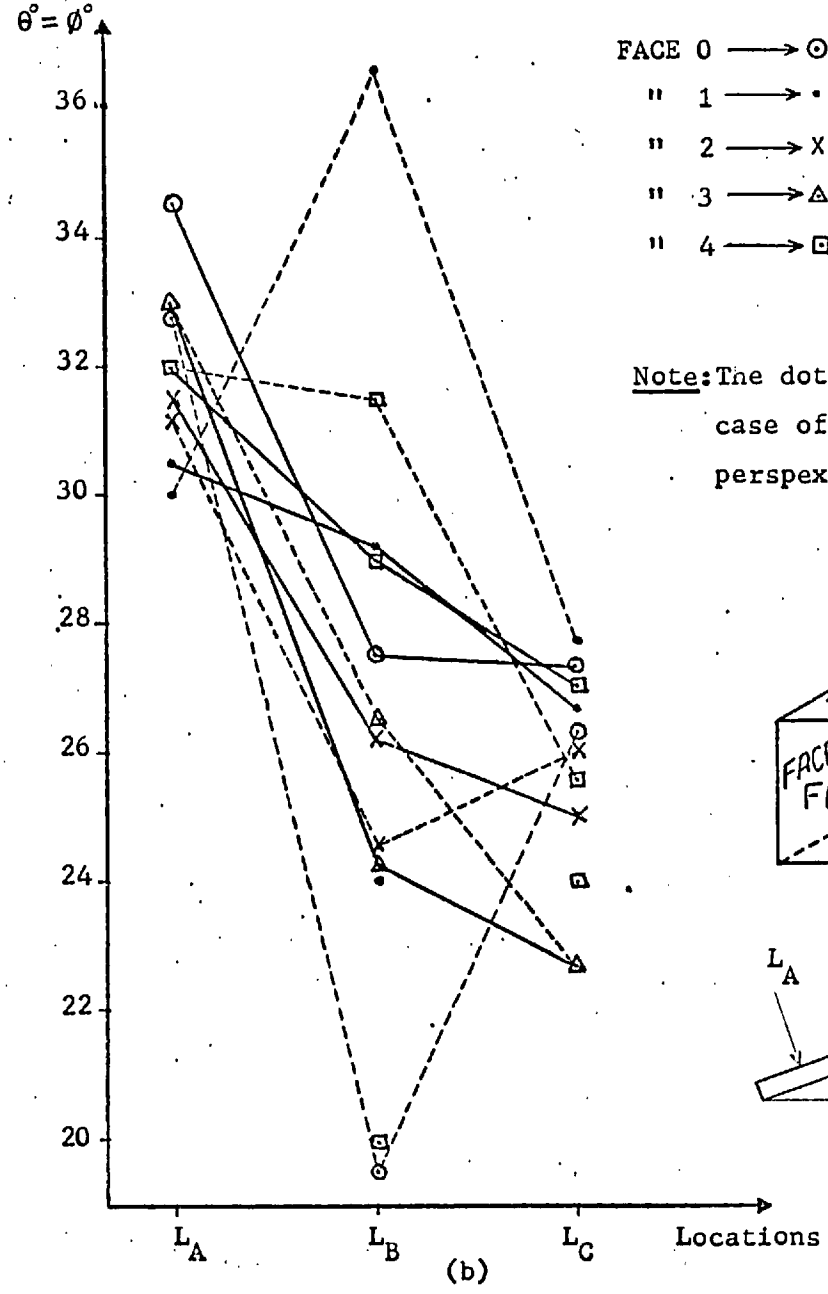

Note: The dotted lines are for the case of no contact to the perspex back of the block.

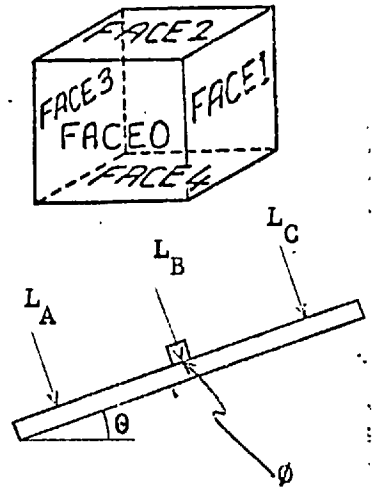

Figure 3.3- Variation of friction angle(∅) of a plaster block(1 inch cube): (a) for different faces, (b) at different locations.

3.3.1 Single Column Tests

Using the tilting frame the author wanted to verify the single block criterion of toppling put forward by Ashby[3] and reproduced unexceptionally in every piece of work concerned with toppling. As it is now known to everybody, this criterion defines the toppling with the position of the weight vector, which passes through the centre of gravity of the body, in relation to the base of the block resting on an inclined surface. Figure 3.4 illustrates the agreement between the theoretical consideration (solid line) and the tilting frame test results of continuous columns (broken line with dots). The third curve, i.e. the broken line, represents the test results of columns made up of 1 inch cubical blocks placed one on another. As compared to Ashby's criterion, the continuous columns appeared to be more unstable when they were short (failed one degree of inclination earlier); but as the columns got taller the difference disappeared. This was probably due to the increasing sensitivity of tall columns to toppling. The critical tilting angle for columns made up of blocks was roughly 1^{o} less than the theoretical prediction for almost all a/b ratios. Therefore, this case represents the least stable of all three. The conformity observed between continuous and block columns was confined to small heights. As the number of blocks composing the column increased, the stability decreased implying the adverse effect the joints have on the behaviour by reducing the flexural stiffness.

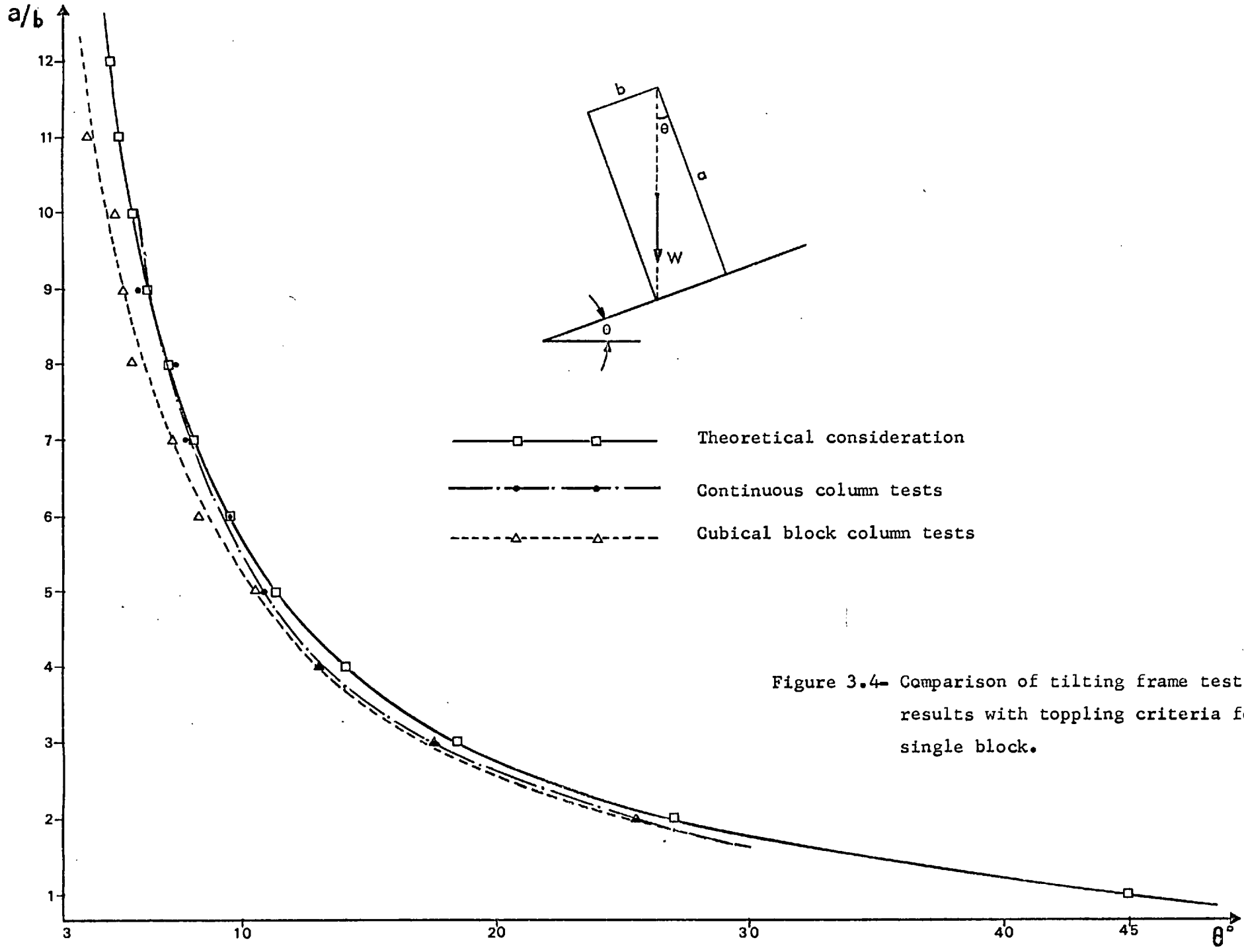

Figure 3.4- Comparison of tilting frame test results with toppling criteria for single block.

3.3.2 Multiple Column Tests

The influence of the interface between two adjacent columns was examined before doing a series of multiple column tests with columns of equal and different heights. Figure 3.5 simply shows the contribution of neighbouring columns to stability which may be in any of three ways:

a. Inter-columnar friction which should be overcome to facilitate rotation.

b. Friction between the toe of the column and the base which opposes the expansion necessary for rotation, though it may be insignificant.

c. The deterrent action of the neighbouring column if it is shorter than the one under consideration, and if it is located on the down side of the slope.

3.3.2.1 - Columns of equal height -

Two, three and four column cases for heights of 2" to 9" inclusive were studied. These tests were made for the following purposes:

a. To find out to what extent the inter-columnar and base frictions are controlling the toppling.

b. To verify the analytical approach, and to compare with the computer results which are the subjects of the fourth and fifth Chapters respectively. Although they were simple, a considerable amount of attention was paid to the tests because of the importance attached to the second aim in particular. The effect of the friction at the base was checked using a strip of tin (friction

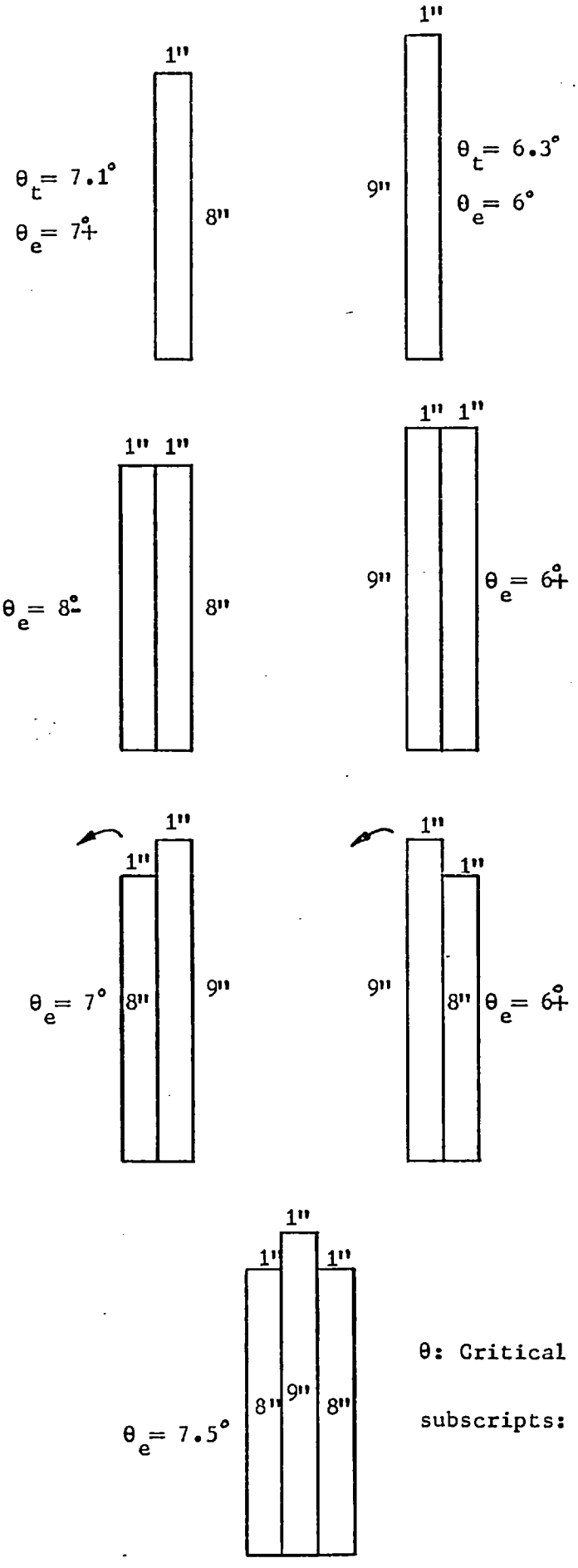

θ: Critical tilting angle

subscripts: t= theoretical
e= experimental

Figure 3.5- Adjacent column influence

angle = ψ = 17^{o} - 19^{o}).

When the number of columns increased the critical tilting angle also increased as shown in Figure 3.6. This increase in stability should be associated with the inter-columnar friction because the resistance provided by the base-toe interaction was insignificant, as illustrated by the broken & dotted curve in Figure 3.6. The critical tilting angles for the tin and plaster base materials, regarding the double column case, were quite close.

Qualitatively speaking, in tests on double columns it was found that short columns toppled suddenly; as they got taller the contact area increased and the interface sliding became more evident and lasted longer. Regarding the triple and quadruple columns: Toppling of all columns usually did not take place simultaneously, but either one by one or in groups in short intervals depending on the nature of the contact between the columns.

To investigate the effect of the nature of the contact between the column faces further tests were conducted with 3" height blocks (double). Tests were conducted to see if the results would be affected by

a. initially placing the blocks on the plane so that they were only gently touching
b. initially pushing the blocks hard together
c. initially allowing a slight separation between the columns (as might occur with out-of-square surfaces)
d. using blocks with slightly differing heights.

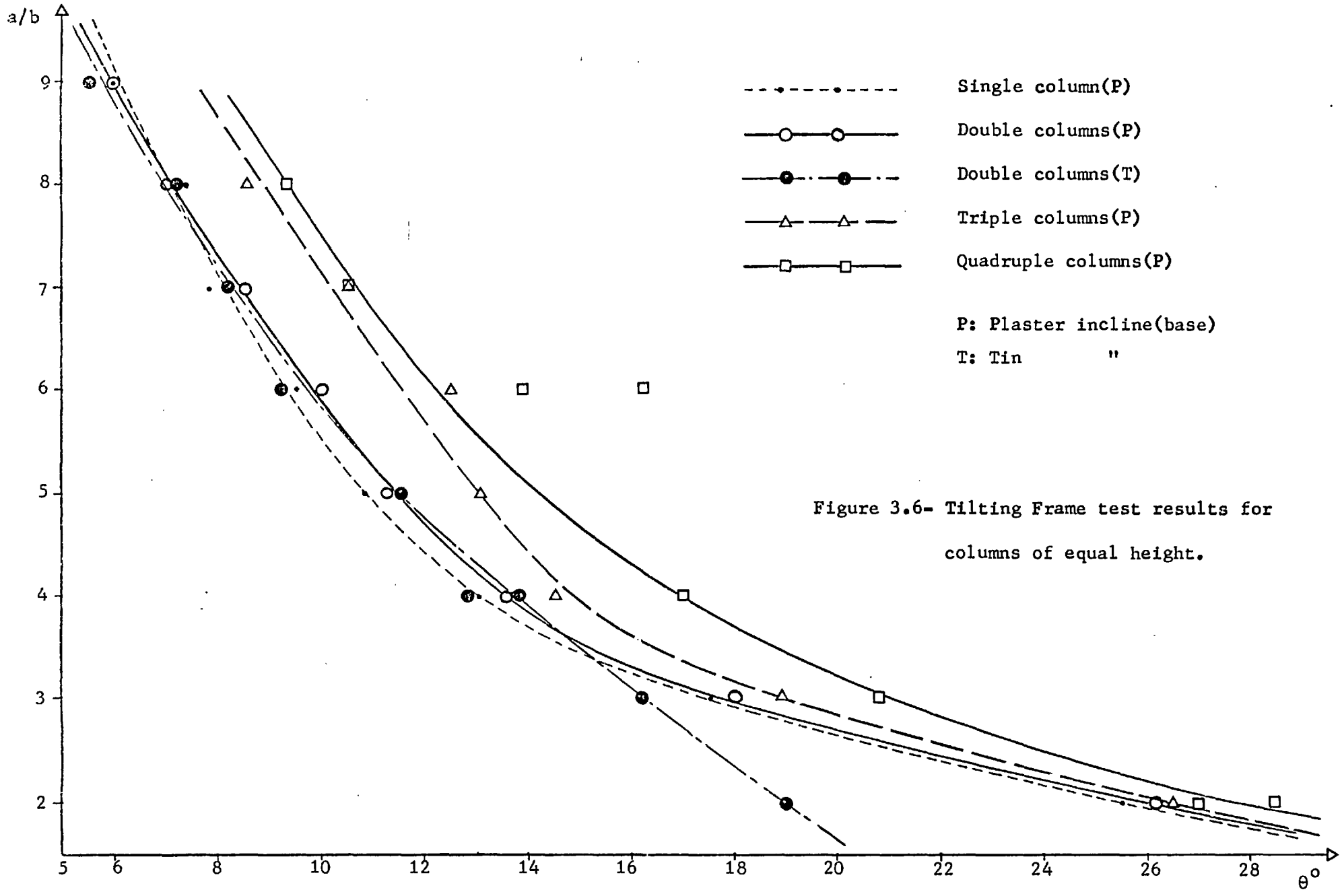

Figure 3.6- Tilting Frame test results for columns of equal height.

The following results were observed:

1. When the blocks were pushed hard together almost no change in critical tilting angle was observed (0.5° increase sometimes). But, while the "gently touching" columns separated before toppling, the "pushed hard" ones toppled suddenly because incipient sliding was avoided in this way.
2. Changing the column positions yielded almost no change in toppling behaviour.
3. Quite a variation was observed in inter-block friction angle, which was determined by simple sliding, changing from 8° - 9° to 36.5° as incipient and full sliding inclinations respectively.

3.3.2.2 - Differential height columns -

Obviously, the models made up of gradually increasing and then decreasing height columns would give the contours of a real slope when tilted. Ashby[3] and Soto[5] have constructed their slopes in this manner, the incline representing a through-going discontinuity in the rock mass. They dealt primarily with the slopes of stacks of blocks rather than the slopes of continuous columns. To obtain some insight into the behaviour of slopes of columnar structure, models composed of up to 18 columns were tested. Formation of the first tension crack was considered as the sign of instability, and the corresponding tilt angles were plotted against the number of columns in Figure 3.7.

Plate 3-XIV illustrates one of the tests (9 column

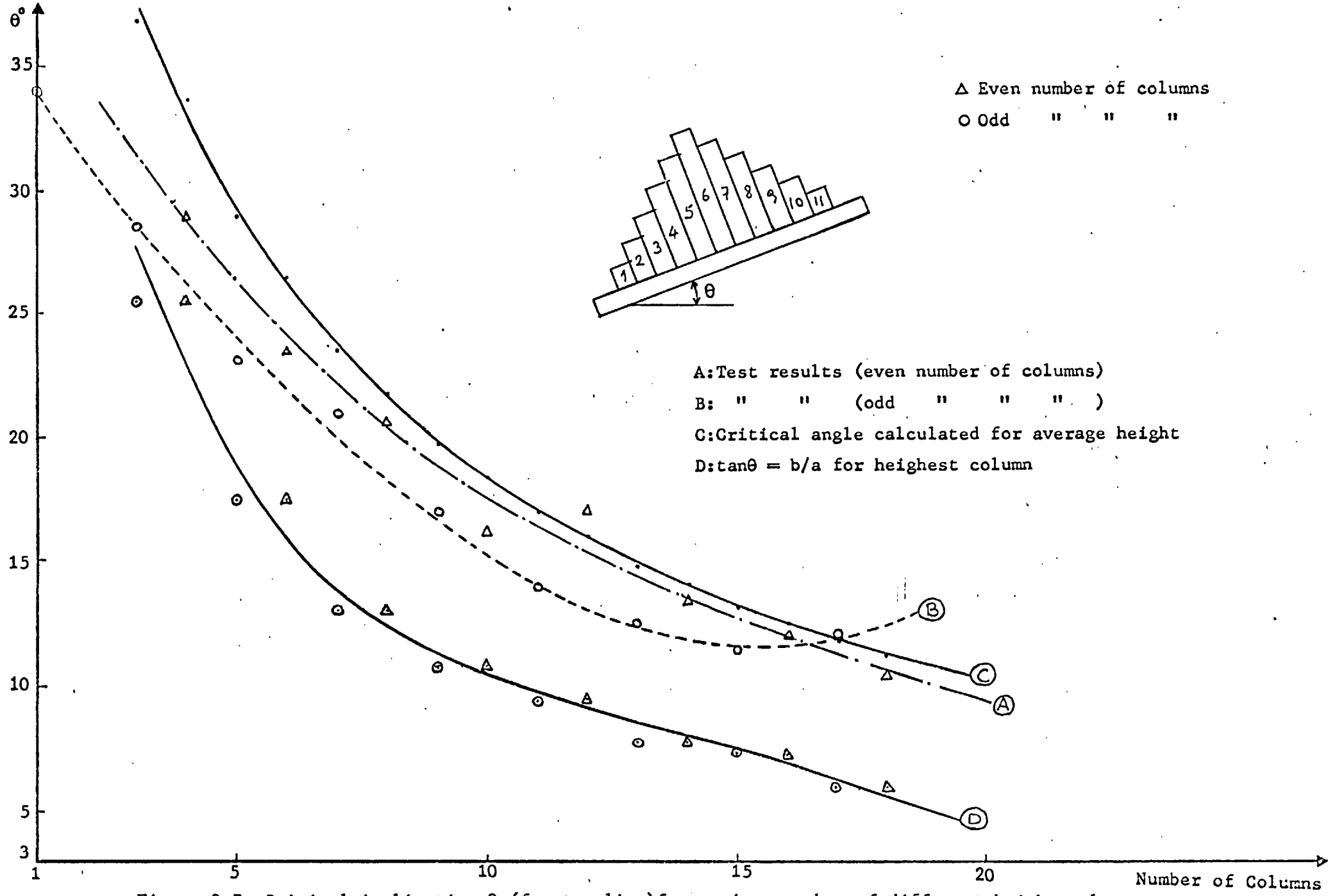

Figure 3.7- Critical inclination,θ,(for toppling)for various number of different height columns

model). It shows the formation of a tension crack between the sixth and seventh columns as a result of rotation of a series of columns (2nd to 6th), the first block having been forced to slide, at the inclination of 16^{o} (photograph (b)). Photograph (c) shows the stable configuration at the inclination of 30^{o} posing the following questions: Why was the stability maintained even at such a high inclination which should have let the 7th and 8th columns topple? What kept back the overhanging columns from collapse? The answers might be the following:

a. The rotated columns could not slide down because they were standing on their edges with an increased friction due to ploughing action.

b. The rotated columns could not carry on rotation because of (i) obstruction of expansion (in form of sliding) at the base in both ways, (ii) increasing resistance to interface sliding, which would facilitate toppling, primarily due to increased normal force being produced by leaning action of the columns.

c. Though there was a tendency, columns 7 and 8 could not topple because neither forward nor backward sliding at the base was allowed owing to the obstruction provided by columns 6 and 9. When the inclination reached 32^{o} all columns started to slide on their edges (photograph (d)).

Test results indicated that with the increasing number of columns the instability increased. This phenomenon should be associated with the highest column because as the

PLATE 3.XIV- Tilting Frame Multiple Column Model.

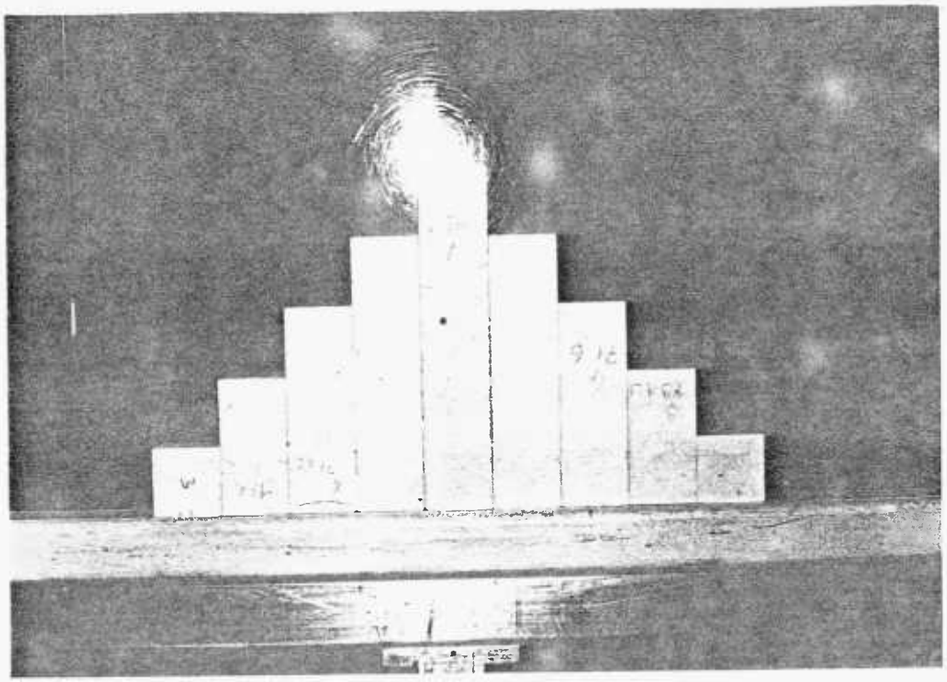

a(start, $\theta = 0^{\circ}$)

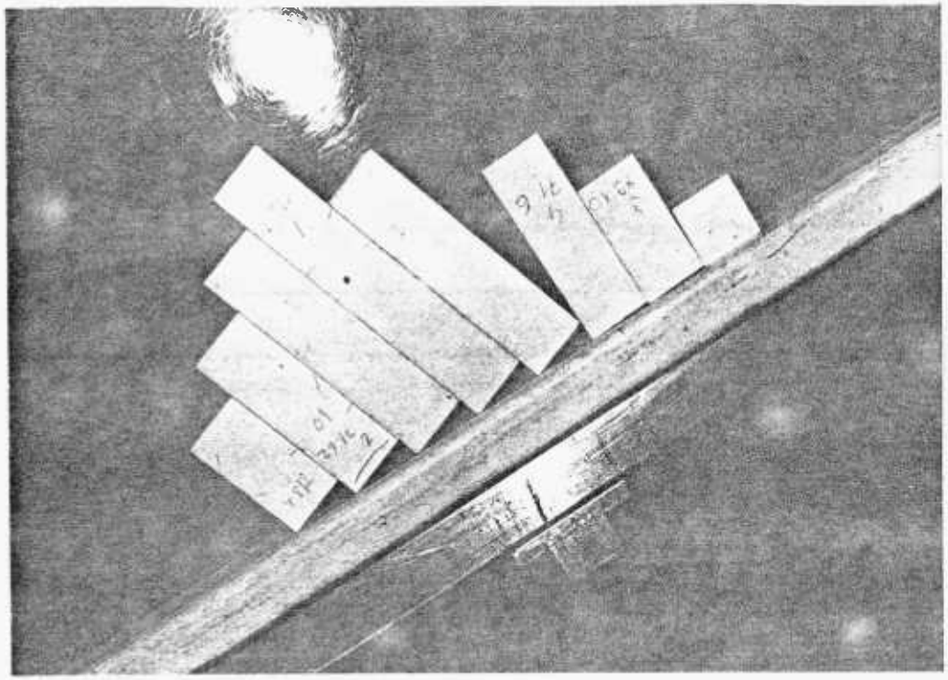

c($\theta = 30^{\circ}$)

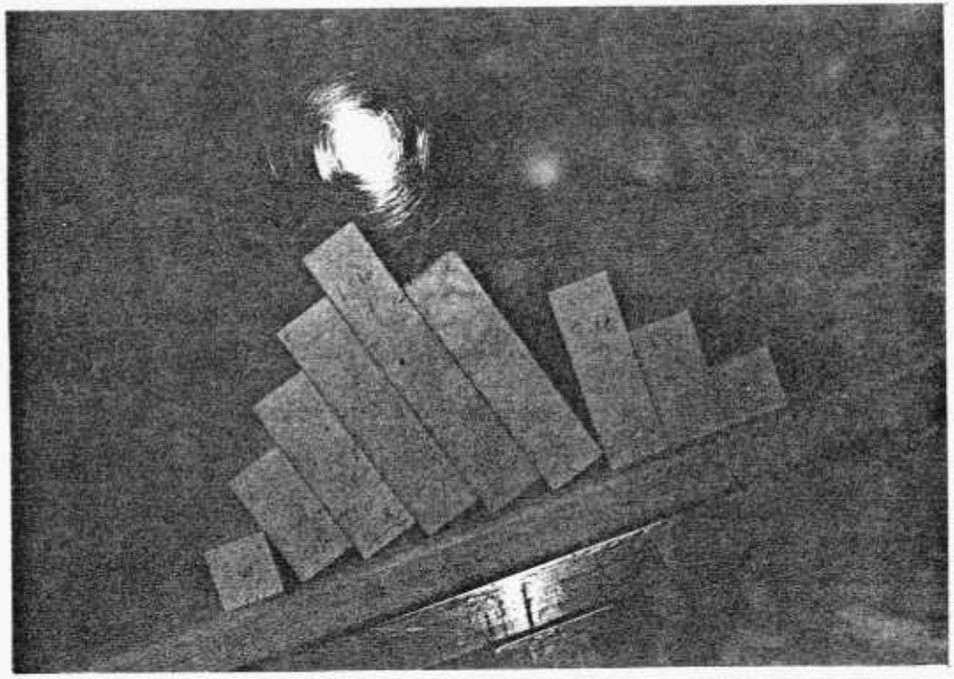

b($\theta = 16^{\circ}$)

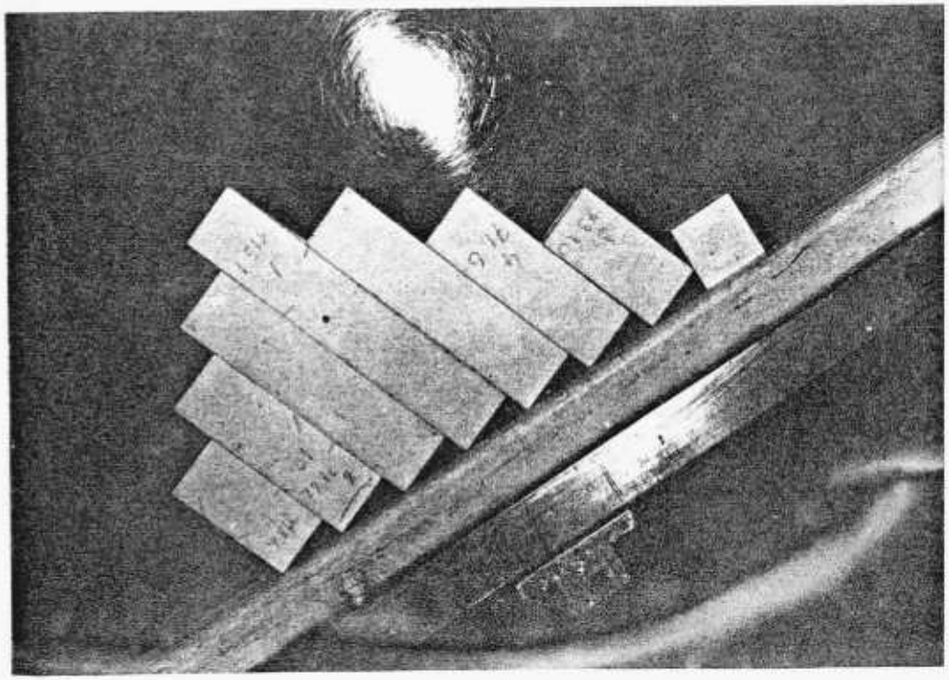

d($\theta = 32^{\circ}$)

number of columns increased the height of the tallest column increased. That is why the curve representing test results shows a profile parallel to that of the highest column. This result is in agreement with Ashby's[3] findings, although there were two basic differences in the models. Ashby's model was physically half of the author's and was made up of blocks rather than continuous columns. While the lower curve (of highest columns) might be considered the lower limit of instability, the upper one, representing the average height of the columns for the particular model, could be designated to serve as the upper limit of instability.

Two other interesting aspects of the tests were the location of first tension cracks, and the differing stability conditions for even and odd numbers of columns For quite a number of models, the number of columns ranging from 8 to 17 (excluding 16), the first tension crack formed at the same location with regard to the stable part at the back, that is, the instability, in the form of rotation spreading backwards, stopped mostly when the 3" height column was reached. The position of the curves for odd and even number of column models indicated that latter models were slightly more stable than the former. It is arguable whether the repetition of the highest column in the middle of the even-column models has any stabilizing effect.

3.4 Discussions and Conclusions

Discussions and conclusions for this chapter, concerning the base friction tests especially, will have to be

in the form of verbal interpretation of observations rather than numerical expression of experiments. That is why only one graphical output could be extracted from several dozens of base friction tests as against three graphs obtained from a limited number of tilting frame tests. This distinction stems from the nature of the techniques themselves.

3.4.1 Base Friction Tests

Although most of the discussions and comments were already made while describing the tests, it would be useful to reiterate some of them in giving the overall picture.

As far as the continuous column tests were concerned the following conclusions could be cited:

a. The flexural strength of the columns together with the degree of restraint against rotation shown by the blocks at the toe seemed to be the dominant factors controlling toppling failure. Tensile fracturing of intact material allowed the columns to rotate. On many occasions, removal of the restraint at the toe gave rise to instability; but toppling might not be prevented altogether if the slope was steep enough, only retarding action could happen then.

b. Fractures first appeared in the middle of the slope mostly, and developed to a critical crack path spreading up and down quickly. Second and third paths followed the first one as the rotation proceeded, the pattern of which was controlled by the resistance of the toe blocks against toppling depending upon their body geometry.

c. The frictional characteristics of the base on

which the slope stands appeared to be affecting the slope behaviour. But, inconsistent results prevent further interpretation.

d. Although the modelling technique and material, and the joint structure were different from those adapted by Ashby[3] it was found that the slopes behaved similarly. Three zones of behaviour cited by Ashby have more or less been observed throughout the tests. They were:

(i) A region of sliding along the slope face.

(ii) A region of toppling columns.

(iii) An approximately triangular stable region.

e. Increase in slope height, unexpectedly, worked in favour of stability, most likely due to the increasing number of columns at the bottom of the slope. This outcome was in contradiction to Ashby's findings as well as the tilting frame results of the author himself.

f. The stability of the slopes was found to be very sensitive to slope angle variation regardless of the number of columns constituting the base of the slope.

g. The slopes constructed to eliminate the boundary effect have not shown a remarkable difference in behaviour. Some of them took longer to fail while the others did not. Few of them had a flatter critical crack path inclination, giving rise to a large volume of rock mass disturbance.

The most useful aspect of the boundary-effect-free models was the observation of the formation of tension cracks. The first tension cracks formed well behind the crest, and

were followed by the others (towards the crest) associated with developing critical crack paths. As toppling proceeded present tension cracks closed down and the new ones developed nearby; this time it was a backward procedure.

As regard to the cross-jointed models the following could be concluded:

a. Cross joints, producing short columns with higher bending tensile strength, gave rise to more stable slopes. Therefore, a lower volume of rock mass was involved and disturbed in the failure.
b. The toes of the slopes were less active regarding the failure initiation and propagation. On the other hand, the crest was the most active part of the slopes.
c. Failure was not as severe as for the columnar slopes because formation of block columns helped stabilization.

Generally speaking: All the slopes having 70° or more slope angle failed very quickly. 60°, even 65°, slopes appeared to be in a limiting equilibrium condition; some of which did not fail at all, while the others were failing under favourable conditions such as restraintless toe, low friction angle base material, etc., and/or after a long lasting test. John[6] suggests toppling analysis for slopes over 60° inclination, supporting the author's findings. But, a great proportion of Soto's[5] slopes failed between 45° - 60°, disagreeing with the author's results.

Critical crack path inclination hardly exceeded 41°, in other words, the friction angle of the modelling material was the boundary of minimum disturbance. It was never less than

20^{o} (roughly half of the friction angle), but mostly between 25^{o} and 35^{o}, agreeing with Soto's results (20^{o} - 34.5^{o}).

3.4.2 - Tilting Frame Tests -

Since the discussions have been made at appropriate sections, the test results will merely be summarised here.

a. Intolerably inconsistent results regarding the friction angle of a single plaster block were noted. It was pointed out that the most likely agent for this inconsistency was the small scale asperities on the surfaces. In the light of this explanation, two alternatives were thought to be applicable to minimize the effect of friction angle variation. They are:
   (i) Blocks should not be used more than once, so, what might be called "peak" friction angle happens to be operative for all models.
   (ii) The first couple of tests should be disregarded for the friction angle to reduce to its "residual" value, that is, the "valid" models have to be constructed from the blocks whose small scale roughness has disappeared.

b. Ashby's theoretical consideration for the toppling of a single block was experimentally confirmed.

c. Existence of an adjacent column increased the critical tilting angle, and the more the number of columns the more stable the configuration became (same height columns).

d. Though quite a variation was observed in inter-columnar friction angle (ϕ) of for both "pushed hard" and "gently

touching" blocks, the critical tilting angle did not change significantly indicating that ϕ has little effect on toppling (excluding large scale joint roughness). Ashby came to the same conclusion after his tests.

REFERENCES

1. HAMMETT, R.D. A study of the behaviour of discontinuous rock masses. Ph.D. Thesis, James Cook Univ. of N. Queensland, Australia, 1975.

2. BARTON, N.R. A model study of the behaviour of steep excavated slopes. Ph.D. Thesis, Univ. of London, (Imperial College), 1971.

3. ASHBY, J. Sliding and toppling modes of failure in models and jointed rock slopes. M.Sc. Thesis, Univ. of London (Imperial College), 1971.

4. GEROGIANNOPOULOS, N. The use of surface displacement monitoring in slopes to predict failure mode and location of failure surface. M.Sc. Thesis, Univ. of London (Imperial College), 1974, 37p.

5. SOTO, C.A. A comparative study of slope modelling techniques for fractured ground. M.Sc. Thesis, Univ. of London (Imperial College), 1974.

6. JOHN, K.W. Three-dimensional stability analyses of slopes in jointed rock. Proc. Symp. on Open Pit Mine Planning, Johannesburg, 1970.

CHAPTER FOUR

LIMITING EQUILIBRIUM APPROACH

4.1 General

The basic mechanism of toppling (together with sliding) for the case of a single block was discussed by Ashby[1] and Hoek and Bray[2] as mentioned in the preceding chapter. Figure 4.1 illustrates the way in which toppling is affected by the geometry of the block. However, this is a very trivial situation and in an actual rock slope consisting of a large number of blocks of irregular shape, toppling such as that shown in Figure 4.1 seldom occurs. In fact, failure by toppling is a complex mechanism which involves both sliding and rotation of the blocks as well as block separation, wedge action, and interlocking as observed in base friction tests in Chapters two and three. No satisfactory analytical techniques, that could be regarded as a design tool, for dealing with this complex situation have yet been developed. In this connection, Cundall[3] continues to improve his Dynamic Relaxation Method of computer simulation. The author, also has made an attempt to take the single block toppling criterion one step further by examining the limiting conditions for multiple blocks. In this context, the mechanistic behaviour of systems comprising two, three and four adjacent blocks were studied. In all cases the blocks were of equal height. Bray[4] used the limiting equilibrium method on his theoretical models of slopes with simple geological structure

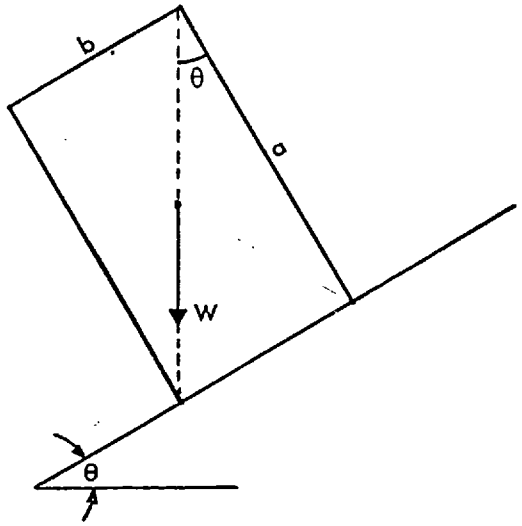

Limiting conditions:

for toppling ⟶ $\tan\theta = a/b$

for sliding ⟶ $\tan\theta = \mu$

(a)

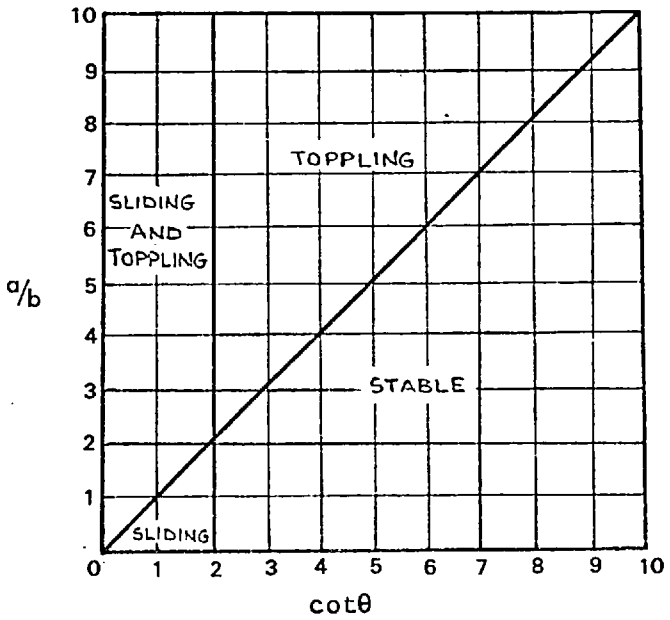

(b)

Figure 4.1- Toppling and sliding criteria for a single block on an inclined plane:(a)block in limiting orientation for toppling; (b)superposed criteria for sliding and toppling (After Goodman & Bray[5]).

to determine the factor of safety for toppling. One of these models, the toppling of blocks on a stepped base, will be discussed at the end of this chapter.

4.2 Toppling of Two Adjacent Blocks

Consider two adjacent blocks of weights W_1 and W_2 resting on a plane surface which is inclined at an angle of θ to the horizontal. The blocks are acted upon by gravity only and hence the weights W_1 and W_2 act vertically downwards as shown in Figure 4.2. While the T components of the weights tend to cause the blocks to topple about the pivot points A and B, the N components oppose it. Since toppling necessitates

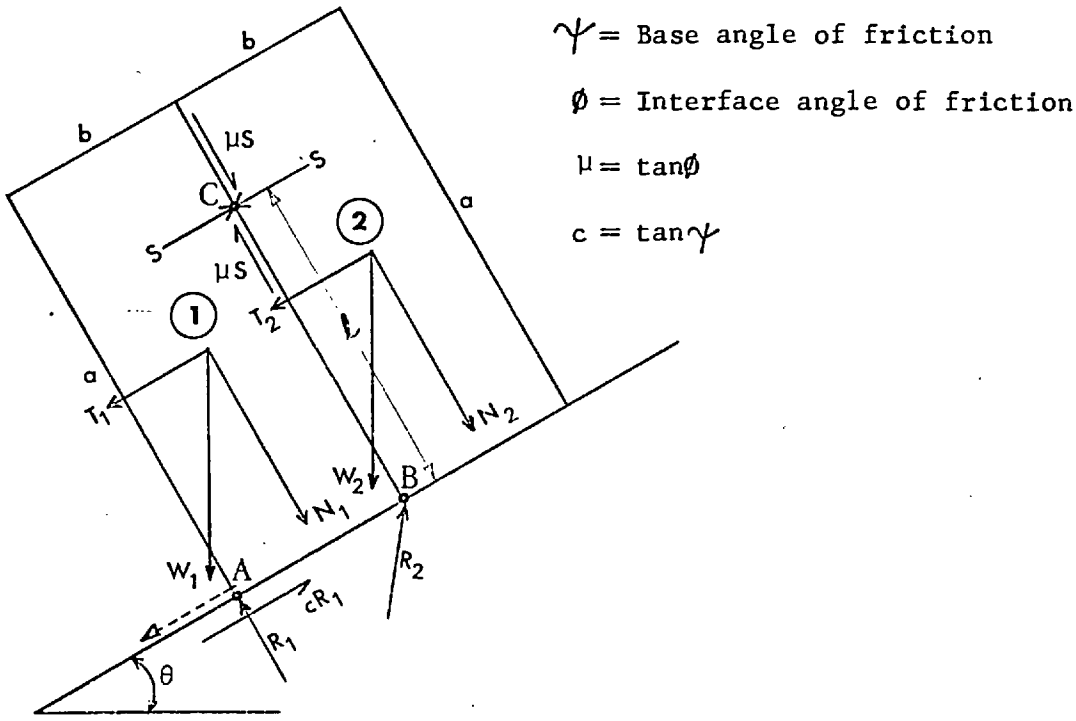

Figure 4.2- Forces acting on two adjacent blocks for toppling mechanism.

sliding movement together with rotation, the forces associated with it (sliding) should be taken into consideration. In this respect, the shear strength along the interface and at corner A must be mobilised assuming the blocks remain in contact along their common face, and corner B does not move. If S is the resultant of the force distribution normal to the interface acting at point C, θ for limiting conditions can be found by resolving the forces on block 1 normal to and parallel to the base plane (equations (1) and (2)), and by taking the moments of forces about pivot points A and B (equations (3) and (4)):

$$R_1 = N_1 + \mu S \tag{1}$$

$$S = CR_1 - T_1 \tag{2}$$

$$\frac{a}{2} T_1 - \frac{b}{2} N_1 + \ell S - b\mu S = 0 \tag{3}$$

$$\frac{a}{2} T_2 - \frac{b}{2} N_2 - \ell S = 0 \tag{4}$$

From (1) and (2) $\quad S = c(N_1 + \mu S) - T_1$

$$S = \frac{cN_1 - T_1}{1 - \mu c} \tag{5}$$

Using (4) and (5) in (3),

$$\frac{a}{2} T_1 - \frac{b}{2} N_1 + \frac{a}{2} T_2 - \frac{b}{2} N_2 - \frac{b\mu(cN_1 - T_1)}{1 - \mu c} = 0 \tag{6}$$

Substituting $\quad T_1 = W_1 \mathrm{Sin}\theta, \quad T_2 = W_2 \mathrm{Sin}\theta$

$$N_1 = W_1 \mathrm{Cos}\theta, \quad N_2 = W_2 \mathrm{Cos}\theta$$

and rearranging equation (6) gives:

$$\tan\theta = \frac{b\left[(W_1+W_2)(1-\mu c) + 2W_1\,\mu c\right]}{a(W_1+W_2)(1-\mu c) + 2W_1 b\mu} \qquad (7)$$

which reduces to equation (8) when $W_2 = W_1 = W$

$$\tan\theta = \frac{b}{a(1-\mu c) + b\mu} \qquad (8)$$

and further to (9) if $c = \mu$

$$\tan\theta = \frac{b}{a(1-\mu^2) + b\mu} \qquad (9)$$

Rearranging equation (8) into,

$$\tan\theta = \frac{b}{a - \mu(ac-b)}$$

and substituting $c = \frac{b}{a}$ gives

$\tan\theta = \frac{b}{a}$ for limiting equilibrium. This indicates that when the friction angle at the base is equal to the critical inclination for the toppling of single block ($\theta_{cr.}$) which is determined by the block geometry, the interface friction no longer operates and the blocks topple as if they were single. Obviously, this value is the lowest possible inclination for the block geometry in consideration. Figure 4.3, where the relationship between θ and ψ for various values of ϕ is plotted, shows the diminishing influence of ϕ as ψ approaches $\theta_{cr.}$. Although the tilting frame test results for single and double block cases were quite close, this cannot be explained by the above mechanism because it occurred for all sizes of blocks.

The results obtained from tilting frame tests were

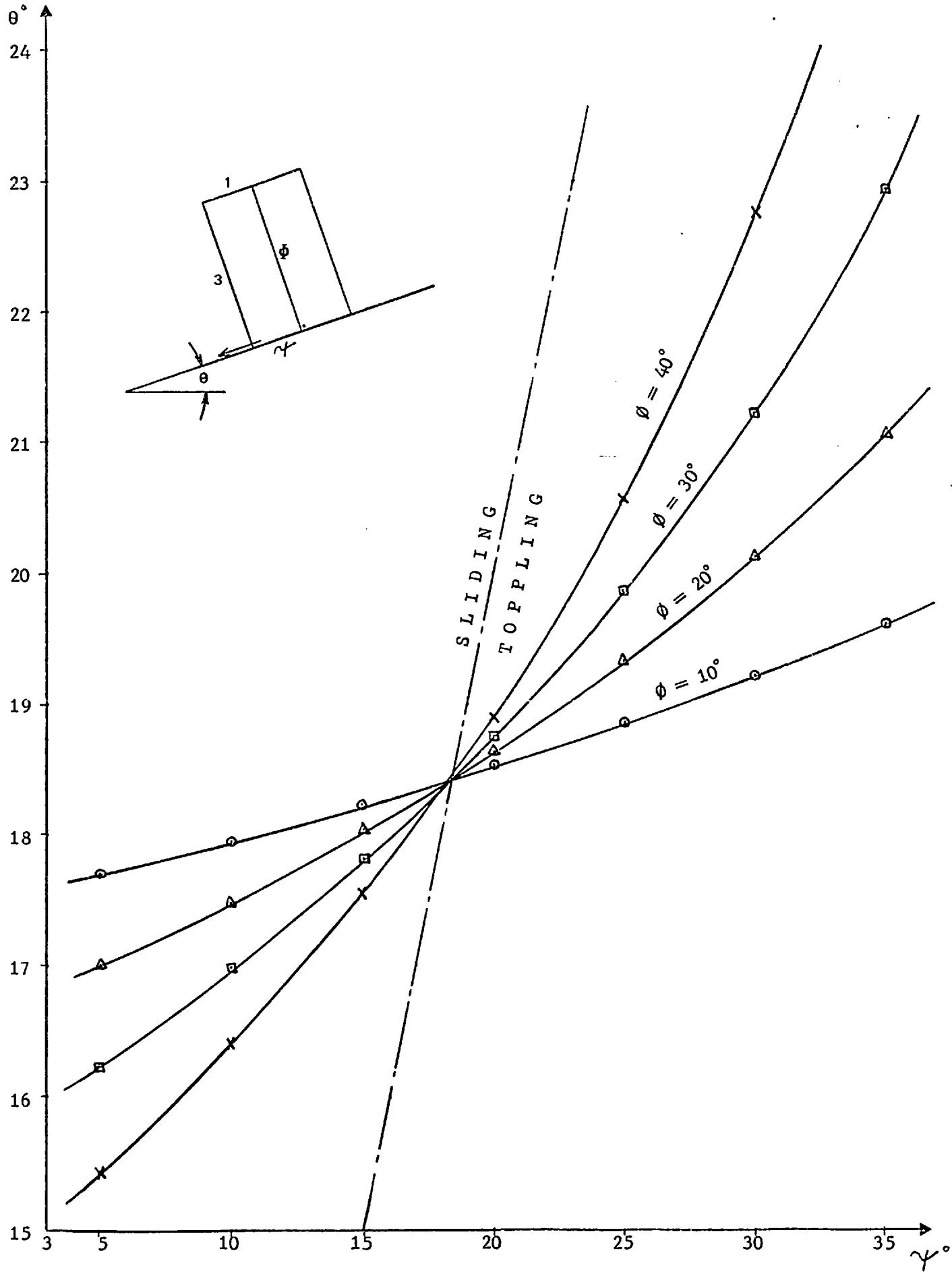

Figure 4.3- Effect of variations in friction angles on tilting angle for toppling.

less stable as compared to the limiting equilibrium solutions. The reasons for this was looked for, and the following alternatives were considered:

(i) the mobilised friction angle in the experiment is smaller than the one used in limiting equilibrium calculations, or

(ii) the assumptions regarding the mode of behaviour of blocks for limiting equilibrium analysis are wrong.

The friction angle along the contact surface of the columns (ϕ) was determined by simple sliding to use in equation (8). Complete sliding took place between 29 and 35 degrees, but prior to this short slips at inclinations ranging from 8^{o} to 22^{o} were present. The calculations based on the latter (a friction angle of 20^{o}) rather than the full sliding of 35^{o}, gave reasonably close θ values to the test results as shown in Figure 4.4 (broken line).

So far, the limiting equilibrium analysis was based on the assumption that only the lower block would slide down during the toppling while the upper one was pivoted on its lower corner. It was obvious that the blocks would behave in a mode rendering the least resistance to failure. Therefore, the other possible mode of behaviours had to be taken into account as one of them might be more unstable approaching the tilting frame test results. The possible other modes are:

1. The upper block slides upward while rotation is taking place; thus the shear strength at corner B should be mobilised. This case is just the reverse of the previous

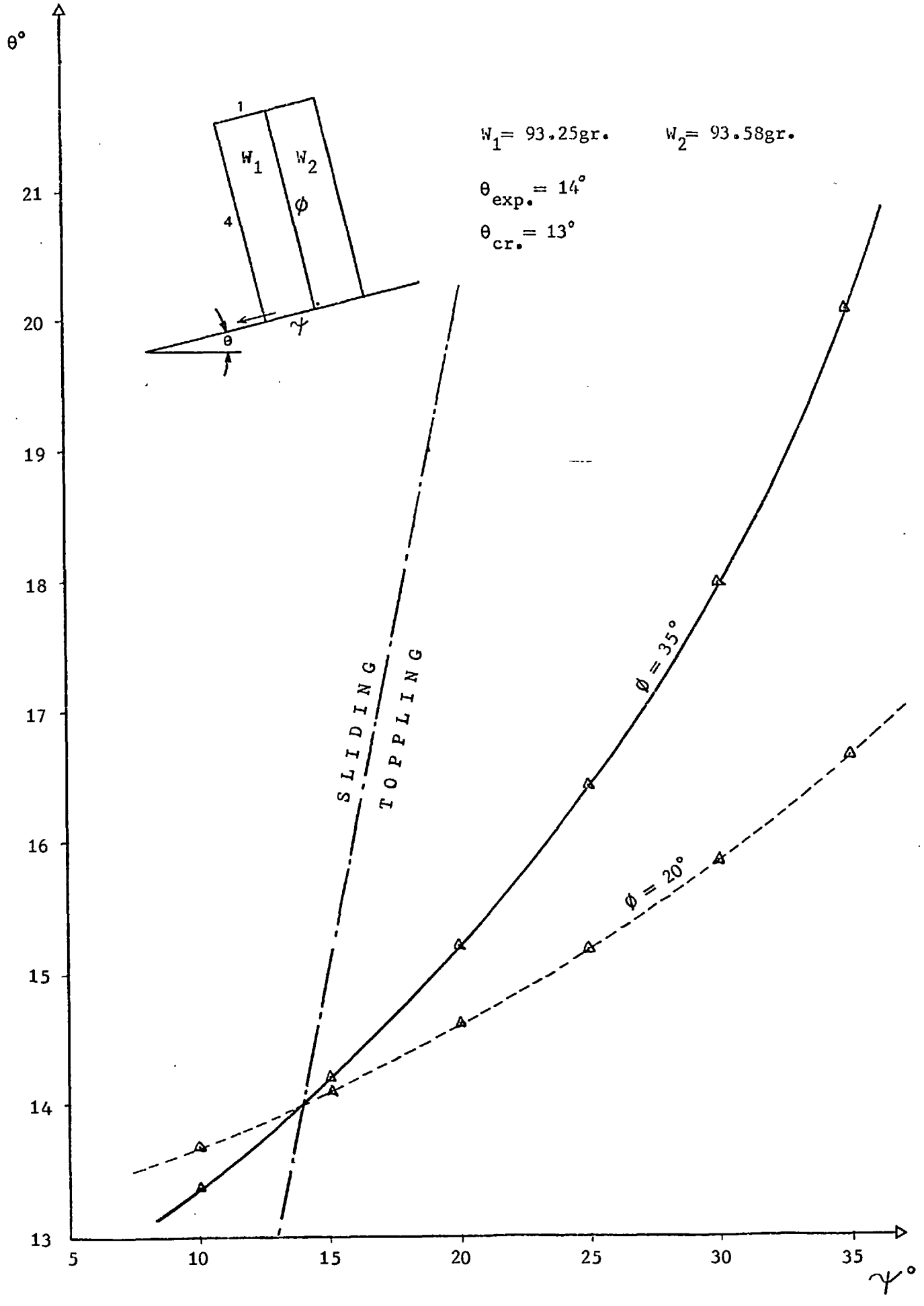

Figure 4.4- Variation of tilting angle for toppling (for limiting equilibrium)with respect to friction angles.

consideration as illustrated in Figure 4.5(a). The limiting conditions are now given by the following equation:

$$\tan\theta = \frac{b[(W_1+W_2)(1+\mu c) + 2W_2\mu c]}{a(W_1+W_2)(1+\mu c) - 2W_2 b\mu} \qquad (10)$$

2. Both of the blocks slide, the lower one downwards, the upper one upwards as shown in Figure 4.5(b). There are two different solutions in this case:

(a) When the equations giving the S forces for each block are equalized:

$$\tan\theta = \frac{W_1 c(1+\mu c) - W_2 c(1-\mu c)}{W_1(1+\mu c) + W_2(1-\mu c)} \qquad (11)$$

The peculiarity with equation (11) is that it does not involve any of the block dimensions. Therefore it cannot be regarded as a correct solution.

(b) From either of the moment equilibrium equations: Then the solution is either equation (7) or equation (10) depending on the source of S used in the moment equation; i.e., the solution is equation (7) when S is derived from Block 1, and equation (10) when S from Block 2 is used. Since this mode of behaviour did not bring anything new it was not considered further. On the other hand, the former possible mode seemed to merit further consideration. In this context, this mode of behaviour was compared with the first consideration for a range of a/b ratios. Graphs relating θ and ψ for ϕ = 20° and 35° were drawn. Figure 4.6 shows one of these graphs

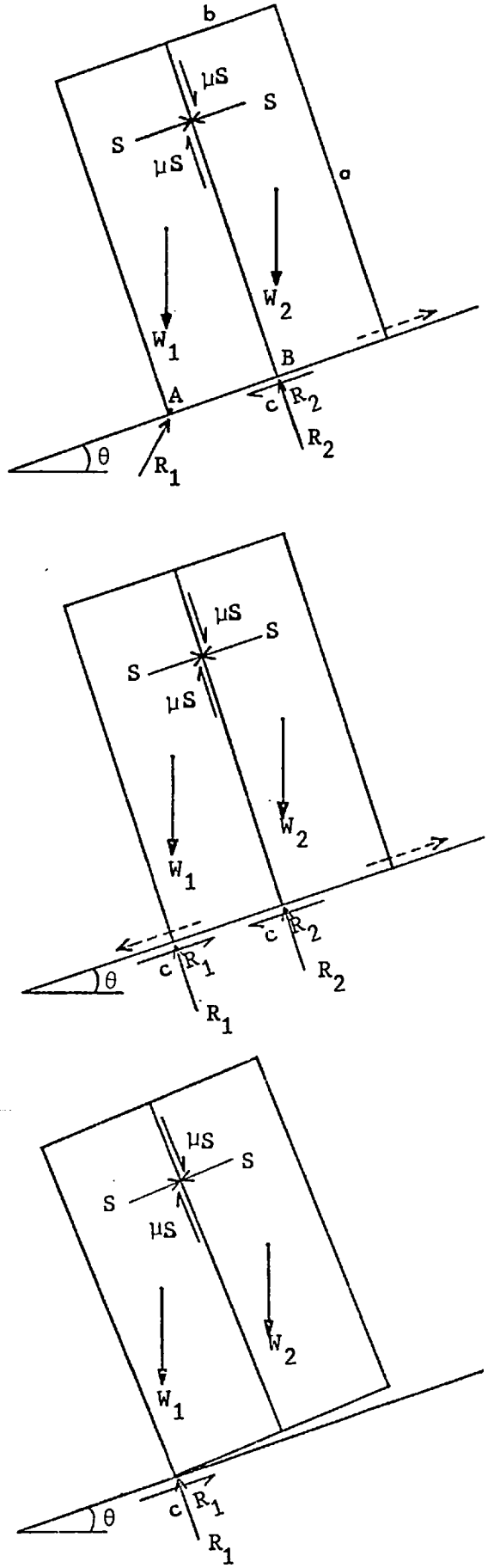

Figure 4.5- Other modes of failure for two adjacent blocks.

for a/b = 3, the others being for the ratios of 2, 4, 5, 6, 7, 8, 9, 10, 15, 20, 30, 40 and 50. The calculations for the ratios of up to 9 (inclusive) were made using the actual weights of blocks tested on the tilting frame for comparison purposes. For the other ratios, the weights were assumed to be the same. The failure takes place with the forward sliding mode for both ϕ values as shown in Figure 4.6. But as the a/b ratio increases the backward sliding mode assumes control after certain ψ values. For example, for a/b = 9 the backward sliding mode becomes operative when ψ is greater than 25.3° and 32.6° for ϕ s of 35° and 20° respectively as illustrated in Figure 4.7. As the columns get taller, what might be called the boundary friction angle at the base (ψ_b) separating the two modes of behaviour decreases, thus the possibility of backward sliding increases. A similar effect was observed when the inter-columnar friction angle (ϕ) increased as shown in Figure 4.8.

3. The third possibility, Figure 4.5(c), is that the two blocks adhere to one another without slip and rotate as a single unit about A. Then the single block criterion applies: $\tan\theta = 2b/a$. Since the width, b, of the toppling unit is doubled this case represents the most stable of all.

4. A further case presents itself due to the practical impossibility of making the blocks identical. If $(a/b)_1 > (a/b)_2$, then when $\tan\theta = (b/a)_1$ block 1 rotates, while block 2 is stable. Though in a way exaggerated, tilting frame test results of the previous chapter (Figure 3.5) confirm this.

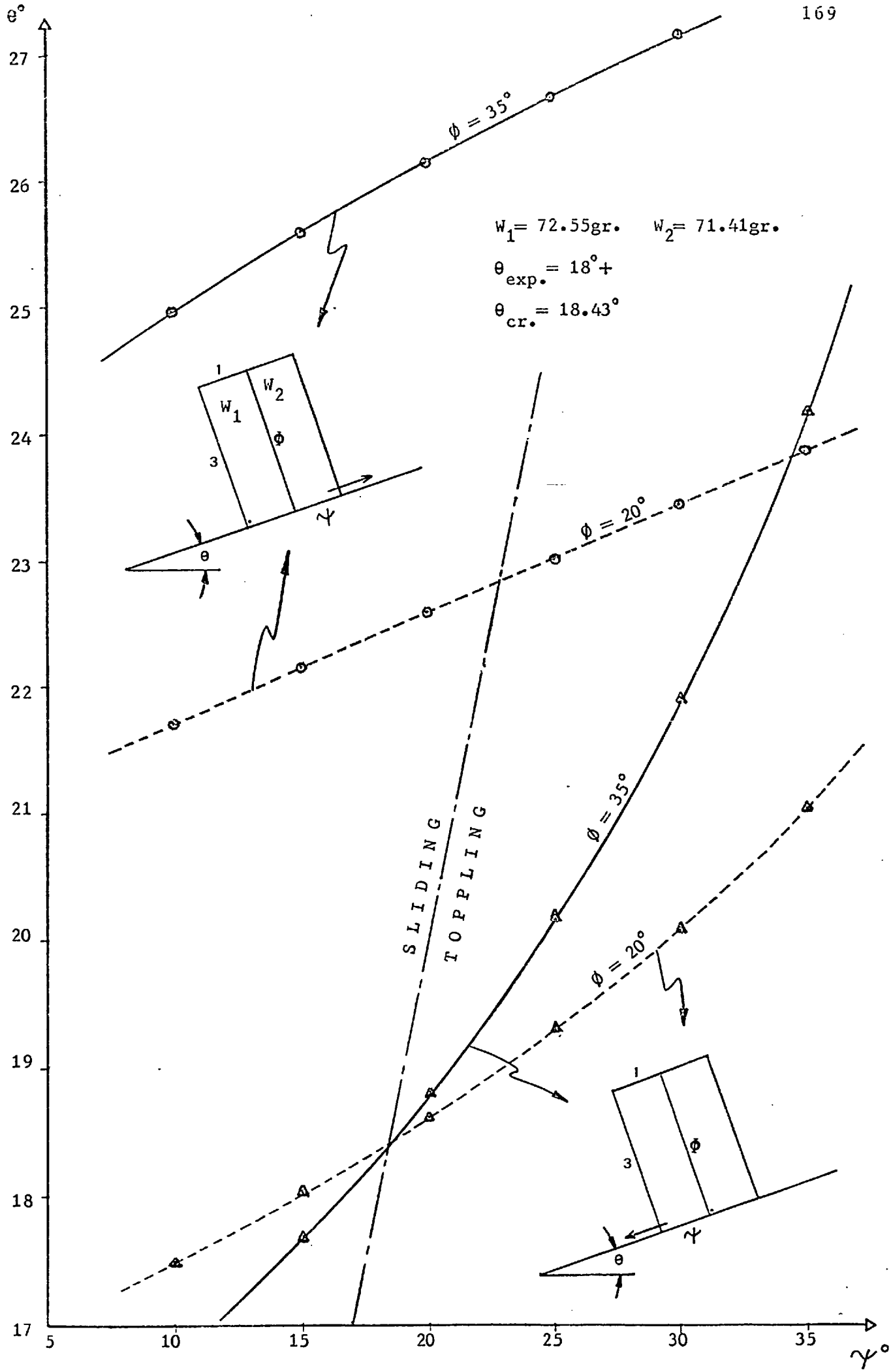

Figure 4.6- Tilting angle variation for forward and backward sliding modes.

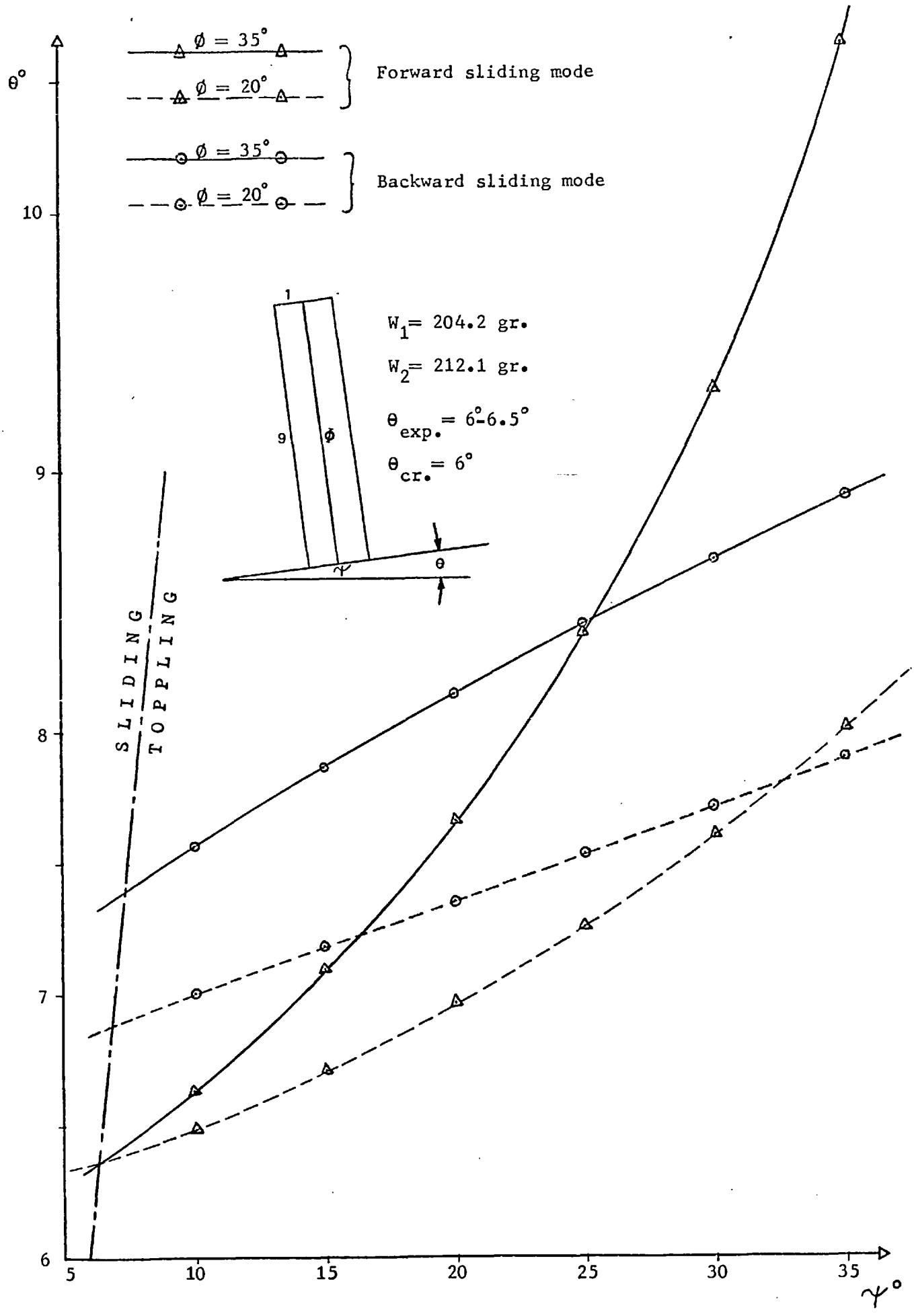

Figure 4.7- Tilting angle variation for two sets of analyses of the double block system and the friction angles.

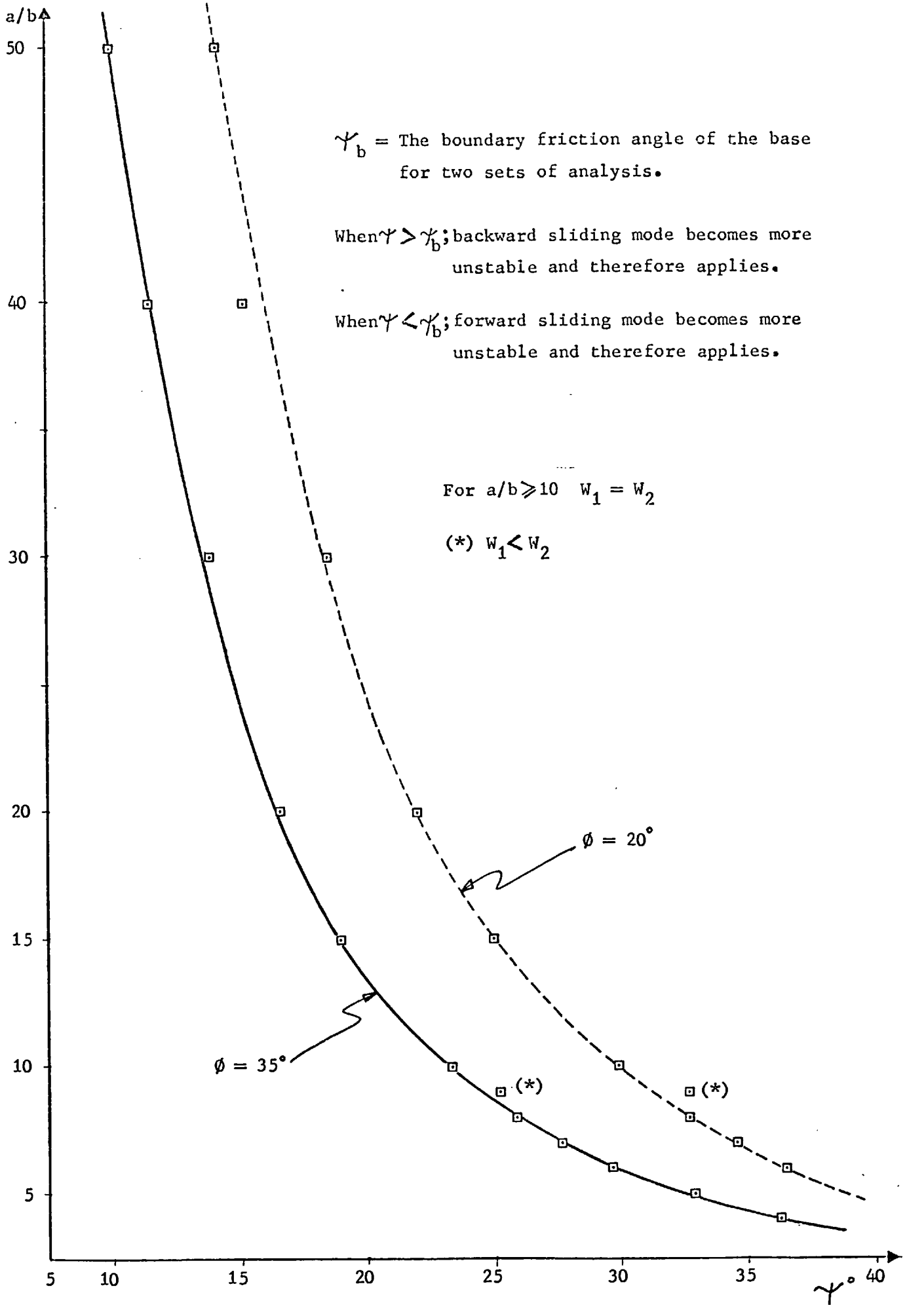

Figure 4.8- Boundary friction angle for the two sets of analysis of double block system with varying a/b ratios and intercolumnar friction angles.

In the beginning it was assumed that the blocks remain in contact along their common face with a resultant force of S. Since the nature of this force (compressive or tensile) depends on other variables, it should be analysed for the different modes of behaviour.

(i) For the case of forward sliding:

$$\text{From (5)} \qquad S = \frac{W_1(\tan\psi.\cos\theta - \sin\theta)}{1 - \tan\psi.\tan\phi} \qquad (12)$$

when,

$\psi > \theta$ and $1 > \tan\psi.\tan\phi$ $(\phi + \psi < \pi/2)$

or

$\psi < \theta$ and $1 < \tan\psi.\tan\phi$ $(\phi + \psi > \pi/2)$

$\Longrightarrow$ S = +ve (COMPRESSIVE)

$\psi < \theta$ ↓ Allows for sliding; therefore should be disregarded.

$\psi > \theta$ and $1 < \tan\psi.\tan\phi$ $(\phi + \psi > \pi/2)$

or

$\psi < \theta$ and $1 > \tan\psi.\tan\phi$ $(\phi + \psi < \pi/2)$

$\Longrightarrow$ S = -ve (TENSILE)

$\psi < \theta$ ↓ Allows for sliding; therefore should be disregarded.

$\{\psi = \theta\} \rightarrow S = 0$

Consequently, for the blocks to be in touch with each other, that is for the S to be compressive, the sum of friction angles along the interface (ϕ) and at the base (ψ) must be less than

90^{o} in addition to the main condition that ψ must be greater than θ to preclude sliding failure. If the frictional characteristics of the surfaces (base and interface) are the same ($\psi = \phi$), then the friction angle must not be more than 45^{o}.

When the friction angle at the base is equal to the critical inclination the blocks are said to be meta-stable, being on the threshold of sliding and toppling failure together without any interaction. Therefore, the blocks behave independently. This phenomenon is merely the expression of the earlier finding obtained in another way.

(ii) For the case of backward sliding:

$$S = \frac{W_2(\sin\theta + \tan\psi.\cos\theta)}{1 + \tan\psi.\tan\phi} \qquad (13)$$

The equation (13) gives a positive S always indicating the presence of interaction between the blocks for all values of ψ, ϕ and θ when the backward sliding mode is operative.

4.3 Triple and Quadruple Block Analysis

As the number of adjacent columns increases so does the number of possible modes of behaviour. Figure 4.9 shows the likely modes for triple and quadruple block systems. To find out the mode giving the least stable conditions all cases should be subjected to limiting equilibrium analysis one by one. But, because of limited time, four of the five possible modes for triple blocks, and only one of the seven possible modes for quadruple blocks were examined.

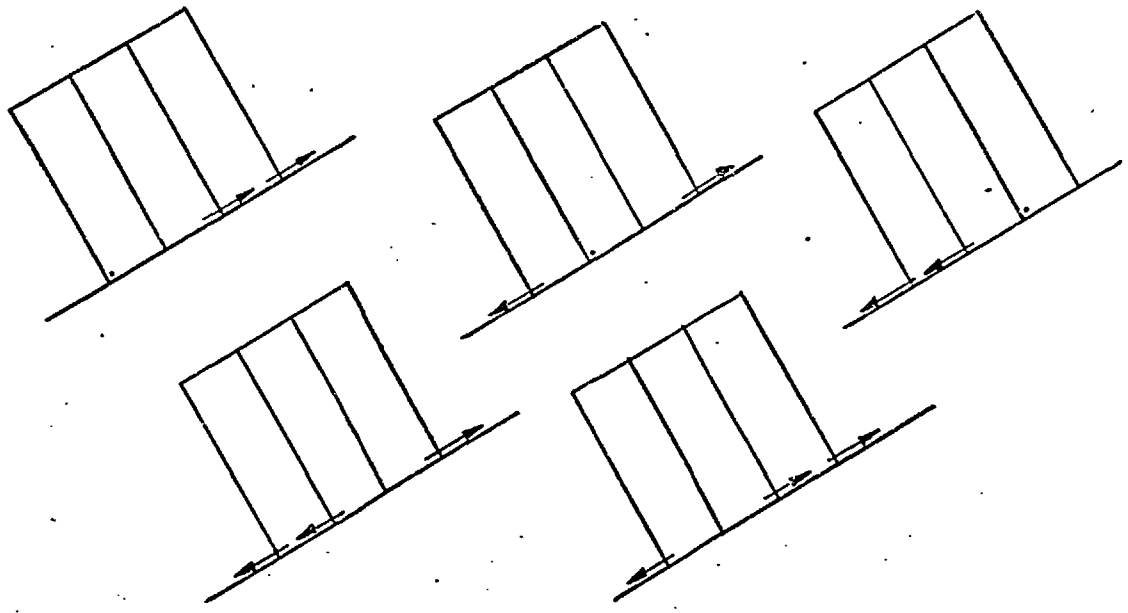

(a)

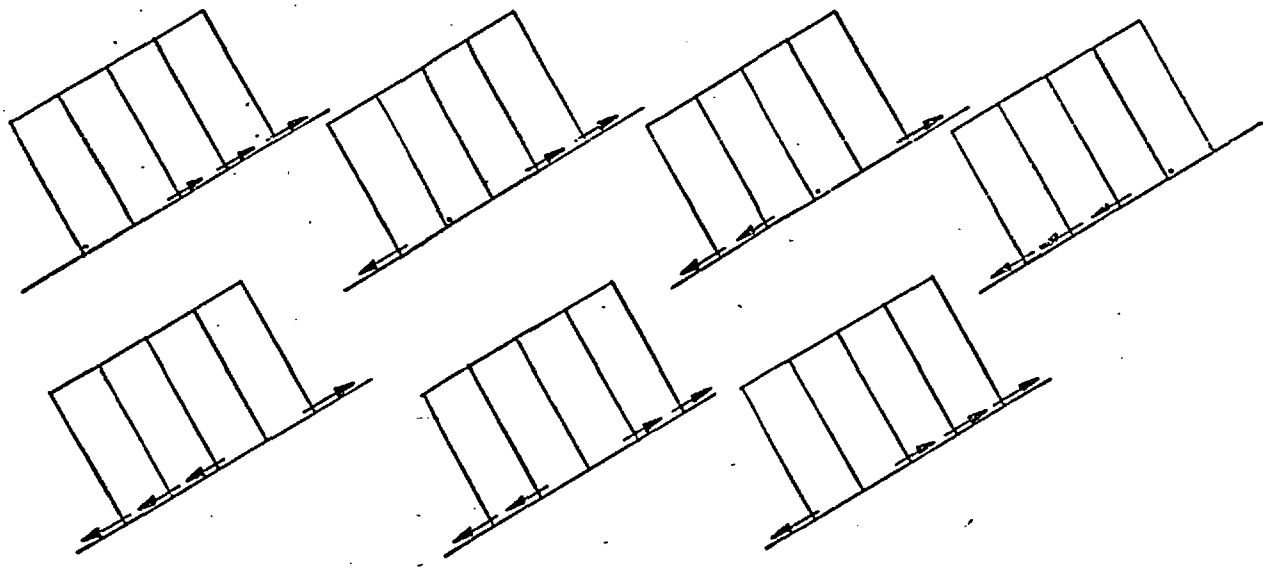

(b)

Figure 4.9- Possible modes of failure for (a)triple block system, (b)quadruple block system.

4.3.1 - Triple Block Analysis -

The analysis was merely the extension of double block case to triple block. The equations for limiting conditions are given below, assuming $W_3 = W_2 = W_1 = W$.

a.

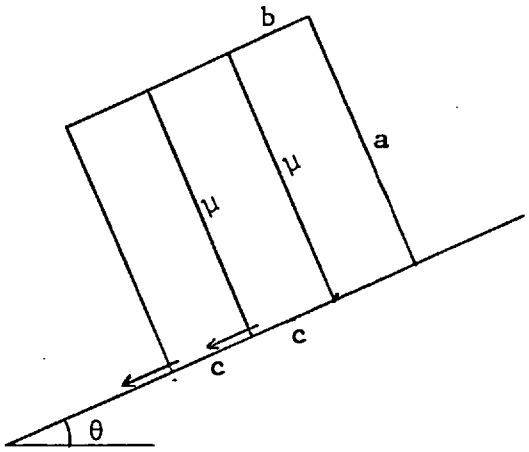

$$\tan\theta = \frac{b}{a(1-\mu c) + b\mu} \qquad (14)$$

b.

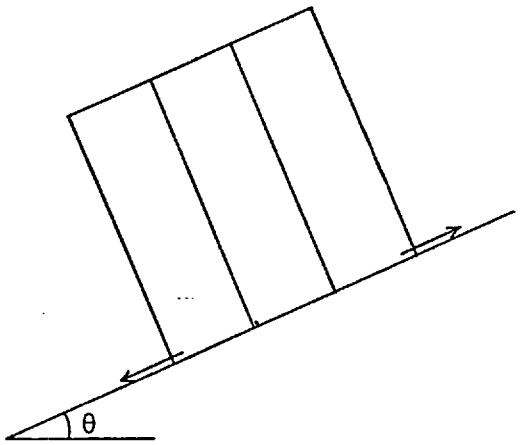

$$\tan\theta = \frac{3b(1-\mu^2c^2) + 4b\mu c}{3a(1-\mu^2c^2) + 4b\mu^2c} \qquad (15)$$

c.

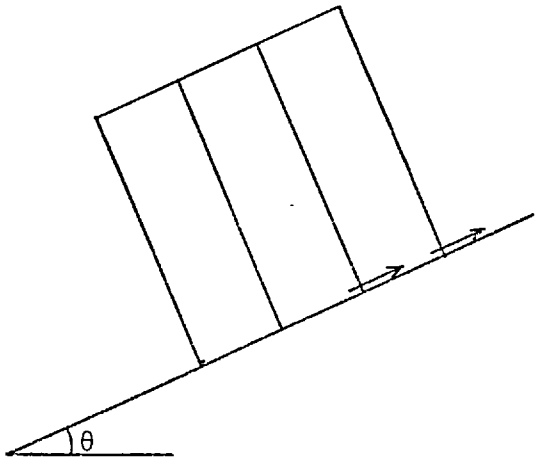

$$\tan\theta = \frac{b(3\mu c+1)}{a(\mu c+1) - 2b\mu} \qquad (16)$$

d.

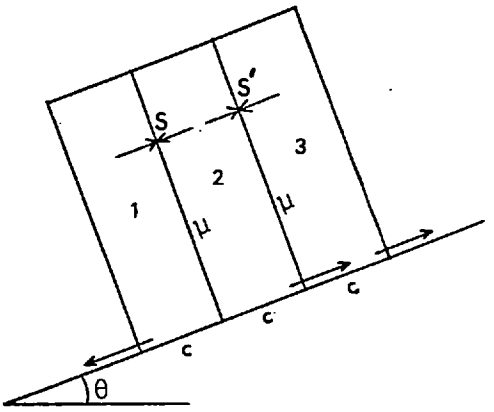

Two different solutions are available in this case.

(i) From the equality of S forces:

$$\tan\theta = \frac{\mu c^2(2+3\mu c) - c}{\mu c(2-\mu c) + 3} \qquad (17)$$

(ii) From either of the moment equations for block 1 or 2:

The solution is equation (15) when S derived from block 1 is used in any of the moment equations for block 1 or 2.

The solution is equation (16) when S derived from block 2 is used in any of the moment equations for block 1 or 2.

Since the equations (8) and (14) are the same, it becomes:

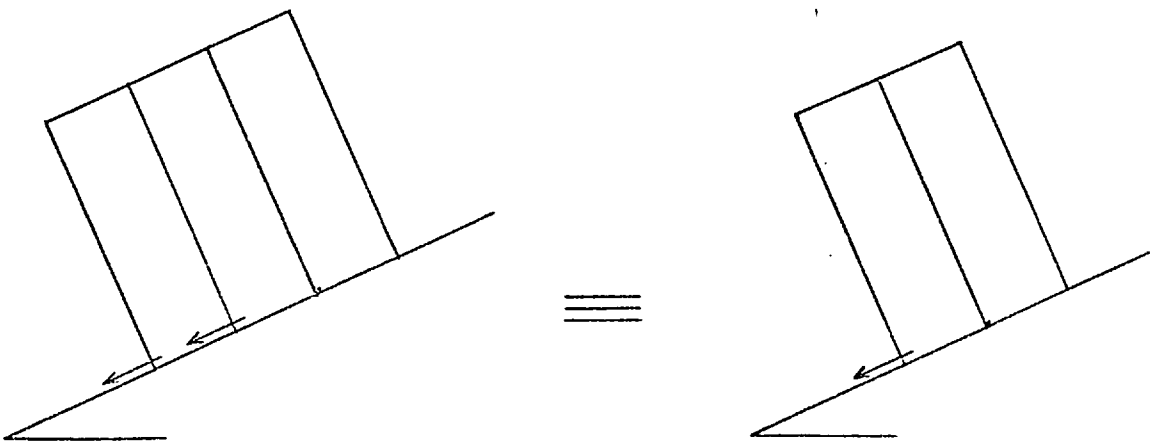

So, mode (a) represents the least stable of all because it reduces to two block behaviour. This is confirmed in Figure 4.10 where the critical inclination at the base (θ) is plotted against the friction angle along the contact surfaces ($\phi = \psi$) for the a/b ratios of 3,5, and 7. As also could be seen in Figure 4.10, case (c) happens to be the most unlikely mechanism of toppling.

4.3.2 - Quadruple Block Analysis -

Only the following case was analysed because of limited time against the lengthy equations to be solved.

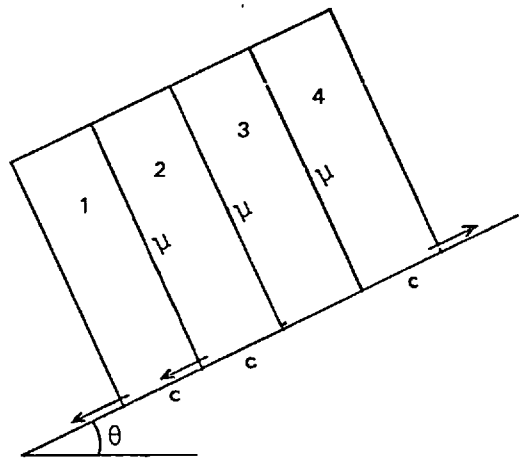

Assuming $W_4 = W_3 = W_2 = W_1 = W$,

$$\tan\theta = \frac{b\left[c^2(2c-1)\mu^3 - 7c^2\mu^2 + (3c+1)\mu + 4\right]}{2\left[a(1-2\mu c+\mu^2c^2) + 2b\mu(1-\mu c)\right](2+\mu c) - 4b\mu(1-\mu c)^2} \qquad (18)$$

reduces to (19) when $c = \mu$

$$\tan\theta = \frac{b\{\mu^4[(2\mu-3)(\mu+1) - 4] + [(3\mu+4)(\mu-1) + 8]\}}{(\mu+1)(\mu-1)\{2[a(\mu+1)(\mu-1) - 2b\mu](\mu^2+2) + 4b\mu(\mu+1)(\mu-1)\}} \qquad (19)$$

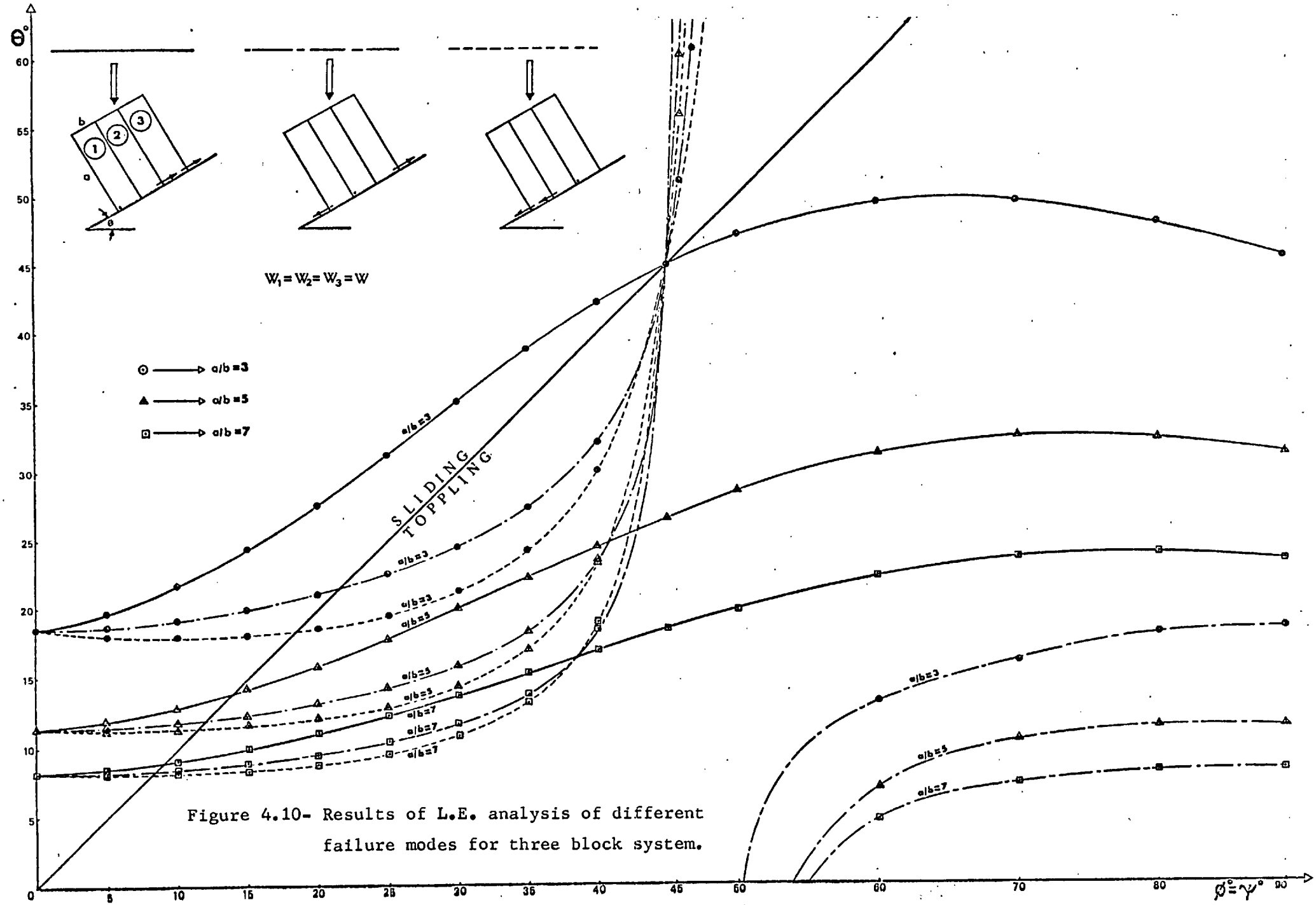

Figure 4.10- Results of L.E. analysis of different failure modes for three block system.

4.4 Multiple Block Analysis

Bray's[4] approach for a series of monolithic columns comprising the slope comes nearer to a real case. For the following analysis he assumes a fully drained slope made up of rigid columns which neither fracture nor deform. Sliding on its own is still a mode of failure for part of the slope as shown in Figure 4.11 below.

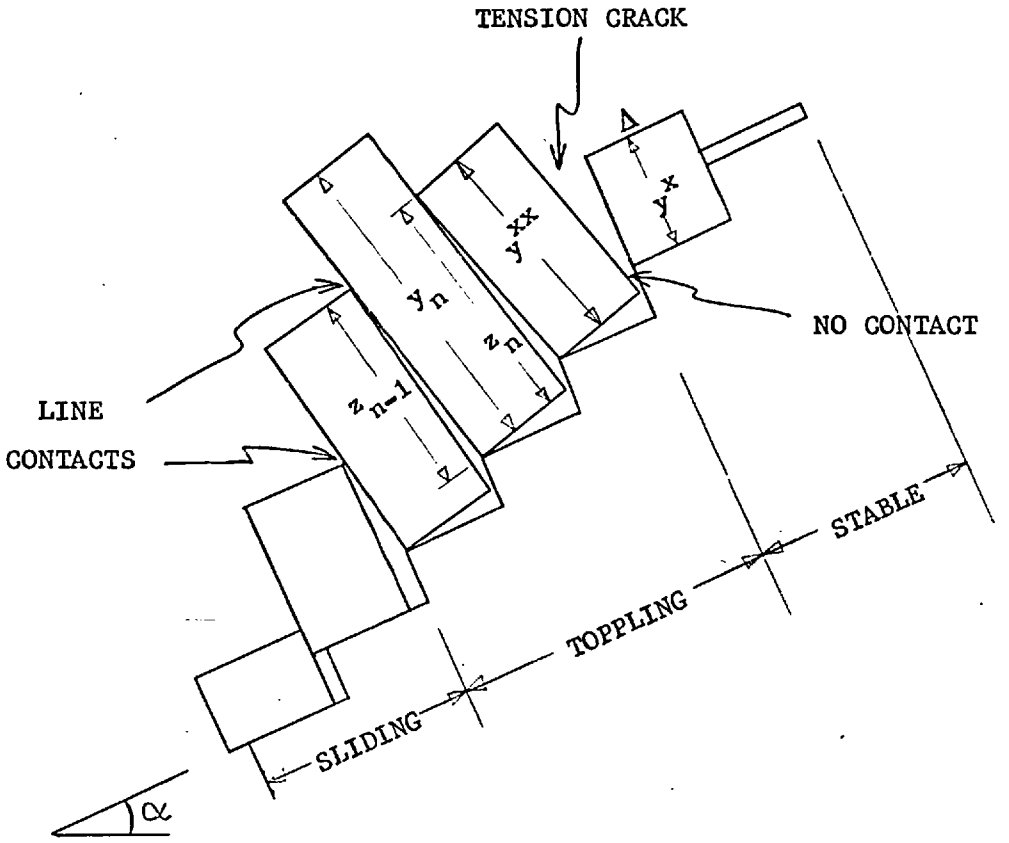

Figure 4.11- Toppling on a Stepped Base (After Bray[4]).

The location of the tension crack which separates the stable zone from the moving part is determined by the single block criterion for toppling. Therefore,

for the block above the tension crack $y^x < \Delta Cot\alpha$ and, for the block below the tension crack $y^{xx} > \Delta Cot\alpha$.

Limiting conditions for a typical column can be analysed considering the forces acting on the nth. block as in Figure 4.12.

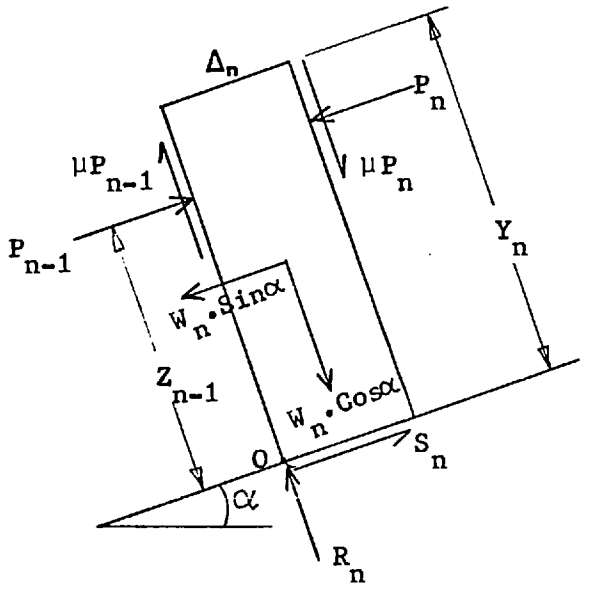

Figure 4.12- Forces acting on the nth. block.

Then, the force P_n to cause toppling is given by equation (20) by taking moments about O.

$$P_n.Z_n - \mu P_n.\Delta_n = P_{n-1}.Z_{n-1} + W_n Cos\alpha.\Delta_n/2 - W_n.Sin\alpha.Y_n/2$$

$$P_n = \frac{P_{n-1}.Z_{n-1} + W_n/2(\Delta n.Cos\alpha - Y_n.Sin\alpha)}{Z_n - \mu\Delta_n} = P_n'' \qquad (20)$$

And, the force P_n to cause sliding can be obtained resolving the forces parallel to R_n and S_n.

$$R_n = W_n.Cos\alpha + \mu(P_n - P_{n-1})$$

$$S_n = W_n.Sin\alpha + (P_n - P_{n-1})$$

For slip $S_n = R_n.\mu$

$$W_n.\text{Sin}\alpha + (P_n - P_{n-1}) = \mu.w_n.\text{Cos}\alpha + \mu^2(P_n - P_{n-1})$$

$$P_n = P_{n-1} + \frac{w_n(\mu.\text{Cos}\alpha - \text{Sin}\alpha)}{1 - \mu^2} = P_n' \qquad (21)$$

Consequently, if $P_n' < P_n'' \rightarrow P_n = P_n'$ Block slides

if $P_n'' < P_n' \rightarrow P_n = P_n''$ Block topples

The analysis is carried out to find the friction coefficient, μ, required for limiting equilibrium. For this purpose one should iterate μ until the end conditions are satisfied, i.e. until $P_n = 0$ for the block neighbouring tension crack. Then, the factor of safety for toppling can be defined as:

$$\text{F.S.} = \frac{\mu \text{ available in the field}}{\mu \text{ required for limiting eq.}}$$

The reader is referred to Goodman and Bray[5], and Hoek and Bray[6] for the details of the analysis and the examples. A simple computer program written by the author to find μ for limiting equilibrium is given in Appendix A.

4.5 Conclusions

Although few results of practical use were obtained, the findings regarding the behaviour of double and triple blocks are of interest. In both cases, toppling was accompanied by forward sliding of the lower block(s), this being the least stable mode by reducing to single and double block behaviour. However, a tendency towards the backward sliding mode was seen as the columns got taller as far as the double

block case was concerned. A similar effect happens when intercolumnar friction angle (ϕ) increases. Considering the interaction between the blocks, the sum of the friction angles ($\phi+\psi$) should be less than 90^{o} for the contact to be maintained i.e. for S to be compressive.

The limiting equilibrium analysis gave more stable configurations as compared to the tilting frame test results, probably due to the experimental conditions in the latter such as the vibrations created by the motor, inaccurate block dimensions, varying frictional characteristics, etc.

Although Bray's[4] analysis is very versatile offering a factor of safety for toppling failure, it needs to be improved to take the groundwater conditions and the joint characteristics into account, and perhaps most important of all it should be able to handle slopes composed of blocks rather than monolithic columns.

REFERENCES

1. ASHBY, J. Sliding and toppling modes of failure in models and jointed rock slopes. M.Sc. Thesis, Univ. of London (Imperial College), 1971, 40p.

2. HOEK, E. and BRAY, J.W. Rock Slope Engineering. The Inst. of Mining and Metall. (Publisher), London, 1974, 309p.

3. CUNDALL, P. The use of rigid block models to study discontinuum problems. Rock Mechanics Seminar, Imperial College, London, 1976.

4. BRAY, J.W. Rock Slope Stability Lecture Notes, Imperial College, London, Nov. 1976.

5. GOODMAN, R.E. and BRAY, J.W. Toppling of rock slopes. Proc. Conf. on Rock Engineering for Foundations & Slopes, ASCE, Boulder, Colo. Vol. 2, 1976.

6. HOEK, E. and BRAY, J.W. Rock Slope Engineering (2nd Edition). The Inst. of Mining & Metallurgy, London, 1977.

CHAPTER FIVE

DYNAMIC RELAXATION METHOD

5.1 General

It would be unwise not to make use of a numerical technique at such a time when they are abundant. The Dynamic Relaxation method (D.R.) was thought to be the best approach available because Cundall[1] had shown its versatility with his spectacular computer drawings, and there was a "package" program ready to run written by Hocking[2]; but it needed to be tested against the established toppling criterion and to be modified to handle different size blocks.

Thus, as the mode of failure was automatically selected, the field configurations would be better modelled as compared to the limiting equilibrium approach which requires an estimate of the failure mode if not known. Also, the individual study of the effects of variation of various parameters on the failure mode would be possible which otherwise would be extremely difficult or impossible with physical modelling techniques.

5.2 Basic Principles

The Dynamic Relaxation Method was first introduced by Otter[3] and his co-workers as a new numerical technique to solve the finite difference formulations of the equations of elasticity. It was originally designed to model an isotropic elastic continuum; but, later on, Cundall[1] adopted the idea

and developed a computer program for treating discontinuous rock problems.

Cundall's program was capable of simulating progressive, large scale movements in blocky rock systems, the interaction between blocks being governed by realistic friction laws and simple stiffness parameters. The underlying assumption of the whole program was that all the blocks were perfectly rigid and that all deformations were completely controlled by block sliding and rotation movements. Thus the program was only suitable for the analysis of problems in which substantial block movements were likely to occur. The elastic deformation within each block was assumed to be negligible when compared with mechanistically controlled block movements. An additional assumption was that when blocks (any parallelogram shape) interact along a common face the response could be modelled through the corner contact points only.

The analysis sequence began with an out of balance force acting at the centroid of each block, and from this an acceleration was calculated using the momentum equation:

$$\text{Force} = \text{Mass} \times \text{Acceleration}$$

This acceleration was then integrated with respect to a given time step, firstly to calculate the velocity of each block, and then its position at the end of the time step. The new geometrical arrangement of all the blocks was then used to compute the overlap of each block corner with its neighbours (in case of no overlap the existence of a gap between blocks was recognised), and the forces acting at each corner were

calculated according to the normal stiffness and the proposed shear force-displacement relationship. These contact forces were then algebraically summed to act at the block centroid and the calculations were repeated for a number of iterative cycles.

The equations governing the response of each block centroid were:

$$\left\{\begin{array}{ll} a = \frac{F}{M} & \ddot{u} = \frac{M}{I} \\ V_{n+1} = V_n + a.\Delta t & \dot{u}_{n+1} = \dot{u}_n + \ddot{u}.\Delta t \\ S_{n+1} = S_n + V_{n+1}.\Delta t & u_{n+1} = u_n + \dot{u}_{n+1}.\Delta t \end{array}\right\} \quad (I)$$

Those governing the interaction of each block corner were:

$$\left\{\begin{array}{l} F_n = k_n.\delta_n \\ F_s = k_s.\delta_s \end{array}\right\} \quad (II)$$

(I) and (II) were linked by the following equations.

$$\left\{\begin{array}{l} F = \Sigma F_n + \Sigma F_s + \text{Applied Forces} \\ M = \Sigma F_n.r + \Sigma F_s.r + \text{Applied Moments} \end{array}\right\} \quad (III)$$

where:

M = Moment acting on the block

a = acceleration

F = accumulative force acting at the block centroid (has X and Y components)

m = block mass

$\ddot{u}$ = angular acceleration for the block

I = moment of inertia

V_{n+1} = new block velocity (has X and Y components)

V_n = previous block velocity (has X and Y components)

$\dot{u}_{n+1}$ = new angular velocity

$\dot{u}_n$ = previous angular velocity

S_{n+1} = new block position (has X and Y components)

S_n = previous block position (has X and Y components)

u_{n+1} = new block orientation

u_n = previous block orientation

F_n = contact force due to normal overlap

F_s = contact force due to shear overlap

k_n = stiffness of normal overlap

k_s = stiffness of shear overlap

δ_n = normal overlap

δ_s = shear overlap

r = moment arm (moments taken about the block centroid)

The calculation steps outlined above could be summarised as in Figure 5.1.

Hocking[2] made some improvements in Cundall's program and brought it into the form of a "package". This version of the program, which will be the subject of the next section, was extensively tested and used, eventually modified (for handling blocks of unequal height) by the author. Gerogiannopoulos[4] also modified Cundall's program for handling triangular blocks. Recently, Hocking[5] tried to simulate the crushing of the blocks besides the progressive large scale movements incorporating a finite element program with the D.R..

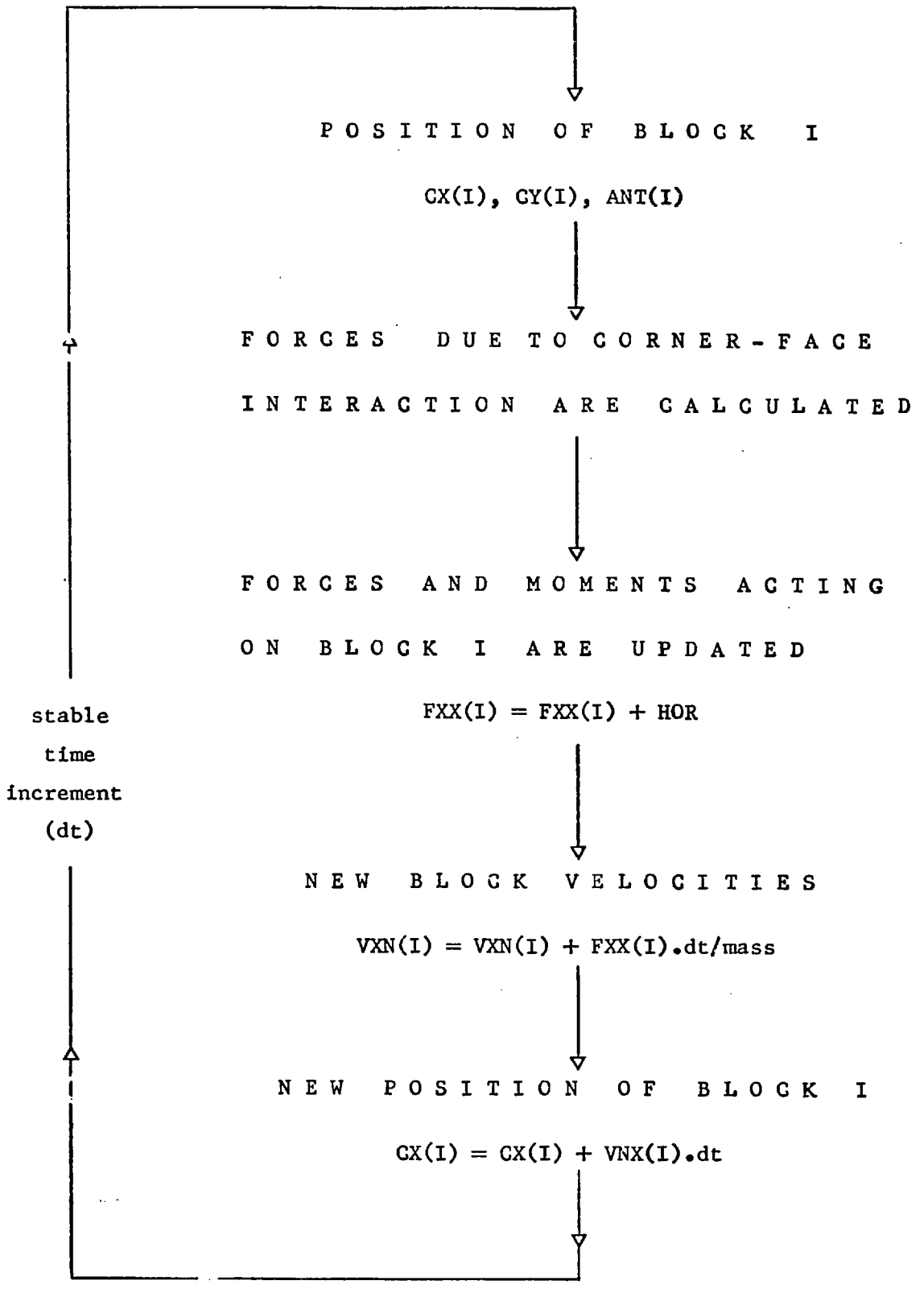

Figure 5.1- Main iteration cycle.

5.2.1 - Details of the Program -

Hocking's program is restricted to blocks all of the same parallelogram shape and dimensions. They are defined by the orientations and the spacings of the discontinuities read into the program as dips and spacings. DIPA has a westerly dip direction (assuming a two dimensional configuration) and DIPB has an easterly dip direction as shown in Figure 5.2.

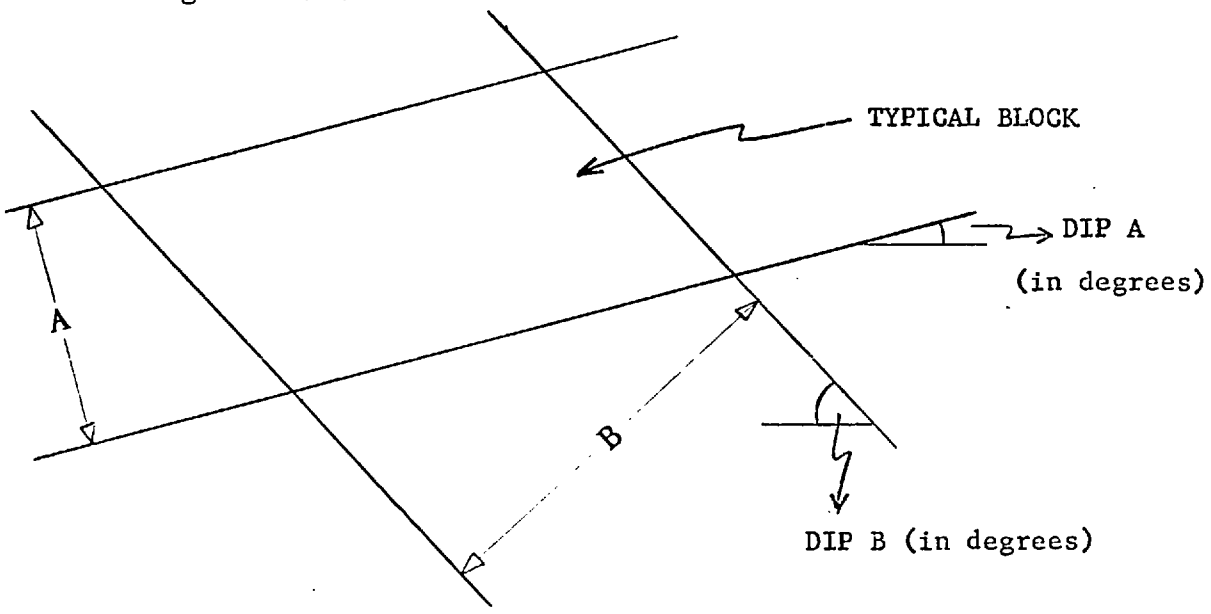

Figure 5.2- Intersecting discontinuities forming parallelogram shaped blocks.

The position of all of the block centroids is to be generated in subroutine GEN. Subroutine CONSOL is for the consolidation of the blocks before simulating a mining extraction. In order to assess the block interactions a record of each block's nearest neighbours must be kept and updated. This is done with subroutine NEIGHB at regular cycle intervals depending on the type of problem and the amount of block

movements expected each cycle. Each block has a maximum of eight neighbouring blocks as compared to six neighbours in Cundall's program.

Other features included in the program are:

i. a restart option so that the analysis can be continued from the end of the last cycle of the previous run,

ii. print edits, and

iii. block position and velocity vector plots at regular intervals.

5.2.2 - Important Input Parameters -

The accuracy of the solutions produced depends on whether the following input parameters are well optimized.

i. the time step for each iteration

ii. the stiffness across and along each discontinuity

iii. the amount of damping to be applied to each block interaction.

Although it is desirable to use as large a time step as possible for each iteration in order to keep the computer costs to a minimum, it cannot be arbitrarily large because rapid changes in the geometry of the block system would not be modelled accurately. The limit comes from the fact that, being a dynamic system, each block must oscillate in a stable manner, and Cundall has shown that for translatory motion this condition is satisfied if,

$$\Delta t < 2\sqrt{\frac{m}{K}} \qquad (1)$$

and for angular motion if,

$$\Delta t < 2\sqrt{\frac{I}{K_r}} \qquad (2)$$

where: Δt = time step

m = block mass

I = moment of inertia

K = block translation stiffness

K_r = block angular stiffness ($= \frac{\text{change in torque}}{\text{change in angle}}$)

K and K_r are the apparent stiffnesses that a block feels when it is in contact with other blocks. The stable time step is, then, the lowest value of Δt obtained from the equations (1) and (2) for all of the blocks.

To compute the forces from the block corner-side interaction a finite stiffness must be assigned for both normal and shear responses. If the interactions are made too stiff the stable time step becomes very small (as the equations 1 and 2 suggest), and a very large number of iterations need to be run to define block movements. If, on the other hand, the stiffness of the discontinuity is too low, unrealistically large overlaps can develop which may influence the deformation mechanism. Therefore, a balance is needed between the two extremes.

In order to make the program quick and simple it is assumed that the normal stiffness of a joint plays very little part in the failure processes of rock mass brought about by joint shearing or tensile separation stemming from the fact that the normal stiffness of many joints is often far higher

than the shear stiffness. So, the normal force between two blocks is assumed to be proportional to the linear overlap between them. The shear spring stiffness, however, may have a greater physical significance since it affects the form of the non-linear shear load-deformation behaviour as will be discussed in the next section. For the solutions described in this thesis, the normal and shear spring stiffnesses were assumed to be equal.

To obtain statically determinate solutions some form of energy dissipation mechanism is needed, otherwise the blocks will continually vibrate and never come to an equilibrium position. This can be accomplished by mathematically connecting viscous dashpots in parallel with both the shear and normal stiffness of each contact point as described by Cundall[6]. The way in which the viscous damping is applied is shown diagrammatically in Figure 5.3.

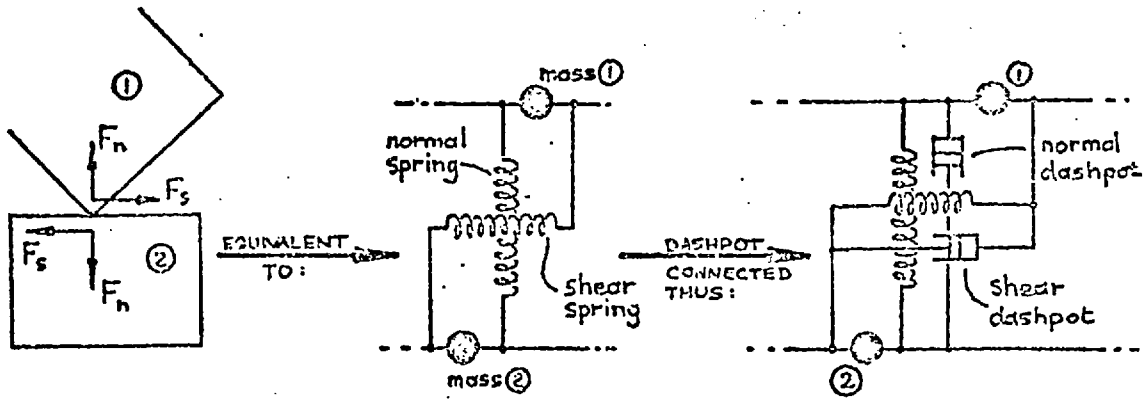

Figure 5.3- Manner of application of viscous damping (After Cundall[6]).

The damping constant of the dashpot is expressed as a fraction of the critical damping, i.e. the dead beat response of the mass-spring system, which is given by:

$$\lambda = 2\sqrt{m.k}$$ where: m = mass, k = stiffness

The shear dashpot is removed if the contact point begins to slide (inelastically) since the energy dissipated by friction is an adequate form of damping by itself.

5.2.3 - Normal and Shear Load-Deformation Response -

The normal load-deformation response is fundamentally elastic in compression with a zero tensile strength characteristics as shown diagrammatically in Figure 5.4(a).

The shear behaviour can be readily modified depending on the nature of the problem to be solved. The present program correctly models an elastic-plastic relationship (Figure 5.4(b), and needs only a small modification to model a peak-residual type relationship (Figure 5.4(c)).

5.3 Tests with D.R. Block Program

Initially it was thought and hoped that Hocking's program was ready to use, but the trial runs revealed the need for some corrections. Most important of all, an error in the logic of the program in connection with the selection of the neighbouring blocks had to be corrected because wrong neighbours were being assigned due to an overriding zero. The removal of the shear dashpot when the contact point in-

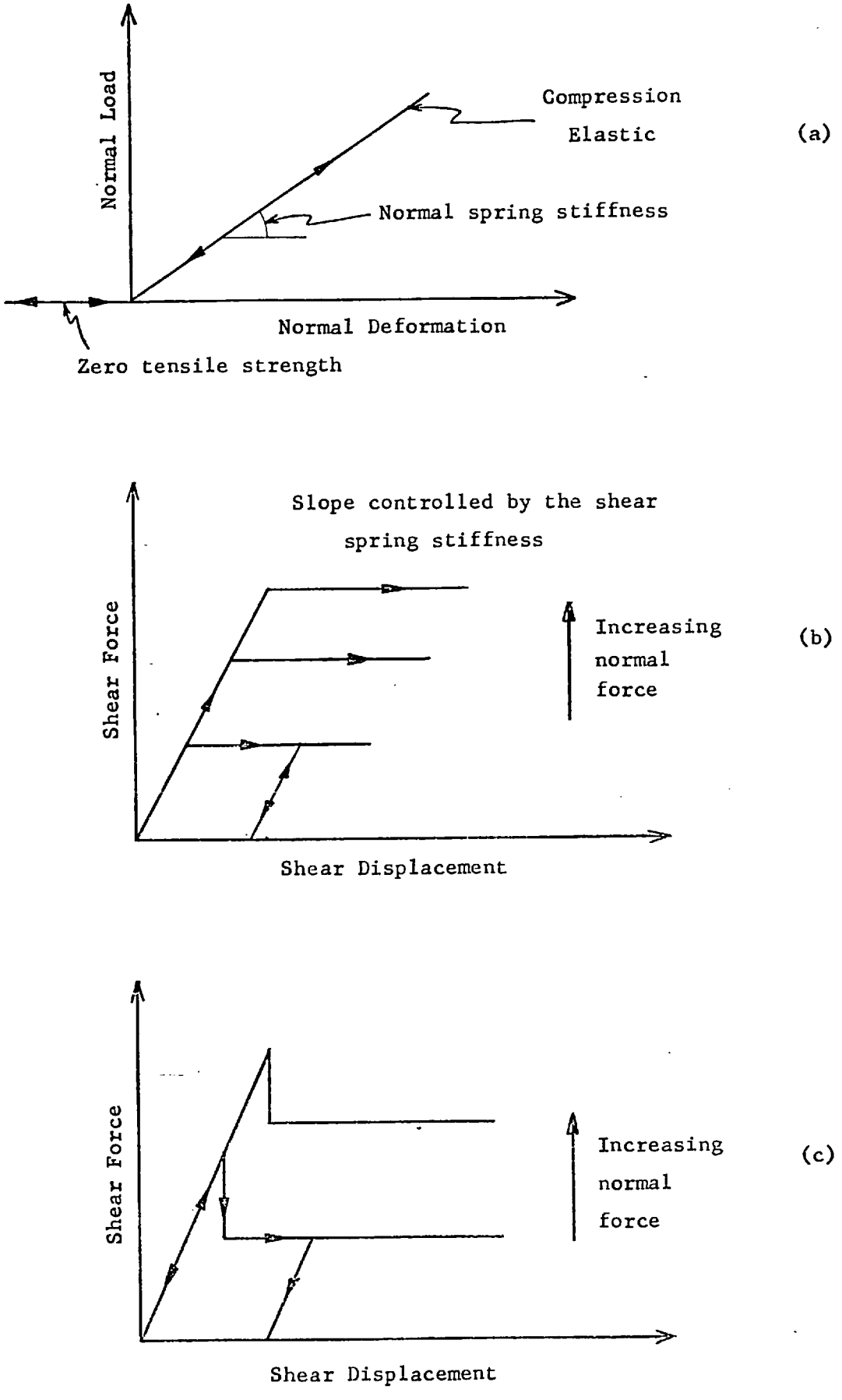

Figure 5.4- Constitutive relations: (a)normal load-deformation response, (b)elastic-plastic shear response,(c)brittle shear response (After Hocking[2]).

elastically slides was missed as well as initialising the velocities. These, together with other minor things, were all completed. Appendix B gives the complete listing of the program which is in working order.

Determination of the optimum values of the input parameters time-step, stiffness and damping factor was given very careful consideration. In this connection total kinetic energy of each block during the course of failure was calculated to monitor the time step and the damping factor as suggested by Hocking[7]. Contradictory results were initially obtained. Eventually 0.0001 as the time step and 0.5 as the damping factor was found to be optimum and they were retained throughout the analysis. Cundall[1,6] used 0.00009 and 0.6 for the time step and the damping factor respectively in generating his famous toppling columns of blocks. A stiffness of 2×10^6 N/m per unit column height was found to be feasible for the interactions to yield realistic block movements in conjunction with the chosen time step (0.0001). SI units were used throughout the analysis.

During the initial stage of the analysis the aim was to obtain results as close as possible to the established single block criterion for toppling. For this purpose, various ways and means such as "preconsolidated" start, application of shear reaction, and tilting (i. from a horizontal position, ii. from a stable inclination) were tried to obtain the best possible solution, i.e. to approach to a more stable configuration because the toppling of the single block was taking place below the critical angle postulated

by the limiting equilibrium analysis. But none of these means worked in favour of stability, contrary to the expectations. Even the process of tilting from a horizontal position (like the tilting frame tests of Chapter 3) gave rise to a very unstable situation as shown in Figure 5.5. This was most likely due to continuous tilting, and therefore the method of "tilting in very small increments at every 10 or 20 cycles" was adopted. This method, as will be seen in the following pages, proved to be successful.

Before going ahead with the test results it should be noted that the check on a freely rotating column indicated that almost the same rotational displacement occurs within the same time for real and computer simulated block. The linear displacement (sliding) has already been checked and found to be perfectly in agreement with the real case by Hocking[7].

5.3.1 - Single Block Tests -

Tests were conducted with the block having height to width ratio of 3. The critical tilting angle ($\theta_{cr.}$) for this geometry, for limiting equilibrium, is 18.43^{o}. The first tests were carried out for a fixed inclination; later on, for better solutions, the method of progressively tilting from a stable inclination was adopted. Unless specified, the time step (DT) was 0.0001 and damping factor (FAC) was 0.5 for all the cases reported below. Figure 5.6 shows a typical arrangement for a single block test.

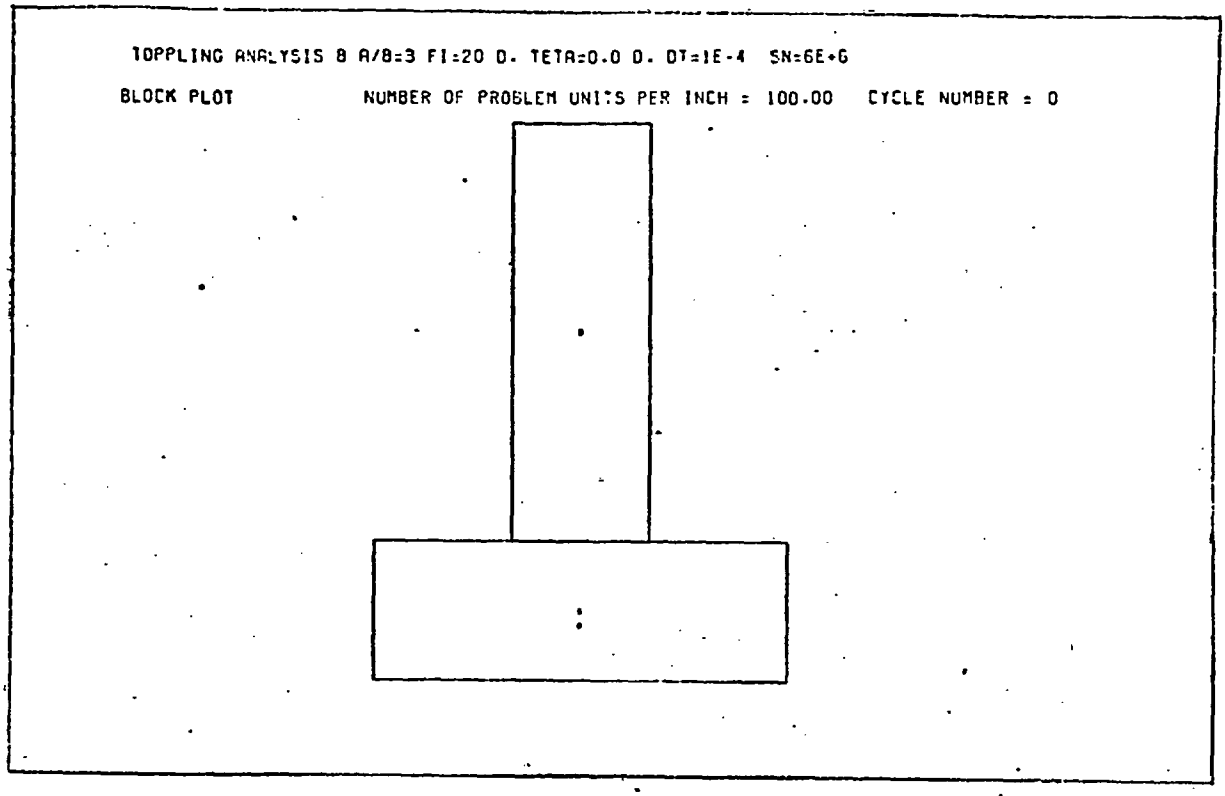

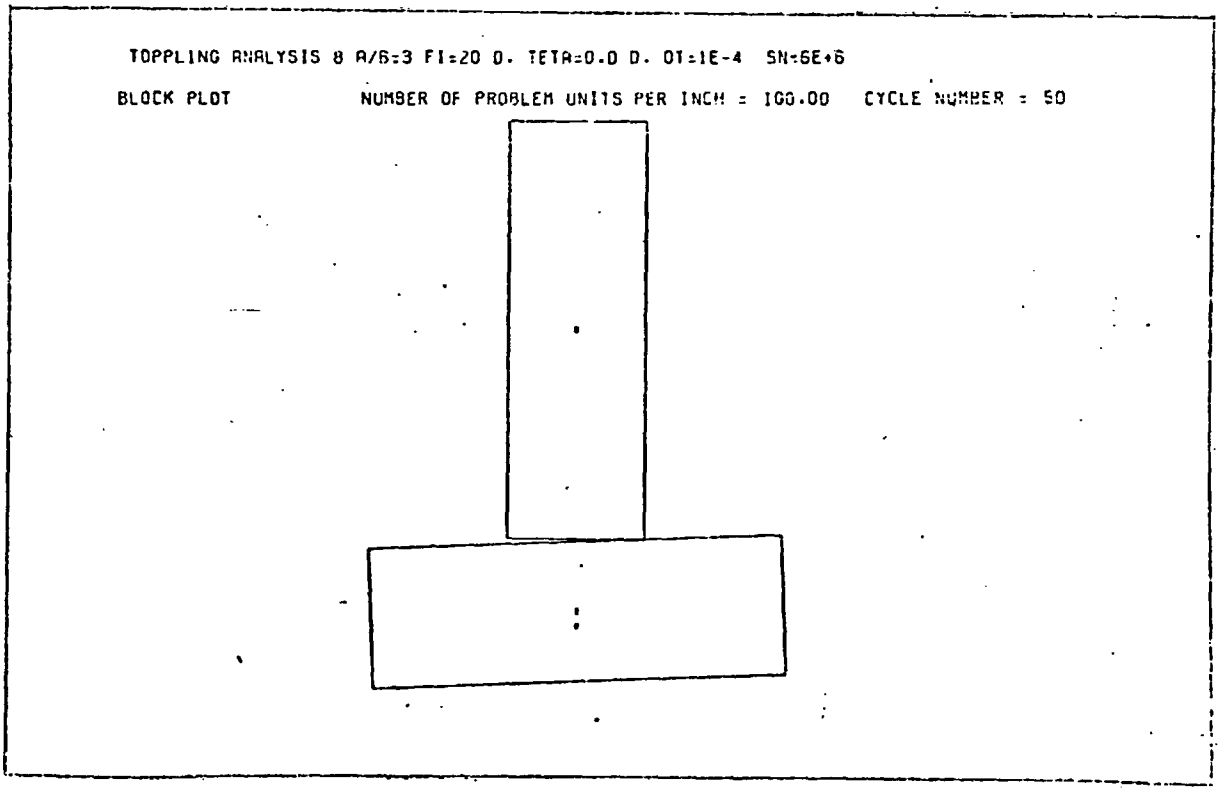

Figure 5.5- Tilting from horizontal to topple a single block.

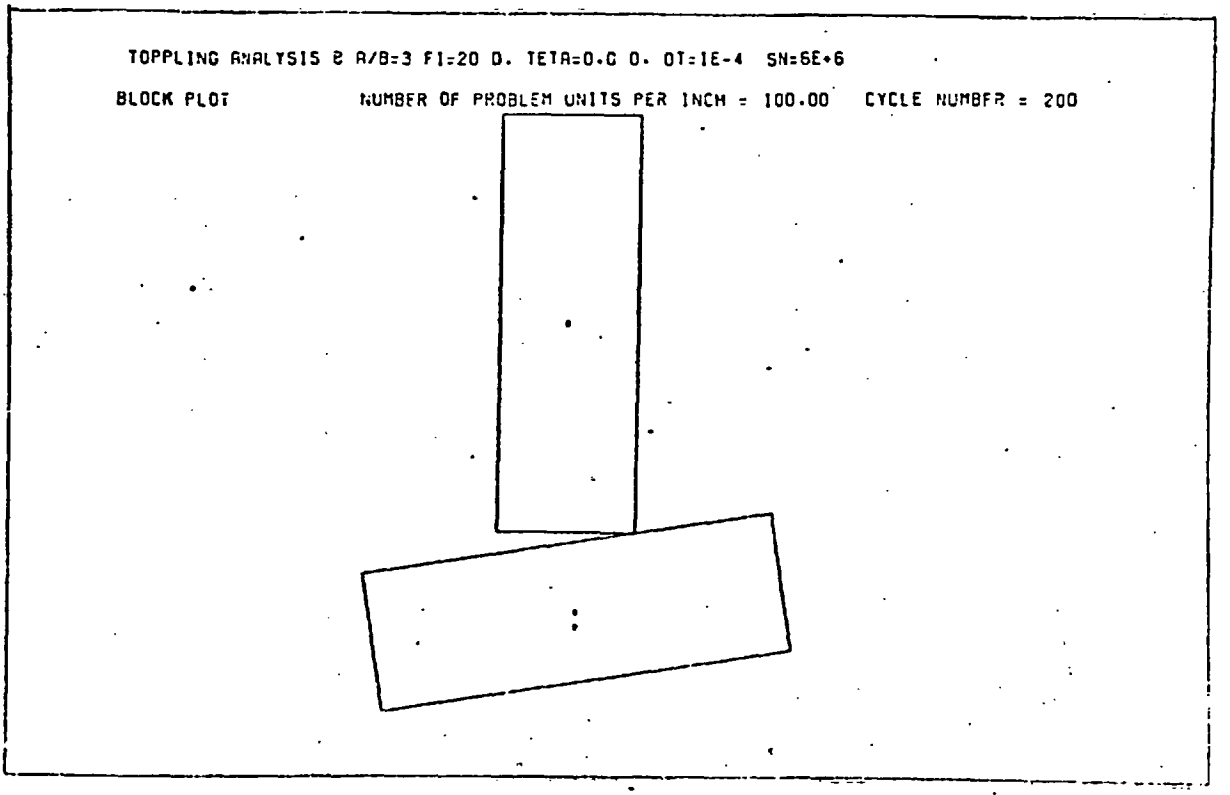

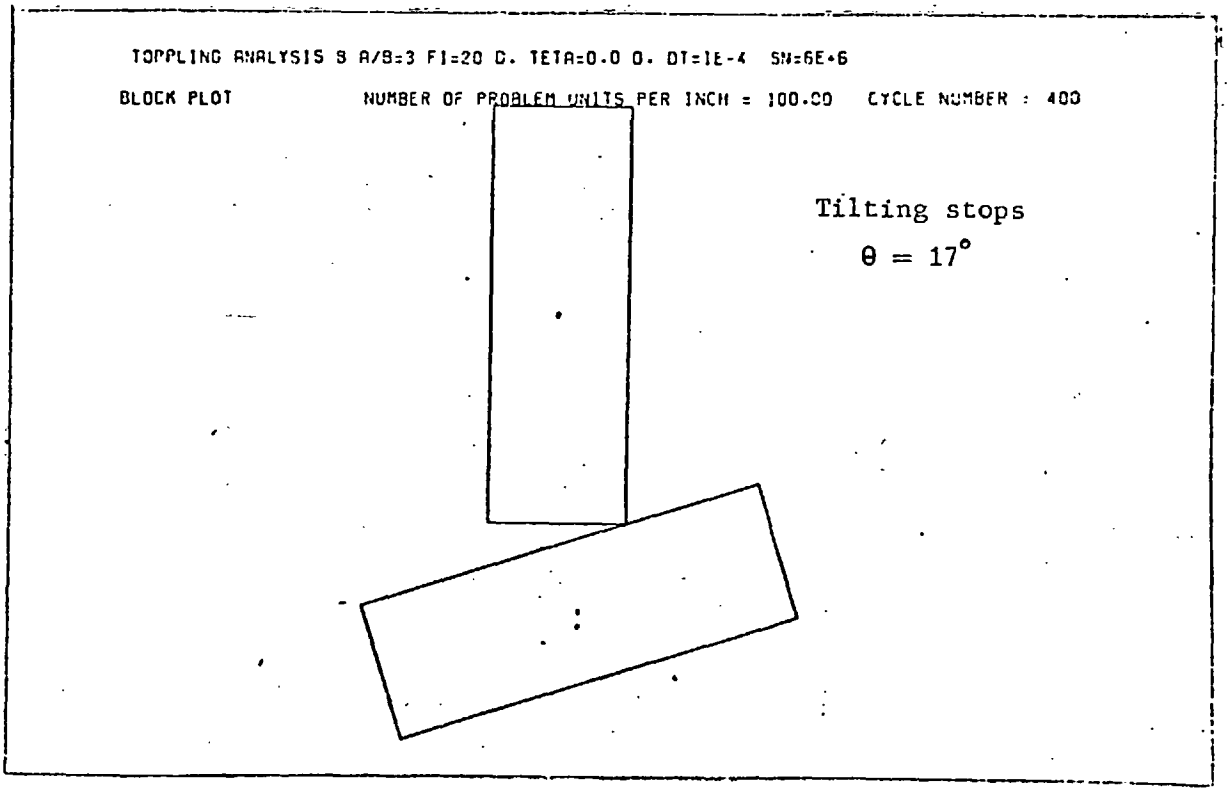

Figure 5.5- Continued.

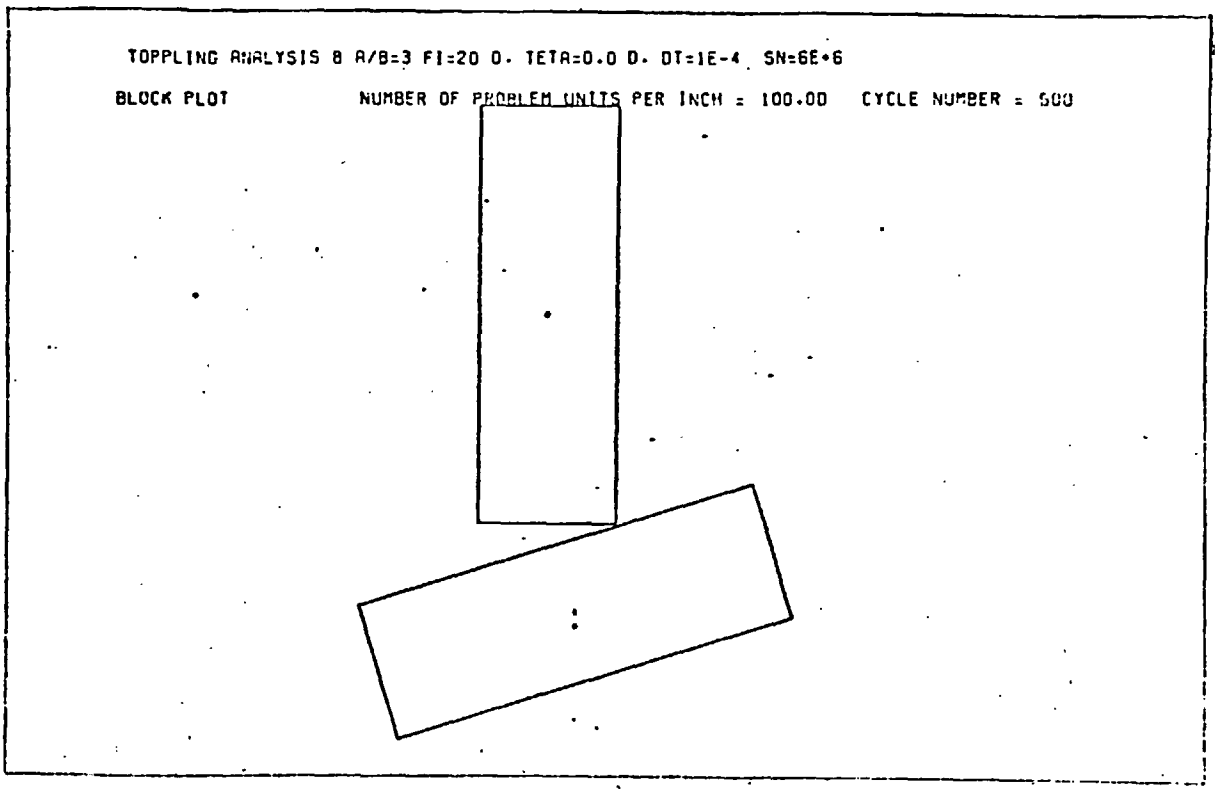

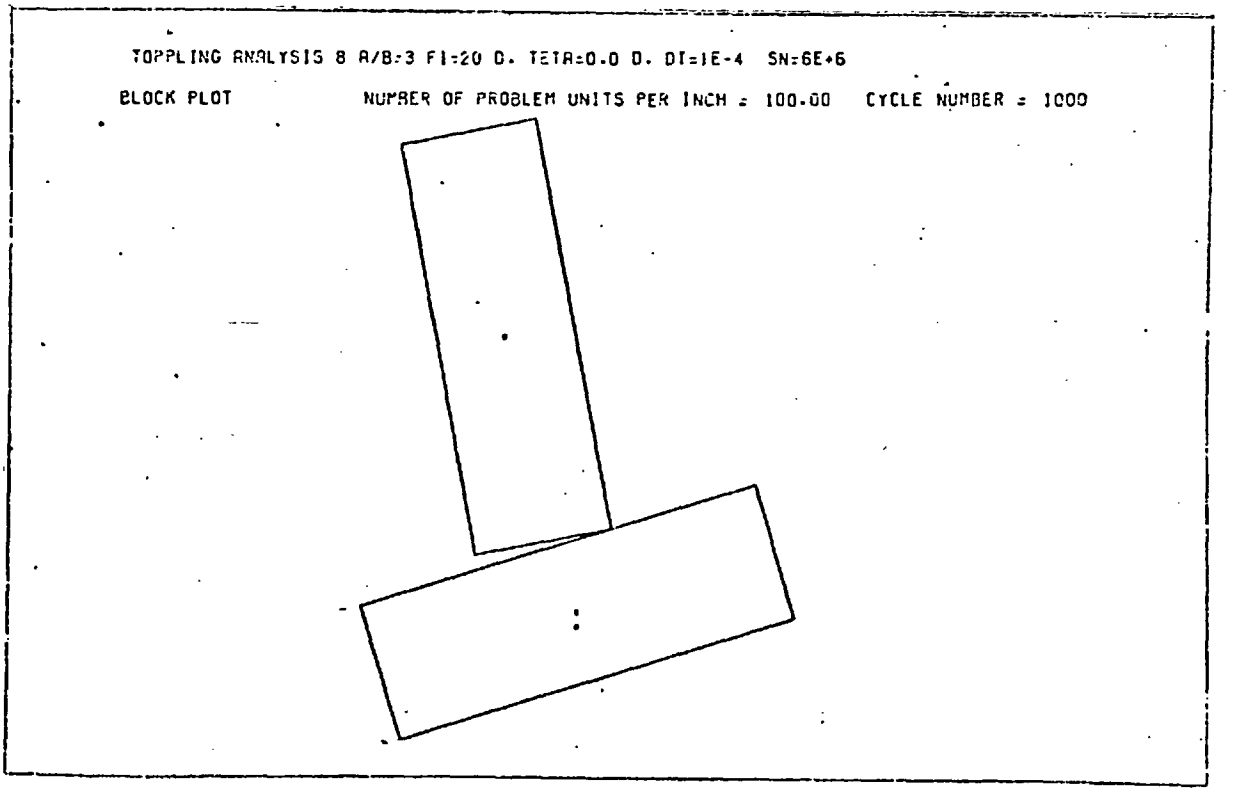

Figure 5.5- Continued.

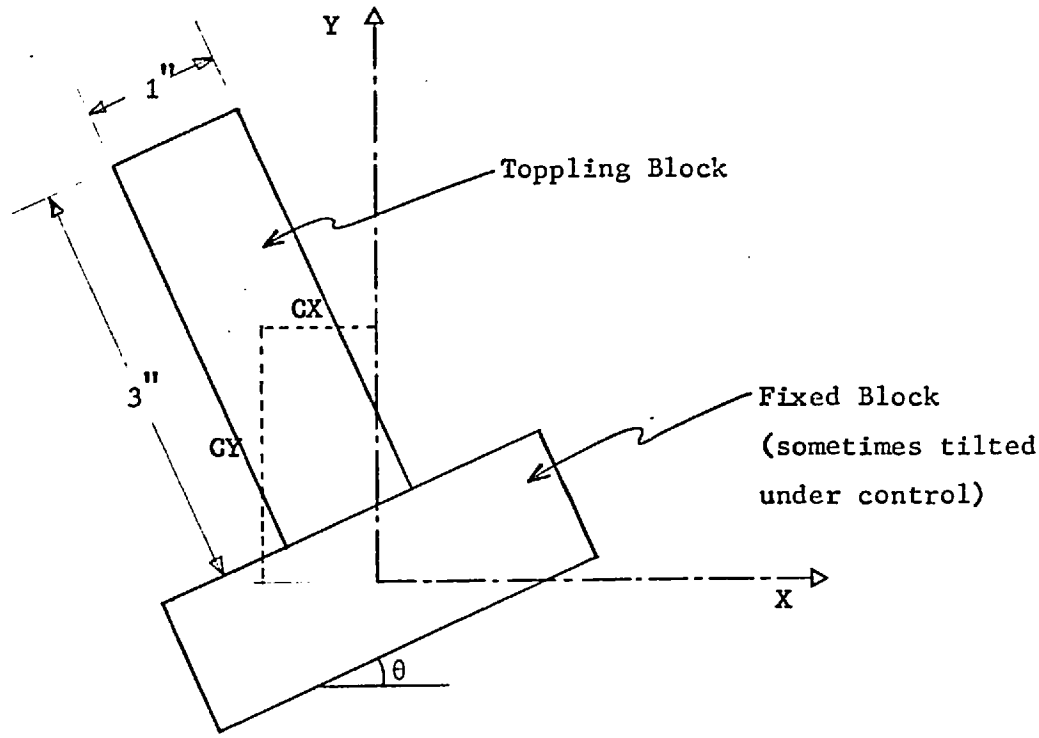

Figure 5.6- Typical single block geometry.

A. Fixed-Inclination

$\theta = 17^{\circ}$	Stabilized at	800	(CX)	and	900	(CY)	cycles	
$\theta = 17.5^{\circ}$	"	"	1100	"	"	1200	"	"
$\theta = 18^{\circ}$	"	"	2200	"	"	2200	"	"
$\theta = 18^{\circ}$ (FAC=1)	"	"	1100	"	"	800	"	"
$\theta = 18.1^{\circ}$	"	"	3200	"	"	2900	"	"
$\theta = 18.15^{\circ}$	"	"	4900	"	"	5000	"	"
$\theta = 18.2^{\circ}$	Failed							

As the results indicate, the number of iterations needed to attain a stable configuration increased with increasing inclination (θ). Figure 5.7 illustrates the transient oscillations for $\theta = 18.10^{\circ}$ and $\theta = 18.15^{\circ}$. What was re-

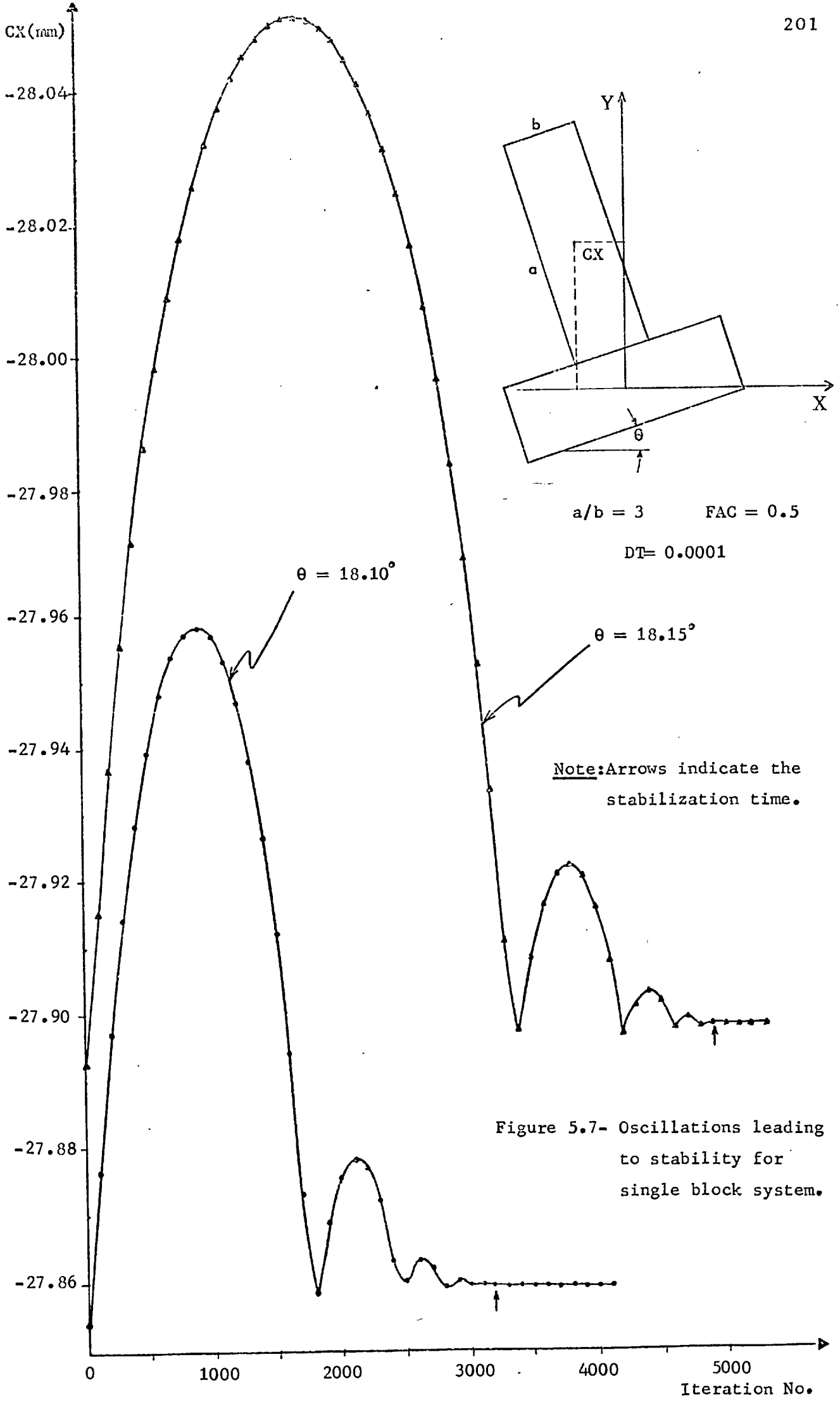

Note: Arrows indicate the stabilization time.

Figure 5.7- Oscillations leading to stability for single block system.

markable was that, the amplitude and the period of the first oscillation with $\theta = 18.15^{o}$ was almost twice that with $\theta = 18.10^{o}$ showing how the system is sensitive to small changes in θ. A similar phenomenon was observed for the damping factors of 1.0 and 0.5. Stabilization time was halved by doubling the damping factor as shown in Figure 5.8.

B. Tilting From a Stable Inclination

Tilting was started from two different stable inclinations: 18.00^{o} and 18.15^{o}.

i. Tilting from 18^{o}: The following steps were pursued:

a. Consolidation for 2500 cycles at 18^{o}.

b. Tilting in very small increments at every 10 cycles (0.1^{o}/1000 cycles).

c. Sufficient number of iterations until failure or stabilization.

$\theta = 18^{o} \rightarrow 18.2^{o}$ Stabilized at 6700 (CX) and 6000 (CY) cycles

$\theta = 18^{o} \rightarrow 18.3^{o}$ " " 11000 " " 9200 " "

$\theta = 18^{o} \rightarrow 18.4^{o}$ Failed (rotation gained momentum after cycle 8000).

ii. Tilting from 18.15^{o}: Same steps were followed but the consolidation took 5500 cycles.

$\theta = 18.15^{o} \rightarrow 18.3^{o}$ Stabilized at 12100 (CX) and 10600 (CY) cycles

$\theta = 18.15^{o} \rightarrow 18.4^{o}$ Failed (rotation gained momentum after cycle 10700).

As can be seen, with the method of tilting from a stable inclination $\theta_{cr.}$ (= 18.43^{o}) was approached as closely as 18.3^{o}

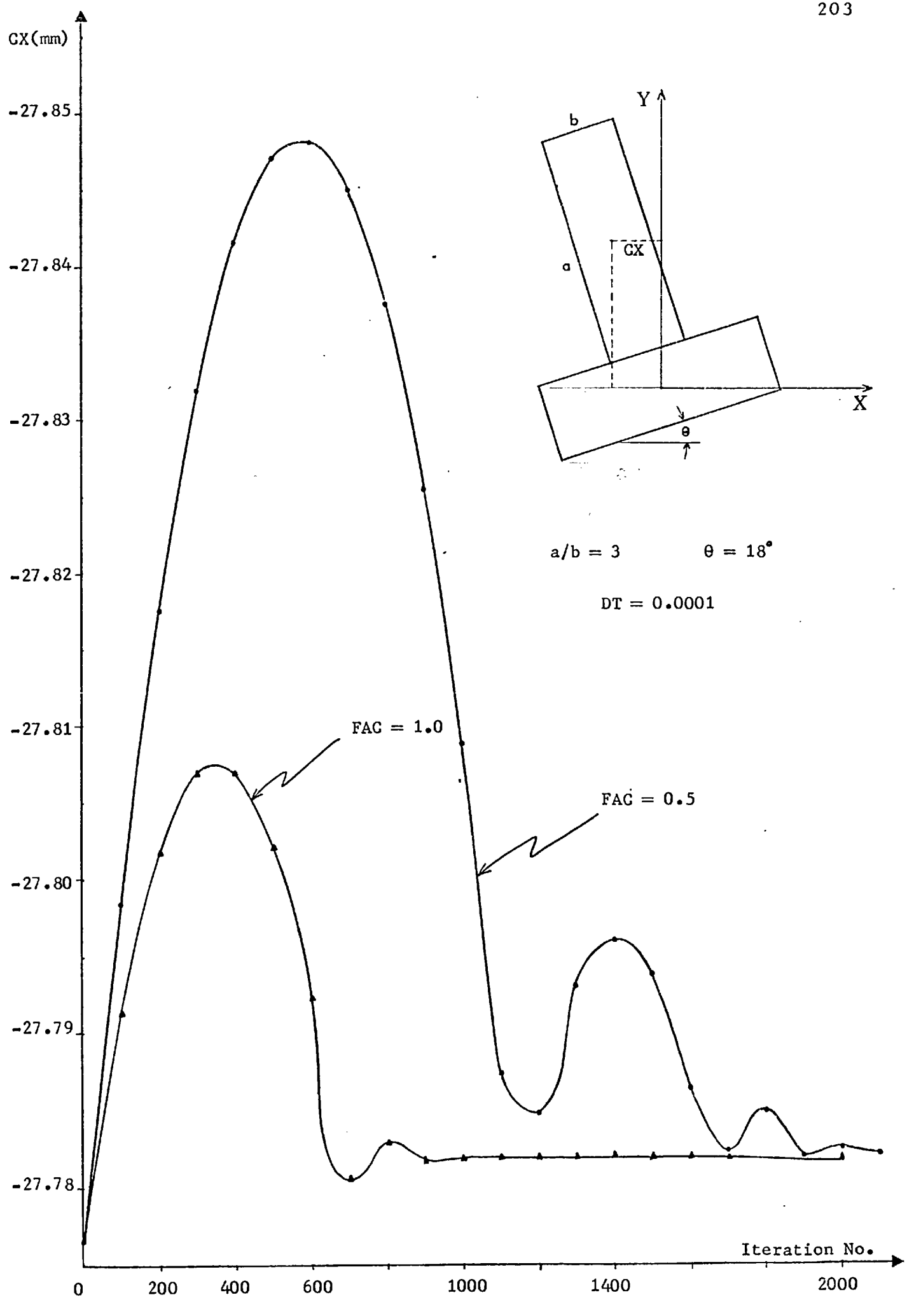

Figure 5.8- Effect of damping factor(FAC) for single block system.

(possibly 18.35°!). The inclination at which the tilting starts did not change the ultimate stable angle. The results, including the 18.15° obtained from the fixed-inclination test, should be considered very satisfactory.

5.3.2 - Double Block Tests -

Most of the tests were performed with the blocks of height to width ratio (R) 3, but the ratios of 5, 7 and 10 were also tried to investigate the influence of the column slenderness on the mode of behaviour. The friction angle assigned for the contact surfaces was 20°. The following is the summary of the test results for the ratio of 3. The geometry is shown in Figure 5.9.

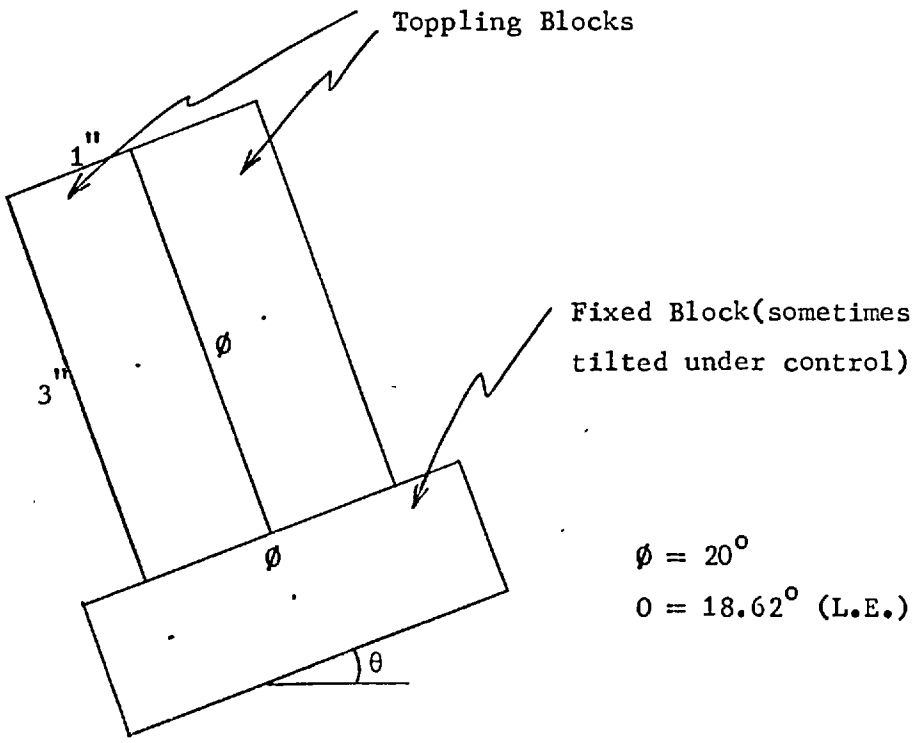

Figure 5.9- Double block arrangement.

A. Fixed-Inclination

$\theta = 18.3^{\circ} \rightarrow$ Stabilized

$\theta = 18.4^{\circ} \rightarrow$ Failed

B. Tilting From a Stable Inclination

Three different inclinations were tried to get the best results. The numbers above the arrows indicate the frequency of iterations for tilting (0.1°/1000 cycles for 10, 0.1°/2000 cycles for 20).

i. Tilting from 18.3°:

$\theta = 18.3^{\circ} \overset{10}{\rightarrow} 18.5^{\circ}$ failed

$\theta = 18.3^{\circ} \overset{10}{\rightarrow} 18.4^{\circ}$ failed

$\theta = 18.3^{\circ} \overset{20}{\rightarrow} 18.4^{\circ}$ failed

ii. Tilting from 18.2°:

$\theta = 18.2^{\circ} \overset{10}{\rightarrow} 18.3^{\circ}$ failed

$\theta = 18.2^{\circ} \overset{20}{\rightarrow} 18.3^{\circ}$ stabilized

iii. Tilting from 18°:

$\theta = 18^{\circ} \overset{10}{\rightarrow} 18.3^{\circ}$ failed

$\theta = 18^{\circ} \overset{10}{\rightarrow} 18.2^{\circ}$ stabilized

Contrary to the single block behaviour, the tilting method did not increase the stable inclination in the double block system. Even the fixed-inclination stable angle (18.3°) was hardly attained by tilting. On the other hand, the fixed-inclination stable angle increased from 18.15° to 18.3° due to the presence of an adjacent column. The same "tilting-stable-angles" (18.3°) for the single and double

block systems implied the lack of any contact between the columns in the latter. Indeed this was the situation. Figure 5.10 shows how the blocks behaved independently when tilting was applied. The reason(s) for this peculiar behaviour was sought.

a. was it because of a micro crack between the blocks, or

b. was it a specific failure mode?

The first possibility was checked through magnification in the Quick-Look Machine of Interactive Graphics System (Imperial College Computer Centre). A micro crack eventually was discovered between the adjacent blocks. To close this gap the following procedure was applied.

i. Consolidation of the system at a stable inclination.

ii. Fixing the lower block and reducing the friction angle at the base for the upper block to slide down and make a full contact with the fixed one.

iii. The usual consolidation, tilting, and iteration process.

However, the closing of the gap did not alter the independent block behaviour as can be seen in Figure 5.11.

Comparison of all the tilted and fixed models led to the conclusion that the tilting itself was the real cause of the independent block behaviour because none of the fixed models ever failed independently. Therefore, to avoid any wrong impression and decision about the behaviour of a model, it is concluded that progressive tilting should not be used. On the other hand, it seems unjustified to jump to such a general conclusion from the observation of double block models

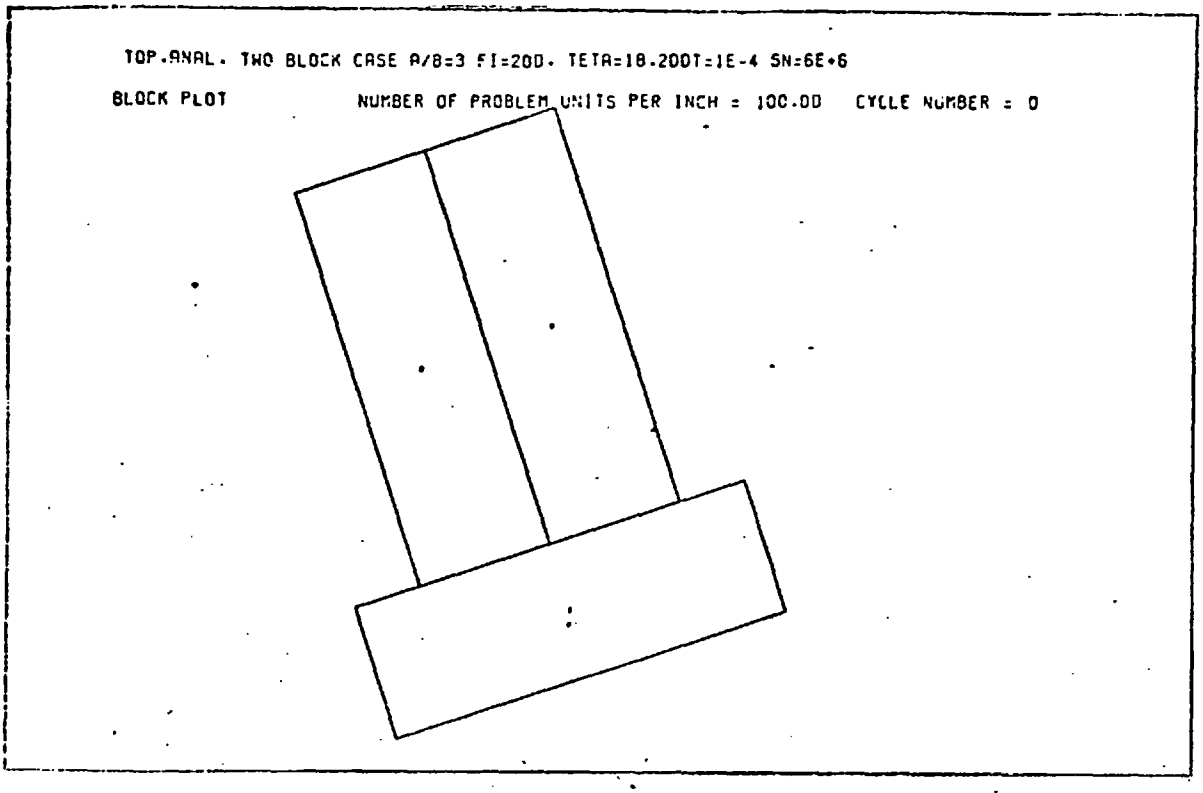

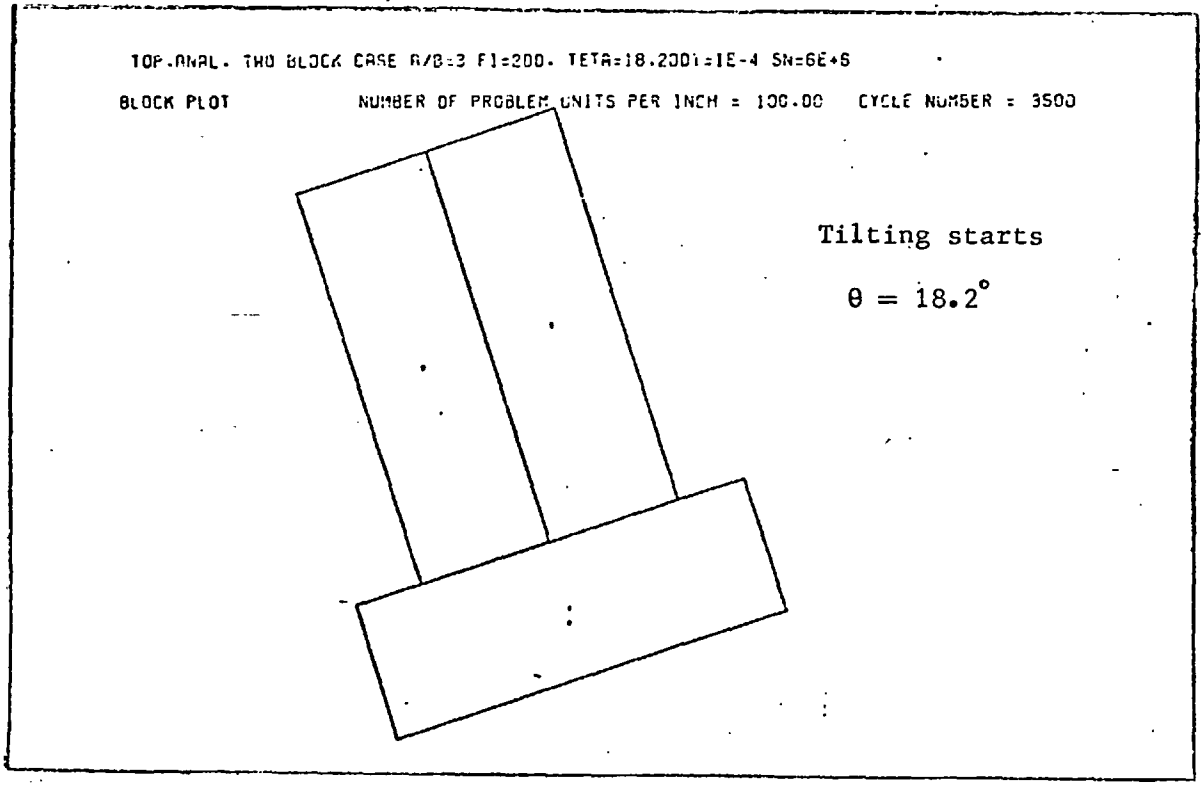

Figure 5.10- Tilting from a stable inclination for double block system.

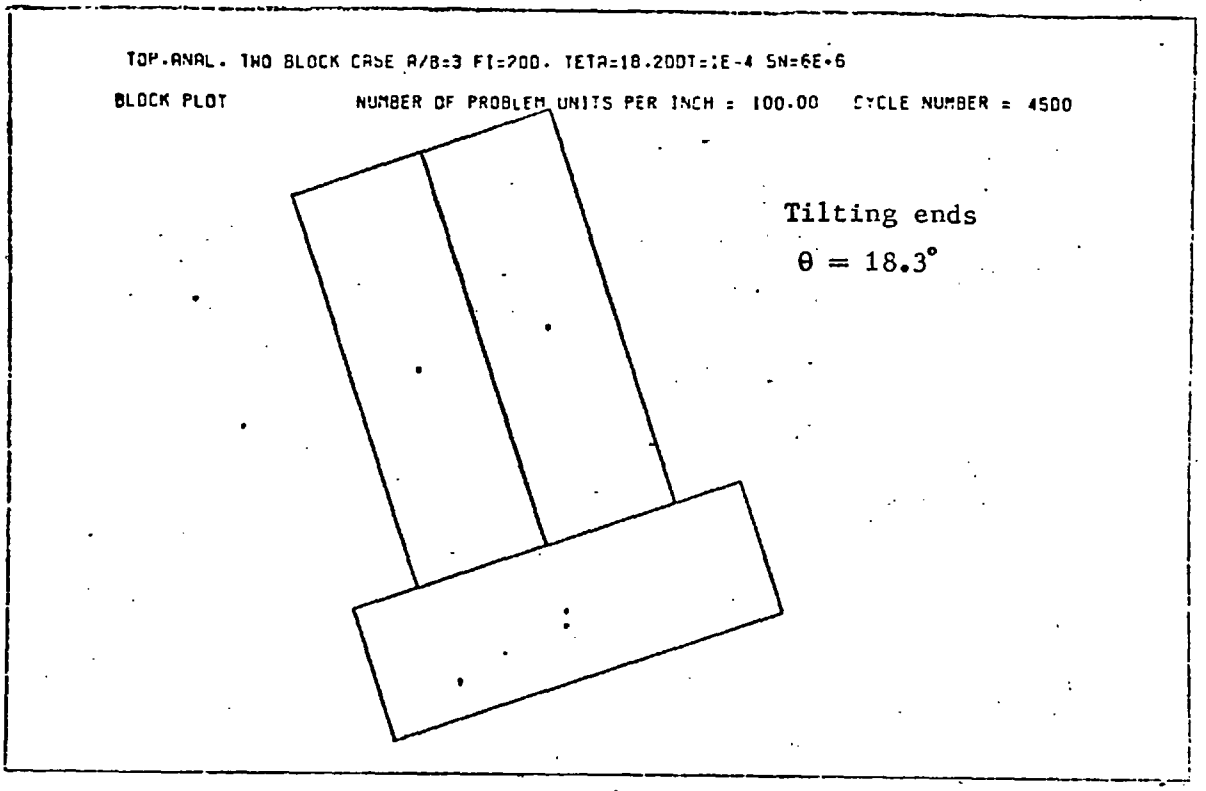

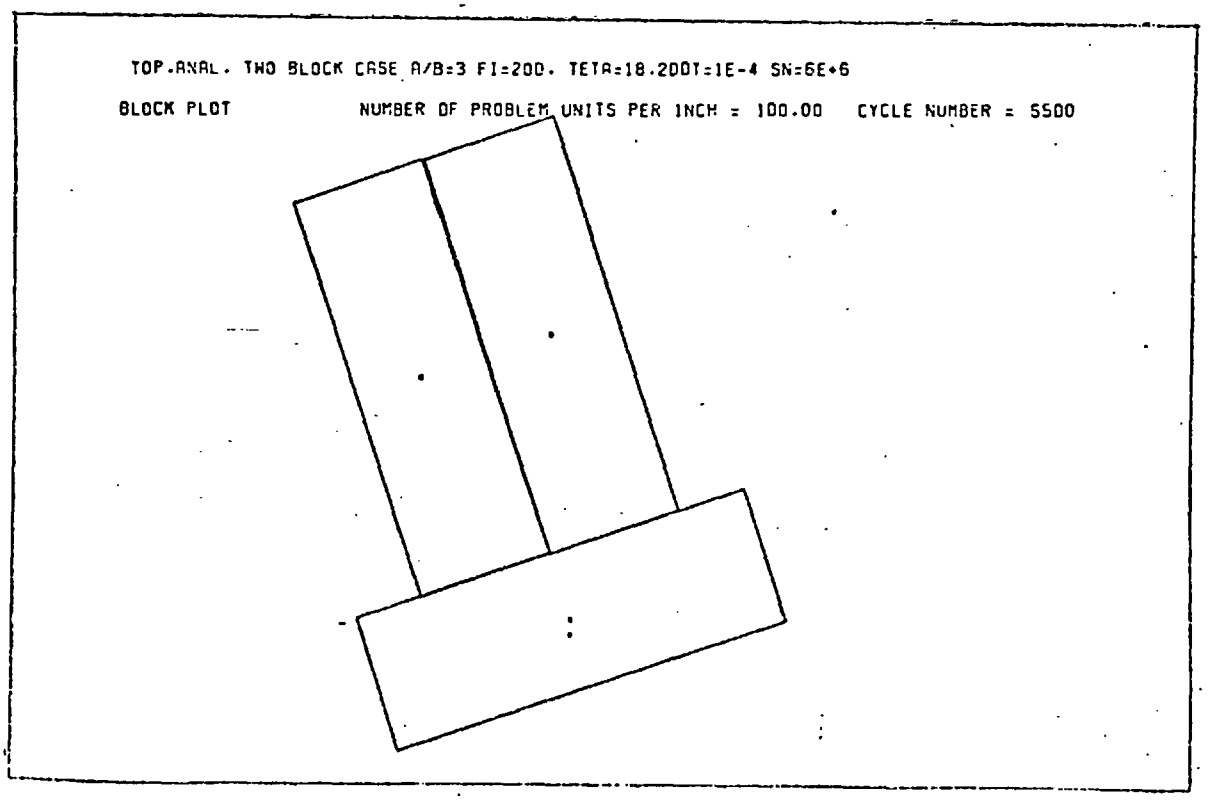

Figure 5.10- Continued.

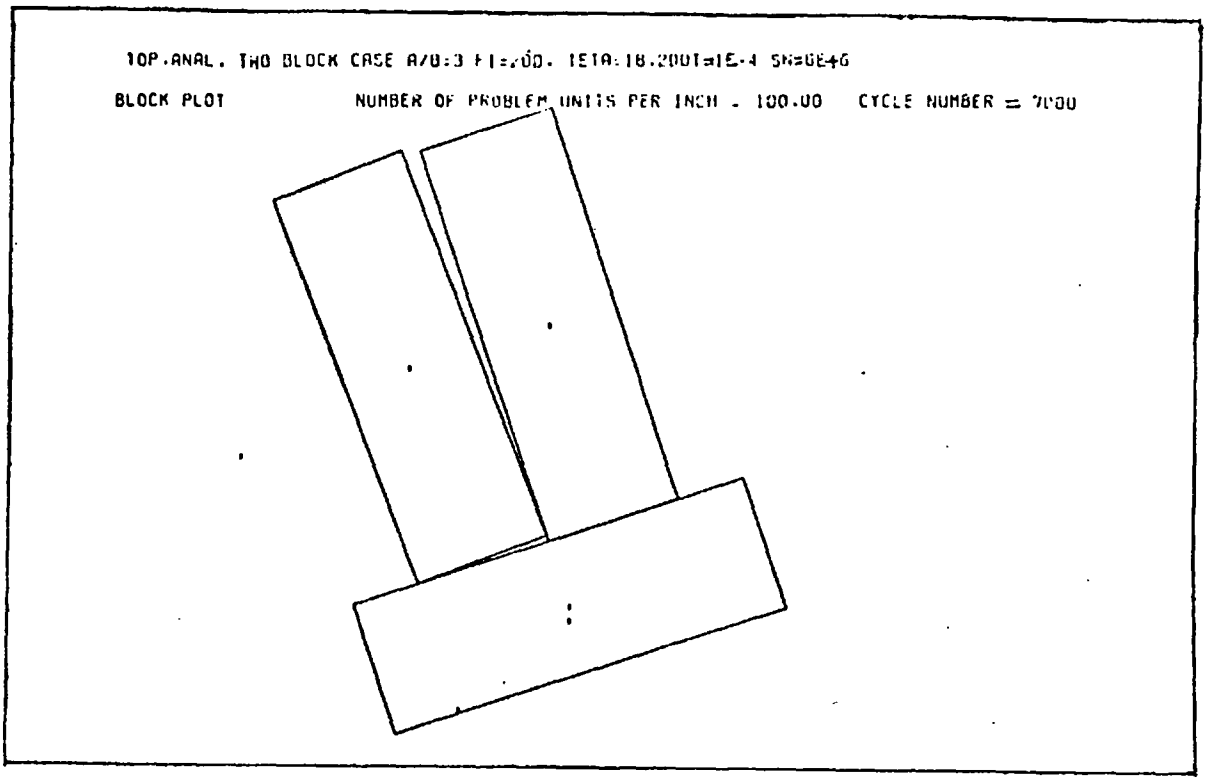

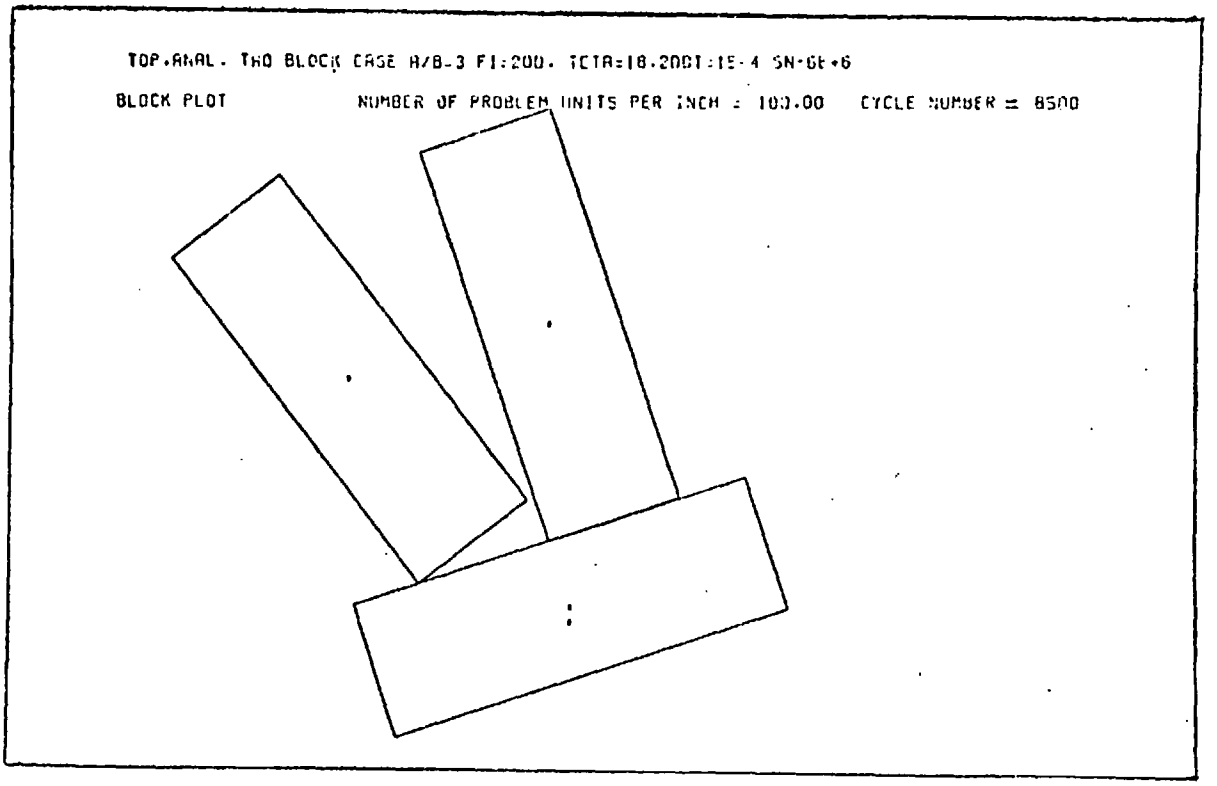

Figure 5.10- Continued.

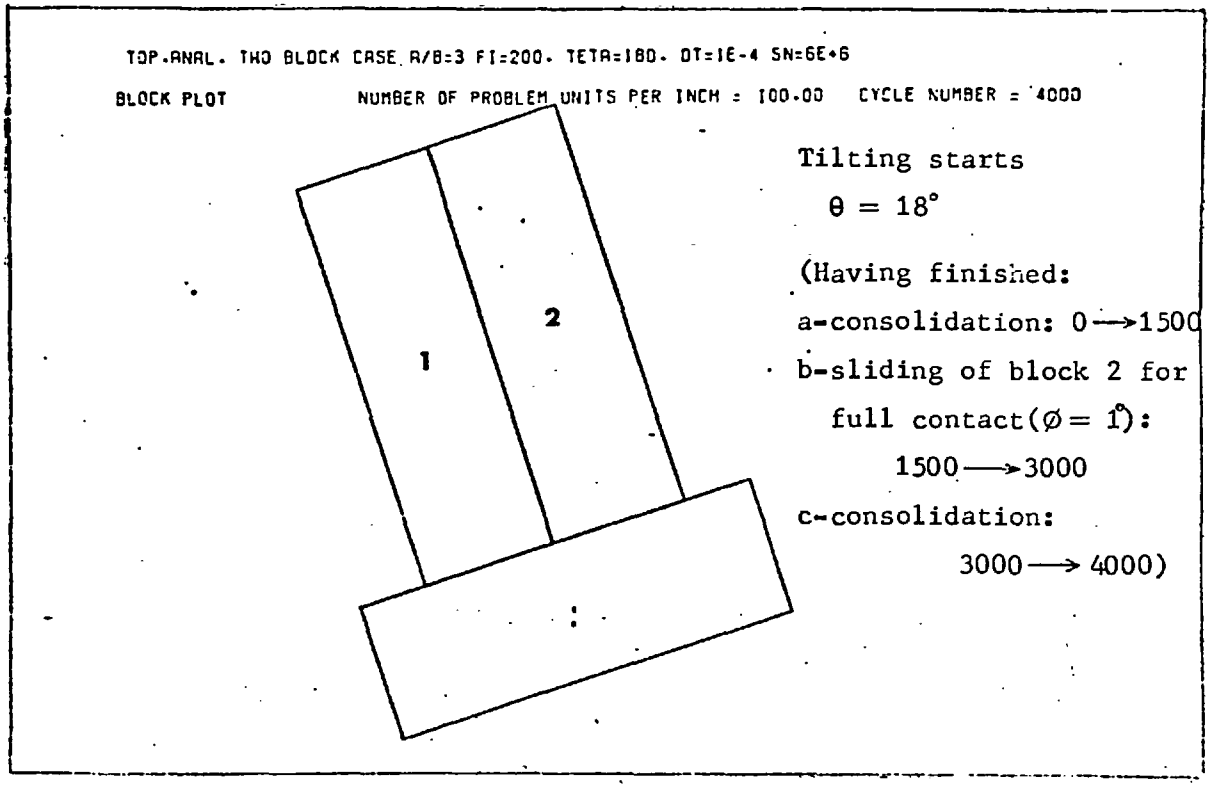

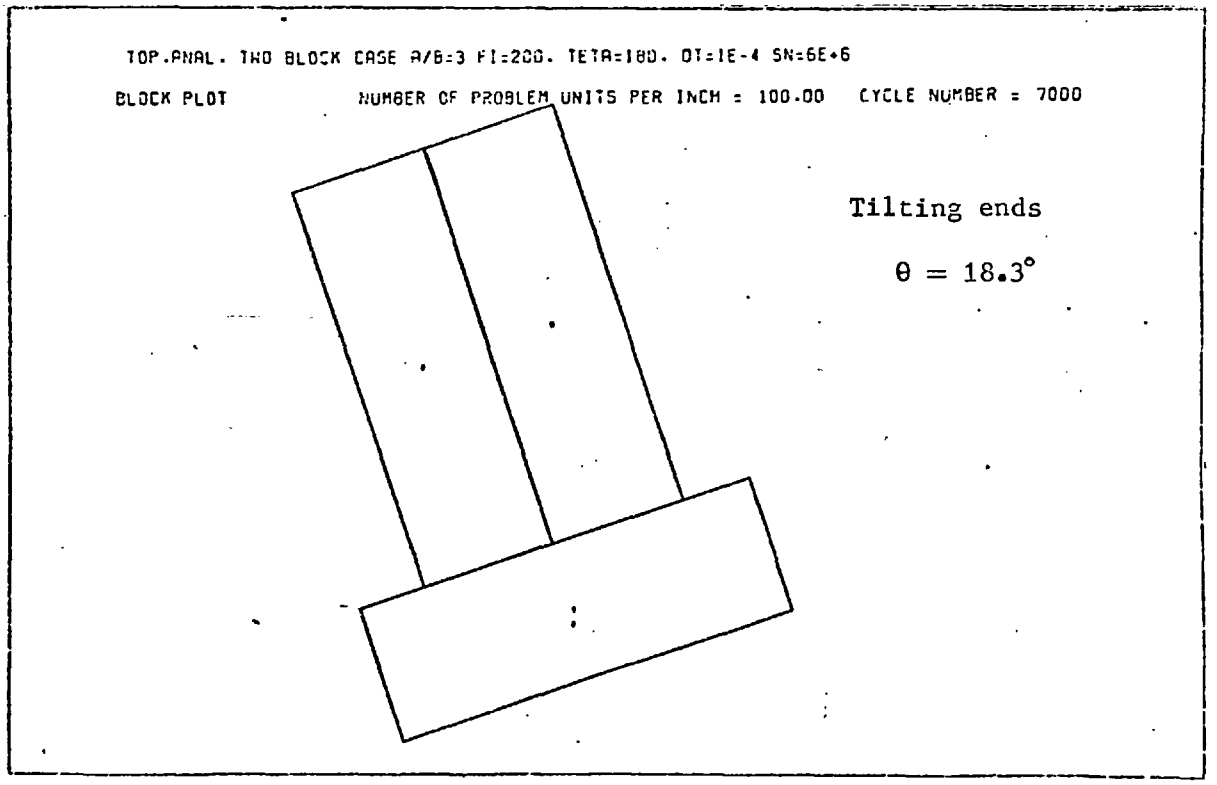

Figure 5.11- Independent block behaviour in spite of ensuring full contact between blocks 1 and 2.

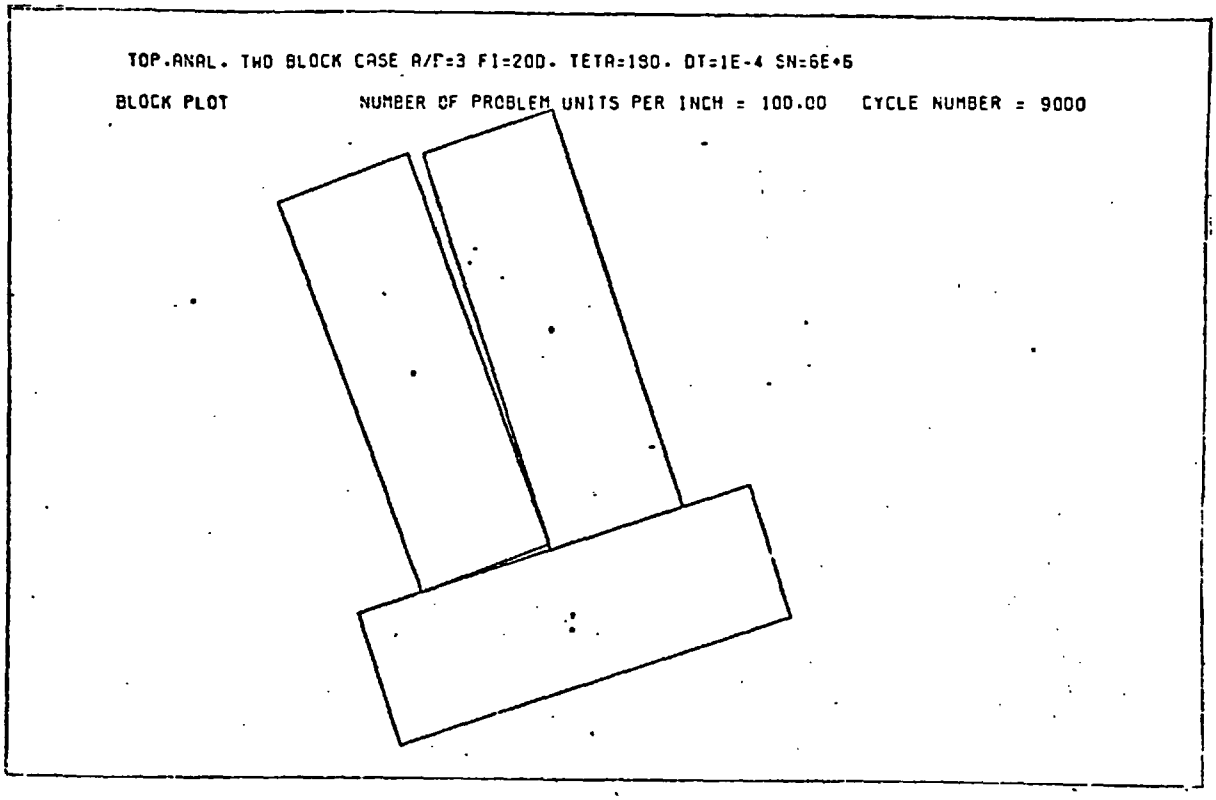

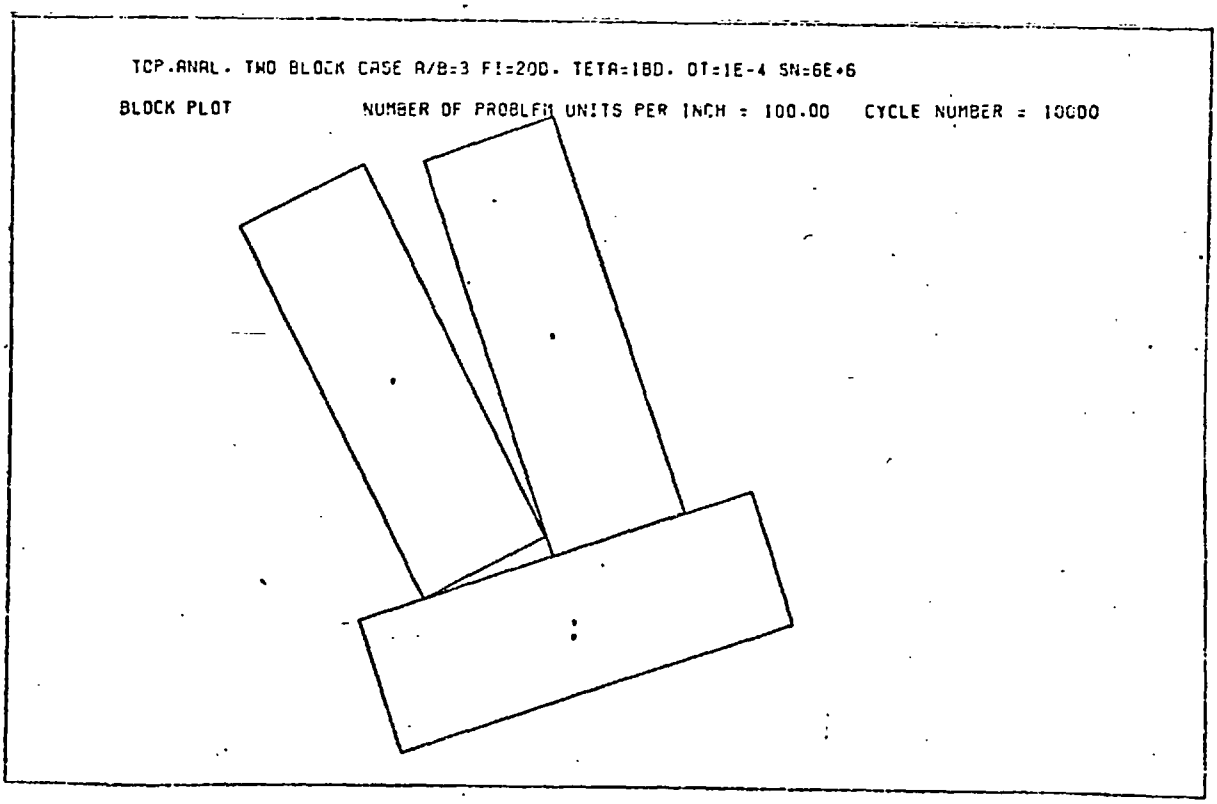

Figure 5.11- Continued.

which apparently is a highly sensitive configuration for this method (D.R.).

As stated earlier, models with blocks of various Rs were to be tested to investigate the mode of behaviour. The movements of the block corners were monitored using shear and normal forces developed. Quite an agreement was seen with the limiting equilibrium results. For all ratios (R = 3, 5, 10) the lower block slid downward first and continued to slide for a while with the rotation. In the later stages of failure it was found that the upper block slid uphill. As R became greater the backward sliding started to take place at earlier stages of the failure. This is illustrated in Figure 5.12 which shows the 3", 5", and 10" height blocks after 4500 cycles when the backward sliding was initiated.

While the 3, 5 and 10 inch height blocks were behaving consistently without any sign of numerical distortion, the 7" height model acted unusually with a sudden blow out at cycle 677 as shown in Figure 5.13. There was nothing odd as far as the input parameters and operational procedure were concerned. As a matter of fact the program gave stable solutions up to the 677 th. cycle. One wonders whether a particular statement in the program triggers off such a violent response when very specific conditions are met. This would have been checked by carrying out all the calculations manually for the 677 th. cycle if the author had enough time.

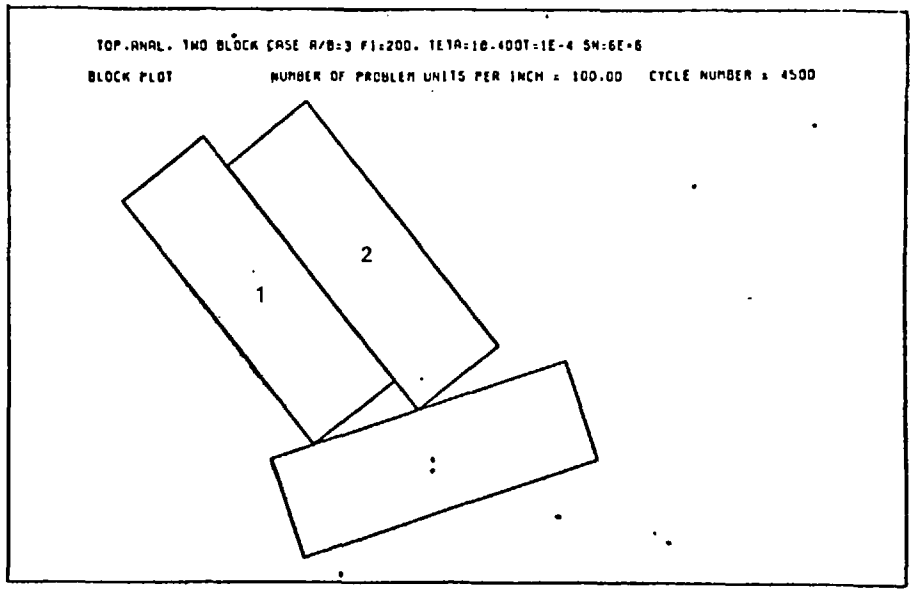

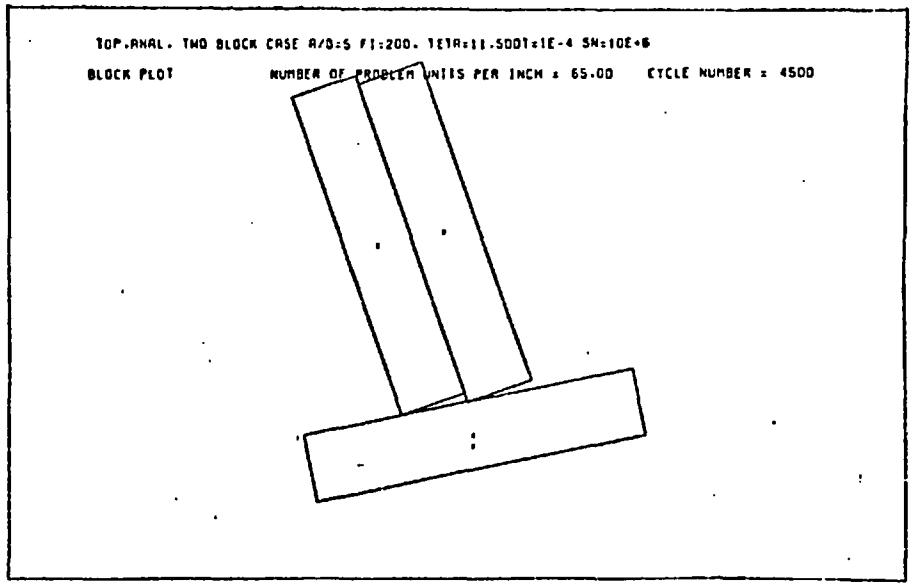

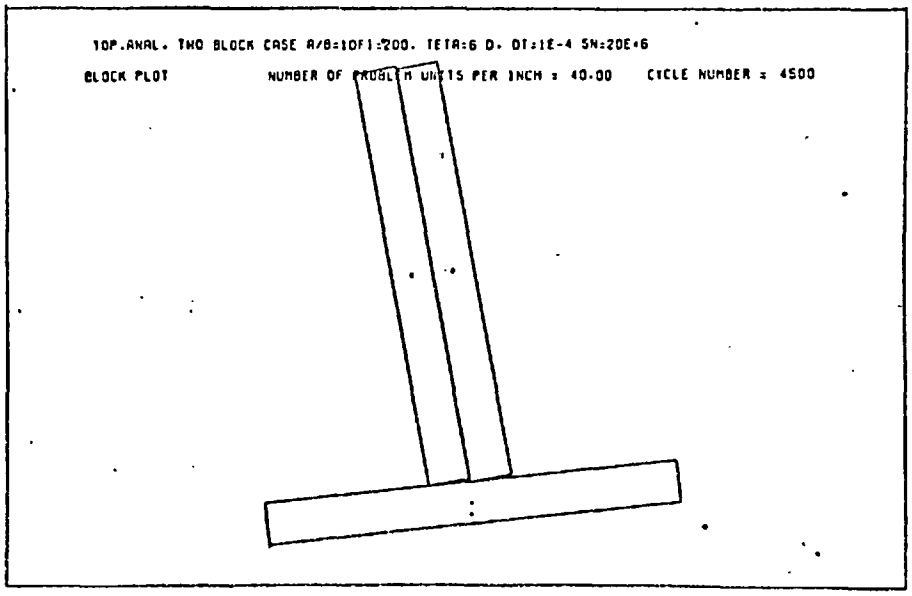

Figure 5.12- Initiation of backward sliding(of block 2) for different ratios,R.

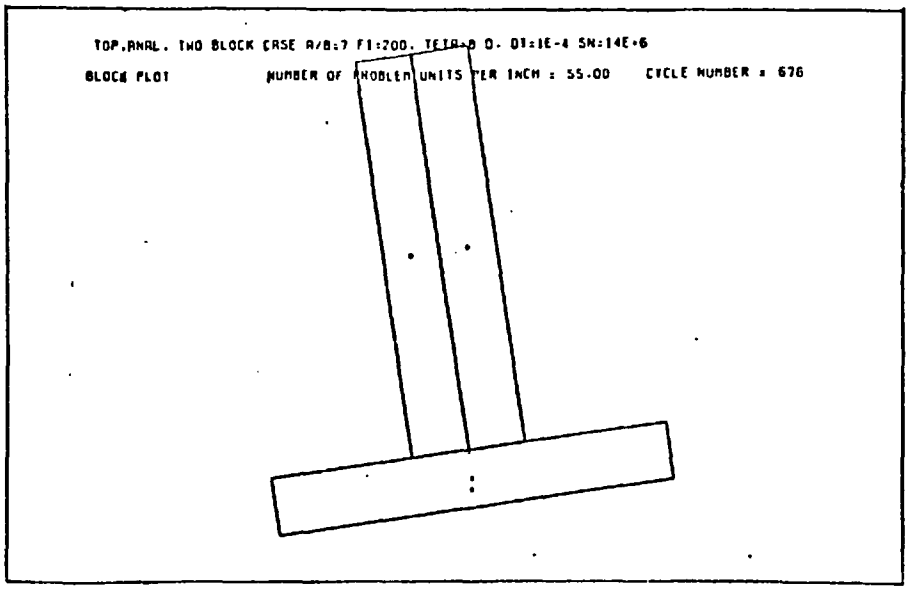

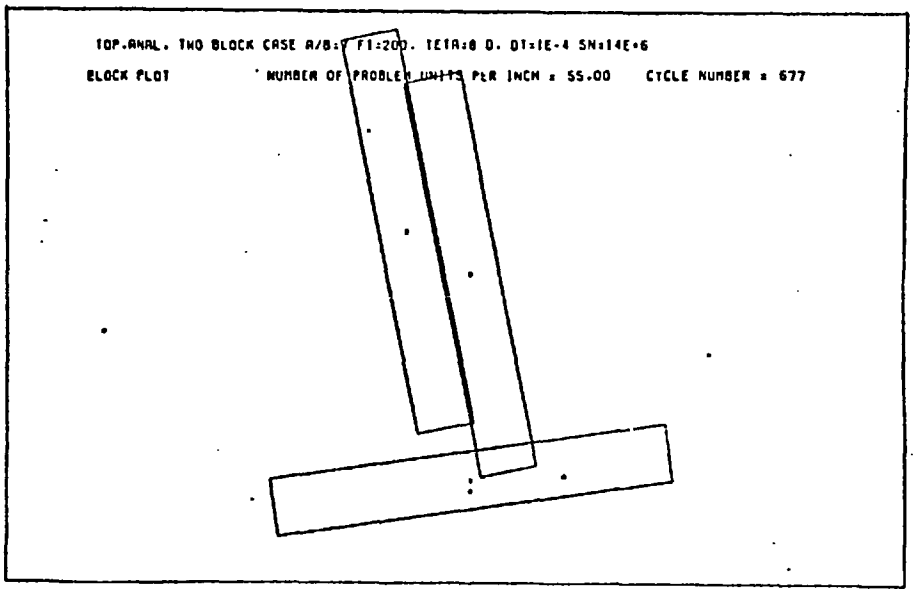

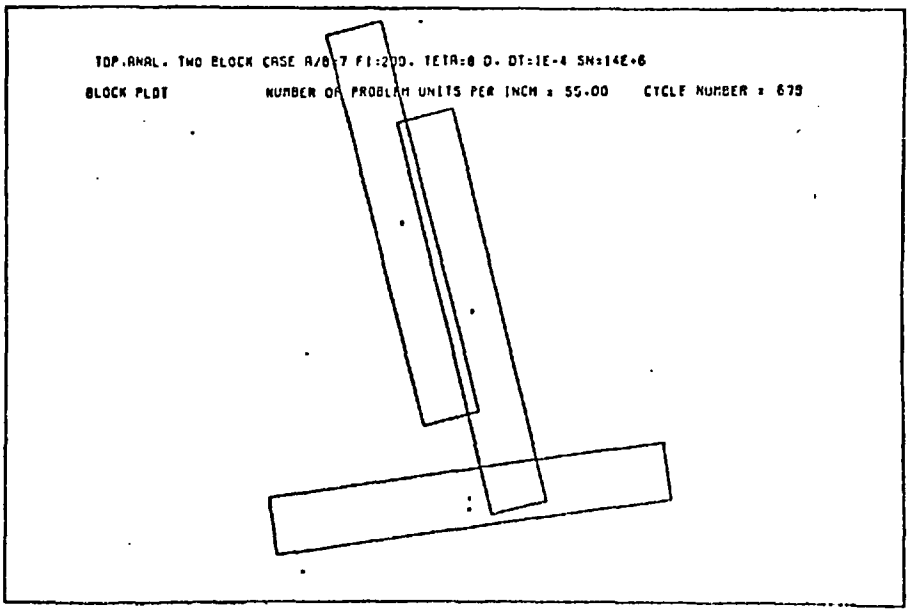

Figure 5.13- Anamolous behaviour of the 7" height blocks.

The following observations were also made regarding the double block behaviour:

1. A reduction of 6 times in the stiffness (SN) caused the stable system to fail.

$SN = 6 \times 10^6$ N/m → stable
$SN = 1 \times 10^6$ N/m → unstable

$\theta = 18.3^\circ$
DT = 0.0001
FAC = 0.5

2. It was thought by doing the opposite, i.e. increasing the stiffness, the reverse effect would be obtained. But this did not, in fact, happen. When the stiffness was doubled, the already unstable system failed faster.

$SN = 6 \times 10^6$ N/m → cycle 7000
$SN = 12 \times 10^6$ N/m → cycle 2500
same disp.

$\theta = 18.4^\circ$
DT = 0.0001
FAC = 0.5

3. Halving the time step (DT) increased the number of iterations more than twice for the same displacement.

DT = 0.0001 → cycle 2500
DT = 0.00005 → cycle 6000
almost same disp.

$\theta = 18.4^\circ$
$SN = 12 \times 10^6$ N/m
FAC = 0.5

4. Variation of damping factor (FAC) gave inconsistent results.

FAC = 0.5 slowest
FAC = 0.6 fastest
FAC = 0.7 in between

$\theta = 18.4^\circ$
DT = 0.0001
$SN = 6 \times 10^6$ N/m

5.3.3 - Triple and Quadruple Block Tests -

Having obtained satisfactorily accurate solutions for the toppling failure of single and double block models,

the triple and quadruple block tests were conducted. This was mainly to examine the failure modes, needed for a reliable limiting equilibrium analysis. As the following test results will indicate there was not a definite pattern of movements for the whole failure process. But it became possible to get an idea about the general character of the failure mode from the overall block movements recorded at regular intervals. None of the models in this series were ever subjected to progressive tilting. The already established values were assigned for the important input parameters, such as DT = 0.0001, FAC = 0.5, SN = 2×10^6 N/m per unit block height.

5.3.3.1 - Triple block tests -

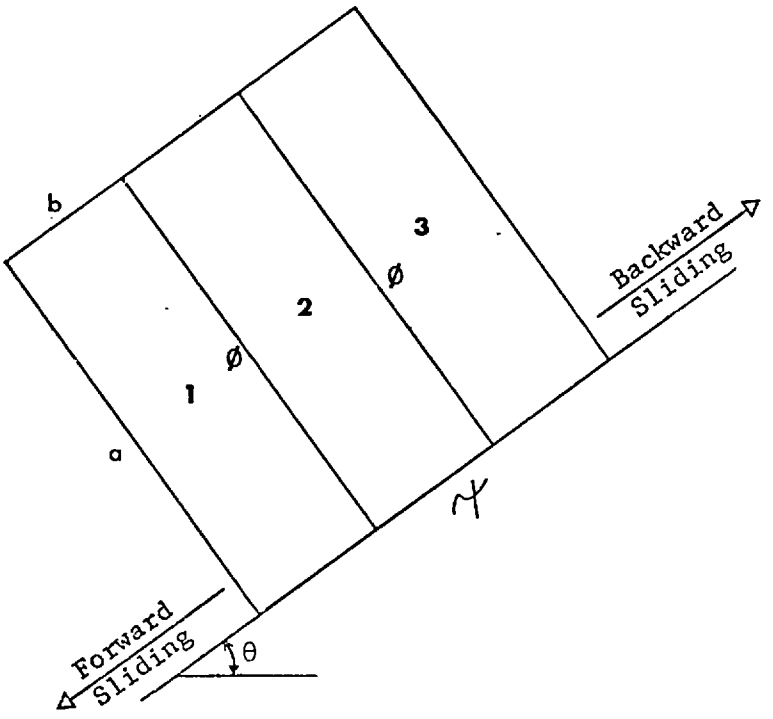

i. $a/b = 3$, $\theta = 25^{\circ}$, $\phi = \psi = 26^{\circ}$ — Blocks (1) and (2) always slid forward. Block (3) first slid forward then stopped sliding and finally started to slide backward.

ii. $a/b = 3$, $\theta = 35^{\circ}$, $\phi = 20^{\circ}$, $\psi = 40^{\circ}$ — Block (1) started sliding forward at cycle 400. Block (3) slid backward starting at cycle 600. Backward sliding at cycle 1500 took place for block (2).

This test is illustrated in Figure 5.14.

iii. $a/b = 5$, $\theta = 15^{\circ}$, $\phi = \psi = 20^{\circ}$ — First, block (1) slid forward, then (1) and (2) forward, (3) backward, finally (1) forward, (3) backward.

iv. $a/b = 5$, $\theta = 15^{\circ}$, $\phi = \psi = 30^{\circ}$ — Block (1) slid forward always. Block (2) slid backward mostly. Block (3) slid backward mostly.

To sum up, Blocks (1) and (3) happened to be more active than block (2) because they were less restrained. Block (1) always slid forward. Block (3) preferred backward sliding mostly but occasional downhill slips occurred when ψ was high. Block (2), when moved, seemed to be more affected by the frictional resistance at the base (ψ) in the same way as Block (3).

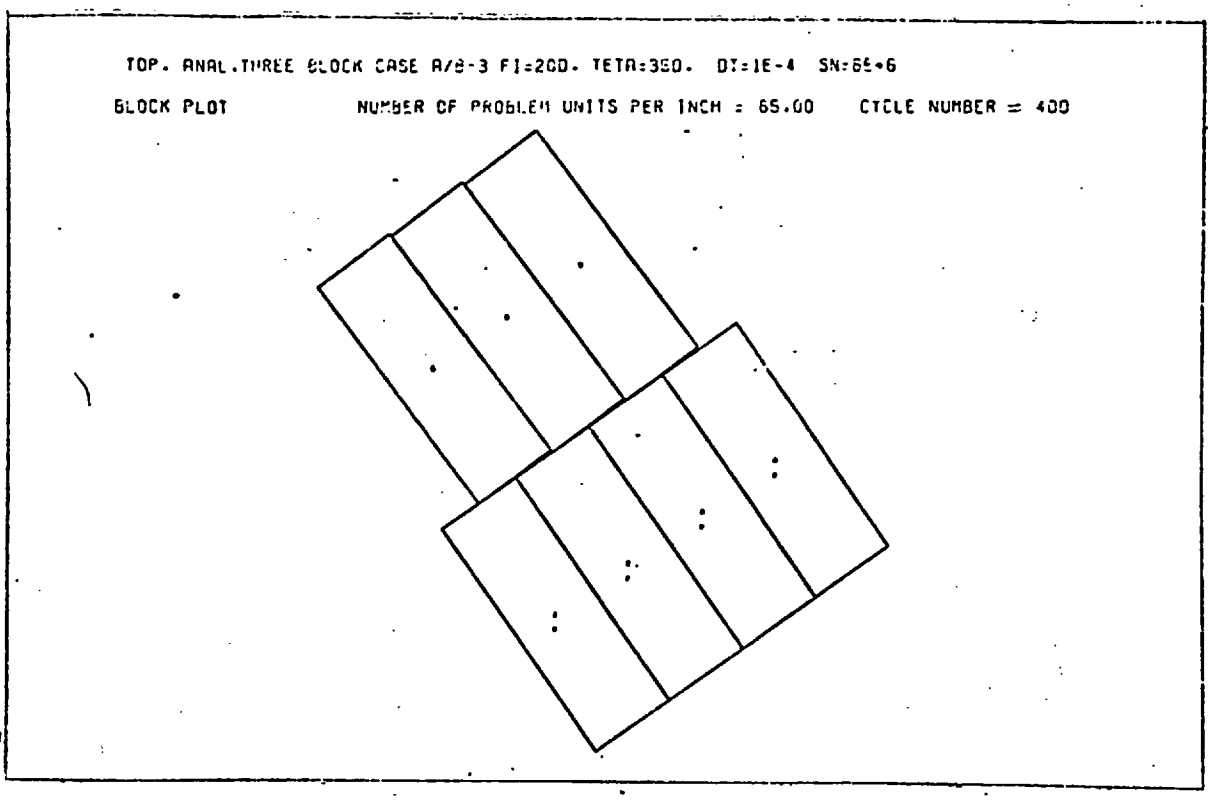

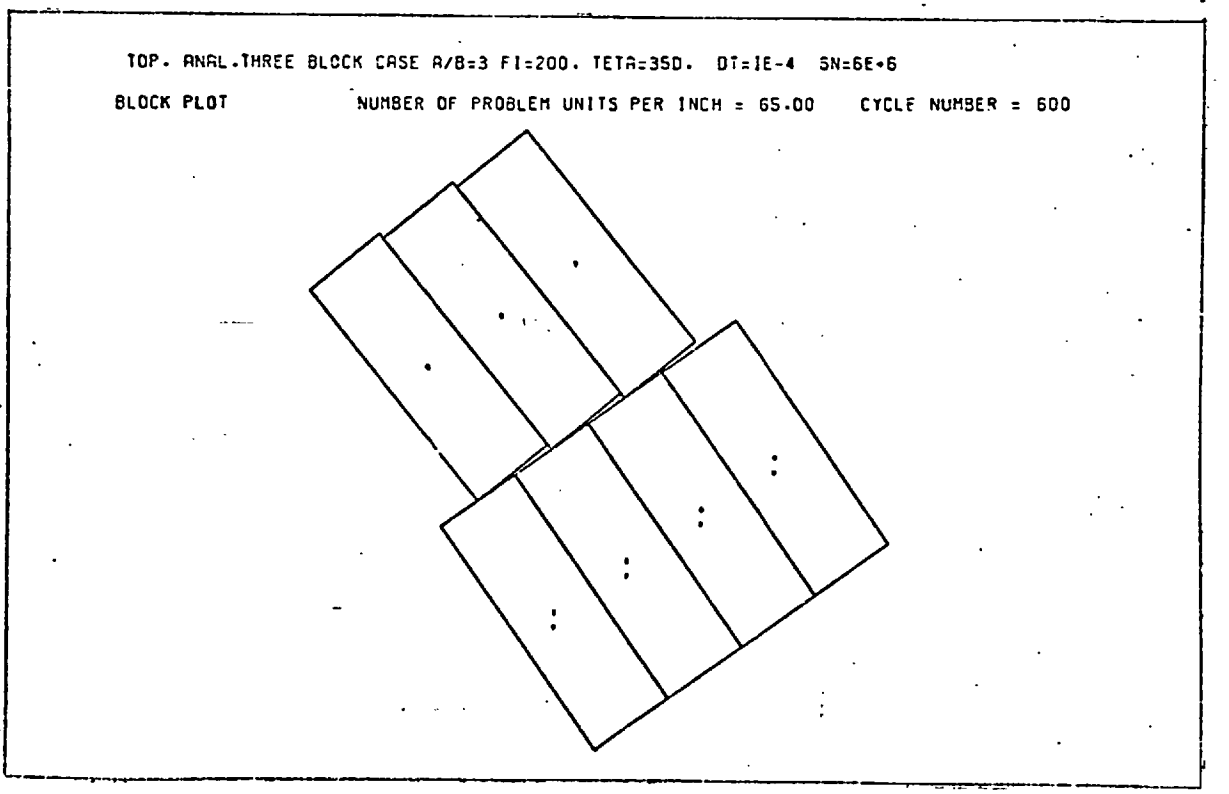

Figure 5.14- Toppling of triple block system.

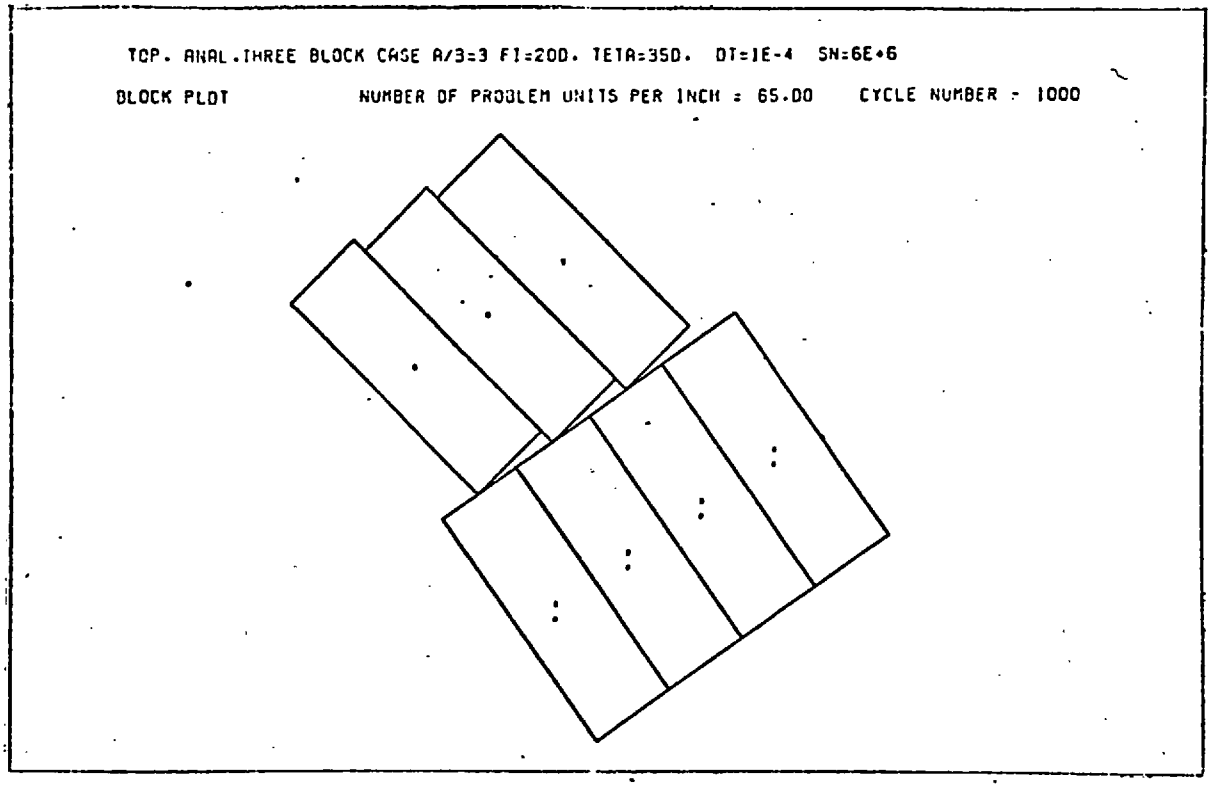

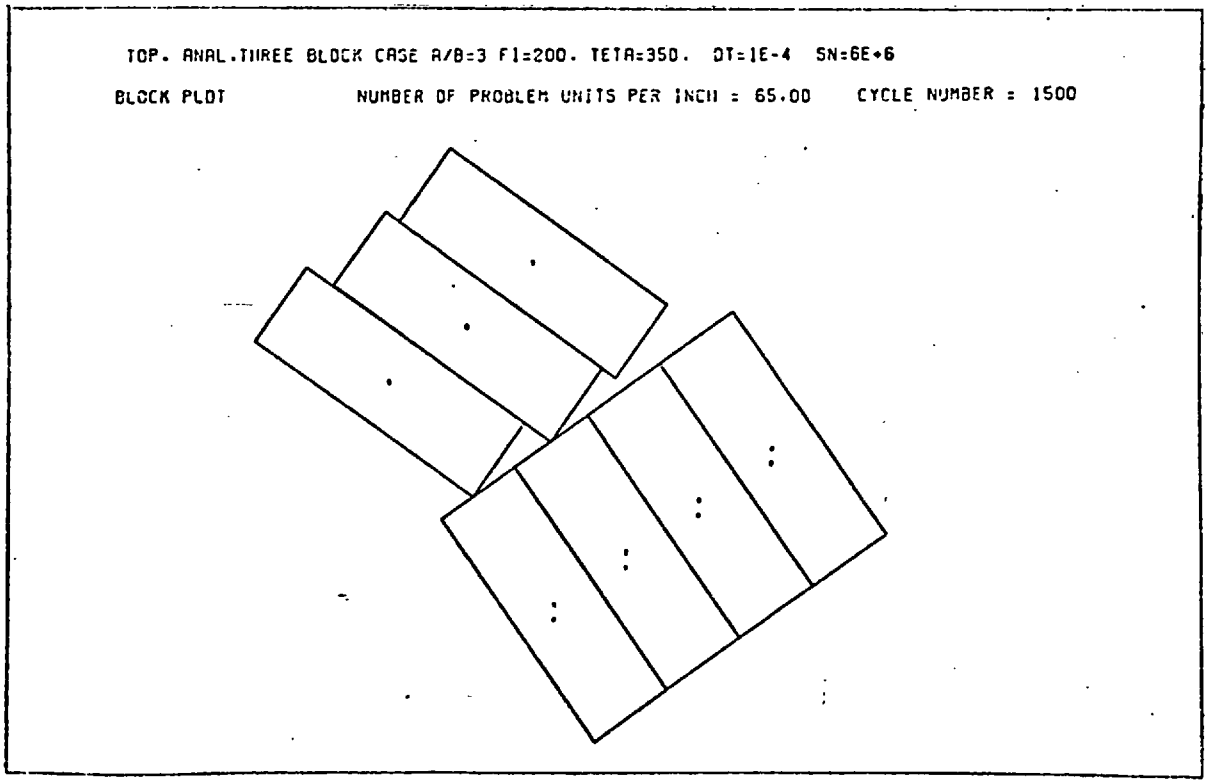

Figure 5.14- Continued.

5.3.3.2 - Quadruple Block Tests -

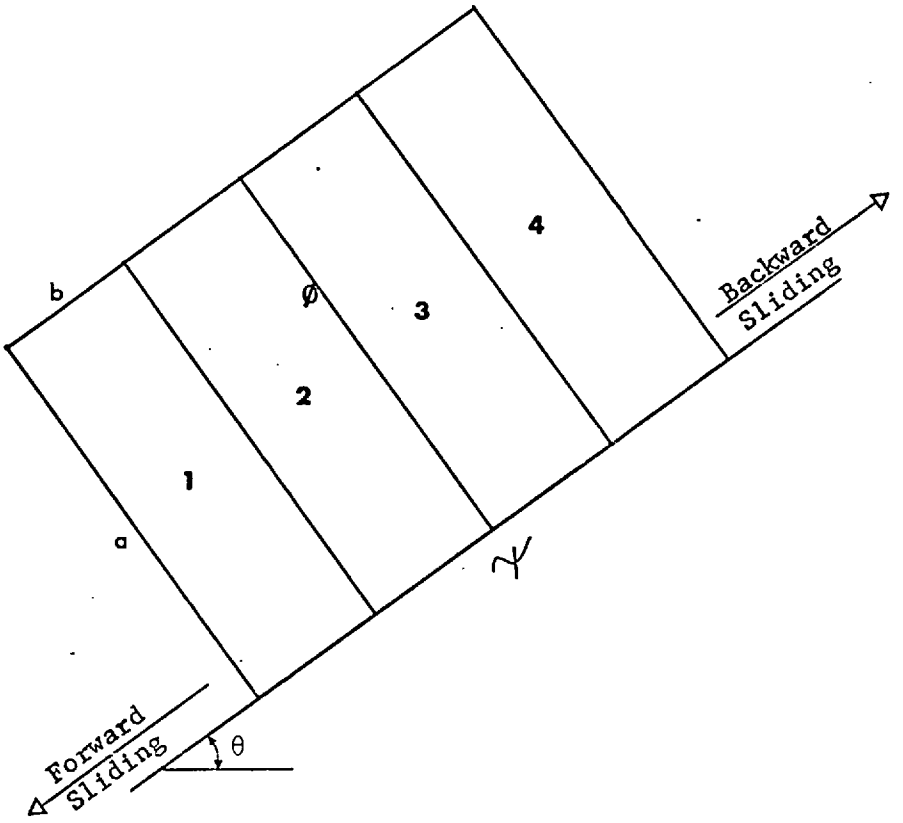

The observations are tabulated to show how the block movements vary at different stages of the failure process.

i. $a/b = 5$, $\theta = 20^{\circ}$, $\phi = \psi = 30^{\circ}$

CYCLE NO.	BLOCK (1)	BLOCK (2)	BLOCK (3)	BLOCK (4)
400	-	F.S.	-	F.S.
500	F.S.	-	-	-
600	-	F.S.	-	B.S.
700	F.S.	F.S.	B.S.	F.S.
800	F.S.	-	-	-
900	-	F.S.	-	B.S.
1000	-	-	B.S.	B.S.
1100	F.S.	-	-	B.S.
1200	F.S.	F.S.	F.S.	B.S.
1300	F.S.	F.S.	B.S.	B.S.
1400	F.S.	-	-	B.S.
1500	F.S.	-	-	B.S.
1600	F.S.	B.S.	B.S.	B.S.
1700	F.S.	-	B.S.	B.S.
1800	F.S.	B.S.	-	B.S.
1900	F.S.	-	B.S.	B.S.
2000	F.S.	-	?	-
2100	F.S.	F.S.	B.S.	B.S.
2200	F.S.	B.S.	B.S.	-
2300-2500	F.S.	-	-	-
TOTAL	F.S. = 18 N.S. = 4	N.S. = 12 F.S. = 7 B.S. = 3	N.S. = 12 B.S. = 8 F.S. = 1	B.S. = 13 N.S. = 7 F.S. = 2

Note:
F.S. Stands for "Forward Sliding"
B.S. Stands for "Backward Sliding"
N.S. and (-) Stands for "No Sliding"
? No record available

Table 5.1 History of block movements for quadruple-block model (i).

ii. $a/b = 5$, $\theta = 18.5^{o}$, $\phi = 40^{o}$, $\psi = 20^{o}$

This test is illustrated in Figure 5.15.

CYCLE NO.	BLOCK (1)	BLOCK (2)	BLOCK (3)	BLOCK (4)
400	F.S.	-	F.S.	-
500	F.S.	F.S.	-	-
600	F.S.	-	F.S.	-
700	-	-	F.S.	-
800	F.S.	F.S.	F.S.	B.S.
900	F.S.	F.S.	F.S.	-
1000	F.S.	F.S.	-	B.S.
1100	F.S.	F.S.	-	F.S.
1200	F.S.	F.S.	-	B.S.
1300	F.S.	F.S.	-	B.S.
1400	F.S.	F.S.	F.S.	B.S.
1500	F.S.	F.S.	F.S.	B.S.
1600	F.S.	F.S.	-	B.S.
1700	F.S.	F.S.	-	B.S.
1800	F.S.	F.S.	B.S.	B.S.
1900	F.S.	-	-	B.S.
2000	F.S.	F.S.	B.S.	B.S.
2100	F.S.	F.S.	B.S.	B.S.
2200	F.S.	-	-	B.S.
2300	F.S.	F.S.	B.S.	B.S.
2400	F.S.	B.S.	B.S.	?
2500	F.S.	F.S.	-	B.S.
2600	F.S.	B.S.	-	-
2700	F.S.	B.S.	-	-
2800-3000	F.S.	-	-	-
TOTAL	F.S. = 26 N.S. = 1	F.S. = 16 N.S. = 8 B.S. = 3	N.S. = 15 F.S. = 7 B.S. = 5	B.S. = 15 N.S. = 10 F.S. = 1

Table 5.2 History of block movements for quadruple-block model (ii).

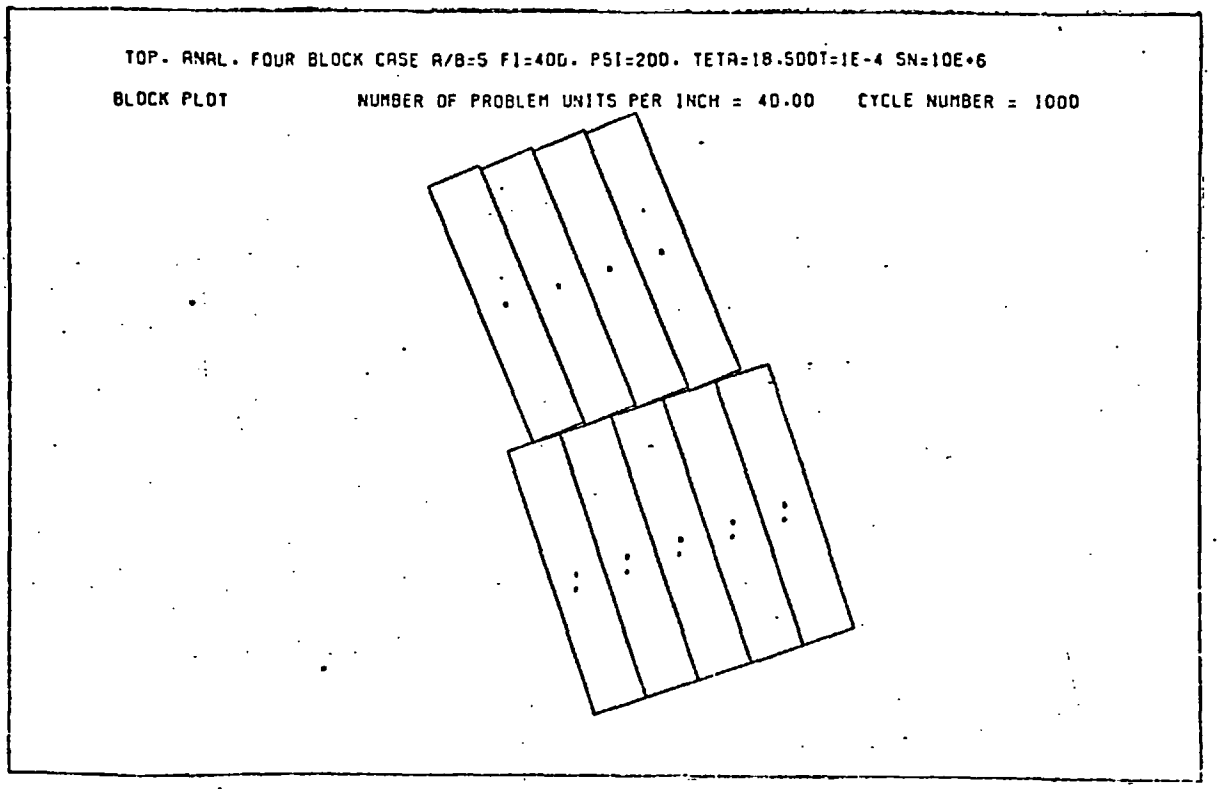

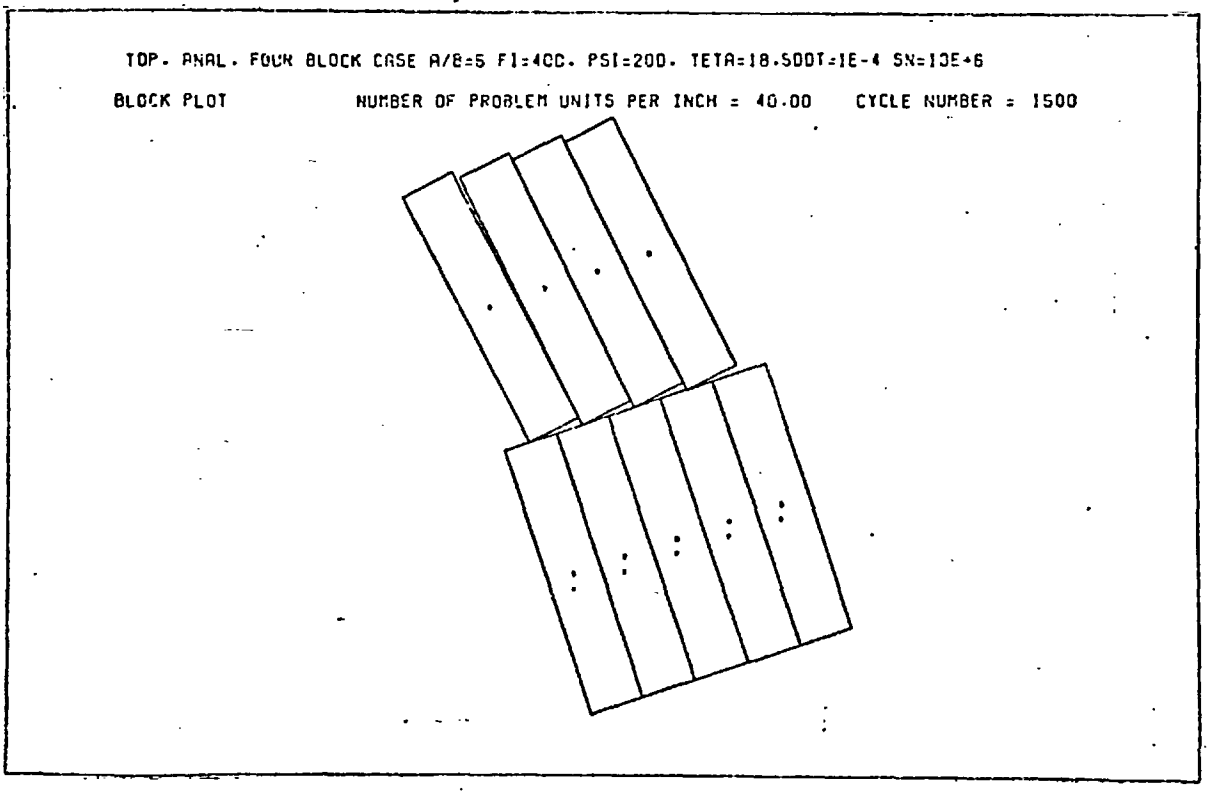

Figure 5.15- Failure of quadruple block system.

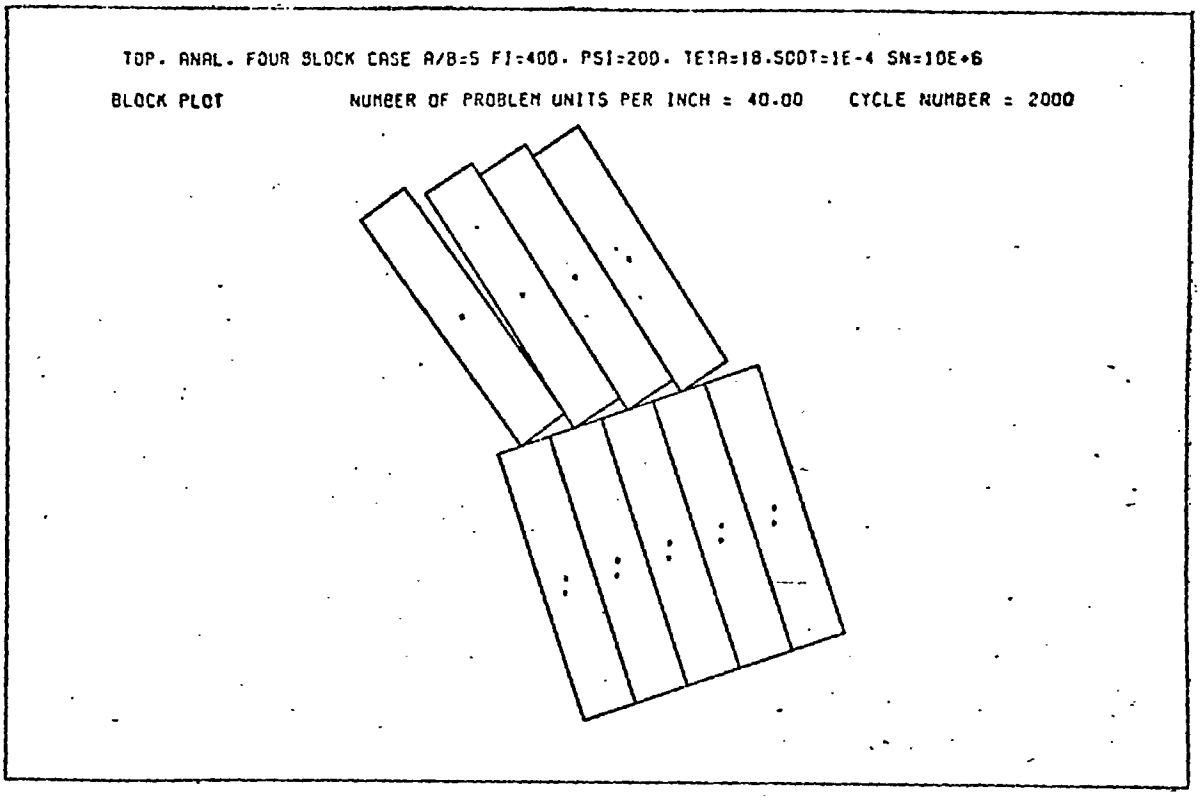

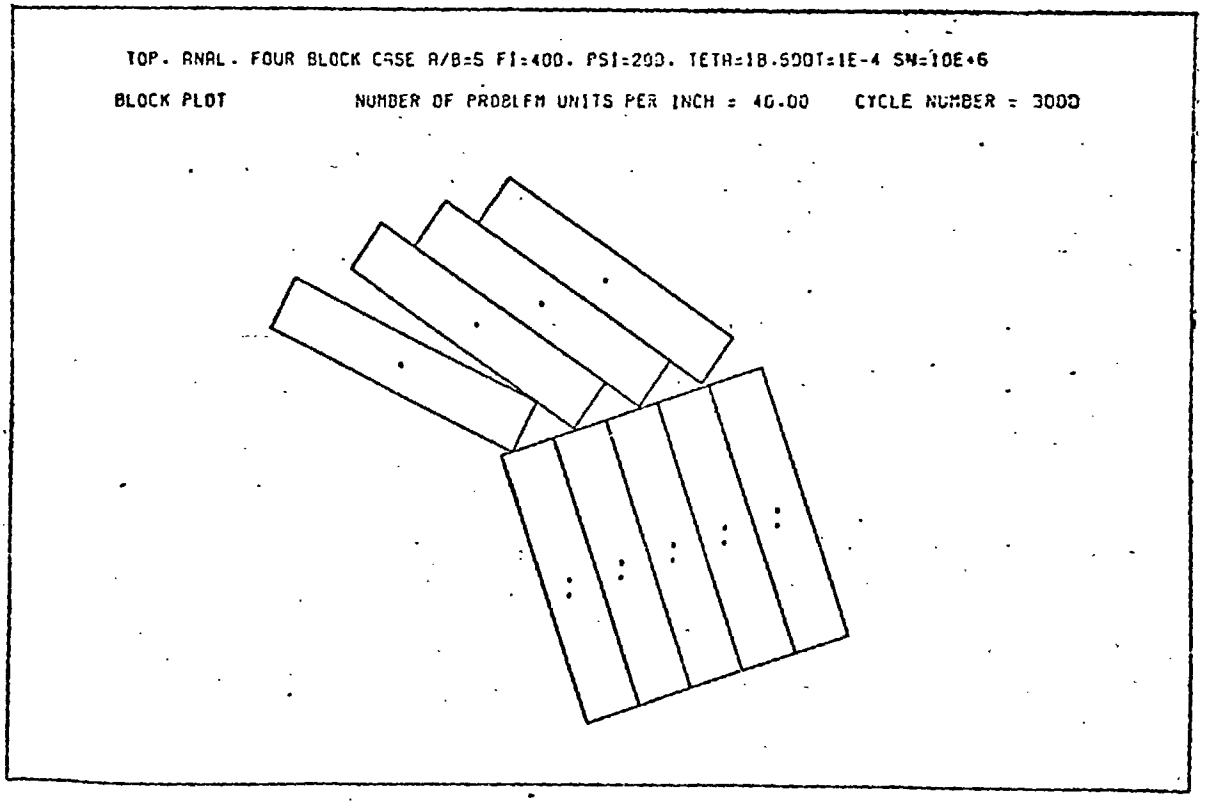

Figure 5.15- Continued.

iii. $a/b = 7$, $\theta = 10.5^{\circ}$, $\phi = \psi = 20^{\circ}$

CYCLE NO.	BLOCK (1)	BLOCK (2)	BLOCK (3)	BLOCK (4)
300	F.S.	-	-	-
700	F.S.	-	-	-
900	F.S.	-	-	-
1000	F.S.	F.S.	-	B.S.
1100	F.S.	-	-	-
1200	F.S.	B.S.	-	B.S.
1300	F.S.	-	-	-
1400	-	-	B.S.	B.S.
1500	F.S.	-	-	B.S.
1600	-	F.S.	F.S.	-
1700	-	-	F.S.	-
1800-1900	-	F.S.	B.S.	B.S.
2000	F.S.	B.S.	B.S.	B.S.
2100	F.S.	F.S.	-	-
2200	F.S.	F.S.	B.S.	-
2300	F.S.	-	-	F.S.
2400	F.S.	F.S.	-	B.S.
2500	F.S.	F.S.	F.S.	-
2600	F.S.	B.S.	B.S.	B.S.
2700	F.S.	-	B.S.	B.S.
2800	-	F.S.	B.S.	B.S.
2900	F.S.	-	-	B.S.
3000	F.S.	F.S.	B.S.	B.S.
TOTAL	F.S. = 18 N.S. = 6	N.S. = 11 F.S. = 10 B.S. = 3	N.S. = 12 B.S. = 9 F.S. = 3	B.S. = 13 N.S. = 10 F.S. = 1

Table 5.3 History of block movements for quadruple-block model (iii).

iv. $a/b = 7$, $\theta = 33^{\circ}$, $\phi = \psi = 40^{\circ}$

CYCLE NO.	BLOCK (1)	BLOCK (2)	BLOCK (3)	BLOCK (4)
300	-	-	B.S.	B.S.
400	-	B.S.	-	-
500	-	-	B.S.	-
600	F.S.	?	-	?
700	F.S.	F.S.	-	B.S.
800	F.S.	-	-	-
900	F.S.	B.S.	-	B.S.
1100	F.S.	-	-	B.S.
1200	F.S.	B.S.	-	-
1500-1600	F.S.	-	-	-
1800	F.S.	-	-	-
2000	F.S.	-	-	-
2400-2800	F.S.	-	-	-
TOTAL	F.S. = 15 N.S. = 3	N.S. = 13 B.S. = 3 F.S. = 1	N.S. = 16 B.S. = 2	N.S. = 13 B.S. = 4

Table 5.4 History of block movements for quadruple-block model (iv).

v. $a/b = 10$, $\theta = 11.5^{\circ}$, $\phi = \psi = 30^{\circ}$

CYCLE NO.	BLOCK (1)	BLOCK (2)	BLOCK (3)	BLOCK (4)
700	-	F.S.	-	-
1100	-	B.S.	-	-
1200	F.S.	B.S.	-	-
1300	F.S.	F.S.	-	-
1400	F.S.	-	-	B.S.
1500	-	-	F.S.	B.S.
1600	-	B.S.	-	B.S.
1700	F.S.	-	B.S.	B.S.
1800	-	B.S.	F.S.	-
1900	F.S.	F.S.	-	B.S.
2000	F.S.	B.S.	-	B.S.
2100	F.S.	-	B.S.	B.S.
2200	F.S.	B.S.	F.S.	B.S.
2300	-	B.S.	B.S.	B.S.
2400	F.S.	B.S.	-	-
2500	F.S.	B.S.	-	B.S.
2600	F.S.	F.S.	B.S.	B.S.
2700	-	-	B.S.	B.S.
2800	F.S.	B.S.	-	B.S.
2900	F.S.	-	-	B.S.
3000	-	B.S.	-	B.S.
3100	F.S.	B.S.	-	B.S.
TOTAL	F.S. = 14 N.S. = 8	B.S. = 12 N.S. = 6 F.S. = 4	N.S. = 14 B.S. = 5 F.S. = 3	B.S. = 16 N.S. = 6

Table 5.5 History of block movements for quadruple-block model (v).

Here too, the flank blocks (1) and (4) almost always slid downhill and uphill respectively, the former being more pronounced. Block (2) was mostly stationary, otherwise tended to slide forward except when the ratio R was high

when it preferred uphill sliding. Block (3) was even less active in respect of sliding and almost always remained fixed, otherwise it slid backwards.

5.3.4 - Blocks of Unequal Size -

Having obtained satisfactory solutions for the models of equal height blocks, the scope of the D.R. program was extended to handle unequal height block systems. Although, at first, it appeared to be quite an easy job to modify the program, it was, in fact, the opposite. The part connected with selection and updating of the neighbours needed substantial changes, and therefore to save time, information regarding the neighbours for each block was fed into the program in the form of data. Appendix B gives a listing of the modified version of the program.

Two different models were constructed: one with a plane base, and the other with a stepped base. The former was a replica of the physical model reported in Chapter 3. The latter was to compare with Bray's[8] limiting equilibrium solution.

5.3.4.1 - Plane Base Model -

The geometry of the model was that of the 9-column tilting frame model described in Chapter 3 (page 147). The failure of the computer model took place in a very similar way to that of the physical model as shown in Figure 5.16. The first block (1" height) slid forward having been pushed down by a set of toppling columns. A couple of blocks at

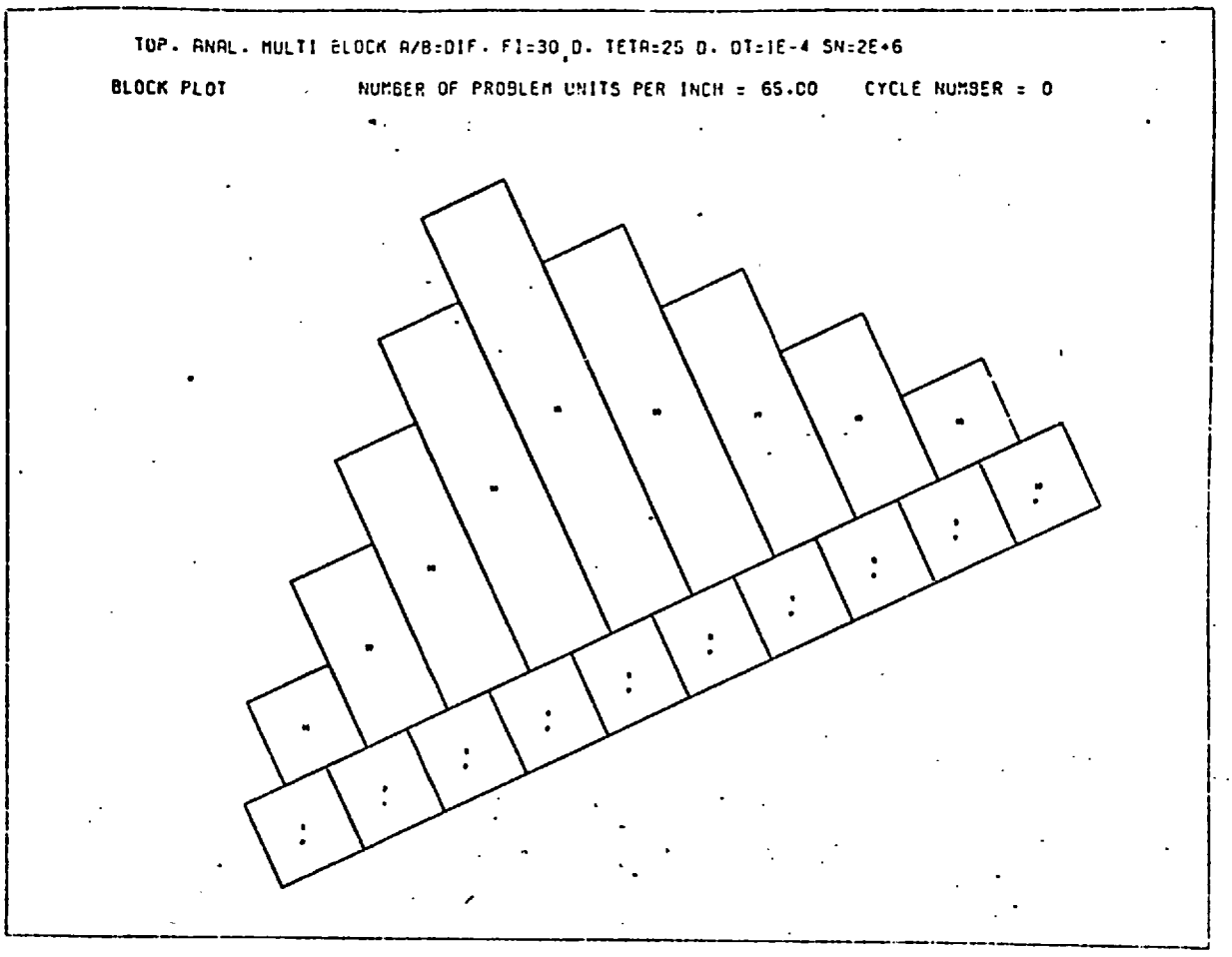

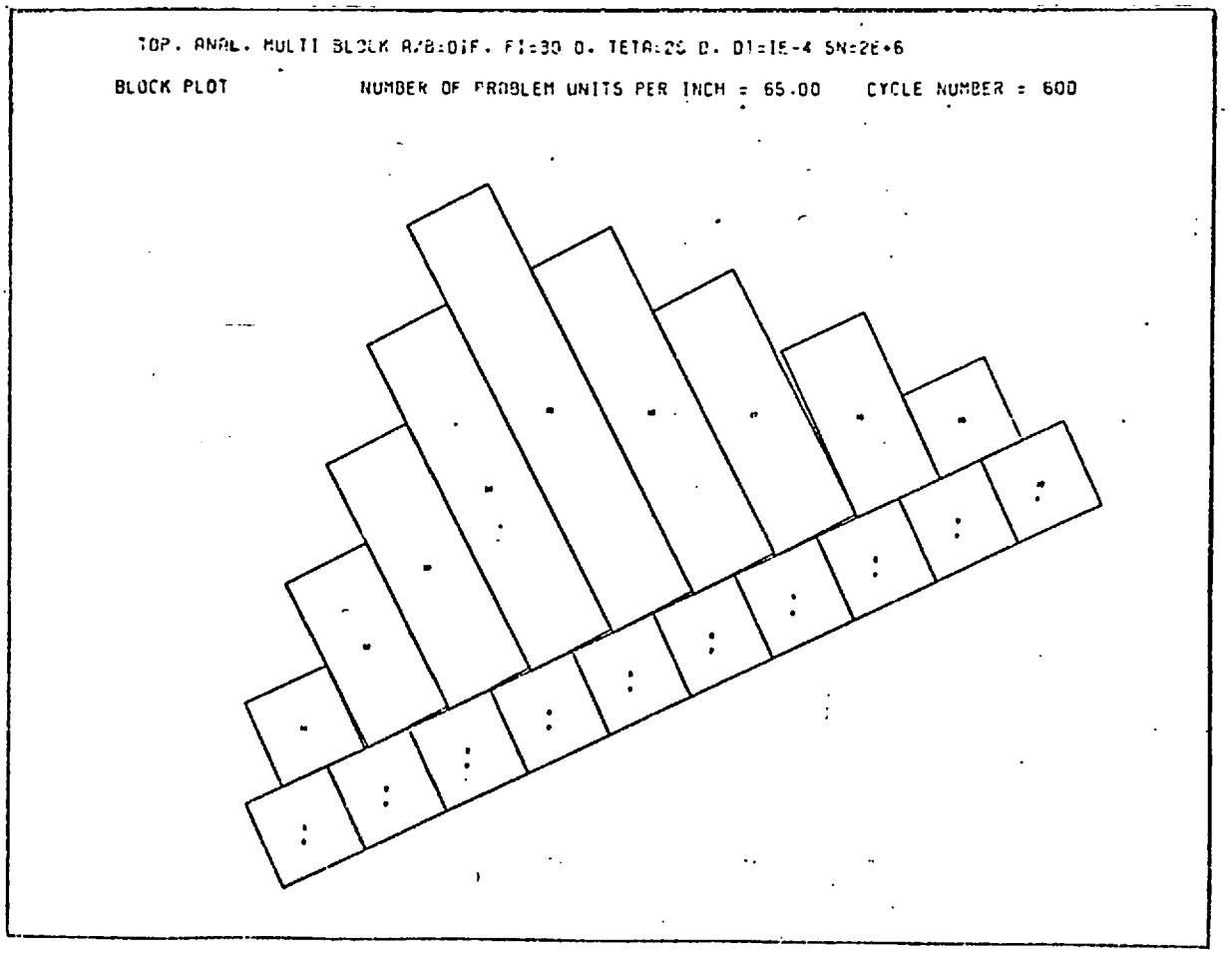

Figure 5.16- Plane base multiple block model.

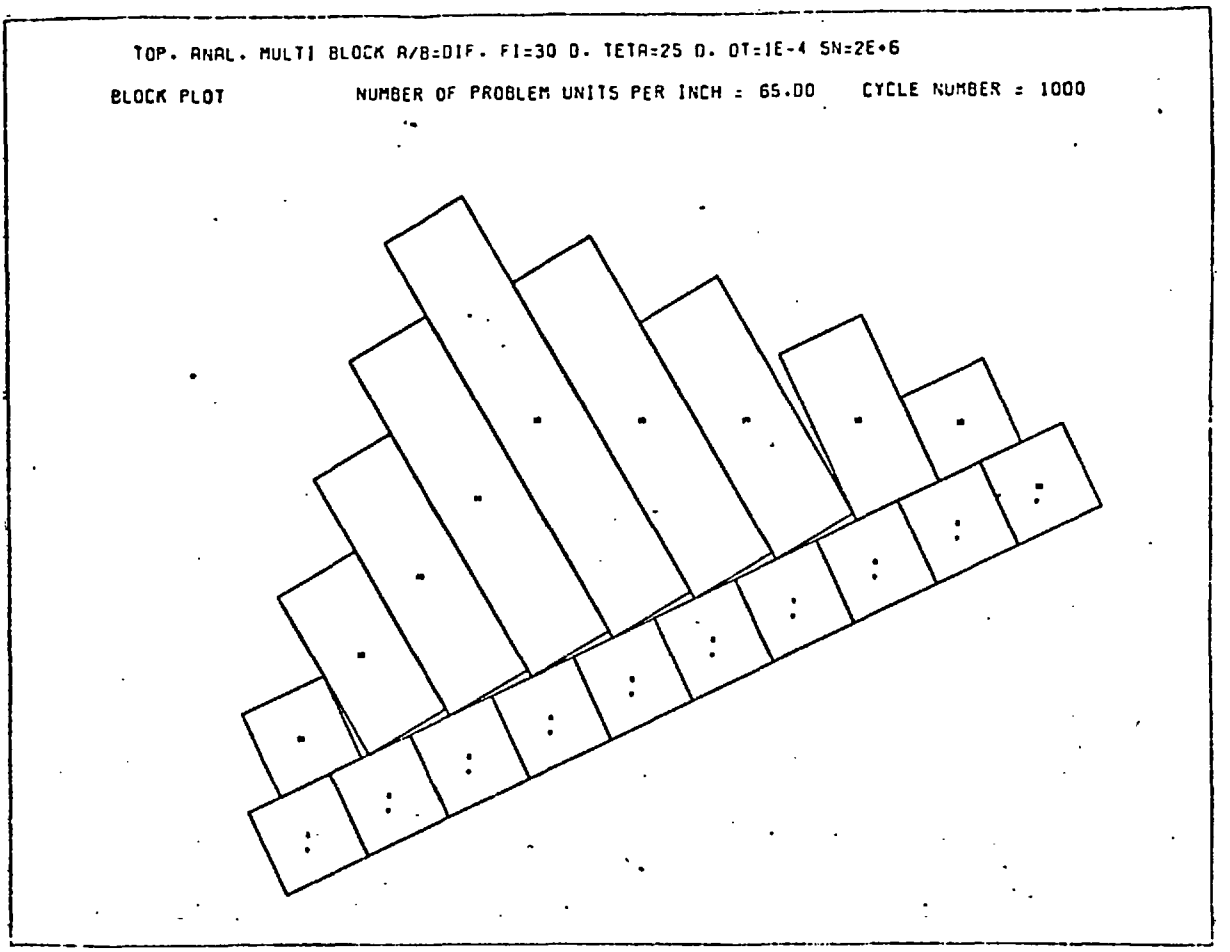

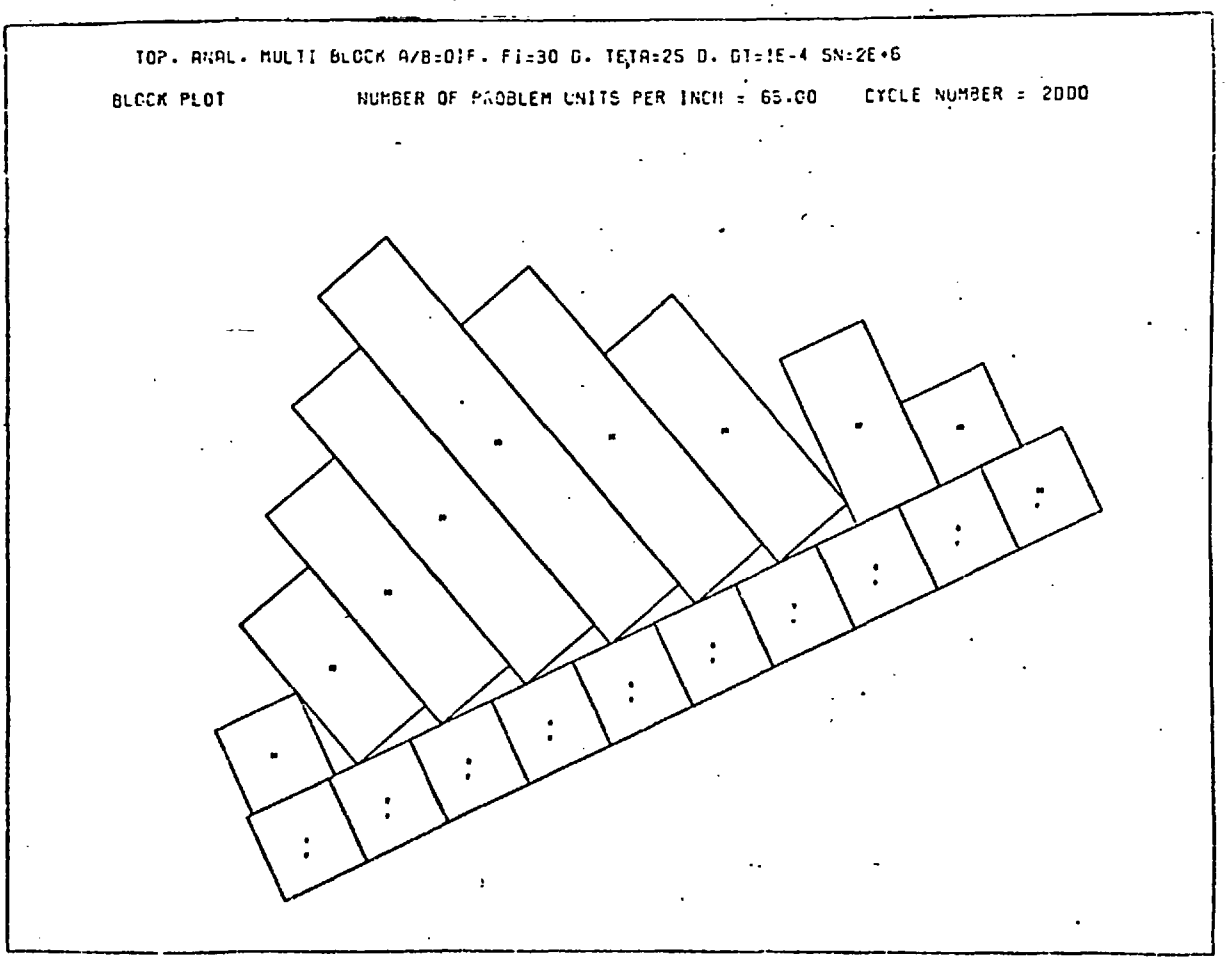

Figure 5.16- Continued.

the back stood still, helping the formation of a tension crack. The reader's attention is drawn to the similarity between the photograph (b) of plate 3.XIV (page 150) and the drawing for cycle 2000 of Figure 5.16 (the 3" height block at the back toppled in the computer model owing to the 25° inclination of the base plane to the horizontal (θ) as compared to 16° in the physical model).

5.3.4.2 - Stepped Base Model -

Bray's[8] analysis for the geometry illustrated in Appendix A gives a friction angle of 41.14° for limiting conditions. The same geometry was reproduced as the computer model and the friction angles of 38, 40, 42, 44 and 46 degrees were tried. The models with ϕ equals 38°, 40° and 42° failed. Obviously, the number of iterations to define the block movements increased with increasing ϕ. Models with the friction angle of 44° and 46°, first showed the sign of instability with a slight opening between the 5th and 6th columns, but this should have been due to consolidation since they remained stable. More important than the agreement in friction angle was the remarkable similarity in behaviour between the limiting equilibrium analysis and the Dynamic Relaxation Method. As illustrated in Figure 5.17, block 1 slid down, blocks 2, 3, 4 and 5 toppled, 6, 7 and 8 remained stable exactly as in the limiting equilibrium analysis. The tension crack formed at the location as predicted by the L.E. method. The similarity between the Figure 4.12 of Chapter 4 and the drawing for cycle 13000 of Figure 5.17 demonstrates this visually. Such a comprehensive

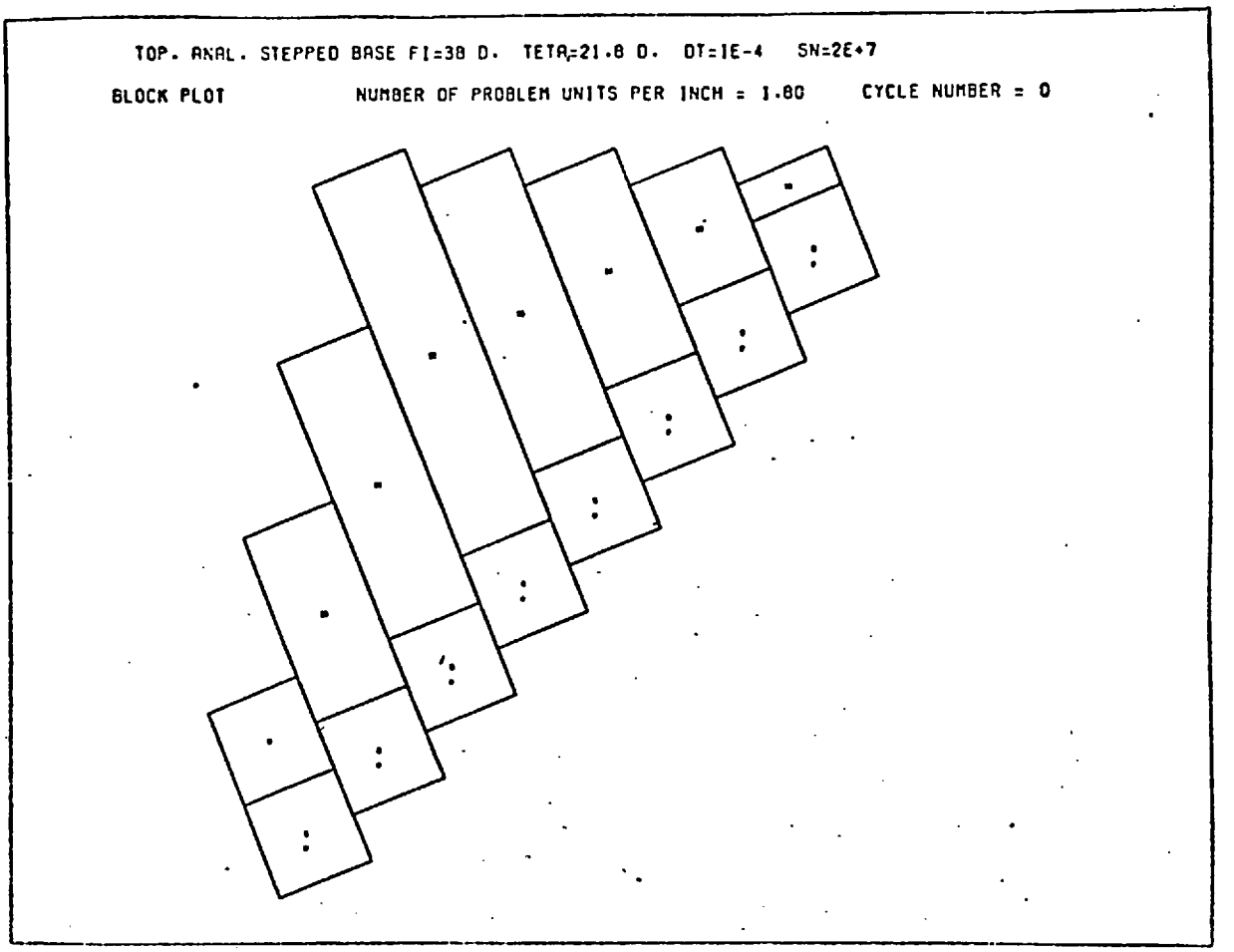

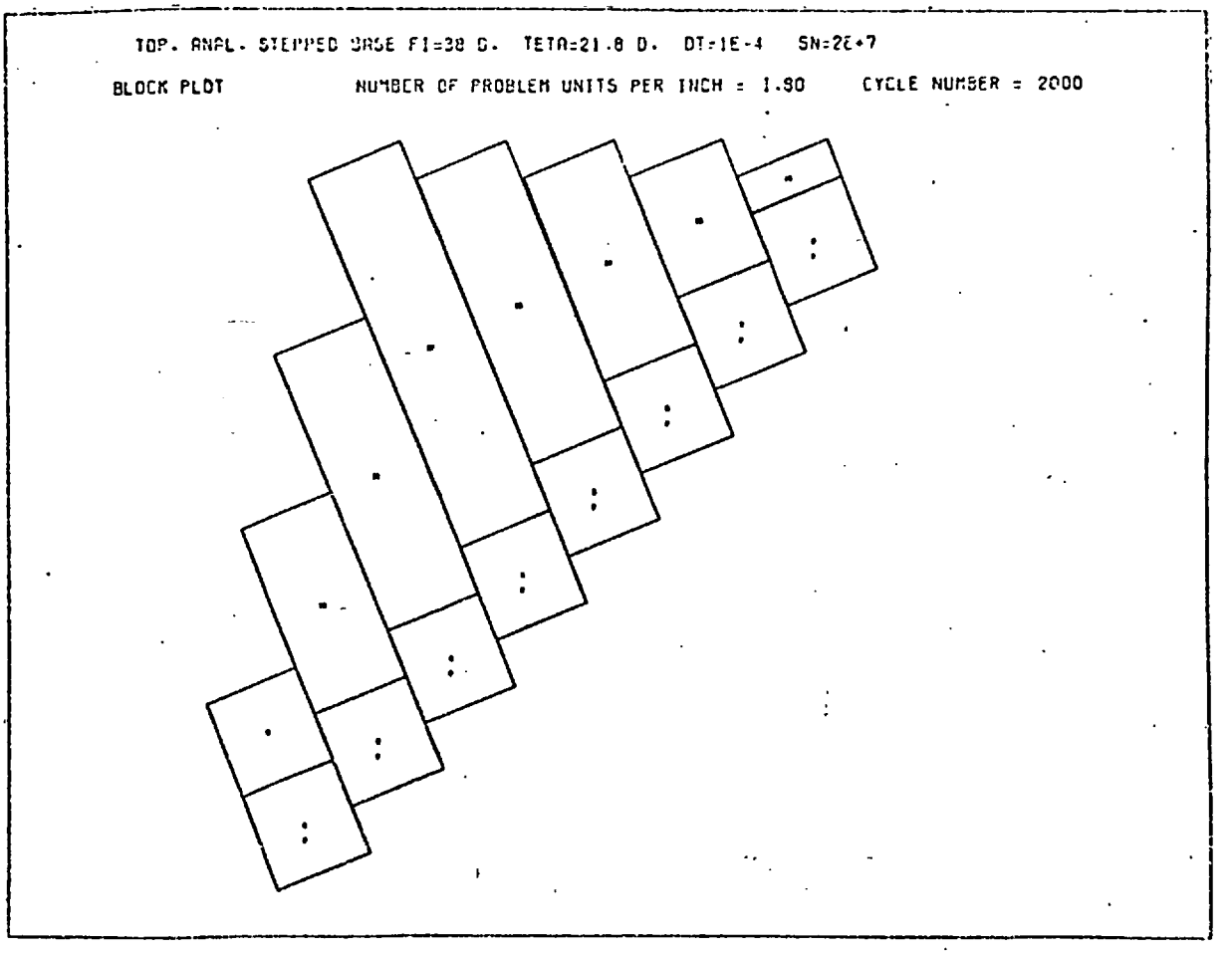

Figure 5.17- Stepped base multiple block model.

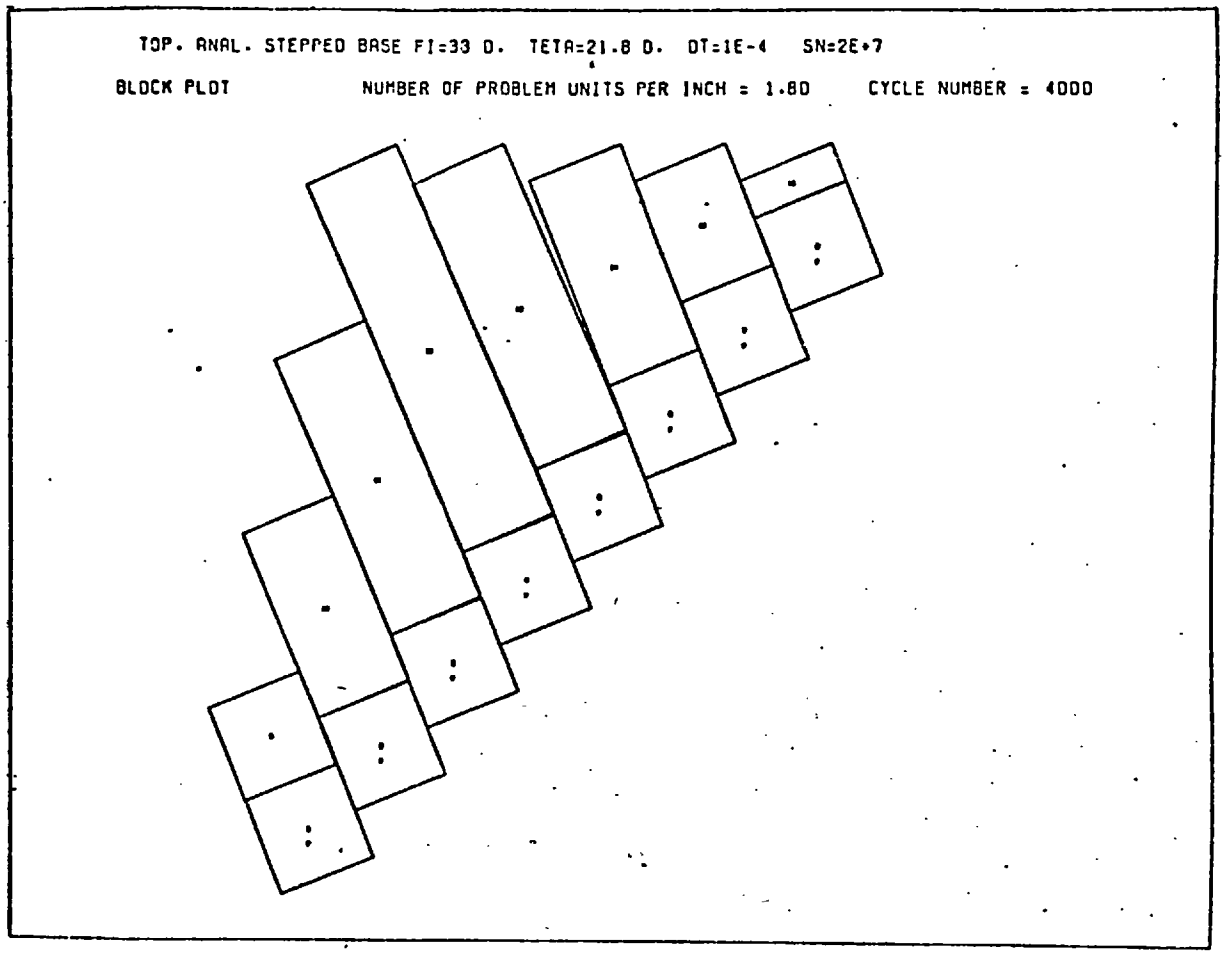

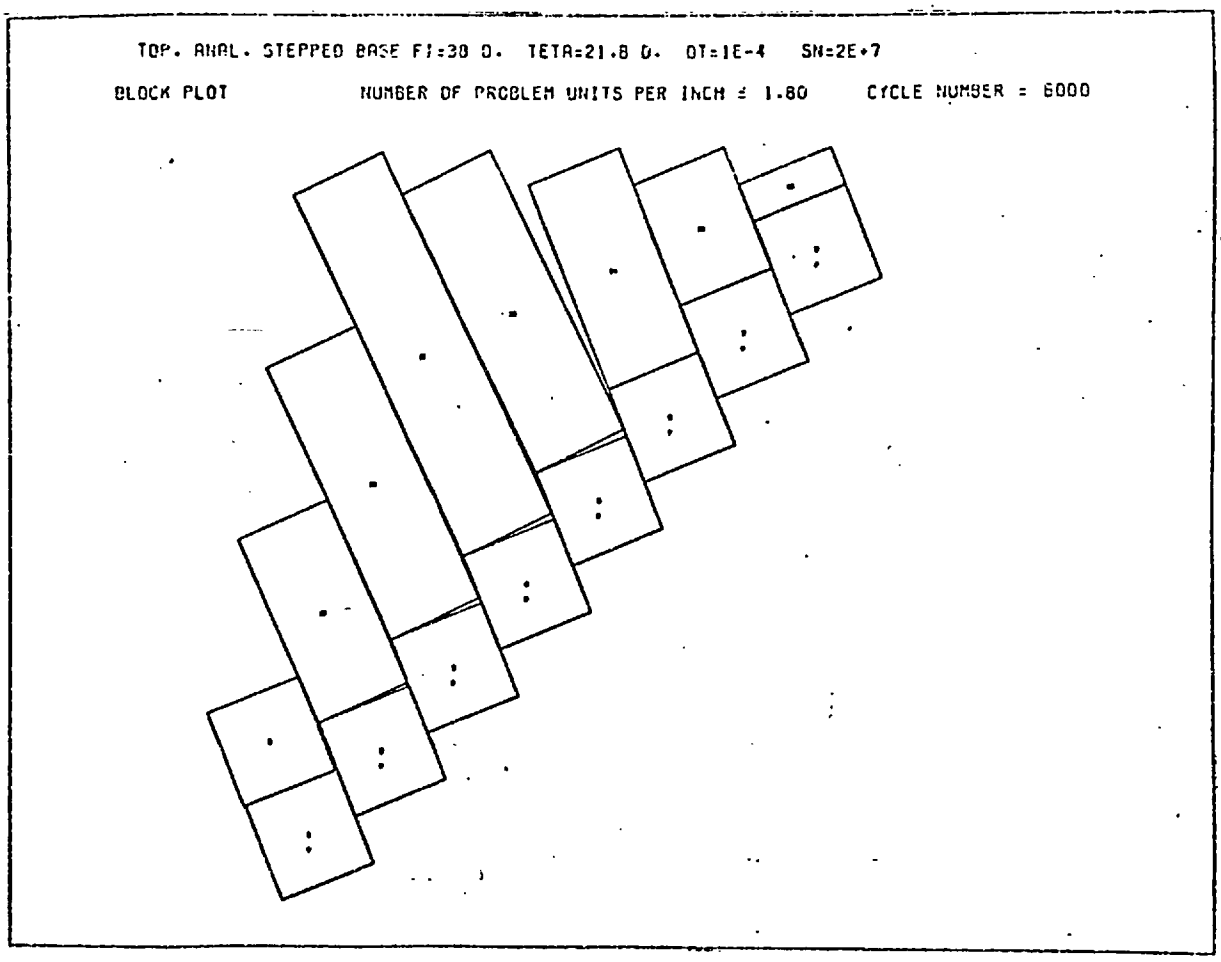

Figure 5.17- Continued.

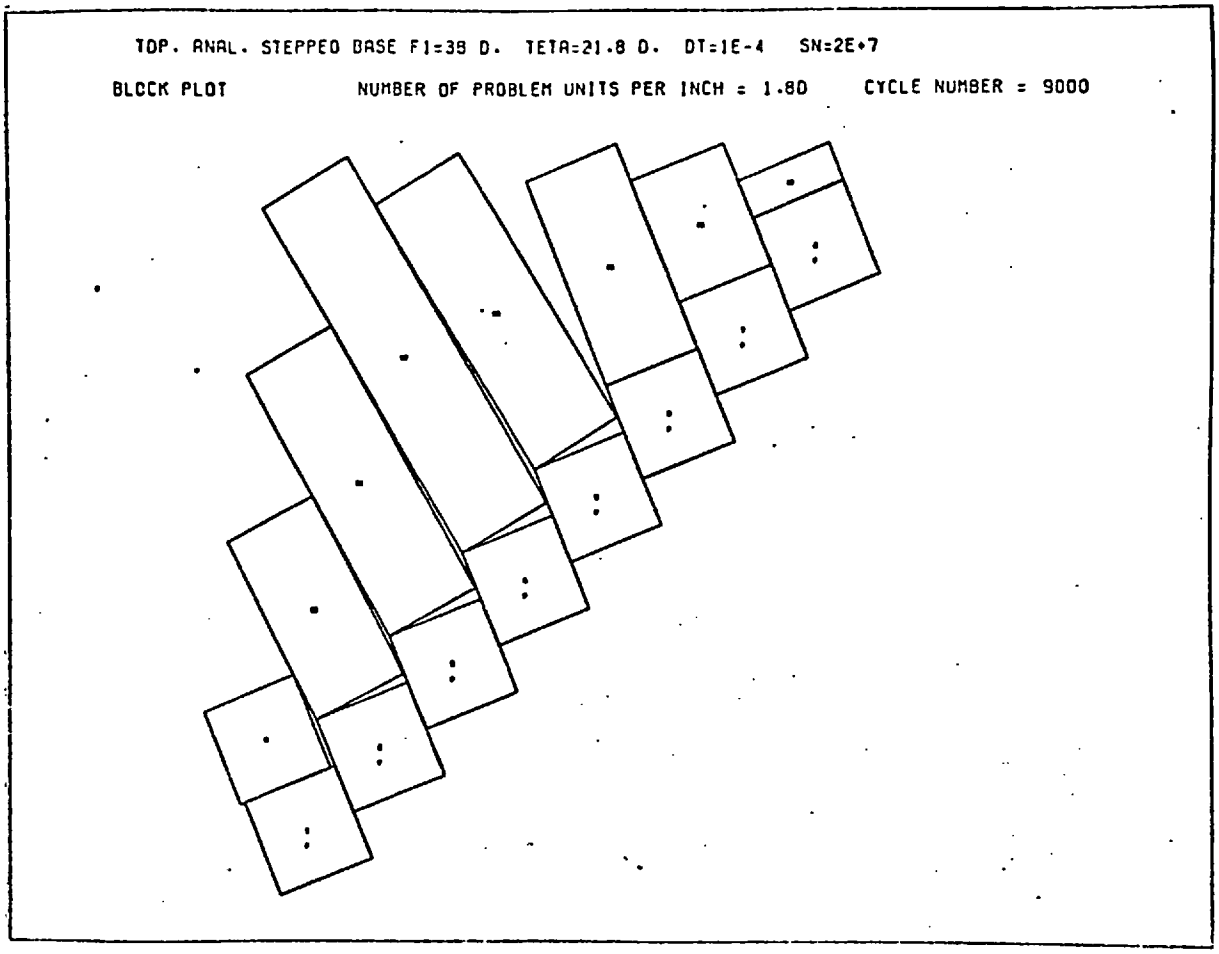

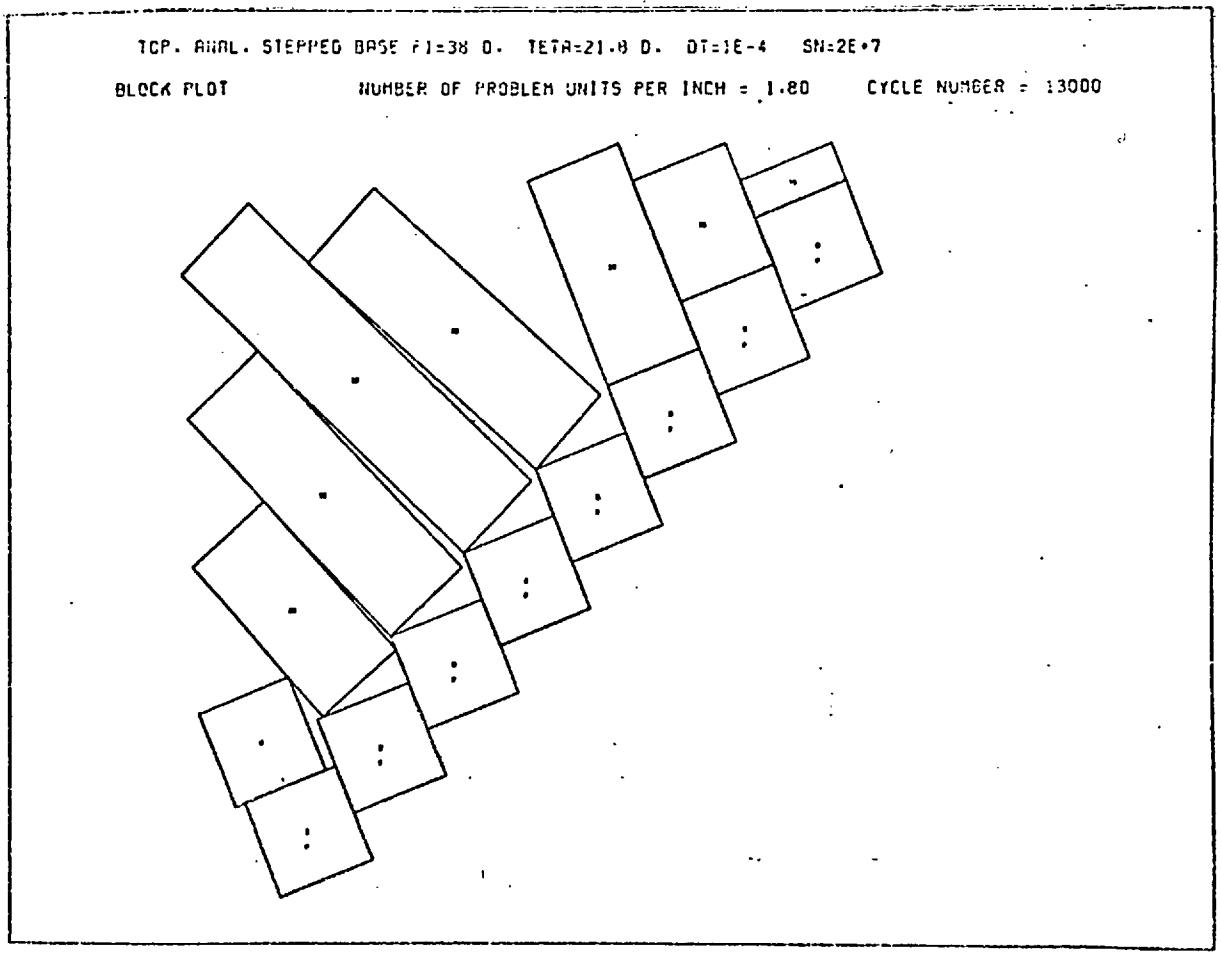

Figure 5.17- Continued.

agreement obviously increases the credibility of both techniques.

5.4 Conclusions

From the tests conducted the following conclusions emerged:

1. The D.R. program accurately simulated toppling as well as sliding.
2. Single and double block tests, agreeing with the L.E. solutions, gave satisfactory results. However, the use of progressive tilting as an experimental procedure to obtain better solutions was found to produce conflicting results.
3. The investigation for failure modes of triple and quadruple block systems yielded the fact that there was not a unique pattern of movement for the whole failure process but various modes at different stages.
4. The models of multiple blocks with unequal heights failed agreeing with the physical (tilting frame) and theoretical (L.E.) models.

Despite its shortcomings (perfectly rigid blocks only) and the difficulties involved in reaching acceptable solutions (high inertia forces, the brevity of stable time step), the D.R. method proved to be applicable for the analysis of toppling failure in a blocky rock system where mechanistically controlled movements play the dominant part in failure process.

REFERENCES

1. CUNDALL, P.A. A computer model for simulating progressive large-scale movements in blocky rock systems. Proc. Symposium on Rock Fracture, Nancy, France 1971.
2. HOCKING, G. Notes on dynamic block modelling program. Golder Associates, April 1975.
3. OTTER, J.R.H., CASSELL, A.C. and HOBBS, R.E. Dynamic Relaxation. Proc. Inst. Civ. Engrs. V.35, Dec. 1966.
4. GEROGIANNOPOULOS, N. A critical state approach to Rock Mechanics. Ph.D. Thesis, Univ. of London (Imperial College), 1977.
5. HOCKING, G. Development and application of the Boundary Integral and Rigid Block methods for geotechnics. Ph.D. Thesis, Univ. of London (Imperial College), 1977, 287 p.
6. CUNDALL, P.A. The measurement and analysis of accelerations in rock slopes. Ph.D. Thesis, Univ. of London, (Imperial College), Feb. 1971.
7. HOCKING, G. Personal communication, Imperial College, 1975.
8. BRAY, J.W. "Rock Slope Stability" Lecture Notes, Imperial College, London, 1976.

CHAPTER SIX

SUMMARY OF CONCLUSIONS

In dealing with slopes, Rock Mechanics has long been influenced by the principles of Soil Mechanics. Therefore, "sliding" has been considered until recently the basic mode of behaviour for rock slopes.

However, recent theoretical developments, supported by physical and numerical model studies and by field observations have led to increased interest in toppling as a mode of failure in rock slopes. Although the present level of knowledge for this mode of behaviour is in no way adequate for design purposes. practising slope engineers should be aware of its dangers especially when steep slopes are to be cut in columnar structures formed by subvertical joint sets.

Despite their qualitative character, base friction models were found to be producing useful information in various ways. It was shown that in the 1967 failure at Old Delabole slate quarry (Cornwall) toppling was the predominant mechanism, models being constructed, initially on a trial-and-error basis, to attempt to match the post-failure features observed in the field.

The physical model tests in the exploration of toppling gave results consistent with the previous investigators in most areas. Base friction models of continuous columns and cross-jointed columns, and tilting frame models of con-

tinuous columns were constructed and tested. The base friction test results for the continuous column models revealed that the flexural strength of the columns together with the degree of restraint shown by the toe block(s) were the dominant factors controlling toppling failure. More stable slopes were obtained with increasing slope height due to the accompanying increase in the number of columns comprising the base of the slope. On the contrary, the stability of the slope appeared to be very sensitive to the variation in slope angle, regardless of the number of columns constituting the base of the slope. The cross-jointed slopes were found to be more stable than the continuous column slopes. They failed less severely with less disturbance at the toe. Taking all the base friction tests into account, the slopes having 60°-65° slope angle seemed to be in limiting conditions. The slopes of 70° ore more all failed quickly.

The accuracy expected from the tilting frame tests was not attained, mainly due to the use of plaster blocks. The wearing off of small scale asperities on the surfaces caused unacceptable variations in the friction angle. Inaccurate block dimensions hindering full surface to surface contact, was another source of distortion, observed particularly in the case of multiple blocks of equal height.

The analysis of limiting conditions for the toppling of multiple column systems revealed that rotation was generally accompanied by forward sliding of the lower block(s). But the likelihood of backward sliding was found to increase

with increasing column height, and with increasing inter-columnar friction angle in the double block case. When compared to the tilting frame models, the limit equilibrium approach was found to be giving more stable solutions.

The Dynamic Relaxation Block Program, producing solutions for both equal and unequal height block systems in agreement with the physical and theoretical models, proved to be capable of handling the overturning mode of failure satisfactorily. Its versatility, obviously, will be doubled when it is used in conjunction with a Finite Element program to simulate the block cracking.

This research has been directed towards the study and improvement of available techniques for toppling analysis rather than developing a method for design. In the light of all the findings the following remarks can be made.

a. Base friction models can safely be used for a preliminary investigation. Complex structures can be modelled with ease. For more reliable results boundary effects should be eliminated. Flexural strength of the columns, being an important parameter, can be adjusted (by the degree of compaction, the percentage of constituent materials, or the thickness of the slab) for a better representation of the field situation.

b. In tilting frame tests, careful consideration must be given to the type of block. If possible plaster blocks should not be used, but perspex or steel instead for consistent frictional properties. This method also suffers

from the imposition of a compulsory incline which may not have a counterpart in the field.

c. Limit equilibrium analysis is probably the most practical of all because it gives a factor of safety at the end. But this method is restricted to simple structures on account of the need for the failure mode to be known.

d. The Dynamic Relaxation technique is superior to limit equilibrium in view of its ability to model progressive failure and complex joint structures. However, this method requires certain amount of experience to optimize a number of input parameters such as time step, joint stiffness and damping factor for a realistic result. Although, at the present, this technique is a research tool rather than a design tool it is very promising for the future.

APPENDIX A

L.E. PROGRAM FOR STEPPED BASE MODEL

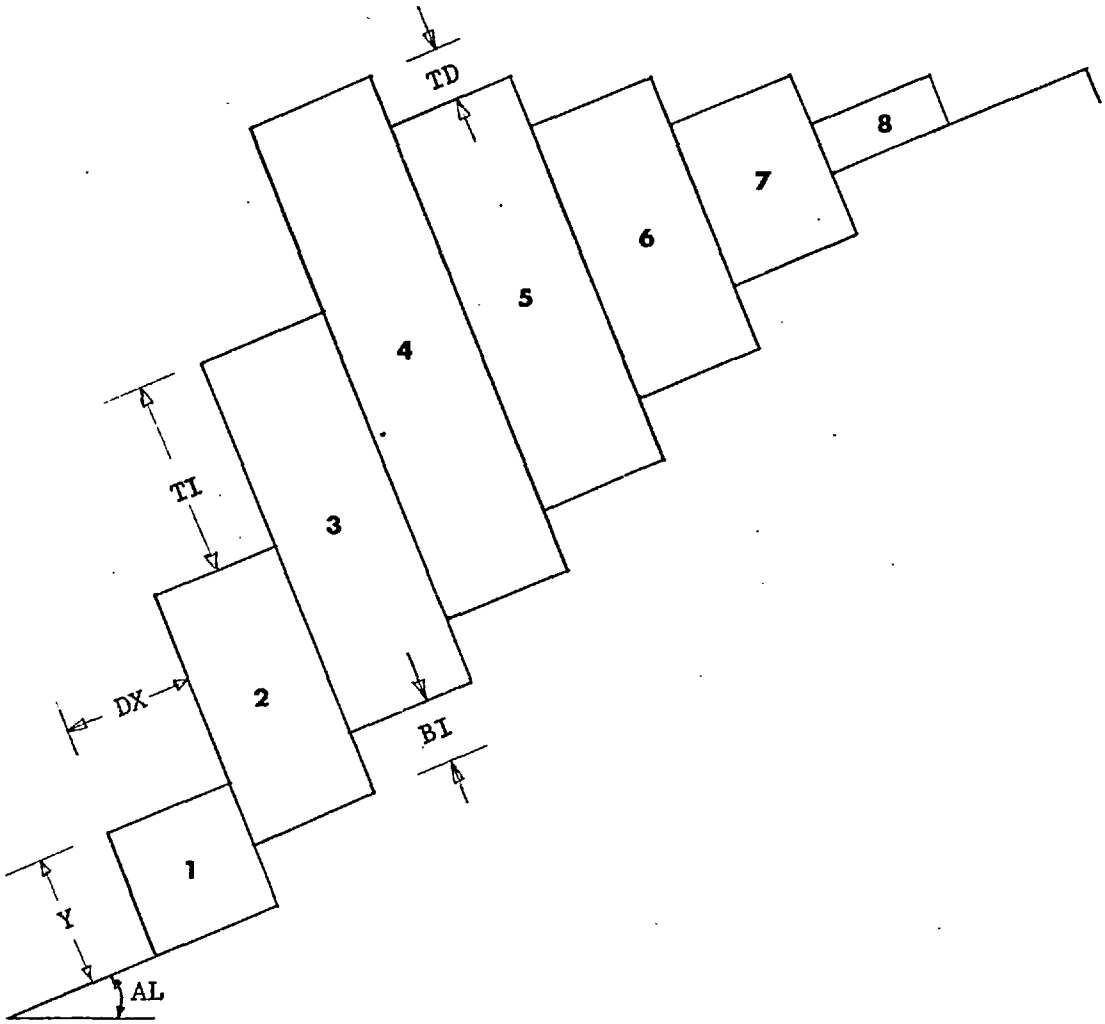


```
PROGRAM CAL(INPUT,OUTPUT,TAPE5 = INPUT,TAPE6 = OUTPUT)
   PARAMETERS-     Y = HEIGHT OF THE COLUMNS
                   W = WEIGHT OF THE COLUMNS
                   P = INTERBLOCK FORCE
                   Z = DISTANCE FROM BASE TO APPLICATION OF P
                  AL = INCLINATION OF THE BASETO THE HORIZONTAL
                  DX = THICKNESS OF COLUMNS
                   G = DENSITY
DIMENSION Y(8),W(8),F(8),Z(8),ZB(8)
AL = 21.8
PI = 3.141592654
G = 1.
DX = 1.
```

```
      TI = 1.5
      TD = 0.4
      BI = 0.5
      NMID = 4
      MAX = 8
      RMU1 = 0.
      WRITE(6,300)AL,G,DX,TI,TD,BI,NMID,MAX
  300 FORMAT(*AL = *,F5.2,5X,*G = *,F5.2, 5X,*DX = *,F5.2,5X,*TI = *,F5.2,5X,*TD
     C = *,F5.2,5X,*BI = *,F5.2,5X,*NMID = *,I3,5X,*MAX = *,I3)
      N = 2
      Y(1) = 1.
      AL = AL*PI/180.
      COAL = 1./TAN(AL)
      TCF = DX*COAL
   20 Y(N) = Y(N-1)+TI-BI
      N = N+1
      IF(N.GT.NMID)GO TO 10
      GO TO 20
   10 Y(N) = Y(N-1)-TD-BI
      N = N+1
      IF(N.GT.MAX)GO TO 30
      GO TO 10
   30 N = NMID
   60 IF(Y(N).GT.TCF)GO TO 40
      I = N-1
      GO TO 50
   40 N = N+1
      IF(N.LE.MAX)GO TO 60
      WRITE(6,100)
  100 FORMAT(* NO TENSION CRACK IS FORMED *)
   50 CONTINUE
  -CONTINUE STATEMENT IS NOT DO TERMINATOR
      M = NIMD-1
      DO 15 N = 1,M
      Z(N) = Y(N)
      W(N) = G*Y(N)*DX
   15 CONTINUE
      DO 25 N = NMID,I
      Z(N) = Y(N) - TD
      W(N) = G*Y(N)*DX
   25 CONTINUE
```

```
      ZB(1) = 0.
      DO 35 N = 2,NMID
      ZB(N) = Y(N) - TI
 35   CONTINUE
      L = NMID + 1
      DO 45 N = L,I
      ZB(N) = Y(N)
 45   CONTINUE
      PNM1 = 0.
      RMU = 0.8
- NAME - RMU SAME AS STANDART FUNCTION AND REMOVES FUNCTION FROM USE
      DELTA = 0.1
 160  CONTINUE
 -CONTINUE STATEMENT IS NOT DO TERMINATOR
      WRITE(6,800)RMU
 800  FORMAT(*----------RMU = *,F8.6,*----------*)
      WRITE(6,600)
 600  FORMAT(* BLOCK NO.*,10X,*P-TOP,*,15X,*P-SIL.*,15X,*PNM1*/*-------
     C-*,10X,*------*,15X*------*,15X,*----*)
      N = 1
 90   PNT = (PNM1*ZB(N)+(W(N)/2.)*(DX*COS(AL)-Y(N)*SIN(AL)))/(Z(N)-RMU*DX)
      PNS = PNM1 + (W(N)*(RMU*COS(AL)-SIN(AL)))/(1.-RMU*RMU)
      IF(PNS.LT.PNT)GO TO 70
      P(N)=PNT
      GO TO 80
 70   P(N) = PNS
 80   CONTINUE
- CONTINUE STATEMENT IS NOT DO TERMINATOR
      IF(P(N).LE.0.)GO TO 170
      PNM1 = P(N)
      WRITE(6,700)N,PNT,PNS,PNM1
 700  FORMAT(4X,I3,9X,E14.6,7X,E14.6,6X,E14.6)
      N = N+1
      IF(N.LE.I)GO TO 90
      WRITE(6,400)
 400  FORMAT(* BLOCK NO.*,10X,*Y*,16X,*W*,18X,*P*,19X,*Z*,16X,*ZB*/*----
     C-----*,9X,*---*,14X,*---*,16X,*---*,17X,*---*,14X,*-----*)
      DO 55 N = 1,I
 55   WRITE(6,500)N,Y(N),W(N),P(N),Z(N),ZB(N)
 500  FORMAT(4X,I3,EX,E14.6,3X,E14.6,5X,E14.6,6XE14.6,4X,E14.6)
      TMU = RMU
```

```
      APN = ABS(P(I))
      IF(APN.GT.0.00001)GO TO 110
      WRITE(6,200)RMU
200   FORMAT(* COEFFICIENT OF FRICTION = *,E15.6/1X,*----------------
     C---*)
      GO TO 120
110   CONTINUE
      IF(P(I).GT.0.)GO TO 130
-CONTINUE STATEMENT IS NOT DO TERMINATOR
170   RMU = RMU+DELTA
      GO TO 140
130   CONTINUE
      IF(RMU.EQ.RMU1)DELTA = DELTA/10.
-CONTINUE STATEMENT IS NOT DO TERMINATOR
-IS FLOATING POINT EQUALITY TO BE EXPECTED
      RMU1 = RMU
      RMU = RMU-DELTA
140   CONTINUE
-CONTINUE STATEMENT IS NOT DO TERMINATOR
      IF(RMU.LE.0.)GO TO 150
      IF(RMU.GE.1.)GO TO 150
      PNM1 = 0.
      GO TO 160
150   DELTA = DELTA/10.
      RMU = TMU
      PNM1 = 0.
      GO TO 160
120   STOP
      END
```

APPENDIX B

D.R. PROGRAM FOR DIFFERENT HEIGHT BLOCKS

Notes:

1. The program is run in three steps:
   a- creation of the program library
   b- updating
   c- feeding the input data
2. The neighbours of each block should be fed into the program in the form of data.
3. The plotting routines are for the Imperial Coll ge display system.

List of Variables:

NRREST = 0 ⟶ Start run (=2 ⟶ Restart run)

A- spacings of westerly dipping discontinuities

B- spacing of easterly dipping discontinuities

DIPA- dip of westerly dipping discontinuities(degrees)

DIPB- dip of easterly dipping discontinuities(degrees)

NROV- number of rows of block

NBASE- number of base blocks for generating block assemblage

DT- time step(based on equivalent block stiffness)

FAC- damping factor

NCYLE- no. of cycles for the run(for restart run accumulative total)

IPRINT- the regular cycle interval at which printer output is required

ITR- iteration number

IWHEN- similar to IPRINT but for plotter output

IZCYC = 0 ⟶ no zero cycle plot is generated

IZCYC = 1 ⟶ zero cycle plot is generated

NWREST = 0 ⟶ no restart tape is written

NWREST = 1 ⟶ restart tape is written after program has run for a required number of cycles

SCAL- block geometry scaling for plotting

SCALT- not used

VECL- length of maximum velocity vector in inches for plotting

XORIG- x position of origin for plotting

YORIG- y position of origin for ploting

NEIB- interval at which neighbour blocks are updated - this is automatically done at the commencement of a restart

SN- normal stiffness (= shear stiffness)

RSD- residual friction angle (degrees)

DMU- peak friction angle (degrees)

RHO- material density

GRAV- gravitational acceleration (vertical)

NREM- number of blocks removed

BMASS- mass of block

BMOI- moment of inertia

NON- total number of blocks

FXX- force in x direction acting on block

FYY- force in y direction acting on block

SMM- moment acting on block

OVLN- normal overlap of corner

OVLS- shear overlap of corner

SF- shear force acting on corner

VXN- velocity in x direction of block

VYN- velocity in y direction of block

AVN- angular velocity of block

CX- x coordinate of block centroid

CY- y coordinate of block centroid

ANT- angle of major axis with x axis(c.c.w $\longrightarrow$+ ve)

```
*COMDECK GENALL
      COMMON/GENALL/CX(100),CY(100),ANT(100),A(100),AA(100),BB(100),
     C              ANN(100),BNN(100),BMASS(100),BMOI(100),FF(100),B,
     C              DIPA,DIPB,RHO,NBASE,NROW,HH,NON,SN,GRAV,RAT10,SCAL,
     C              PI,SCALT,ITR,IZCYC,TITLE (20),IAXIS(100)
*COMDECK MAIN
      COMMON/MAIN/FXX(100),FYY(100),SMM(100),OVLN(100,12)OVLS(100,12),
     *              SF(100,12),VXN(100),VYN(100),AVN(100),FPCYC(100),
     *              SMPCYC(100)
*COMDECK CNEIGH
      COMMON/CNEIGH/NEIGH(100,8),N(4,3)NREMOV(30),NREM
*COMDECK CCOOR
      COMMON/CCOOR/DMOVE(100),WEIGHT(100),BETA1(100),BETA2(100),XORIG,
     C              YORIG,IFIXED,IFIX(50)
*DECK MAINL
      PROGRAM TEST (INPUT = 1002,OUTPUT,TAPE5 = INPUT,TAPE6 = 1002,TAPE62,
     *TAPE4 = 1002)
*CALL GENALL
*CALL MAIN
*CALL CNEIGH
*CALL CCOOR
      DIMENSION GEN(1236),AMAI(4400),CNE(843),CC1(453),REMOV(7)
      EQUIVALENCE (CX,GEN),(FXX,AMAI),(NEIGH,CNE),(DMOVE,CC1)
      DATA DEGREE,PI/0.017453292519943,3.1415926358979/
      READ(5,198)(TITLE(I),I = 1,8)
      ITR = 0
198   FORMAT(8A10)
      READ(5,700)DUM,RREST
700   FORMAT(A5,F10.0)
      NRREST = RREST
      IF(NRREST.NE.2)GO TO 703
      READ(4)(GEN(I),I = 1,1236),(AMAI(I),I = 1,4400),(CNE(I),I = 1,843),
     *(CC1(I),I = 1,453)
703   CONTINUE
      WRITE(6,197)(TITLE(I),I = 1,8)
197   FORMAT(1H,8A10)
      WRITE(6,399)
399   FORMAT( *  CARD      FIELD 1      FIELD 2      FIELD 3
     *FIELD4      FIELD 5      FIELD 6      FIELD 7*,//)
      WRITE(6,701)DUM,RREST
701   FORMAT(1H,A5,E15.6)
      READ(5,100)NC,HEIGHT,B,DIPA,DIPB,ANROW,ANBASE
      NROW = ANROW
```

```
      NBASE = ANBASE
      WRITE(6,101)NC,HEIGHT,B,DIPA,DIPB,ANROW,ANBASE
      READ(5,100)NC,DT,FAC,CYCLES,PRINT,WHEN,ZCYCLE,WREST
      NWREST = WREST
      NCYCLE = CYCLES
      IWHEN = WHEN
      IZCYC = ZCYCLE
      IPRINT = PRINT
      WRITE(6,101)NC,DT,FAC,CYCLES,PRINT,WHEN,ZCYCL,WREST
      READ(5,100)NC,SCAL,SCALT,VECL,XORIG,YORIG,ANEIB
      NEIB = ANEIB
      WRITE(6,101)NC,SCAL,SCALT,VECL,XORIG,YORIG,ANEIB
      READ(5,100)NC,SN,RSD,DMU,RHO,GRAV
100   FORMAT(15,7F10.0)
      WRITE(6,101)NC,SN,RSD,DMU,RHO,GRAV
101   FORMAT(1H,I5,7E15.6/)
      READ(5,100)NC,(REMOV(I),I = 1,7)
      WRITE(6,101)NC,(REMOV(I),I = 1,7)
      NREM = REMOV(1)
      DO 713 I = 2,7
713   NREMOV(I-1) = REMOV(I)
      IF(NREM.LE.6)GO TO 714
      J = 6
      DO 711 IIJ = 1,10
      READ(5,100)NC,(REMOV(I),I = 1,7)
      WRITE(6,101)NC,(REMOV(I),I = 1,7)
      IF(NC.EQ.99)GO TO 714
      DO 711 IJ = 1,7
      J = J + 1
711   NREMOV(J) = REMOV(IJ)
714   CONTINUE
      IPCON = 1
      CALL PL(IPCON)
      RSD = TAN(RSD*PI/180.)
      DMU = TAN(DMU*PI/180.)
      NTILT = 0
      VV = 0.01
      PII=PI*2.
      RATIO = 0.
      DIPA = DIPA*PI/180.
      DIPB = DIPB*PI/180.
```

```
      DELTA = DIPA
      A(1) = HEIGHT
      FF(1) = A(1)/SIN(DIPA+DIPB)
      DO 228 I = 2,9
      A(I) = A(1)
      FF(I) = FF(1)
228   CONTINUE
      MID = 12
      NON = 16
      DO 222 I = 10,NON
      IF(I.GT.MID)GO TO 333
      A(I) = (I-1)+1.
      GO TO 444
333   A(I) = A(I-1)-0.9
444   FF(I) = A(I)/SIN(DIPA+DIPB)
222   CONTINUE
      HH = B/SIN(DIPA + DIPB)
      ST = SN
      DISMAX =0.01
      IF(NRREST.EQ.2)GO TO 501
      CALL COORDS
501   DO 189 I = 1,NON
      WEIGHT(I) = BMASS(I)*GRAV
189   CONTINUE
      DO 1401 I=1,NON
      READ(5,1402)(NEIGH(I,L),L =1,8)
1402  FORMAT(8I10)
1401  CONTINUE
      IF(NRREST.EQ.2)GO TO 502
      CALL CONSOL
502   CONTINUE
      IF(NRREST.EQ.2)GO TO 500
      DO 206 I = 1,NON
      FXX(I) = 0.
      FYY(I) = 0.
      SMM(I) = 0.
      VXN(I) = 0.
      VYN(I) = 0.
      AVN(I) = 0.
      DO 206 J = 1,12
```

```
      OVLN(I,J) = 0.
      OVLS(I,J) = 0.
206   SF(I,J) = 0.
500   ITR = ITR + 1
      DO 44  I = 1,NON
      FXX(I) = 0.
      FYY(I) = 0.
      SMM(I) = 0.
   44 CONTINUE
      DO 68  I = 1,NON
      DAMPN = (FAC*2.*SQRI(SN*BMASS(I)))/DT
      DAMPS = (FAC*2.*SQRT(ST*BMASS(I)))/DT
      IF(NREM.EQ.0)GO TO 256
      DO 156 J = 1,NREM
      IF(NREMOV(J).EQ.I)GO TO 68
156   CONTINUE
256   CONTINUE
      K = 1
      ANTI = ANT(I)
      SI = SIN(ANTII)
      CO = COS(ANTII)
      IF(IAXIS(I).EQ.1)GO TO 40
      ANTIC = DIPA + DIPB + ANTI
      SS = SIN(ANTIC)
      CC = COS(ANTIC)
      ANTII = DIPA + DIPB +ANTI - PI/2.
      SOI = SIN(ANTII)
      COI = COS(ANTII)
      GO TO 41
   40 ANTIC = ANTI + PI - DIPA - DIPB
      SS = SIN(ANTIC)
      CC = COS(ANTIC)
      ANTII = ANTI + PI/2. - DIPA - DIPB
      SOI = SIN(ANTII)
      COI = COS(ANTII)
   41 CONTINUE
      UAA = AA(I)*CO
      VAA = AA(I)*SI
      UBB = BB(I)*CC
```

```
      VBB = BB(I)*SS
      DO 65 IL = 1,4
      LL = 2*IL
      GO TO (1,2,3,4)IL
    1 XX = CX(I) + UAA + UBB
      YY = CY(I) + VAA + VBB
      GO TO 52
    2 XX = CX(I) + UAA - UBB
      YY = CY(I) + VAA - VBB
      GO TO 52
    3 XX = CX(I) - UAA - UBB
      YY = CY(I) - VAA - VBB
      GO TO 52
    4 XX = CX(I) - UAA + UBB
      YY = CY(I) - VAA + VBB
   52 J = NEIGH(I,LL - 1)
      GO TO 60
   54 J = NEIGH(I,LL + 1)
      GO TO 60
   55 J = NEIGH(I,1)
      GO TO 60
   53 J = NEIGH(I,LL)
   60 CONTINUE
      LTOUCH = 1
      L = K
      IF(J.EQ.0)GO TO 66
      KONTER = 0
      KONYEJ = 0
      KHECKS = 0
      XD = XX - CX(J)
      YD = YY - CY(J)
      ALPHAJ = ANT(J)
      SSI = SIN(ALPHAJ)
      CCO = COS(ALPHAJ)
      IF(IAXIS(J).EQ.1)GO TO 69
      ALPHAI = DIPA + DIPB + ALPHAJ - PI/2.
      SII = SIN(ALPHAI)
      COO = COS(ALPHAI)
      ALPHII = DIPA + DIPB + ALPHAJ
      SOJ = SIN(ALPHII)
      COJ = COS(ALPHII)
```

```
      GO TO 70
   69 ALPHAI = ALPHAJ + PI/2. - DIPA - DIPB
      SII = SIN(ALPHAI)
      COO = COS(ALPHAI)
      ALPHII = ALPHAJ + PI - DIPA - DIPB
      SOJ = SIN(ALPHII)
      COJ = COS(ALPHII)
   70 CONTINUE
      AJJ =-XD*SSI + YD*CCO
      TJJ = XD*CCO + YD*SSI
      AII = XD*COO + YD*SII
      TII = XD*SII - YD*COO
      ANI = ABS(AII)
      ANJ = ABS(AJJ)
      IF(ANI.GT.ANN(J).OR.ANJ.GT.BNN(J))GO TO 66
C  WHEN IF STATEMENT CORRECT NO CONTACT EXSTS BETWEEN I AND J
C  FIND WHAT FACE CORNER PENERTRATES BY THE USE OF ANGLES. CORNER ONE
C  HAS ANGLE OF ZERO.
      IF(ALPHAJ.GT.PII)GO TO 88
      ALP = ALPHAJ
      GO TO 89
   88 KALP = ALPHAJ/PII
      ALP = ALPHAJ - KALP*PII
   89 ALPP = ALP + BETA1(J)
      IF(ALPP.GT.PII)ALPP = ALPP - PII
      ALP1 = 0.
      ALP4 = PI - BETA1(J) - BETA2(J)
      ALP3 = PI
      ALP2 = PI + ALP4
      UCC = AA(J)*CCO
      VCC = AA(J)*SSI
      UDD = BB(J)*COJ
      VDD = BB(J)*SOJ
C  FINDS WHICH FACE OF BLOCK J, THE CORNER PENERTRATES
      KONTER = 1
      KONTEJ =1
      K1 = 0
      K2 = 0
      KA = 0
      GM = ABS(CCO)
      IF(GM.LE.1E - 5)GO TO 94
      AF1 = SSI/CCO
```

```
121     GM = ABS(COJ)
        IF(GM.LE.1E - 5)GO TO 95
        AF2 = SOJ/COJ
        GO TO 86
 94     K1 = 1
        GO TO 121
 95     K2 = 1
 86     XO = XX - CX(I)
        YO = YY - CY(I)
        GM = ABS(XO)
        IF(GM.LE.1.E - 5)XO = 1.E - 5
        ACTOC = YO/XO
        BCTOC = YD -XD*ACTOC
        KTOUCH = 0
        KFF = 0
        DO 87 KF = 1,4
        GO TO (96,97,98,99)KF
    96  UU = UCC + UDD
        VV = VCC + VDD
        AF = AF1
        AP1 = 0
        AP2 = ALP4
        KA = K1
        GO TO 106
    97  UU = UCC - UDD
        VV = VCC - VDD
        AF = AF1
        AP1 = ALP3
        AP2 = ALP2
        KA = K1
        GO TO 106
    98  UU = UCC - UDD
        VV = VCC -VDD
        AF = AF2
        AP1 = ALP2
        AP2 = PII
        KA = K2
        GO TO 106
    99  UU = - UCC - UDD
        VV = - VCC - VDD
        AF = AF2
```

```
      AP1 = ALP4
      AP2 = ALP3
      KA =K2
106    IF(KA.EQ.1)GO TO 126
      BF = VV - UU*AF
      XF = (BCTOC -BF)/(AF - ACTOC)
      YF = BF + XF*AF
      GO TO 127
126   XF = UU
      YF = BCTOC + XF*ACTOC
127   GM = ABS(XF)
      IF(GM.LE.1E - 5) XF = 1E - 5
      AG = ATAN2(YF,XF)
      IF(AG.LT.0.)AG = PII + AG
      AG = AG - ALPP
      IF(AG.LT.0.)AG = AG+PII
      IF(AG.LE.AP2.AND.AG.GE.AP1)GO TO 107
      GO TO 87
  107 IF(KFF.NE.0.)GO TO 102
      KFF = KF
      XFF = XF
      YFF = YF
      KTOUCH = 1
      GO TO 87
  102 KFO = KF
      XFO = XF
      YFO = YF
      KTOUCH = 2
      GO TO 103
   87 CONTINUE
      IF(KTOUCH.EQ.0)GO TO 104
      GO TO (56,77,73,72)KFF
  103 XGF = XFF + CX(J) - CX(I)
      YGF = YFF + CY(J) - CY(I)
      DGF = SQRT(XGF*XGF + YGF*YGF)
      XGF = XFO + CX(J) - CX(I)
      YGF = YFO + CY(J) - CY(I)
      DGO = SQRT(XGF*XGF + YGF*YGF)
      IF(DGF.GT.DGO)KFF = KFO
      GO TO (56,77,73,72)KFF
   77 KONTER = -1
```

```
      GO TO 79
   56 CONTINUE
C  CORNER PENERTRATES A FACE PARALLEL TO A MAJOR AXIS (MAJOR FACE)
   79 FFJ = SN*(BNN(J) - ANJ)
      OVLNO = OVLN(I,L)
      IF(OVLNO.EQ.0.)OVLNO = ANJ
      DNF = FFJ + DAMPN*(OVLNO - ANJ)
      DSF = 0.
C  DSF EQUALS ZERO, BECAUSE ONLY NORMAL FORCES ARE INVOLVED IN COMMON
C  BLOCK INTERACTIONS, SINCE THERE IS NO SLIDING PLANE INVOLVED
      OVLSO = OVLS(I,L)
      IF(OVLSO.EQ.0.)OVLSO = TJJ
      SHDJ = TJJ - OVLSO
C  SHDJ = DISTANCE OF SHEARING MOTION ALONG A MAJOR FACE
      FSJ = SF(I,L) + SHDJ*ST
      NOFSEF = ITR/IPRINT
      NOFSEF = NOFSEF*IPRINT
      IF(NOFSEF.NE.ITR)GO TO 2324
      WRITE(6,2526)ITR,I,FFJ,FSJ
 2526 FORMAT(* CYCLE NO. = *,15,5X,*BLOCK NO.*,12,5X,*NORMAL FORCE = *,1PE16
     C.8.5X,*SHEAR FORCE = *,1PE16.8)
 2324 CONTINUE
      DSF = FSJ + SHDJ*DAMPS
      SMAX = FFJ*DMU
      ABF = ABS(FSJ)
      IF(NOFSEF.NE.ITR)GO TO 9512
      IF(SMAX.GT.ABF)GO TO 9293
      WRITE(6,9394)
 9394 FORMAT(100X,*.....SLIDING*)
 9293 CONTINUE
 9512 CONTINUE
      IF(ABF.LE.SMAX)GO TO 719
      FSJ = RSD*FFJ*ABF/FSJ
      DSF = FSJ
  719 CONTINUE
      OVLN(I,L) = ANJ
      OVLS(I,L) = TJJ
      HOR = ( - ONF*SSI)*KONTER - DSF*CCO
      VER = (DNF*CCO)*KONTER - DSF*SSI
   64 CONTJNUE
      FXX(I) = FXX(I) + HOR
```

```
      FYY(I) = FYY(I) + VER
      FXX(J) = FXX(J) - HOR
      FYY(J) = FYY(J) - VER
      SMM(J) = SMM(J) + HOR*YD - VER*XD
      SMM(I) = SMM(I) - HOR*YO + VER*XO
      SF(I,L) = DSF
      LTOUCH = 2
      GO TO 66
104   CONTINUE
      WRITE(6,201)
201   FORMAT(* ERROR IN BLOCK INTERACTION*)
      GO TO 66
 72   KONTEJ = -1
      GO TO 74
73    CONTINUE
C C   CORNER PENERTRATES A FACE PARALLEL TO A MINOR AXIS (MINOR FACE)
 74   FFI = SN*(ANN(J) - ANI)
      OVLNO = OVLN(I,L)
      IF(OVLNO.EQ.0.)OVLNO = ANI
      DNF = FFI + DAMPN*(OVLNO - ANI)
      DSF = 0.
      OVLSO = OVLS(I,L)
      IF(OVLSO.EQ.0.)OVLSO = TII
      SHDI = TII - OVLSO
      FSI = SF(I,L) + SHDI*ST
      MINNOS = ITR/IPRINT
      MINNOS = MINNOS*IPRINT
      IF(MINNOS.NE.ITR)GO TO 2728
      WRITE(6,2829)ITR,I,FFI,FSI
 2829 FORMAT(*CYCLE NO. = *,15,5X,*BLOCK NO.*,12,5X,*NORMAL FORCE(MIN) = *,
     C1PE16.8,5X,*SHEAR FORCE(MIN) = *,1PE16.8)
 2728 CONTINUE
      DSF = FSI + SHDI*DAMPS
      SMAX = FFI*DMU
      ABF = ABS(FSI)
      IF(MINNOS.NE.ITR)GO TO 7123
      IF(SMAX.GT.ABF)GO TO 7273
      WRITE(6,8283)
 8283 FORMAT(110X,*.....SLIDING(MIN)*)
 7273 CONTINUE
 7123 CONTINUE
```

```
      IF(ABF.LE.SMAX)GO TO 720
      FSI = RSD*FFI*ABF/FSI
      DSF = FSI
  720 CONTINUE
      OVLN(I,L) = ANI
      OVLS(I,L) = TII
      HOR = (DNF*COO)*KONTEJ - DSF*SII
      VER = (DNF*SII)*KONTEJ + DSF*COO
      GO TO 64
   66 CONTINUE
      IF(LTOUCH.EQ.2)GO TO 67
      SF(I,L) = 0.
      OVLN(I,L) = 0.
      OVLS(I,L) = 0.
67    K = K + 1
      GO TO (65,54,53,65,54,53,65,54,53,65,55,53,65)K
65    CONTINUE
   68 CONTINUE
      DO 71 I = 1,NON
      DSST = DT/BMASS(I)
      DOIT = DT/BMOI(I)
      FYY(I) = FYY(I) - WEIGHT(I)
      VXN(I) = VXN(I) + FXX(I)*DSST
      VYN(I) = VYN(I) + FYY(I)*DSST
      AVN(I) = AVN(I) + SMM(I)*DOIT
   71 CONTINUE
C  THIS SUBROUTINE SETS FIXED BLOCKS VELOCITIES TO ZERO
      DO 10 I = 1,IFIXED
      J = IFIX(I)
      VXN(J) = 0.
      VYN(J) = 0.
      AVN(J) = 0.
   10 CONTINUE
      DO 26 I = 1,NON
      CX(I) = CX(I) + VXN(I)*DT
      CY(I) = CY(I) + VYN(I)*DT
      ANT(I) = ANT(I) + AVN(I)*DT
   26 CONTINUE
      IP = ITR/IPRINT
      IP = IP*IPRINT
      IF(IP.EQ.ITR)CALL PRIN
      IT = ITR/IWHEN
```

```
      IT = IT*IWHEN
      IF(IT.EQ.ITR)CALL BLOCK
      IT = ITR/NEIB
      IT = IT*NEIB
      IF(ITR.NE.NCYCLE)GO TO 500
      IF(NWREST.NE.1)GO TO 704
      REWIND 4
      WRITE(4) (GEN(I),I = 1,1236),(AMAI(I),I = 1,4400),(CNE(I),I = 1,843),
     *(GC1(I),I = 1,453)
704   CONTINUE
      IPCON = 2
      CALL PL(IPCON)
      STOP
      END

*DECK COORDS
      SUBROUTINE COORDS
*CALL GENALL
*CALL CCOOR
      XCC = COS(DIPA)*HH
      YCC = SIN(DIPA)*HH
C  HH IS DISTANCE BETWEEN CENTROIDS OF BLOCKS IN SAME ROW
      DO 111 I = 1,NON
      XFF = COS(DIPA)*FF(I)
      YFF = SIN(DIPB)*FF(I)
C  FF IS DISTANCE BETWEEN CENTROIDS OF BLOCKS IN SAME COLUMN
      DD = HH/2.
      EE = FF(I)/2.
C  DD AND EE ARE HALF LENGHS OF AXES
      IF(EE.GT.DD)GO TO 80
C  IAXIS IS EQUAL TO ONE WHEN THE MAJOR AXIS IS PARALLEL TO DIPA
C  EQUAL TO TWO WHEN PARALLEL TO DIPB
      AA(I) = DD
      ANN(I) = B/2.
      BB(I) = EE
      BNN(I) = A(I)/2.
      ANT(I) = DIPA
      IAXIS(I) = 1
      GO TO 81
   80 AA(I) = EE
```

```
      ANN(I) = A(I)/2.
      BB(I) = DD
      BNN(I) = B/2.
      ANT(I) = PI - DIPB
      IAXIS(I) = 2
   81 CONTINUE
C    AA = HALF LENGTH OF MAJOR AXIS     BB = HALF LENGTH OF MINOR AXIS
C    ANN = DISTANCE FROM CENTROID TO MINOR FACE
C    BNN = DISTANCE FROM CENTROID TO MAJOR FACE
C    AGG = ANGLE ANTICLOCKWISE POSITIVE BETWEEN X AXIS AND MAJOR AXIS
C    CALCULATE BETA SO THAT CORNER POSITIONS CAN BE FOUND
      PP = BB(I)*(COS(PI - DIPA - DIPB)
      IF(IAXIS(I).EQ.1)GO TO 82
      AG = AA(I) - PP
      AH = AA(I) + PP
      GO TO 83
 82   AG = AA(I) + PP
      AH = AA(I) - PP
   83 CONTINUE
      BETA1(I) = ATAN(BNN(I)/AG)
      BETA2(I) = ATAN(BNN(I)/AH)
      BMASS(I) = HH*A(I)*RHO
      BE = ABS(FF(I)*COS(DIPA +DIPB))
      BC = (HH - BE)/2.
      BMOI1 = HH*(A(I)**3)/12.
      BMOI2 = 2.*A(I)*((BC**3)/3. + (BE**3)/36. + BE*(BC + BE/3.)*(BC + BE/3.)/2.)
      BMOI(I) = (BMOI1 + BMOI2)*RHO
 111  CONTINUE
C  THIS IS A SIMPLE CASE OF NINE BLOCKS STACKED IN THREE ROW AND THREE
      CALL GEN
      IF(IZGYC.EQ.1)CALL BLOCK
      RETURN
      END
*DECK NEIGHB
      SUBROUTINE NEIGHB
*CALL GENALL
*CALL CNEIGH
      DIMENSION NEIG(30)
C  THIS SUBROUTINE FINDS A MAXIMUM OF EIGHT NEIGHBOURING BLOCKS AND
C  ARRANGES THEM IN AN ANTI -CLOCKWISE ORDER SO THAT EACH CORNER OF
C  THE BLOCK HAS A MAXIMUM OF THREE NEIGHBOURING BLOCKS
```

```
      DO 136 I = 1,NON
      DO 136 J = 1,8
136   NEIGH(I,J) = 0
      DO 41 I = 1,NON
      XNN = COS(DIPA)*HH + COS(DIPB)*FF(I)
      YNN = SIN(DIPA)*HH + SIN(DIPB)*FF(I)
      RES = SQRT(XNN*XNN + YNN*YNN)
      DIF = 1.1*RES
      IF(NREM.EQ.0)GO TO 235
      DO 135 J = 1.NREM
      IF(NREMOV(J).EQ.I)GO TO 41
135   CONTINUE
235   CONTINUE
      NEX = 0
      DO 33 L = 1,4
      DO 33 M = 1,3
      N(L,M) = 0.
   33 CONTINUE
      DO 32 J = 1,30
   32 NEIG(J) = 0.
      XG = CX(I) + DIF
      XL = CX(I) - DIF
      YG = CY(I) + DIF
      YL = CY(I) - DIF
      DO 24 J = 1,NON
      IF(NREM.EQ.0)GO TO 237
      DO 137 IJ = 1,NREM
      IF(NREMOV(IJ).EQ.J)GO TO 24
137   CONTINUE
237   CONTINUE
      IF(J.EQ.I)GO TO 24
      IF(CY(J).GT.YG.OR.CY(J).LT.YL)GO TO 24
      IF(CX(J).GT.XG.OR.CX(J).LT.XL)GO TO 24
      NEX = NEX + 1
      NEIG(NEX) = J
   24 CONTINUE
      SI = SIN(ANT(I))
      CO = COS(ANT(I))
      IF(IAXIS(I).EQ.1)GO TO 34
      SS = SIN(DIPA + DIPB +ANT(I))
```

```
      CC = COS(DIPA + DIPB + ANT(I)
      GO TO 38
   34 SS = SIN(ANT(I) + PI - DIPA - DIPB)
      CC = COS(ANT(I) + PI - DIPA - DIPB)
   38 CONTINUE
      UAA = AA(I)*CO
      VAA = AA(I)*SI
      UBB = BB(I)*CC
      VBB = BB(I)*SS
      ANN = ANN(I) + 0.9*BNN(I)
      BNN = 1.9*BNN(I)
      DO 25 K = 1,4
      GO TO (1,2,3,4)K
    1 XX = CX(I) + UAA +UBB
      YY = CY(I) + VAA +VBB
      GO TO 26
    2 XX = CX(I) + UAA - UBB
      YY = CY(I) + VAA - VBB
      GO TO 26
    3 XX = CX(I) - UAA - UBB
      YY = CY(I) - VAA - VBB
      GO TO 26
    4 XX = CX(I) - UAA + UBB
      YY = CY(I) - VAA + VBB
   26 CONTINUE
      MM = 0
      DO 25 J = 1,NEX
      JJ = NEIG(J)
      SSI = SIN(ANT(JJ))
      COO = COS(ANT(JJ))
      IF(IAXIS(JJ).EQ.1)GO TO 39
      SII = SIN(DIPA + DIPB + ANT(JJ) - PI/2.)
      CCO = COS(DIPA + DIPB +ANT(JJ) - PI/2.)
      GO TO 40
   39 SII = SIN(ANT(JJ) + PI/2. - DIPA - DIPB)
      CCO = COS(ANT(JJ) + PI/2. - DIPA - DIPB)
   40 CONTINUE
      XD = XX- CX(JJ)
      YD = YY - CY(JJ)
      AJJ = ABS( - XD*SSI + YD*COO)
      AII = ABS(XD*CCO + YD*SII)
```

```
      IF(AJJ.GE.BBN.OR.AII.GE.AAN)GO TO 25
      MM = MM + 1
      N(K,MM) = JJ
   25 CONTINUE
      DO 23 J = 1,3
      DO 23 K = 1,3
      DO 23 L = 1,3
      DO 23 M = 1,3
      L1 = N(1,J)
      L2 = N(2,K)
      L3 = N(3,L)
      L4 = N(4,M)
      IF(L1.EQ.L2.AND.L1.NE.0)GO TO 27
   42 IF(L2.EQ.L3.AND.L2.NE.0)GO TO 28
   43 IF(L3.EQ.L4.AND.L3.NE.0)GO  TO 29
   44 IF(L4.EQ.L1.AND.L4.NE.0)GO TO 30
      GO TO 23
   27 NEIGH(I,3) = L1
      GO TO 42
   28 NEIGH(I,5) = L2
      GO TO 43
   29 NEIGH(I,7) = L3
      GO TO 44
   30 NEIGH(I,1) = L4
   23 CONTINUE
      DO 35 M = 1,3
      L1 = N(1,M)
      L2 = N(2,M)
      L3 = N(3,M)
      L4 = N(4,M)
      IF(L1.EQ.NEIGH(I,1).OR.L1.EQ.NEIGH(I,3)GO TO 31
      NEIGH(I,2) = L1
   31 CONTINUE
      IF(L2.EQ.NEIGH(I,3).OR.L2.EQ.NEIGH(I,5)GO TO 36
      NEIGH(I,4) = L2
   36 CONTINUE
      IF(L3.EQ.NEIGH(I,5).OR.L3.EQ.NEIGH(I,7)GO TO 37
      NEIGH(I,6) = L3
   37 CONTINUE
      IF(L4.EQ.NEIGH(I,7).OR.L4.EQ.NEIGH(I,1)GO TO 35
      NEIGH(I,8) = L4
```

```
    35 CONTINUE
41      CONTINUE
        RETURN
        END

*DECK  CONSOL
        SUBROTINE CONSOL
C     THIS IS A DUMMY CONSOLIDATION SUBROUTINE
C     REMEMBER TO INCLUDE COMMON BLOCKS
      RETURN
      END

*DECK  GEN
        SUBROUTINE  GEN
C    THIS IS A DUMMY SUBROUTINE , YOU SHOULD DELETE AND INSERT YOUR
C    PARTICULAR BLOCK GENERATION ROUTINE INCLUDING BLOCK FIXING
C    REMEMBER THAT COMMON BLOCKS GENALL AND CCOOR ARE TO BE CALLED.
        NON = 16
        READ(5,10)(CX(I),CY(I),I = 1,NON)
  10    FORMAT(4F20.0)
        IFIXED = 8
        READ(5,20)(IFIX(I),I = 1,IFIXED)
   20   FORMAT(2014)
        RETURN
        END

 *DECK PL
        SUBROUTINE PL(IPCON)
        GO TO (10,20)IPCON
10      CALL START (2)
        CALL PEN (1)
        RETURN
20      CALL ENPLOT
        RETURN
        END

 *DECK BLOCK
        SUBROUTINE BLOCK
 *CALL GENALL
 *CALL CNEIGH
 *CALL CCOOR
```

```
C  THIS SUBROTINE PLOTS ALL BLOCKS WITH THEIR RESPSCTIVE NUMBER
C  SCAL = NUMBER OF PROBLEM UNITS TO THE INCH AND DEPDNDS ON SIZE OF NUM
C  AND PAPER AI  (AO = LARGE  A1 = MEDIUM  A2 = SMALL)
C*************
C*************
      CALL TITLES(1,SCAL)
      DO 10 I = 1,NON
      IF(NREM.EQ.0)GO TO 150
      DO 50 IJ = 1,NREM
      IF(NREMOV(IJ).EQ.I)GO TO 10
50    CONTINUE
150   CONTINUE
      SI = SIN(ANT(I))
      CO = COS(ANT(I))
      IF(IAXIS(I).EQ.1)GO TO 20
      SS = SIN(DIPA + DIPB + ANT(I))
      CC = COS(DIPA +DIPB +ANT(I))
      GO TO 21
   20 SS = SIN(ANT(I) + PI - DIPA - DIPB)
      CC = COS(ANT(I) + PI - DIPA - DIPB)
   21 CONTINUE
      UAA = AA(I)*CO*SCAL
      VAA = AA(I)*SI*SCAL
      UBB = BB(I)*CC*SCAL
      VBB = BB(I)*SS*SCAL
      XX = CX(I)*SCAL
      YY = CY(I)*SCAL
      XX1 = XX + UAA + UBB
      YY1 = YY +VAA +VBB
      XX2 = XX + UAA - UBB
      YY2 = YY +VAA - VBB
      XX3 = XX - UAA - UBB
      YY3 = YY - VAA - VBB
      XX4 = XX - UAA + UBB
      YY4 = YY - VAA + VBB
      AAA = I
      CALL PLOT(XX1,YY1,3)
      CALL PLOT(XX2,YY2,2)
      CALL PLOT(XX3,YY3,2)
      CALL PLOT(XX4,YY4,2)
      CALL PLOT(XX1,YY1,2)
```

```
      H = 0.07
      IF(I.GT.9)GO TO 22
      XC = XX - H/2.
      YC = YY - H/2.
      GO TO 24
   22 IF(I.GT.99)GO TO 23
      XC = XX - H
      YC = YY - H
      GO TO 24
   23 XC = XX -1.5*H
      YC = YY -1.5*H
   24 CONTINUE
      CALL NUMBER(XC,YC,H,AAA,0.0, - 1)
      DO 26 K = 1,IFIXED
      J = IFIX(K)
      IF(I.EQ.J)GO TO 27
26    CONTINUE
      GO TO 10
27    YCA = YC - 0.28
      CALL SYMBOL(XC,YCA,H,1HF,0.0,1)
   10 CONTINUE
      CALL NEWPAGE
      RETURN
      END

*DECK PRIN
      SUBROUTINE PRIN
C     COMMON PRINT FOR NOMINATED CYCLES
*CALL GENALL
*CALL MAIN
*CALL CNEIGH
*CALL CCOOR
      WRITE(6,10)ITR
10    FORMAT(1H1,*CYCLE NUMBER*,15)
      WRITE(6,20)
20    FORMAT(* BLOCK     X       Y       ANG       V
     *X          VY           OMEGA       *)
      DO 30 I = 1,NON
      WRITE(6,40)  I,CX(I),CY(I),ANT(I),VXN(I),VYN(I),AVN(I)
40    FORMAT(15,7E15.6)
30    CONTINUE
```

```
      RETURN
      END

*DECK VELOC
      SUBROUTINE VELOC(VECL)
C  PLOTS VELOCITIES AS VECTORS WITH MAXIMUM VELOCITY EQUAL TO VECL INCHE
*CALL GENALL
*CALL MAIN
*CALL CNEIGH
*CALL CCOOR
      VO = 0.
      DO 10 I = 1,NON
      IF(NREM.EQ. 0)GO TO 30
      DO 40 IJ = 1,NREM
      IF(NREMOV(IJ).EQ.I)GO TO 10
 40   CONTINUE
 30   CONTINUE
      VN = SQRT(VXN(I)*VXN(I) + VYN(I)*VYN(I))
      IF(VN.LE.VO)GO TO 10
      VC = VN
   10 CONTINUE
      FG = VECL/VO
C   VECL IS LENGTH OF MAXIMUM VELOCITY IN INCHES
      GG = 1./FG
      CALL TITLES(2,GG)
      DO 20 I = 1,NON
      IF(NREM.EQ.0)GO TO 50
      DO 60 IJ = 1,NREM
      IF(NREMOV(IJ).EQ.I)GO TO 20
60    CONTINUE
50    CONTINUE
      X = CX(I)/SCAL
      Y = CY(I)/SCAL
      VX = VXN(I)*FG
      VY = VYN(I)*FG
      CALL VECTOR(X,Y,VX,VY)
   20 CONTINUE
      CALL NEWPAGE
      RETURN
      END
```

```
*DECK VECTOR
      SUBROUTINE VECTOR(X,Y,VX,VY)
*CALL GENALL
      CALL PLOT(X,Y,3)
      X = X + XV
      Y = Y + YV
      CALL PLOT(X,Y,2)
      VT = (SQRT(XV*XV + YV*YV))/5.
      GM = ABS(XV)
      IF(GM.LE.1.E - 5)XV = 1.E - 5
      ABA = ATAN2(YV,XV)
      IF(ABA.LT.0.)ABA = 2.*PI + ABA
      ABA1 = PI + ABA - 0.25
      ABA2 = ABA1 + 0.5
      XA = X + VT*(COS(ABA1))
      YA = Y + VT*(SIN(ABA1))
      CALL PLOT(XA,YA,2)
      CALL PLOT(X,Y,3)
      XA = X + VT*(COS(ABA2))
      YA = Y + VT*(SIN(ABA2))
      CALL PLOT(XA,YA,2)
      RETURN
      END

*DECK TITLES
      SUBROUTINE TITLES(IPLOT,DIS)
*CALL GENALL
*CALL CCOOR
      CALL SYMBOL(0.5,15.0,0.21,TITLE,0.,80)
      GO TO (10,11,12,13,14)IPLOT
   10 CONTINUE
C  THIS IS FOR A BLOCK PLOT
      CALL SYMBOL(0.5,14.25,0.21,10HBLOCK PLOT,0.,10)
      GO TO 15
   11 CONTINUE
C  THIS IS FOR A LINEAR VELOCITY PLOT
      CALL SYMBOL(0.5,11.25,0.21,13HVELOCITY PLOT,0.,13)
      GO TO 15
   12 CONTINUE
      CALL SYMBOL(0.5,11.25,0.21,17HCORNER FORCE PLOT,0.,17)
      GO TO 15
```

```
   13 CONTINUE
C  THIS IS FOR A DISPLACEMENT PLOT
      GO TO 15
   14 CONTINUE
C  THIS IS FOR A STRESS PLOT
   15 CONTINUE
      CALL SYMBOL(5.0,14.25,0.21,34HNUMBER OF PROBLEM UNITS PER INCH = ,0
     *..34)
      CALL NUMBER(12.4,14.25,0.21,DIS,0.,2)
      FL = ITR
      CALL SYMBOL(14.3,14.25,0.21,14HCYCLE NUMBER = ,0.,14)
      CALL NUMBER(17.5,14.25,0.21,FL,0.,-1)
      CALL PLOT(XORIG,YORIG,-3)
      RETURN
      END
```